

UNIVERSITÀ
DEGLI STUDI
DI PADOVA

Università degli Studi di Padova

Sede Amministrativa: Università degli Studi di Padova

Dipartimento di Scienze Chimiche

CORSO DI DOTTORATO DI RICERCA IN: SCIENZE MOLECOLARI
CURRICOLO: SCIENZE CHIMICHE
CICLO: XXXII

VANADIUM-CATALYZED AEROBIC C-C BOND OXIDATIVE CLEAVAGE: FROM SIMPLE MODELS TO LIGNIN DEPOLYMERIZATION

Coordinatore: Ch.mo Prof. Leonard Jan Prins

Supervisore: Ch.ma Prof.ssa Giulia Marina Licini

Dottorando: Davide Carraro

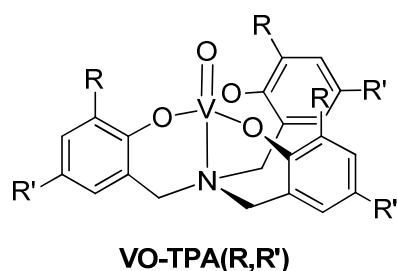
02/12/2019

INDEX

Summary	i
Riassunto.....	iii
Chapter 1	1
1.1 Biomass and Biorefineries.....	2
1.2 Lignocellulosic Biomass	3
1.3 Lignin Pretreatments	6
1.4 Lignin Depolymerization Strategies	9
1.4.1 Lignin Reductive Depolymerization Strategies	12
1.4.2 Lignin Redox-Neutral Depolymerization Strategies.....	14
1.4.3 Lignin Oxidative Depolymerization Strategies	15
1.5 Triphenolamines	17
1.6 Coordination Chemistry of TPAs	19
1.7 Vanadium (V) Aminotriphenolate Complexes VO-TPA(R, R')	21
1.8 Aim of the Thesis	23
Chapter 2.....	25
2.1 Introduction	26
2.2 Aerobic Oxidative C-C Cleavage of Vicinal Diols: Reaction Conditions Optimization.....	28
2.3 Catalytic Activity Studies and Substrate Scope	35
2.4 Catalyst Stability under Turnover Conditions.....	44
2.5 Proposed Reaction Mechanism	45
2.6 C-C Cleavage of <i>meso</i> -hydrobenzoin in Xylene	48
2.7 Oxidation of Aldehydes to Carboxylic Acids	52
2.8 Conclusions	59
2.9 Experimental.....	60
Chapter 3.....	71
3.1: Introduction	72
3.1.1 Lignin Oxidative Depolymerization.....	72
3.1.2 Vanadium (V) Complexes in Lignin Oxidative Depolymerization.....	75
3.2 Synthesis of β -O-4 Lignin Models	80
3.3 V^V Catalyzed Aerobic Oxidative Cleavage of non-phenolic Dimeric β -O-4 Lignin Models.....	83
3.4 Aerobic Oxidation of Phenolic β -O-4 Lignin Models	93
3.5 V^V Catalyzed Aerobic Oxidative Cleavage of a Trimeric β -O-4 Lignin Model.....	95
3.6 Structure-Reactivity Relationship: Aerobic Oxidation of Lignin Model Derivatives	101

3.7 Conclusions	103
3.8 Experimental.....	104
Chapter 4.....	121
4.1 Introduction	122
4.2 Lignin Samples Characterization.....	126
4.3 Steam Exploded SCB and WS Organosolv Lignin Depolymerization	130
4.3.1 2D-HSQC NMR Spectroscopy.....	130
4.3.2 Quantitative ³¹ P NMR Spectroscopy	134
4.3.3 FT-IR Analysis.....	137
4.3.4 GPC Analysis	138
4.3.5 MALDI-TOF-MS Analysis	142
4.4 Conclusions	146
4.5 Experimental.....	147
General Conclusions.....	151
List of Abbreviations.....	155

Summary



- V1:** R = ^tBu, R' = H
V2: R = R' = ^tBu
V3: R = ^tBu, R' = OMe
V4: R = ^tBu, R' = NO₂
V5: R = R' = Cl

This PhD thesis describes the use of vanadium(V) aminotriphenolate complexes **VO-TPA(R,R')** as catalysts for aerobic oxidative cleavage of vicinal diols, β -O-4 lignin models and lignin itself. In *Chapter 1* a general overview of the concept of biorefinery is given. In an ideal biorefinery, lignocellulosic biomass is transformed in order to obtain electric energy, biofuels (such as bioethanol) and fine chemicals. Among the lignocellulosic biomass fractions, lignin is considered the most earth-abundant renewable source of aromatic compounds, therefore, throughout the last few years researchers tried to develop more efficient depolymerization techniques. In particular, oxidative depolymerization should allow to obtain high value-added aromatic aldehydes (such as vanillin). With the purpose of finding a more efficient strategy for this process, in the research group in which this PhD thesis was carried out, **VO-TPA(R,R')** complexes have been synthesized and already effectively employed as catalysts for oxidation reactions.

In *Chapter 2*, the use of **VO-TPA(R,R')** complexes as catalysts for aerobic C-C cleavage of vicinal diols is described. *Meso*-hydrobenzoin was chosen as a model substrate in order to elucidate the ligand, solvent and temperature effects to the reactivity/selectivity. The best reaction performances, in terms of TONs, TOFs and selectivity towards benzaldehyde formation were achieved using **V5**, bearing six chloro substituents on the ligand backbone, in toluene and O₂ as oxidant. The reaction is quite general and effective with a large substrate scope, including tertiary, benzylic diols and also aliphatic linear and cyclic diols, obtaining in the majority of cases complete conversion towards the relative carbonyl compounds.

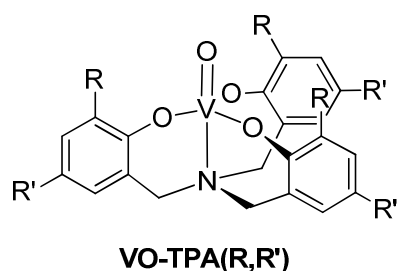
Catalyst stability during the reaction course was verified by ¹H-NMR and ESI-MS. Moreover, a reaction mechanism based on DFT calculation has been proposed. The reaction can be divided into three main steps: i. formation of a vanadium(V) non oxo-glycolate complex with formal elimination of a water molecule, ii. C-C bond cleavage of the substrate, with the formation of the relative carbonyl compounds by a two-fold electron transfer mechanism and generation of a V(III) species. iii. re-oxidation to V(V) by O₂ via formation of V(IV)-peroxo-species. Noticeably, when increasing the reaction temperature (xylenes at 130°C), a change in selectivity towards the further oxidized benzoic acid was observed. We therefore investigated aerobic oxidation of both aromatic and aliphatic aldehydes using complex **V5** as catalyst, collecting preliminary insights on the reaction mechanism.

In *Chapter 3*, aerobic oxidative cleavage of non-phenolic and phenolic β -O-4 lignin models catalyzed by **V5** is described. Differently from what found with 1,2-diols, the reaction occurs with different chemoselectivity affording products deriving from C_{α} - C_{β} , C_{β} -O and C_{α} -H cleavage (benzylic oxidation) mechanisms. The best catalytic performance was obtained using complex **V5**, in toluene under O_2 (1 atm) with catalyst loadings down to 1%. The reaction selectivity is strongly oriented towards benzylic oxidation (C_{α} -H cleavage, 50-85 %), but at lower catalyst loadings (1 %), C_{α} - C_{β} cleavage is favored with unprecedented high selectivity (up to 32%). These results were further confirmed with a non-phenolic trimeric model bearing two β -O-4 bonds (selectivity for C_{α} -H cleavage, 51-70 %, C_{α} - C_{β} cleavage, 12-20 % and C_{β} -O cleavage, 15-30 %). As regards phenolic β -O-4 models, reactions afford ketones deriving from benzylic oxidation as the major products (16-32 % yield), with a low degree of C_{α} - C_{β} cleavage (2-5% yield). Finally, the importance of free benzylic -OH groups in order to have C_{α} - C_{β} bond cleavage was highlighted, whereas the presence of free primary -OH group seems to assist the benzylic oxidation, leading to an enhancement of the selectivity towards ketones formation.

In *Chapter 4* the catalytic behavior of **V5** was tested on lignin samples (wheat straw/sugarcane bagasse), the latter particularly rich in β -O-4 linkage motifs. Lignin samples (20 mg/mL) were treated with **V5** (10% w/w) in dioxane or toluene at 100 °C, under O_2 (1 atm). The course of the reaction was monitored by 2D-HSQC-NMR, ^{31}P -NMR, FT-IR, GPC and MALDI-TOF-MS analyses, showing a significant disappearance of β -O-4 linkages for both samples. In the case of SCB lignin, formation of the corresponding ketones (benzylic oxidation) was observed, whereas reaction with WS lignin yielded the highest degree of depolymerization, not only of β -O-4 linkages, but also of phenylcoumaran and resinol bonds.

In conclusion, this PhD thesis reports the discovery of a new vanadium-based catalyst for effective C-C bond cleavage and lignin oxidative depolymerization, using molecular oxygen as terminal oxidant, in order to obtain valuable aromatic compounds starting from cheap and renewable sources.

Riassunto



- V1:** R = ^tBu, R' = H
V2: R = R' = ^tBu
V3: R = ^tBu, R' = OMe
V4: R = ^tBu, R' = NO₂
V5: R = R' = Cl

Questo lavoro di tesi descrive l'utilizzo di complessi amminotrifenolati di Vanadio (V) **VO-TPA(R,R')** come catalizzatori per la scissione ossidativa in ambiente aerobico di modelli del legame β -O-4 presente nella lignina e nella lignina stessa. Nel *Capitolo 1* viene fornita una panoramica generale del concetto di bioraffineria dove, partendo dalla biomassa lignocellulosica, si possono ottenere energia elettrica, carburanti (bioetanolo) o *fine chemicals*. In particolare, la frazione ligninica della biomassa è considerata la sorgente rinnovabile più economica e disponibile di composti aromatici, pertanto in questi ultimi anni si sono cercate tecniche di depolimerizzazione sempre più efficienti. Tra le varie tecniche finora sviluppate, la depolimerizzazione ossidativa permette di ottenere aldeidi aromatiche ad elevato valore aggiunto (tra cui la vanillina). Con lo scopo di trovare una via catalitica più adatta per questo processo, nel gruppo di ricerca in cui è stata condotta questa tesi, sono stati sintetizzati i complessi **VO-TPA(R,R')**, già efficacemente impiegati come catalizzatori per reazioni di ossidazione.

Nel *Capitolo 2* viene descritto l'impiego dei complessi **VO-TPA(R,R')** nella scissione ossidativa del legame C-C in dioli vicinali, usando il *meso*-idrobenzoino come modello per verificare l'effetto del legante, del solvente e della temperatura sulla reattività/selettività. Le migliori prestazioni in termini di TON e TOF, e selettività della reazione verso la benzaldeide, sono state ottenute con il complesso funzionalizzato con sei atomi di cloro nel legante **V5**, utilizzando toluene come solvente e sotto ossigeno (1 atm). Tale reazione è stata efficacemente impiegata in un'ampia classe di substrati, tra cui dioli terziari, benzilici, ma anche dioli alifatici lineari e ciclici, ottenendo nella maggior parte dei casi conversione completa nei relativi composti carbonilici.

La stabilità del catalizzatore durante la reazione è stata verificata mediante ¹H-NMR ed ESI-MS. È stato proposto inoltre un meccanismo di reazione basato su calcoli DFT. La reazione si può dividere in tre step principali: i. la formazione di un complesso non osso-glicolato di vanadio(V) con eliminazione formale di una molecola d'acqua, ii. la scissione C-C del substrato, con la formazione dei relativi composti carbonilici tramite un meccanismo di doppio trasferimento elettronico e la generazione di una specie di V(III), iii. la ri-ossidazione a V(V) da parte di O₂ tramite la formazione di complessi perossidici di V(IV). Aumentando la temperatura di reazione (xilene a 130°C) è stato osservato un cambiamento nella selettività verso il prodotto di *over*-ossidazione acido benzoico. La reazione di ossidazione di aldeidi sia alifatiche che aromatiche è stata quindi investigata usando il complesso **V5** come catalizzatore, raccogliendo risultati preliminari sul meccanismo di reazione.

Nel *Capitolo 3* viene descritta la scissione ossidativa di modelli non fenolici e fenolici di legame β -O-4 della lignina. A differenza di quanto osservato nel caso di dioli vicinali, la reazione decorre con diverse chemoselettività, portando alla formazione di prodotti derivanti da meccanismi di scissione C_{α} - C_{β} , C_{β} -O e C_{α} -H (ossidazione benzilica). La migliore attività catalitica è fornita dal complesso **V5**, in toluene sotto un'atmosfera di O_2 , con una concentrazione di catalizzatore inferiore all'1%. La selettività del sistema è fortemente diretta verso l'ossidazione benzilica (scissione C_{α} -H, 50-85 %), ma, abbassando la concentrazione di catalizzatore all'1%, si ottengono prodotti derivanti dalla scissione ossidativa C_{α} - C_{β} con rese mai raggiunte da altri sistemi omogenei di V(V) (fino al 32 % di selettività). Questi risultati sono stati confermati anche con un modello trimerico non fenolico contenente due legami β -O-4 (selettività per la scissione C_{α} -H, 51-70 %, scissione C_{α} - C_{β} , 12-20 % e scissione C_{β} -O, 15-30 %). Per quanto riguarda invece i modelli fenolici, le reazioni portano a chetoni derivanti dall'ossidazione benzilica come prodotti maggioritari (16-32 % di resa), con una quantità minoritaria di prodotti derivanti dalla scissione C_{α} - C_{β} (2-5 % di resa). Infine, è stata verificata l'importanza di gruppi -OH benzilici non funzionalizzati per avere scissione C_{α} - C_{β} nei modelli, mentre la presenza di gruppi -OH primari non funzionalizzati sembra favorire l'ossidazione benzilica, aumentando la selettività della reazione verso la formazione di chetoni.

Nel *Capitolo 4*, l'effetto catalitico dei complessi **VO-TPA(R,R')** è stato verificato su campioni di lignina (paglia di grano/bagassa della canna da zucchero), quest'ultimo particolarmente ricco in legami β -O-4. I campioni di lignina (20 mg/mL) sono stati trattati con **V5** (10 % m/m) in 1,4-diossano o toluene, a 100 °C usando O_2 come ossidante terminale. Le reazioni sono state monitorate via 2D-HSQC-NMR, ^{31}P -NMR, FT-IR, GPC e MALDI-TOF-MS, evidenziando una significativa scomparsa dei legami β -O-4 in entrambi i casi. Nel caso della lignina SCB, è stata osservata la formazione delle corrispondenti specie carboniliche (ossidazione benzilica), mentre dalla reazione della lignina WS si è ottenuto il più elevato grado di depolimerizzazione, non solo dei legami β -O-4, ma anche dei legami fenilcumarano e resinolo.

In conclusione, questa tesi di dottorato riporta la scoperta di un nuovo catalizzatore a base di vanadio per la scissione del legame C-C e la depolimerizzazione ossidativa della lignina, usando ossigeno molecolare come ossidante terminale, in modo da ottenere composti aromatici di valore a partire da sorgenti rinnovabili ed economiche.

Chapter 1

General Introduction

1.1 Biomass and Biorefineries

Petroleum is a non-renewable critically important commodity resource that modern society is reliant on as a carbon feedstock for the production of fuel and fine chemicals¹. However, environmental hazards and climate changes caused by thoughtless exploitation of non-renewable sources, gave rise to the need of a transition to renewable systems for the production of bioenergy and biomaterials². Moreover, European Union has outlined several targets to reach within 2020 in order to reduce CO₂ emissions by 20 % with respect to 1990, increase the energy efficiency by 20 %³ and increase the energy coming from renewable sources to 20 %.

With this consequent desirable depletion of fossil fuels as a source for fuels, chemicals, and energy, a strong demand to alternative renewable sources has been rising. Among these sources, biomass is the most natural abundant renewable feedstock⁴. Biomass can be defined as any organic material derived from living organisms or their metabolites⁵. In the context of energy and chemicals production, biomass refers to agricultural residues and forestry wastes or energy crops such as sugarcane, sweet sorghum, and microalgae⁶. The annual production of biomass all over the world is about 10¹¹ tons⁷, making it the fourth major source of energy after oil, coal and natural gas⁸. Furthermore, among these sources, biomass is the only one that can provide value added chemicals, such as commodity chemicals, solvents, pharmaceuticals and agrochemicals⁷. This feature paved the way to the development of biorefinery concept in order to obtain a sustainable and economically attractive strategy for biomass valorization. As in conventional refineries, biorefineries aim to maximize the use of biomasses producing a wide range of fuels and chemicals⁹. In this way, conversion of biomass to biofuels can become a rival process of petroleum refining, although it's unlikely that biomass would replace the demand for oil in the near future. However, currently, biomasses possess a great potential in the production of commodity chemicals and some companies already started to employ biomass as a raw material.

An example of industrial biorefinery is Spero Energy in Indiana (USA), where lignocellulosic biomass is converted into aromatic compounds used as flavors, for fragrances or in pharmaceutical industry¹⁰. In a similar manner, Borregaard in Norway employs wood fibers as raw material. Lignin is extracted

¹ Kärkäs, M. D.; Matsuura, B. S.; Monos, T. M.; Magallanes, G.; Stephenson, C. J.; *Org. Biomol. Chem.* **2016**, 14, 1853.

² Ragauskas, A. J.; *Science* **2006**, 80, 488.

³ Europe 2020 - www.ec.europa.eu/info/business-economy-euro/economic-and-fiscal-policy-coordination/eu-economic-governance-monitoring-prevention-correction/european-semester/framework/europe-2020-strategy_en (August 2019).

⁴ Zakzeski, J.; Bruijninx, P. C. A.; Jongerius, A. L.; Weckhuysen, B. M. *Chem. Rev.* **2010**, 110, 3552.

⁵ Baskar, C. *et al. Biomass conversion: the interface of biotechnology. chemistry and materials science.* Springer (2012).

⁶ Liu, C.; Wu, S.; Zhang, H.; Xiao, R.; *Fuel Process. Technol.*, **2019**, 191, 181.

⁷ Kärkäs, M. D.; *ChemSusChem* **2017**, 10, 2111.

⁸ Li, C.; Zhao, X.; Wang, A.; Huber, G. W.; Zhang, T.; *Chem. Rev.* **2015**, 115, 11559.

⁹ Regalbuto, J.; *Comput. Chem. Eng.* **2010**, 34, 1393.

¹⁰ Spero Energy - www.speroenergy.com (August 2019).

and converted to vanillin by catalytic oxidation, and other lignin-based materials can be employed as dispersants and emulsions. Cellulose is instead used to obtain products that can be employed in construction and oil industries, but also for pharmaceuticals and cosmetics, tablets, foodstuffs, hygiene products, filters, batteries and paints. Finally, part of the extracted sugars is fermented to make bioethanol¹¹. Despite the above-mentioned examples of biomass biorefineries, many efforts have still to be done in order to fully exploit the economic potential of biomass conversion, especially as regards the development of novel chemical transformations for processing biomasses.

1.2 Lignocellulosic Biomass

Nowadays, biomass-based chemicals and fuels are generally derived from sugar- and starch-containing crops such as beet, corn and grain. These crops are also used as feeds, resulting in an undesirable competition between food and fuels¹². It is therefore important to switch raw materials to sources that are currently considered as waste products, as in the case of lignocellulosic biomass deriving from agriculture and forest industries waste products.

Lignocellulosic biomass is the most abundant renewable carbon resource on Earth. It is mainly composed of the carbohydrate polymers cellulose (35 - 45 %) and hemicellulose (25 - 30 %) and the aromatic polymer lignin (20 – 35 %)¹³, depending on the kind of source.

Cellulose (Figure 1.1) is a linear homo-polysaccharide consisting of anhydrous glucose units linked by β -(1-4) bonds. The interconnections between these linear chains give rise to a crystallin structure bearing a significant mechanical resistance¹⁴.

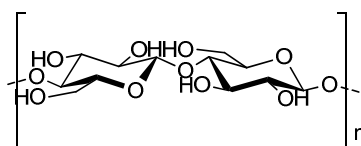


Figure 1.1: Chemical structure of cellulose.

Hemicelluloses (Figure 1.2) is an amorphous polymer consisting of a series of highly cross-linked polysaccharides that have β -(1-4)-linked backbones with an equatorial configuration. It includes both pentoses (xyloglucans, xylans), and hexoses (mannans, glucomannans, and β -(1-3,1-4)-glucans)¹⁵. Hemicellulose provides the structural strength between cellulose and lignin¹⁶.

¹¹ Borregaard – www.borregaard.com (August 2019).

¹² a) Patil, P. T.; Armbruster, U.; Richter, M.; Martin, A.; *Energy and Fuels* **2011**, 25, 4713 b) Gosselink, R. J. *Bioresour. Technol.* **2012**, 106, 173.

¹³ a) Hill, C. *Wood Modification: Chemical, Thermal, and Other Processes*; John Wiley & Sons: Chichester, U.K., **2006**. b) Boerjan, W.; Ralph, J.; Baucher, M.; *Annu. Rev. Plant Biol.* **2003**, 54, 519.

¹⁴ Ralph, J.; Lundquist, K.; Brunow, G.; Lu, F.; Kim, H.; Schatz, P. F.; Marita, J. M.; Hatfield, R. D.; Ralph, S. A.; Christensen, J. H.; Boerjan, W. *Phytochemistry Reviews* **2004**, 3, 29.

¹⁵ Scheller, H. V.; Ulvskov, P.; *Annu. Rev. Plant Biol.* **2010**, 61, 263.

¹⁶ a) Kuhad, R. C.; Singh, A.; Ericksson, K. E.; *Adv. Biochem. Eng. Biotechnol.* **1997**, 57, 45. b) Reddy, N.; Yang, Y.; *Trend Biotechnol.* **2005**, 23, 22. c) Li, B. Z.; Balan, V.; Yuan, Y. J.; Dale, B. E.; *Bioresour. Technol.* **2010**, 101, 1285.

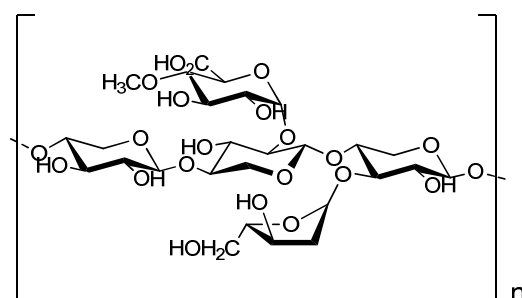


Figure 1.2: Chemical structure of hemicellulose.

Lignin (Figure 1.3) is a three-dimensional amorphous oligomer consisting of methoxylated phenyl propane units¹⁷. In plant cell walls, lignin fills the space between cellulose and hemicellulose and acts like a resin, holding the lignocelluloses matrix together¹⁸. It also protects the cell walls from microbial attack and provides shear and compressive strength to plant tissues¹⁹.

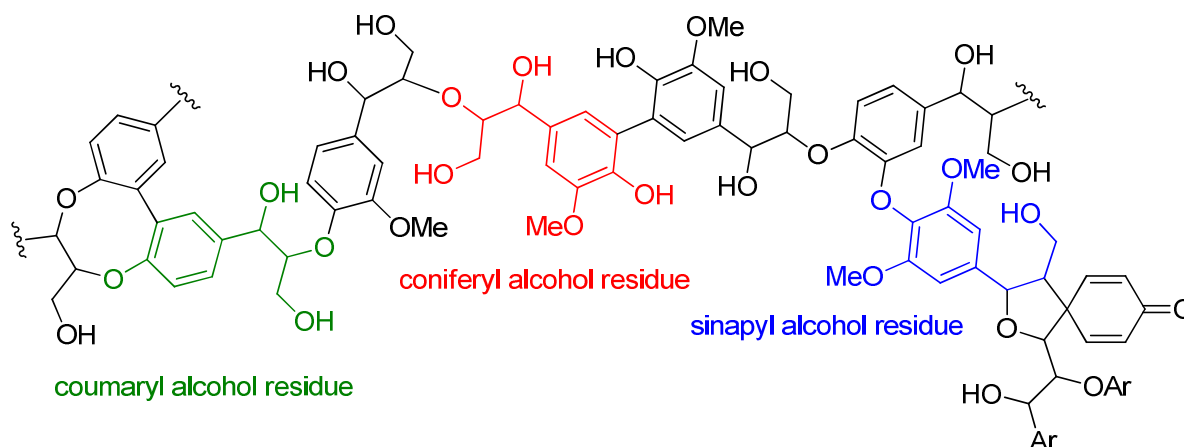


Figure 1.3: Chemical structure of Lignin.

The composition and ratio of lignin in plants varies greatly depending not only to the botanical species²⁰, but also on the type of biomass and even on the part of the plant²¹, with lignin abundance generally decreasing in the order of softwoods > hardwoods > grasses⁴. Indeed, lignin accounts for 30 % by weight in softwoods, while in hardwood lignin content falls to 20 - 25 %²² and in grass it shares 10 -15 % of the total plant mass²³.

¹⁷ Chakar, F. S. Ragauskas, A. J.; *Ind. Crops Prod.* **2004**, 20, 131.

¹⁸ Ritter, S. K.; *Chem. Eng. News* **2008**, 46, 15.

¹⁹ a) Van Haveren, J.; Scott, E. L.; Sanders, J.; *Biofuels. Bioprod. Biorefining* **2008**, 2, 41. b) Sjöström. E. *Wood chemistry: Fundamentals and applications*. Academic. (1993).

²⁰ a) Sarkanen, K. V.; Ludwig, C. H.; (Eds), *Lignins: Occurrence, Formation, Structure, and Reactions*, Wiley, New York (1971). b) Buranov, A. U.; Mazza, G.; *Ind. Crops Prod.* **2008**, 28, 237.

²¹ Hu, L. H.; Pan, H.; Zhou, Y. H.; Zhang, M.; *Bioresources*, **2011**, 6, 3515.

²² Calvo-Flores, F. G.; Dobado, J. A.; *ChemSusChem* **2010**, 3, 1227.

²³ Kamm, B.; Gruber, P. R.; Kamm, M.; *Biorefineries-Industrial Processes and Products*, Wiley-VCH, (2006).

The biosynthesis of lignin is achieved from the random radical polymerization via oxidative phenolic coupling of three different monolignols: Sinapyl Alcohol, Coniferyl Alcohol and *p*-Coumaryl Alcohol (Figure 1.4), known also as syringyl (**S**), guaiacyl (**G**) and *p*-hydroxyphenyl units (**H**).

The content of each monolignol depends upon plant taxonomy. For example, softwood lignin (gymnosperm) contains more **G** units, hardwood (angiosperm) lignin has a mixture of **G** and **S** units, whereas grass lignin is composed by a mixture of all three units⁸.

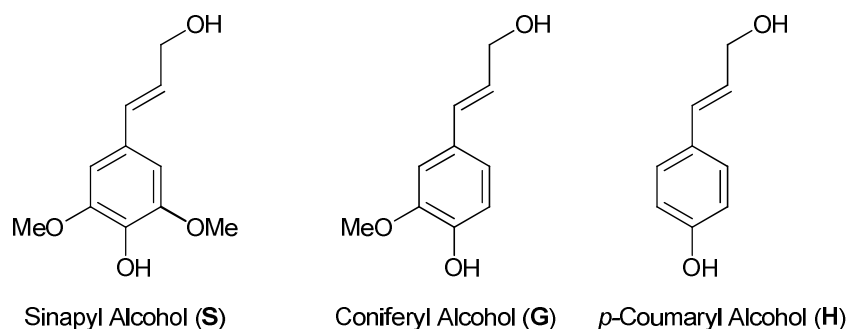


Figure 1.4: The three monolignols, lignin building blocks.

Lignin monomers are predominantly linked by either C-C or C-O bonds⁸, producing a variety of linkages. The most recurring lignin linkage motifs are depicted in Figure 1.5:

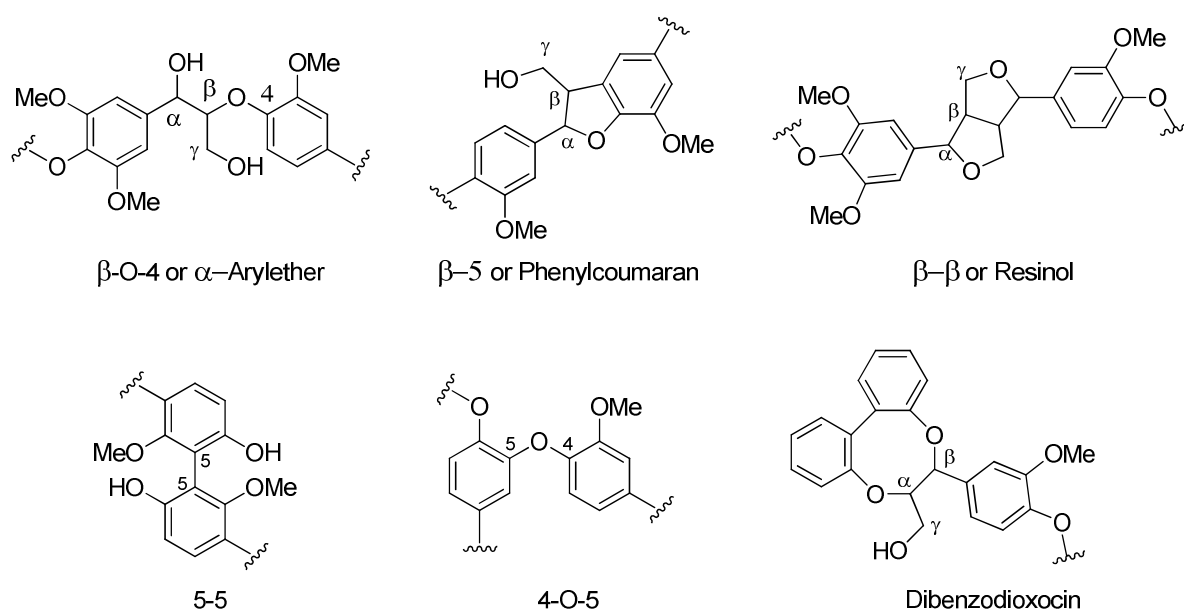


Figure 1.5: Most abundant lignin linkage motifs.

Among the different linkages that characterize lignin, the most abundant is by far the β -O-4 linkage that accounts for 45-60 % of all linkages, with phenylcoumaran, resinol and 5,5 present in significant but less abundant quantities¹. Typical proportions of these linkages in lignin are listed in table 1.1. These data, however, can vary considerably even for the same plant species due to growing environment, area and also analysis methods²⁴.

²⁴ Manara, P.; Zabanitout, A.; Vanderghem, C.; Richel, A.; *Catal. Today* **2014**, 223, 25.

Table 1.1: Linkages distribution in different lignins²⁵.

Linkage	Abundance (%)	
	Softwood	Hardwood
β -O-4	43-50	50-65
5-5	10-25	4-10
β -5	9-12	4-6
4-O-5	4	6-7
Dibenzodioxocin	5-7	1-2
β - β	2-4	3-7

With its unique structure, lignin can be regarded as the most abundant natural source of aromatic units, and therefore over the past few years the attention of research groups was paid in order to find an efficient depolymerization strategy that can eventually lead to the production of valuable aromatic compounds²². However, due to the structural complexity, poor solubility and chemical inertness, the development of an efficient depolymerization strategy still remains a challenge. In absence of any chemical processing technology, lignin is currently treated as a waste product from pulp and paper industry, or it simply burnt in order to supply energy²⁶. It would be therefore desirable to develop a sustainable lignin conversion chemistry that preserves its aromatic structure, according to the carbon-neutral biorefinery concept outlined in section 1.1²⁷. Moreover, since β -O-4 bonds represent the most abundant linkage, lignin depolymerization strategies should be targeted mostly on that kind of bond.

1.3 Lignin Pretreatments

In order to obtain high value-added chemicals from lignin depolymerization, a first separation step of lignin from lignocellulosic biomass must be considered. This critical step called “pulping” involves the mechanochemical separation of raw biomass into two fractions, one consisting of cellulose and hemicellulose that takes into account about 60-75 % of biomass by weight, and the other consisting of lignin¹. Currently, this process can be performed in several ways: physical (ball milling, etc.), organosolv processes, chemical (acidic, alkaline, etc.), and biological (using predominantly fungi)²⁸.

²⁵ a) Evtuguin, D. V.; Neto, C. P.; Silva, A. M. S.; Domingues, P. M.; Amado, F. M. L.; Robert, D.; Faix, O.; *J. Agric. Food Chem.* **2001**, 49, 4252. b) Rodrigues Pinto, P. C.; da Silva, E. A. B.; Rodrigues, A. E.; *Ind. Eng. Chem. Res.* **2011**, 50, 741.

²⁶ Sanderson, K.; *Nature*, **2011**, 474, S12–S14.

²⁷ Clark, J. H.; Luque, R.; Matharu, A. S.; *Annu. Rev. Chem. Biomol. Eng.* **2012**, 3, 183.

²⁸ da Costa Sousa, L.; Chundawat, S. P.; Balan, V.; Dale, B. E.; *Curr. Opin. Biotechnol.* **2009**, 20, 339.

However, each of these so called “lignin pretreatments” give rise to considerable structural modifications of lignin, yielding a very irregular complex polymer. Nowadays, commercially available lignin is mainly produced as a waste product from paper industry²⁹, since the most recurring pretreatments are meant to maximize the amount of recovered cellulose, rather than preserving the native structure of lignin. The most common preprocessing is Kraft pulping³⁰ in which large amounts of NaOH and Na₂S at high temperatures (165-175 °C) are used to cleave the ester bonds between cellulose and lignin, producing a black liquor rich in lignin, which can be obtained from precipitation at low pH. Under these harsh conditions, lignin undergoes structural rearrangements, displacement of aryl ethers with sulfides, promoting C-O and C-C cleavage¹. β-O-4 bonds are broken during this process, and repolymerization with cross condensation, oxidative coupling of guaiacyl moieties and radical cross couplings can occur. The resulting Kraft lignin (Figure 1.6) is generally a highly intractable and recalcitrant hydrophobic polymer with lower molecular weight with respect to native lignin and it becomes unsuitable to undergo further processing, despite its low price and wide availability.

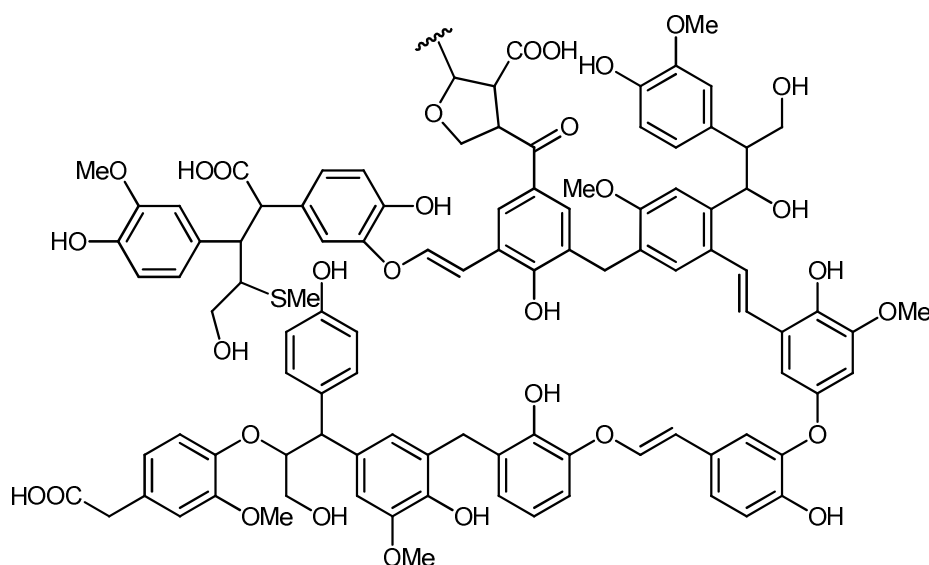


Figure 1.6: Kraft lignin structure³¹.

Another treatment used in paper industry is sulfite pulping, that yields liginosulfonates from the wood³². The process consists of cooking wood in aqueous sulfite solution (HSO₃⁻ or SO₃²⁻) at 125-150 °C for 3-7 h¹⁷. Liginosulfonates are soluble in water from pH = 2 to pH = 12, in organic solvents, and exhibit also a higher molecular weight than Kraft lignin.

²⁹ Bajpai, P.; Biorefinery in the Pulp and Paper Industry, London, UK: Academic Press (2013).

³⁰ a) Gierer, J.; *Wood Sci. Technol.* **1980**, 14, 241. b) Xiao, B.; Sun, X. F.; Sun, R. C.; *Polym. Degrad. Stab.* **2001**, 74, 307. c) Martin-Sampedro, R.; Santos, J. I.; Fillat, U.; Wicklein, B.; Eugenio, M. E.; Ibarra, D.; *Int. J. Biol. Macromol.* **2019**, 126, 18.

³¹ a) Lange, H.; Decina, D.; Crestini, C.; *Eur. Polym. J.* **2013**, 49, 1151. b) Crestini, C.; Lange, H.; Sette, M.; Argyropoulos, D. S.; *Green Chem.* **2017**, 19, 4104.

³² a) Cui, F.; Wijesekera, T.; Dolphin, D.; Farrell, R.; Skerker, P.; *J. Biotechnol.* **1993**, 30, 15. b) Liu, C.; Xu, J.; Hu, J.; Zhang, H.; Xiao, R.; *Chem. Eng. Technol.* **2017**, 40, 1092.

Currently, lignosulfonates are used in the production of binders, surfactants, lubricants and emulsifiers³³. However, the very high sulfur content (up to 8 %) makes lignosulfonates unusable for catalytic valorization³⁴. A milder delignification process is organosolv treatment, which consists in pulping lignocellulosic biomass with organic solvents (EtOH, MeOH etc.) and water at temperatures of about 180-200°C³⁵. The most successful treatment is Alcell Process, in which wood is extracted with a mixture of ethanol and water (1:1 v/v)³⁶ at 200 °C under a pressure of 35 bar. This process allows to obtain a very good separation between lignin and hemicellulose fractions which remain in the solution, and cellulose, which can be obtained in high-purity fibers³⁷. Lignol Energy Corporation modified this pretreatment with an integrated process involving solvent pretreatment of lignocellulosic biomass, saccharification and fermentation³⁸. This process could afford high-quality lignin with a broad range of potential applications³⁹. Moreover, organosolv lignin is characterized also by a lower sulfur content with respect to Kraft lignin or lignosulfonates, a feature that can prevent poisoning of catalysts for further processing. As regards structural modification, it has been demonstrated that technical lignin afforded by organosolv pretreatment retains the majority of β-arylether linkages. Generally speaking, organosolv pretreatment is considered an environmentally friendly process though it suffers from the high costs of solvent recovery³⁴. Unfortunately, organosolv processes still remain non-commercial. One extraction technique used to isolate lignin with little structural changes is extraction of ball milled wood with 9:1 dioxane:water volume ratio⁴⁰. This so-called Björkman process⁴¹ allows to obtain milled wood lignin (MWL), whose structure is considered to be one of the most similar to that of untreated lignin because of mild extraction conditions and the neutral solvent used, although MWL does not represent the whole lignin because of possible depolymerization during extensive milling or the low extraction yield (25-50 %)⁴². Another non-commercial lignin pretreatment that is worth noting is steam explosion. This technique involves the impregnation of lignocellulosic biomass with high-pressure steam (13 – 34 bar, 180 – 230 °C) for short contact times (1-20 min) in an autoclave reactor, followed by a rapid pressure release and an extraction with diluted NaOH or organic solvents⁴³.

³³ a) Knözinger, H. & Kochloefl, K. *Ullmann's Encyclopedia of Industrial Chemistry*. Wiley-VCH (2003). b) Tejado, A.; Peña, C.; Labidi, J.; Echeverria, J. M.; Mondragon, I.; *Bioresour. Technol.* **2007**, 98, 1655.

³⁴ Bozell, J. J.; Holladay, J. E.; Johnson, D.; White, J. F.; Top Value-Added Candidates from Biomass, Volume II: Results of Screening for Potential Candidates from Biorefinery Lignin; Pacific Northwest National Laboratory: Richland, WA, (2007).

³⁵ a) Liu, C.; Hu, J.; Zhang, H.; Xiao, R.; *Fuel* **2016**, 182, 864. b) Yao, L.; Chen, C. X.; Yoo, C. G.; Meng, X. Z.; Li, M.; Pu, Y. Q.; Ragauskas, A. J.; Dong, C. Y.; Yang, H. T.; *ACS Sust. Chem. Eng.* **2018**, 6, 14767.

³⁶ Pye, E. K.; Lora, J. H.; *Tappi J.* **1991**, 74, 113.

³⁷ a) Kleinert, T. Tayenthal, K. V.; *Angew. Chem.* **1931**, 44, 788.

³⁸ Rinaldi, R.; Jastrzebski, R.; Clough, M. T.; Ralph, J.; Kennema, M.; Bruijninx, P. C. A.; Weckhuysen B. M.; *Angew. Chem. Int. Ed.* **2016**, 55, 8164.

³⁹ a) Michels, J.; Wagemann, K.; *Biofuels Bioprod. Biorefin.* **2010**, 4, 263. b) Viell, J.; Harwardt, A.; Seiler, J.; Marquardt, W.; *Bioresour. Technol.* **2013**, 150, 89.

⁴⁰ Guerra, A.; Filipponen, I.; Lucia, L. A.; Argyropoulos, D. S.; *J. Agr. Food Chem.* **2006**, 54, 9696.

⁴¹ Björkman, A.; *Nature* **1954**, 174, 1057.

⁴² Hu, Z.; Yeh, T. F.; Chang, H. M.; Matsumoto, Y.; Kadla, J. F.; *Holzforschung* **2006**, 60, 389.

⁴³ Avellar, B. C.; Glassier, W. G.; *Biomass and Bioenergy* **1998**, 14, 205.

The process allows the separation of the individual biomass components. The resulting steam exploded lignin is characterized by a low content of carbohydrate impurities and a structure that resembles native lignin more than all the other pretreatments, since the chemical modification of lignin structure under these conditions is quite limited. The main drawbacks of this pretreatment are the low pulp yield and the high cost, which make this process not commercialized yet⁴⁴. In this thesis, aerobic catalytic oxidation of steam exploded sugarcane bagasse lignin was studied, as described in *Chapter 4*.

1.4 Lignin Depolymerization Strategies

Over the past few years, interest in the production of value-added chemicals, alternative fuels and platform compounds from lignin depolymerization has grown rapidly, since it can represent a more sustainable alternative to the petrochemical industry⁴⁵. However, the complexity of lignin structure makes its depolymerization very challenging⁴⁶. An ideal depolymerization process should indeed be able to selectively degrade lignin into monomeric high value products and the catalyst should be tolerant towards all the functional groups found in lignin, react selectively and resist to deactivation¹. In the last decades, several thermochemical transformation strategies have been developed in order to convert lignin into value-added products⁴⁷, including combustion, gasification, liquefaction, and pyrolysis (Figure 1.7).

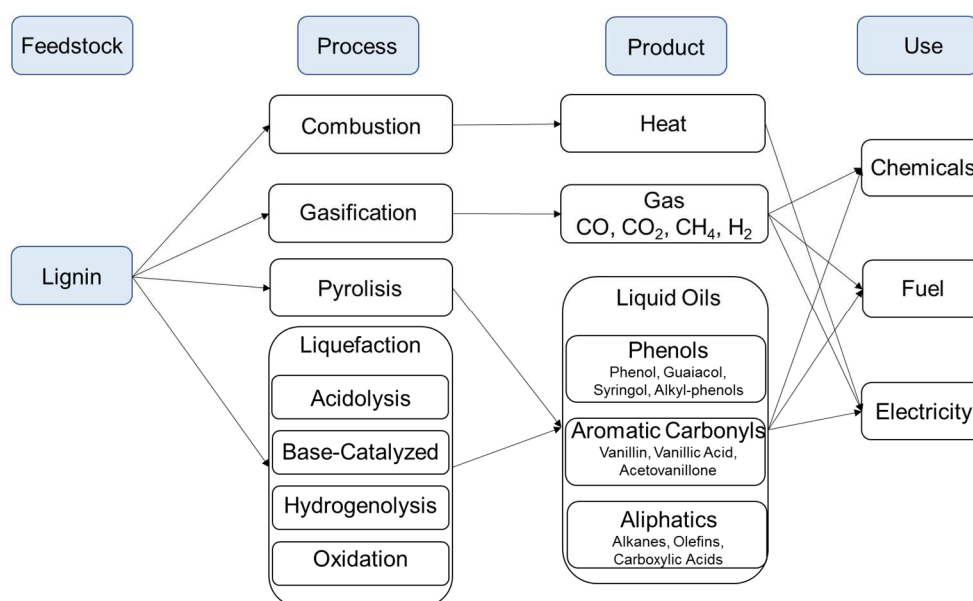


Figure 1.7: Schematic diagram of lignin conversion strategies, potential products and further use.

Adapted with permission from ref. 6, Copyright 2019, Elsevier.

⁴⁴ a) Tanahashi, M.; Tamabuchi, K.; Goto, T.; Aoki, T.; Karina, M.; Higuchi, T.; *Wood Res.* **1988**, 75, 1. b) Dahlmann, G.; Schroeter, M. C.; *Tappi J.* **1990**, 73, 237.

⁴⁵ Gasser, C. A.; Hommes, G.; Schaffer, A.; Corvini, P. F. X.; *Appl. Microbiol. Biotechnol.* **2012**, 95, 1115.

⁴⁶ a) Beckham, R. A. J.; Bidy, G. T.; Chandra, M. J.; Chen, R.; Davis, F.; Davison, M. F.; Dixon, B. H.; Gilna, R.; Keller, P.; Langan, M.; Naskar, P.; Saddler, A. K.; Tschaplinski, J. N.; Tuskan, T. J.; Wyman, G.; Wyman, C. E.; *Science* **2014**, 344, 1246843. b) Chatel, G.; Rogers, R. D.; *ACS Sust. Chem. Eng.* **2014**, 2, 322. c) Jia, S.; Cox, B. J.; Guo, X.; Zhang, Z. C.; Ekerdt, J. G.; *ChemSusChem* **2010**, 3, 1078.

⁴⁷ Pandey, M. P.; Kim, C. S.; *Chem. Eng. Technol.* **2011**, 34, 29.

Lignin gasification is carried out using supercritical water (374 °C, 218 atm), and it is used to produce syngas (CO + H₂), which can be used in production of chemicals. Currently, biomass gasifiers are still in development⁸.

Pyrolysis consists of rapid heating of biomass at temperatures between 450 and 600 °C, under an anaerobic environment. This treatment decomposes biomass into lower molecular weight compounds such as gases, liquid oils and solid char⁴⁸. Pyrolysis with rapid heating (> 100 °C / s) have received a great attention because it produces the highest yield of pyrolysis oil or bio-oil⁴⁹. The composition of bio oil includes hydroxyaldehydes, hydroxyketones, sugars and dehydrosugars, carboxylic acids and phenolic compounds, such as monolignols, guaiacol, catechol or eugenol⁵⁰. The addition of a zeolite catalyst allows to control the product distribution to valuable hydrocarbon compounds, exerting a double effect: the acid sites catalyze lignin depolymerization into more desirable and stable products, whereas the small volume inside pores prevents repolymerization and char formation⁵¹. One main drawback of this process is the low yield of liquid hydrocarbon products (below 30 % w/w). Moreover, the char formed during lignin pyrolysis inside zeolites can cause catalyst deactivation by blocking the pores or active site poisoning. Incorporation of cerium slightly decreased coke formation and shifted the products from BTX to valuable oxygenated chemicals (furans, aldehydes, ketones)⁵². Bio-oil is a potential feedstock or making liquid fuels, although it is an emulsion of several phases with low pH, low energy density and high viscosity, and must be upgraded in order to be employed as a fuel, by decreasing the oxygen / carbon ratio and increasing the overall carbon yield⁸.

Liquefaction can achieve a more target-oriented lignin depolymerization⁶. In particular, base-catalyzed depolymerization employs very cheap reagents such as NaOH, KOH or LiOH⁸, and targets mainly β -O-4 bonds cleavage, since is one of the weakest bonds in lignin, rather than the most abundant⁵³. Recently, Bolm and co-workers developed a solvent-free ball milling process in the presence of solid ^tBuONa or NaOH (3.5 equiv.) for lignin depolymerization. Importantly, they were able to obtain 55-76 % cleavage of β -O-4 linkages of untreated organosolv lignin or even naturally dried beech wood⁵⁴. Although this solvent-free strategy is considered environmentally benign, the amount of base is too large to be used in large scales. Also, in acid-catalyzed delignification of lignocellulosic biomass the hydrolytic cleavage of β -O-4 bond plays a predominant role⁵⁵. In the past years, both mineral acids and Lewis acids have successfully been used for this kind of reaction. Ekerdt et al used phenolic and non-phenolic β -O-4 models in DMSO with a catalytic amount of HCl.

⁴⁸ Goyal, H. B.; Seal, D.; Saxena, R. C.; *Renewable Sustainable Energy Rev.* **2008**, 12, 504.

⁴⁹ Windt, M.; Meier, D.; Marsman, J. H.; Heers, H. J.; de Konong, S.; *J. Anal. Appl. Pyrolysis* **2009**, 85, 38.

⁵⁰ Mohan, D.; Pittman, C. U.; Steele, P. H.; *Energy and Fuels* **2006**, 20, 848.

⁵¹ Ma, Z.; Troussard, E.; van Bockhoven, J. A.; *Appl. Catal. A* **2012**, 423-424, 130.

⁵² Neumann, G. T.; Hicks, J. C.; *ACS Catal.* **2012**, 2, 642.

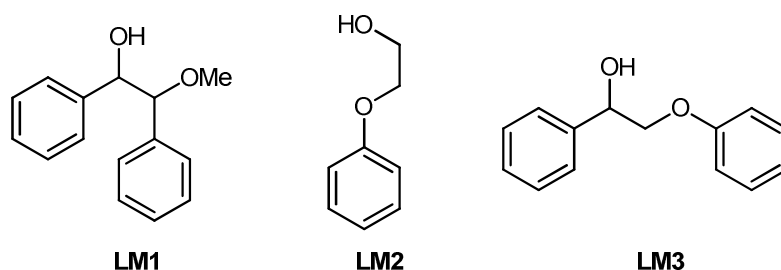
⁵³ Roberts, V. M.; Fendt, S.; Lemonidou, A.; Li, X.; Lercher, J. A.; *Appl. Catal. B* **2010**, 95, 71.

⁵⁴ Kleine, T.; Buendia, J.; Bolm, C.; *Green Chem.* **2013**, 15, 160.

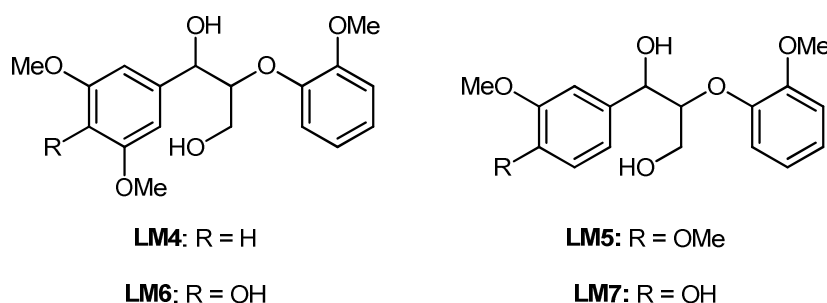
⁵⁵ Meshgini, M.; Sarkanen, K. V.; *Holzforschung* **1989**, 43, 239.

A moderate guaiacol yield was obtained (55%) with 100 % of substrate conversion⁵⁶. More recently, acidic ionic liquids (ILs) were used, since they bear the advantages of readily solubilizing lignin and favoring its depolymerization⁸. Ekerdt et al. employed [Hmim]Cl for the treatment of β -O-4 lignin models, which afforded guaiacol as the main product with a yield higher than 70 % at 150 °C⁵⁶. However, there are several challenges when using ILs including high cost, product separation and high viscosity.

In order to have a green sustainable strategy for lignin valorization, stoichiometric amounts of toxic reagents as well as expensive processes must be avoided. Therefore, catalysis should be used in order to overcome these problems⁵⁷. This thesis will be devoted to homogeneous catalysis, despite heterogeneous catalysis is very important in this field, because of the greater control in reaction selectivity and easier mechanistic studies. Up to now, many investigation studies employ lignin models rather than actual lignin. The most used models rely on β -O-4 bond, as this linkage is the most recurring in lignin⁵⁸. The simplest lignin models **LM** are 1,2-diphenyl-2-methoxyethanol **LM1**, 1,2-phenoxyethanol **LM2**, and 1-phenyl-2-phenoxyethanol **LM3**⁵⁹.



Other more complex models bearing a β -arylether bond are non-phenolic 1-(3,5-dimethoxyphenyl)-2-(methoxyphenoxy)-propane-1,3-diol **LM4** and 1-(3,4-dimethoxyphenyl)-2-(methoxyphenoxy)-propane-1,3-diol **LM5**⁶⁰ and phenolic 1-(4-hydroxy-3,5-dimethoxyphenyl)-2-(methoxyphenoxy)-propane-1,3-diol **LM6** 1-(3-hydroxy-4-methoxyphenyl)-2-(methoxyphenoxy)-propane-1,3-diol **LM7**.



⁵⁶ Jia, S.; Cox, B. J.; Guo, X.; Zhang, Z. C.; Ekerdt, J. G.; *ChemSusChem* **2010**, 3, 1078.

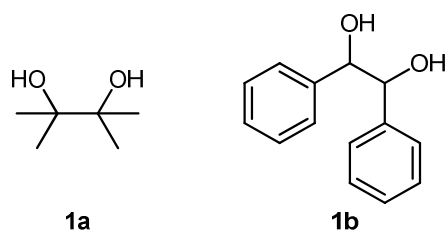
⁵⁷ Kusserow, B.; Schimpf, S.; Claus, P.; *Adv. Synth. Catal.* **2003**, 345, 289.

⁵⁸ a) Adler, E.; *Wood Sci. Technol.* **1977**, 11, 169. b) Sakakibara, A.; *Wood and Cellulose Chemistry*, Hon, D. N. S.; Shiraishi, N.; Marcel Dekker Inc.; New York, **1991**.

⁵⁹ a) Preti, L.; Attanasi, O. A.; Caselli, E.; Favi, G.; Ori, C.; Diavoli, P.; Felluga, F.; Prati, F.; *Eur. J. Org. Chem.* **2010**, 55, 4312. b) Corrie, J. E. T.; Lunazzi, L.; *J. Chem. Soc. Perkin Trans.* **1993**, 2, 1299.

⁶⁰ Cho, D. W.; Parthasarathi, R.; Pimentel, A. S.; Maestas, G. D.; Park, H. J.; Yoon, U. C.; Dunaway-Mariano, D.; Gnanakaran, S.; Langan, P.; Mariano, P. S. *J. Org. Chem.* **2010**, 75, 6549.

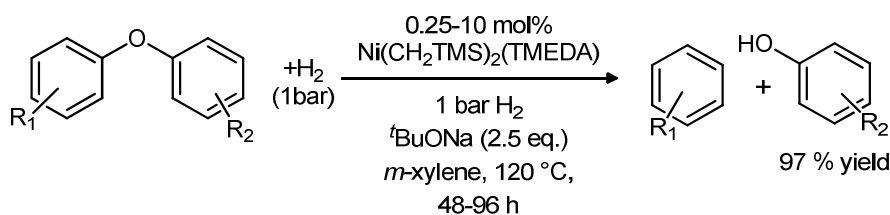
Finally, also vicinal diols such as pinacol **1a** and *meso*-hydrobenzoin **1b** can be considered important models for the investigation of lignin depolymerization, due to their simpler structure that facilitates catalyst optimization⁶¹.



Three main approaches have been exploited so far: oxidative, reductive and redox neutral depolymerizations.

1.4.1 Lignin Reductive Depolymerization Strategies

Since 1930 researchers were interested to find out how much hydrogen lignin could absorb, and the products obtained by lignin hydrogenation. The most common lignin reductive depolymerization methods are hydrogenation and selective hydrogenolysis. Whereas hydrogenation is a result of over-reduction and yields mainly cyclohexyl ether products, selective hydrogenolysis can convert lignin to valuable aromatics such as methoxylated phenols, benzylic alcohols and phenylpropanols. Nowadays, transition metal catalysis based on Ni and Pd for the activation of arene C-O bonds is the principal technique that allows selective lignin hydrogenolysis⁶². Swindell and co-workers first reported that a Ni catalyst, based on the precursor $[\text{Ni}(\text{PCy}_3)\text{Cl}_2]$ can insert into a C-O bond⁶³. Followed by this work, Hartwig et al. reported that $[\text{Ni}(\text{COD})_2]$ and $[\text{Ni}(\text{TMEDA})(\text{CH}_2\text{TMS})_2]$ are able to cleave C-O bonds of diaryl ethers, under 1 bar of H_2 affording high yields of phenols (Eq. 1.1)^{64a}. Later, the same research group showed that in a strong alkaline environment, $[\text{Ni}(\text{COD})_2]$ can form stable nanoparticles suitable for hydrogenation of aryl ethers under 1 atm of H_2 ^{64b}.



Eq. 1.1: Nickel catalyzed hydrogenolysis of aryl ethers.

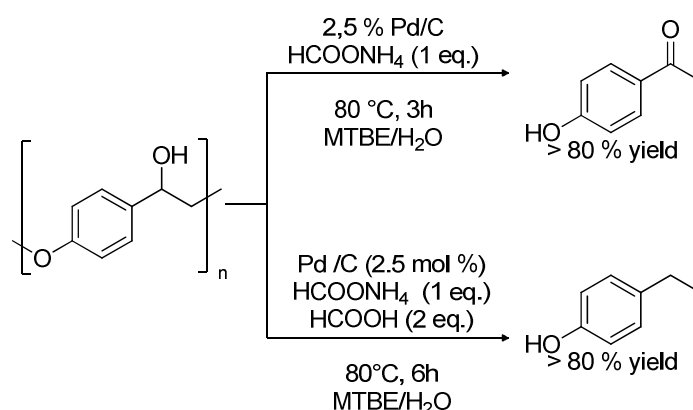
⁶¹ a) Castoldi, M. C. M.; Camara, L. D. T.; Aranda, D. A. G. *React. Kinet. Catal. Lett.* **2009**, 98, 83. b) Román-Leshkov, Y.; Barrett, C. J.; Liu, Z. Y.; Dumesic, J. A. *Nature* **2007**, 447, 982.

⁶² Das, A.; König, B.; *Green Chem.* **2018**, 20, 4844.

⁶³ Wenkert, E.; Michelotti, E. L.; Swindell, C. S.; *J. Am. Chem. Soc.* **1979**, 101, 2246.

⁶⁴ a) Sergeev, A. G.; Hartwig, J. F.; *Science* **2011**, 332, 439. b) Sergeev, A. G.; Webb, J. D.; Hartwig, J. F.; *J. Am. Chem. Soc.* **2012**, 134, 20226.

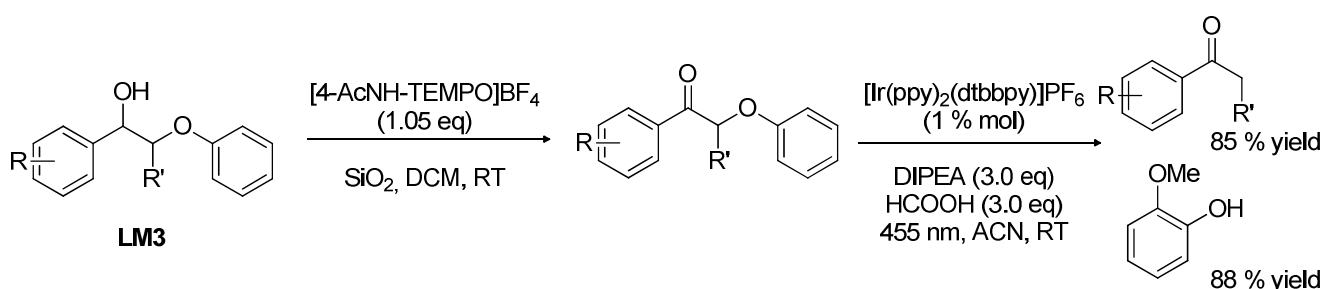
As regards β -O-4 lignin models, Samec et al, demonstrated that the reduction of a lignin model polymer could be performed also with Pd/C in presence of a stoichiometric equivalent of amine (Eq. 1.2)⁶⁵. Moreover, the use of formic acid as reductant afforded a better reduction if compared to H₂.



Eq 1.2: Heterogeneous Pd-catalyzed cleavage of β -O-4 models.

Although Ni and Pd are the most used catalytic systems for lignin reductive depolymerization, other transition metal complexes namely, [Ti(Cp)₂(OTf)₂]⁶⁶ and [Fe(acac)₃]⁶⁷ have been effectively employed for β -O-4 bond cleavage. However, the formation of several side products, catalyst deactivation and low TONs led to the research for alternative catalytic systems⁶².

Other reductive depolymerization strategies involve the use of photocatalysis, which occurs at RT, is compatible with both aqueous and organic solvents and generally insensitive to oxygen and water¹. Stephenson et al. reported a photochemical strategy for C-O reductive cleavage of **LM3** and similar models at RT (Scheme 1.1)⁶⁸. In a first step, a benzylic oxidation of lignin models was performed with [4-AcNH-TEMPO]BF₄ (Bobbitt's Salt). Consequently, C-O bond was cleaved photochemically using [Ir(ppy)₂(dtbbpy)]PF₆ as catalyst, in presence of DIPEA and formic acid as additives under 455 nm light irradiation.



Scheme 1.1: Photocatalytic two-step lignin degradation strategy.

The reaction conditions are mild, and the system is tolerant for several functional groups. In this case, products deriving from both fragmentation sites were obtained in very high yields, more than

⁶⁵ a) Galkin, M. V.; Sawadjoon, S.; Rodhe, V.; Dawange, M.; Samec, J. S. M.; *ChemCatChem* **2014**, 6, 179.

b) Galkin, M. V.; Samec, J. S. M.; *ChemSusChem* **2014**, 7, 2154.

⁶⁶ Desnoyer, A. N.; Fartel, B.; MacLeod, K. C.; Patrick, B. O.; Smith, K. M.; *Organometallics* **2012**, 31, 7625.

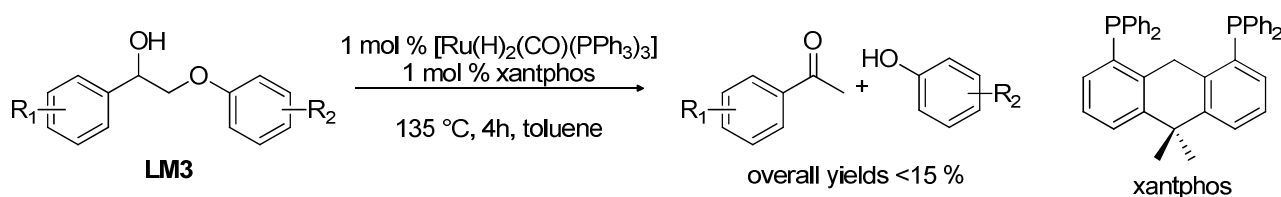
⁶⁷ Ren, Y.; Yan, M.; Wang, J.; Zhang, Z. C.; Yao, K.; *Angew. Chem. Int. Ed.* **2013**, 52, 12674.

⁶⁸ Nguyen, J.D.; Matsuura, B. S.; Stephenson, C. J.; *J. Am. Chem. Soc.* **2014**, 136, 1281.

80 %. The reaction was performed in flow, which resulted in higher efficiency achieved in lower reaction time⁶².

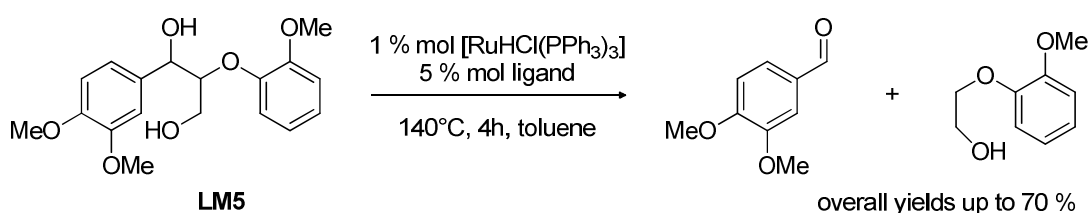
1.4.2 Lignin Redox-Neutral Depolymerization Strategies

Another lignin depolymerization strategy is redox-neutral conversion. In this process, which is considered the most atom economical one¹, the initial oxidation step is used to form reductive equivalents that are subsequently used to cleave C-O bond. The initial studies from Bergman, Ellman and co-workers showed that a catalyst synthesized in-situ from $[\text{Ru}(\text{H})_2(\text{CO})(\text{PPh}_3)_3]$ and xantphos can affect tandem catalytic dehydrogenation and C-O cleavage of **LM3** in a single step without the need of other additives (Eq. 1.3)⁶⁹.



Eq. 1.3: Tandem hydrogenolysis / dehydrogenation of **LM3**.

The major disadvantage of this technique is that the system is completely ineffective for γ -OH containing models (as in the case of compounds **LM4** and **LM5**), since they form a stable complex with Ru which results in catalyst deactivation. This drawback was overcome by Leitner and co-workers who reported a more active Ru-based complex for selective C-C bond cleavage of β -O-4 lignin model **LM5** (Eq. 1.4)⁷⁰. In this example, a Ru precursor, $[\text{Ru}(\text{COD})(\eta^3\text{-C}_4\text{H}_7)]$ in combination with a tripodal phosphine-based ligand acts as a very efficient catalyst in γ -OH containing lignin model substrates.



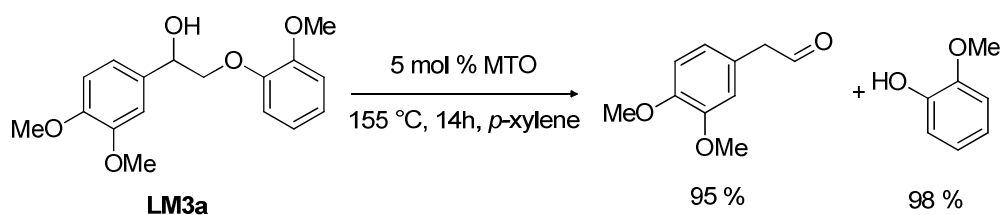
Eq. 1.4: Selective C-C bond cleavage using $[\text{RuHCl}(\text{PPh}_3)_3]$.

Several other transition metal systems have been developed for redox-neutral lignin model depolymerization. For example, it has also been reported that MTO can act as an effective catalyst for C-O cleavage of **LM3a** although the reaction takes place above 155°C to afford phenylacetaldehyde and guaiacol (Eq. 1.5)⁷¹.

⁶⁹ Nichols, J. M.; Bishop, L. M.; Bergman, R. G.; Ellman, J. A. *J. Am. Chem. Soc.* **2010**, 132, 12554.

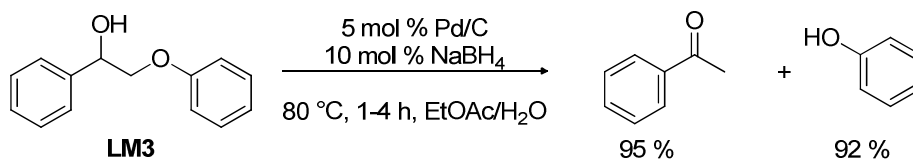
⁷⁰ a) vom Stein, T.; Weigand, T.; Merckens, C.; Klankermayer, J.; Leitner, W.; *ChemCatChem* **2013**, 5, 439. b) vom Stein, T.; den Hartog, J.; Buendia, S.; Stoychev, S.; Mottweiler, J.; Bolm, C.; Klankermayer, J.; Leitner, W.; *Angew. Chem. Int. Ed.* **2015**, 54, 5859.

⁷¹ Harms, R. G.; Markovits, I. I. E.; Drees, M.; Herrmann, W. A.; Cokoja, M.; Kuhn, F. E.; *ChemSusChem* **2014**, 7, 429.



Eq. 1.5: MTO catalyzed redox neutral cleavage of **LM3a**.

Samec and collaborators reported the use of Pd/C that can act as a heterogeneous catalyst for redox neutral cleavage of **LM3** (Eq. 1.6)⁷².



Eq. 1.6: Pd/C catalyzed redox neutral C-O cleavage of **LM3**.

Despite the high overall yields, it was found that this catalytic system was not applicable to more complex lignin models. The majority of the above-mentioned procedures suffer from the use of expensive transition metals with high loadings and usually require long reaction times in order to get a complete substrate conversion. With the concomitant requirement of superstoichiometric amount of additive, these strategies are impractical for a feasible application in a biorefinery.

1.4.3 Lignin Oxidative Depolymerization Strategies

The oxidative depolymerization of lignin is particularly interesting because it leads to the formation of highly valuable oxygen-containing compounds such as aromatic aldehydes, acids and their derivatives, like esters and anhydrides, which are of great significance in our daily life. These compounds are widely used as solvents, food additives, monomers for polymer production and cosmetics. There are several techniques that allow to achieve lignin oxidation, which can be divided in traditional techniques and advanced techniques for valuable platform chemicals⁶. These latter techniques will be described in more detail in *Chapter 3*. As regards traditional lignin oxidative depolymerization strategies, pulp bleaching is one form of lignin oxidation. It is composed by two steps, the first is an oxidative fragmentation and dissolution of residual lignin in pulp, and the second involves the oxidation of chromogenic groups such as quinones and conjugated side chains in residual lignin. The most efficient oxidant for pulp bleaching is chlorine, which produces Cl⁺ ions by heterolysis during the reaction. These cations then react by electrophilic substitution on partial electron-rich sites of aromatic rings, causing linkage cleavage of aliphatic side chains and subsequent fragmentation and dissolution of residual lignin. However, during this process, large amounts of organohalogenes are produced, placing an enormous burden to the environment, since

⁷² Galkin, M. V.; Dahlstrand, C.; Samec, J. S. M.; *ChemSusChem* **2015**, 8, 2187.

they dissolve in bleaching effluents and are difficult to be dealt with. In order to replace chlorine bleaching, elemental chlorine free bleaching technique has been developed. This strategy employs NaOCl as bleaching reagent for chromogenic groups of residual lignin, eventually degrading them into dicarboxylic acids⁷³. In order to get rid of the concerns caused by the use of halogens, a total chlorine free process has been developed. This strategy employs greener H₂O₂ or O₂ under basic conditions for lignin bleaching. In this environment, or with the aid of a metal catalyst, radicals such as OH[·], HOO[·] and superoxide radical anion (O₂^{·-}) are generated, with the purpose of destructing chromogenic groups. The reaction can be also performed with O₃ at low pH, in order to avoid decomposition caused by OH⁻ ions. Ozone is highly reactive with lignin residues, disrupting benzene rings into carboxylic acids and oxidizing double bonds in side chains, alcohols, ethers and aldehydes to carboxylic acids. However, due to high cost of O₃, high consumption and the decreased pulp strength after bleaching, this technique is not widely used in industries. The second most common lignin oxidative depolymerization technique is alkaline nitrobenzene oxidation, which breaks down the non-condensed side-chain linkages within lignin fragments, affording syringaldehyde, vanillin, 4-hydroxybenzaldehyde and their corresponding carboxylic acids⁷⁴. The ratios of yields of such compounds can represent to a certain extent the value of Syringyl:Guaiacyl:*p*-Hydroxyphenyl units ratio of native lignin⁷⁵. However, product yields and distributions are extensively affected by lignin structural properties and β-O-4 linkages content, and this method suffers from a very high toxicity of reagents. The last non-catalytic technique for lignin depolymerization is wet air oxidation. This procedure employs oxygen or air at high temperature and pressure. Typical conditions are a temperature of (180-315) °C, a pressure of (2-15) MPa and a residence time of (15-120) min⁷⁶. In this way, lignin is depolymerized into aliphatic carboxylic acids and aromatic aldehydes, such as vanillin, syringaldehyde and *p*-hydroxybenzaldehyde. This process is also used by Borregaard in Norway to produce vanillin from liginosulfonates, as reported previously¹¹, but is limited only to this process. Therefore, a catalytic version has been developed. Compared to traditional wet air oxidation, the catalytic one has lower energy requirements, better product yields and selectivity, shorter reaction times and the overcome of the limitation to use liginosulfonates as raw material. Currently, copper-based catalysts have demonstrated good performances in the production of aromatic aldehydes from lignin using this process⁷⁷. For example, Lee et al. obtained about 15 % yield of vanillin and syringaldehyde from the oxidation of diluted acid hydrolyzed lignin from

⁷³ Yang, S. H.; *Lignocellulosic Chemistry*, third ed., China Light Industry Press, Beijing, **2001**.

⁷⁴ Chen, C. L.; *Nitrobenzene and Cupric Oxide Oxidations: Methods in Lignin Chemistry*, Springer, **1992**.

⁷⁵ a) Prozil, S. O.; Evtuguin, D. V.; Silva, A. M.; Lopes, L. P.; *J. Agric. Food Chem.* **2014**, 62, 5420. b) Dou, J.; Kim, H.; Li, Y.; Padmakshan, D.; Yue, F.; Ralph, J.; Vuorinen, T.; *J. Agr. Food Chem.* **2018**, 66, 7294. c) Wang, Y.; Sun, S.; Li, F.; Cao, X.; Sun, R.; *Ind. Crop Prod.* **2018**, 116, 116.

⁷⁶ Luck, F.; *Catal. Today* **1999**, 53, 81.

⁷⁷ a) Santos, S. G.; Marques, A. P.; Lima, D. L. D.; Evtuguin, D. V.; Esteves, V. I.; *Ind. Eng. Chem. Res.* **2011**, 50, 291. b) Wu, G. X.; Hetiz, M.; Chornet, E.; *Ind. Eng. Chem. Res.* 1994, 33, 718.

Liriodendron tulipifera using Cu^{2+} as catalyst and Fe^{3+} as cocatalysts in catalytic wet air oxidation process⁷⁸.

1.5 Triphenolamines

In *Chapter 3* transition metal catalyzed lignin oxidative depolymerization is described in much detail. We will show also that, among first-row metals, Vanadium has gained much interest since its complexes are considered the most efficient catalysts up to now⁷⁹. In particular, stereoelectronic properties of ligands in the above-mentioned Vanadium complexes are considerably important in order to drive the reaction selectivity towards different products. Taken this into account, we decided to employ a series of V(V) compounds based on triphenolamines (TPA(R, R')) in aerobic oxidation of lignin models and lignin. TPAs are a class of molecules whose general structure is reported in Figure 1.8.

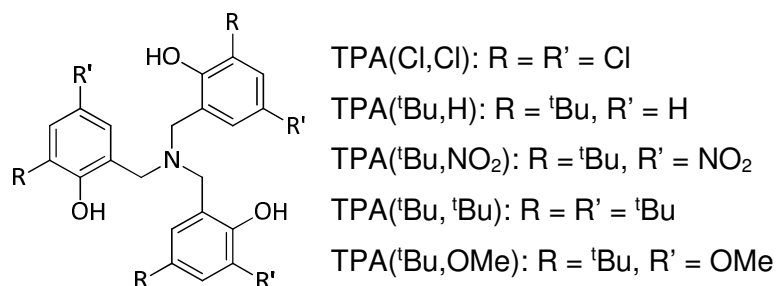
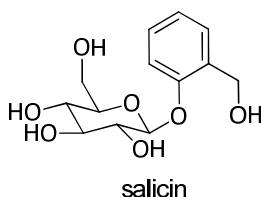


Figure 1.8: General structure of TPA(R, R').

TPAs structure is highly modular due to the ease of variation of *ortho*- and *para*- substituents to the phenolic moiety, which can impose remarkable changes into the system depending on steric encumbering and electronic demanding⁸⁰. The first example of TPA synthesis is dated to 1922, when salicin, a natural product consisting of a β -glycoside extracted from willow bark, was converted to the corresponding benzyl bromide and reacted with ammonia⁸¹.



Nowadays there are three ways to synthesize TPAs⁸²: the first is a Mannich reaction between a 2,4-disubstituted phenol and hexamethylenetetramine (HMTA) (Scheme 1.2)⁸³.

⁷⁸ Xiang, Q.; Lee, Y. Y.; *Appl. Biochem. Biotechnol.* **2001**, 91-93, 71.

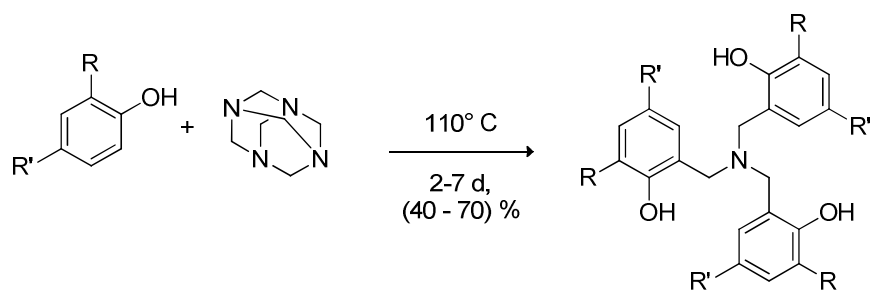
⁷⁹ a) Hanson, S. K.; Baker, R. T.; *Acc. Chem. Res.* **2015**, 48, 2037. Amadio, E.; Di Lorenzo, R.; Zonta, C.; Licini, G.; *Coord. Chem. Rev.* **2015**, 301-302, 147.

⁸⁰ Licini, G.; Mba, M.; Zonta, C.; *Dalton Trans.* **2009**, 5265.

⁸¹ Zemplen, G.; Kunz, A.; *Chem. Ber.* **1922**, 55, 979.

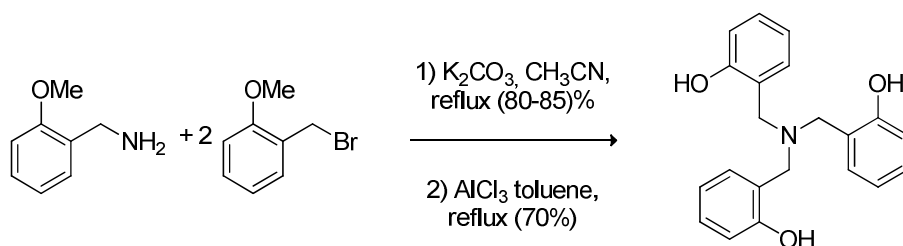
⁸² Hultsch, K.; *Chem. Ber.* **1949**, 82, 16.

⁸³ Chandrasekan, A.; Day, R. O.; Holmes, R. R.; *J. Am. Chem. Soc.* **2000**, 122, 1066.



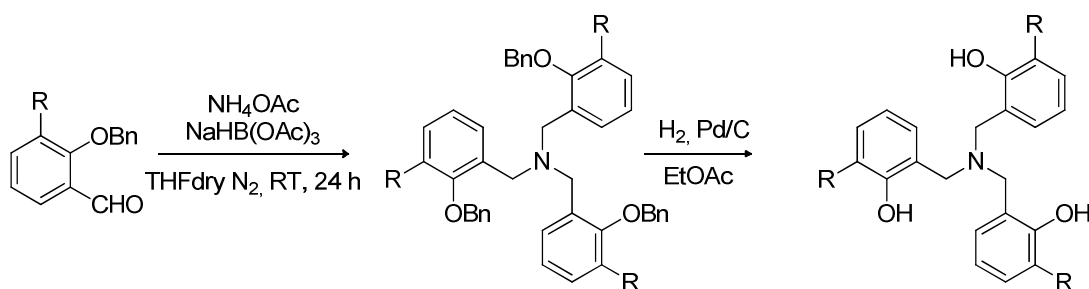
Scheme 1.2: Synthesis of TPAs via Mannich reaction.

The method can be used only for *ortho*, *para*-disubstituted phenols. This reaction has many advantages, it is a one-pot reaction and it occurs in neat conditions, thus avoiding solvent waste. The drawbacks are the very long reaction time, up to two weeks, and harsh reaction conditions that must be applied. The second method of TPAs synthesis is a nucleophilic substitution reaction between 2-methoxybenzylamine and two equivalents of 2-methoxybenzyl bromide (Scheme 1.3)⁸⁴.



Scheme 1.3: Synthesis of TPAs via S_N2.

This reaction requires the independent synthesis of the two partners, which offers the possibility to synthesise asymmetric TPAs, but it is less practical for the synthesis of symmetric ligands. Moreover, phenolic groups must be protected in order to afford reasonable yields. The third method has been developed in our research group. This consist of a three-fold reductive amination from *ortho*-substituted salicyl aldehydes, using NH₄OAc as nitrogen source, and NaHB(OAc)₃ as reducing agent (Scheme 1.4)⁸⁵.



Scheme 1.4: Synthesis of TPAs via three-fold reductive amination.

Salicyl aldehydes, which can come from commercial sources, or synthesised from phenol precursors, are protected as benzyl ethers, which are removed in the final step via hydrogenolysis.

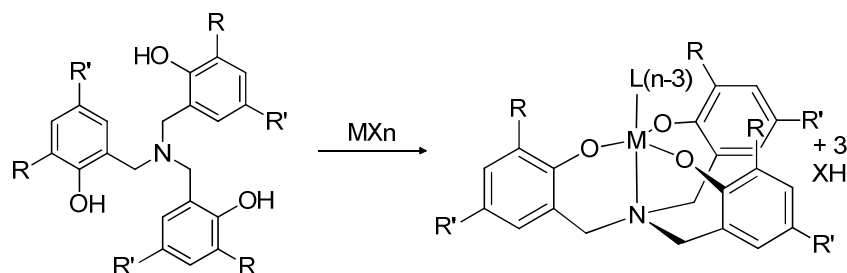
⁸⁴ Hwang, J., Govindaswamy, K., Koch, S. A., *Chem. Comm.* **1998**, 1667.

⁸⁵ Prins, L. J.; Mba Blázquez, M.; Kolarović, A.; Licini, G.; *Tetrahedron* **2006**, 47, 2735.

Moreover, these protecting groups facilitate the crystallisation of intermediates and their purification. This method allows to obtain *ortho*-substituted TPAs by using mild reaction conditions, low reaction times and good yields and purity of the products. Furthermore, starting materials cheapness and availability, together with easy synthetic steps, allow to prepare these C_3 symmetric ligands in gram scale.

1.6 Coordination Chemistry of TPAs

TPAs usually coordinate to metal centers M as tetradentate ligands, with three anionic oxygen atoms occupying equatorial positions and the nitrogen atom occupying one of the axial positions, generating very stable compounds (Eq. 1.7). Generally, the metal centre is positioned slightly above the plane defined by phenolate groups.



Eq. 1.7: Coordination of TPAs with a generic metal ion M.

Aminotriphenolate complexes show generally a trigonal bipyramidal (TBP) structure with C_3 symmetry or an octahedral structure (OCT), while the trigonal monopyramidal structure (TMP) is less observed (Figure 1.9). The geometry can be easily controlled and modulated by variation of *ortho*- and *para*- substituents. *Ortho*- groups to phenol oxygen (R) are in close proximity with metals and therefore there is an influence on steric properties of complexes. *Para*- groups (R'), on the other hand, can modify the electronic properties of ligands without affecting the steric demand. This position can be also used as anchoring site in order to obtain further functionalisation of these molecules.

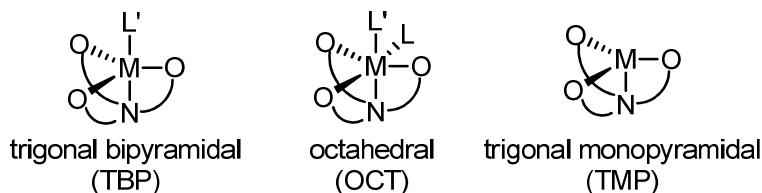


Figure 1.9: Main geometries of aminotriphenolate complexes.

These complexes are characterised by a *propeller-like* shape of the ligand around the metal, when viewed along the metal-nitrogen axis. Even if TPAs are not chiral, coordination to metal furnishes two enantiomeric complexes (Figure 1.10), one laevorotatory (M or Λ) and the other dextrorotatory (P or Δ). At RT, interconversion between the two enantiomers is very rapid, so their resolution is not feasible.

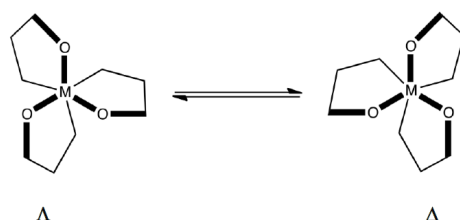


Figure 1.10: Clockwise (Δ) and counter-clockwise (Λ) enantiomeric configurations of TPA complexes.

The donor interaction of nitrogen with the metal, increases electron density on the latter, but it causes also the polarisation of all the bonds, resulting in bond lengthening and therefore in a net increase in metal Lewis acidity⁸⁶. Numerous examples of aminotriphenolate complexes can be found in literature for transition metals (d^0 , d^5 , d^6 and d^7), such as Ti(IV)⁸⁷, Zr(IV)⁸⁸, Fe(III)⁸⁹, Ta(V)⁹⁰, V(V)⁹¹, Co(II) and Co(III)⁹², Mo(VI)⁹³ and for main group elements (Al(III)⁹⁴, Ga(III), In(III)⁹⁵, Si(IV)⁹⁶, P(V)⁹⁷).

⁸⁶ Denmark, S. E.; Beutner, G. L.; Wynn, T.; Eastgate, M. D.; *J. Am. Chem. Soc.* **2005**, 127, 3774.

⁸⁷ a) Bull, S. D.; Davidson, M. G.; Johnson, A. L.; Robinson, D. E. J. E.; Mahon, M. F.; *Chem. Commun.* **2003**, 1750. b) Kol, M.; Shamis, M.; Goldberg, I.; Goldschmidt, Z.; Alfi, S.; Hayut-Salant, E.; *Inorg. Chem. Commun.* **2001**, 4, 177. c) Michalczyk, L.; de Gala, S.; Bruno, J. W.; *Organometallics* **2001**, 20, 5547. d) Kim, Y.; Verdake, J. G.; *Organometallics* **2002**, 21, 2395. e) Kim, Y.; Jnaneshwara, G. K.; Verdake, J. G.; *Inorg. Chem.* **2003**, 42, 1437. f) Wang, W.; Fujiki, M.; Nomura, K.; *Macromol. Rapid. Commun.* **2004**, 25, 504. g) Ugrinova, V.; Ellis, G. A.; Brown, S. N.; *Chem. Commun.* **2004**, 468. h) Fortner, K. C.; Bigi, J. P.; Brown, S. N.; *Inorg. Chem.* **2005**, 44, 2803. i) Kim, Y.; Verdake, J. G.; *Phosphorus, Sulfur Silicon, Relat. Elem.* **2004**, 179, 729. j) Mba, M.; Prins, L. J.; Zonta, C.; Cametti, M.; Valonen, A.; Rissanen, K.; *Dalton Trans.* **2010**, 39, 7384. k) Bernardinelli, G.; Seidel, T. M.; Kündig, E. P.; Prins, L. J.; Kolarovic, A.; Mba, M.; Pontini, M.; Licini, G.; *Dalton Trans.* **2007**, 36, 1573. l) Zonta, C.; Cazzola, E.; Mba, M.; Licini, G.; *Adv. Synth. Catal.* **2008**, 350, 2503.

⁸⁸ Davidson, M. G.; Doherty, C.L.; Johnson, A. L.; Mahon, M. F.; *Chem. Commun.* **2003**, 1832.

⁸⁹ a) Hwang, J.; Govindaswamy, K.; Koch, S. A.; *Chem. Commun.* **1998**, 1667. b) Whiteoak, C. J.; Gjoka, B.; Martin, E.; Mart, M.; Escudero-Adàn, E. C.; Zonta, C.; Licini, G.; Kleij, A. W.; *Inorg. Chem.* **2012**, 51, 10639.

⁹⁰ a) Groysman, S.; Segal, S.; Goldberg, I.; Kol, M.; Goldschmidt, Z.; *Inorg. Chem. Commun.* **2004**, 7, 938. b) Groysman, S.; Segal, S.; Shamis, M.; Goldberg, I.; Kol, M.; Goldschmidt, Z.; Hayut-Salant, E. J.; *Chem. Soc.-Dalton Trans.* **2002**, 3425. c) Kim, Y. J.; Kapoor, P. N.; Verdake, J. G.; *Inorg. Chem.* **2002**, 41, 4834.

⁹¹ a) Groysman, S.; Goldberg, I.; Goldschmidt, Z.; Kol, M.; *Inorg. Chem.* **2005**, 44, 5073. b) Mba, M.; Pontini, M.; Lovat, S.; Zonta, C.; Bernardinelli, G.; Kündig, E.P.; Licini, G.; *Inorg. Chem.* **2008**, 47, 8616.

⁹² Martin, C.; Whiteoak, C. J.; Martin, E.; Escudero-Adàn, E. C. Galàn-Mascaròs, J. R.; Kleij, A. W.; *Inorg. Chem.* **2014**, 53, 11675.

⁹³ Romano, F.; Linden, A.; Mba, M.; Zonta, C.; Licini, G.; *Adv. Synth. Catal.* **2010**, 352, 2937.

⁹⁴ a) Kim, Y.; Verdake, J. G.; *Inorg. Chem.* **2003**, 42, 4804. b) Whiteoak, C. J.; Kielland, N.; Laserna, V.; Escudero-Adàn, E. C.; Martin, E.; Kleij, A. W.; *J. Am. Chem. Soc.* **2013**, 135, 1228.

⁹⁵ Motekaitis, R.; Martell, A. E.; Koch, S. A.; Hwang, J.; Quarless, D. A. Jr.; Welch, M. J.; *Inorg. Chem.* **1998**, 37, 5902.

⁹⁶ a) Timosheva, N. V.; Chandrasekaran, A.; Day, R. O.; Holmes, R. R.; *Organometallics* **2001**, 20, 2331. b) Timosheva, N. V.; Chandrasekaran, A.; Day, R. O.; Holmes, R. R.; *Organometallics* **2000**, 19, 5614.

⁹⁷ Timosheva, N. V.; Chandrasekaran, A.; Day, R. O.; Holmes, R. R.; *J. Am. Chem. Soc.* **2002**, 124, 7035.

1.7 Vanadium (V) Aminotriphenolate Complexes VO-TPA(R, R')

As regards coordination with V(V), TPAs provide a “natural-like” environment for this metal, since their TBP coordination geometry resembles the active center in Vanadium dependent haloperoxidases, a class of enzymes found in some seaweeds or terrestrial fungi, in which a Vanadium center is surrounded by three equatorial oxygen donors, and axial oxygen and nitrogen atoms (histidine residue) (Figure 1.11)⁹⁸

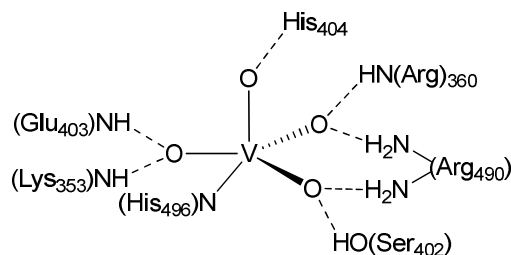
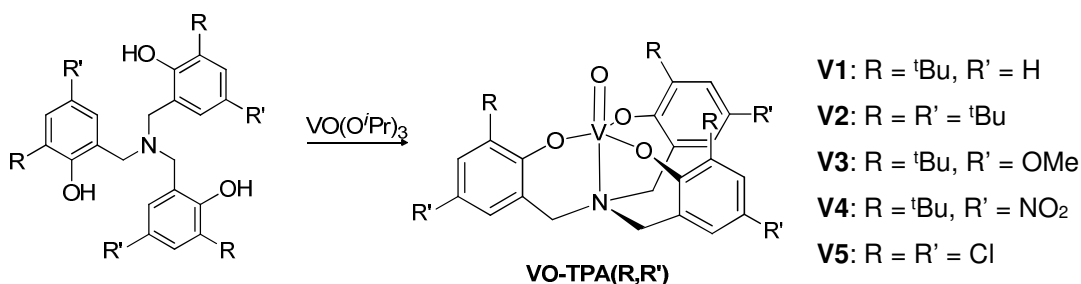


Figure 1.11: Structure of the active site of Vanadium haloperoxidase.

The first example of V(V) Aminotriphenolate complexes has been reported by Kol et al., who obtained such compounds from the reaction between TPAs and metal precursor VO(OⁱPr)₃, according to Eq. 1.8.^{91a}



Eq. 1.8 Coordination of TPAs with VO(OⁱPr)₃.

Later on, our group reported the synthesis of **V1**^{91b}, and **V4**, employed as a dynamic chiral sensor⁹⁹. Complexes **V1-V4** show a TBP geometry, with the oxo group occupying the axial position *trans* to the TPA nitrogen, as shown by the X-Ray structure (Figure 1.12).

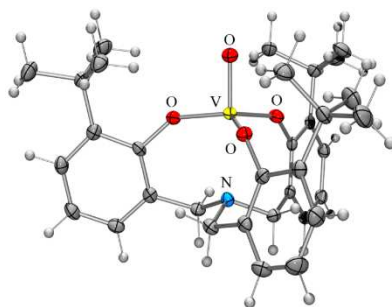


Figure 1.12: X-Ray structure of complex **V1**^{91b}.

⁹⁸ a) Vilter, H.; *Phytochemistry* **1984**, 23, 1387. b) Butler, A.; *Coord. Chem. Rev.* **1999**, 187, 17.

⁹⁹ Zardi, P.; Wurst, K.; Licini, G.; Zonta, C.; *J. Am. Chem. Soc.* **2017**, 139, 15616.

On the other hand, complex **V5** adopts an OCT geometry in which the equatorial position is occupied by a water molecule (Figure 1.13). In this case the ligand does not have a propeller-like arrangement around the metal.

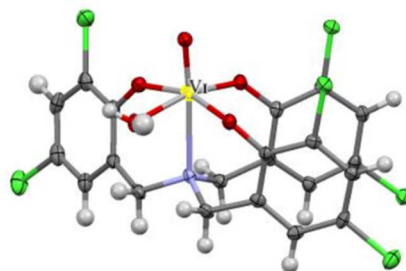


Figure 1.13: X-Ray structure of complex **V5**^{91a}.

The catalytic behavior of these complexes was first investigated by Kol et al. in the oxidation of styrene to styrene oxide, in the presence of ^tBuOOH as oxidant^{91a}. More recently, the catalytic studies of **VO-TPA(R,R')** were focused on sulfoxidations⁹³ and haloperoxidations^{91b}, affording in every case quantitative yields and high selectivity, TONs and TOFs. Besides the efficiency of vanadium aminotriphenolate complexes in oxidation reactions, these versatile species have also been successfully employed in CO₂ fixation for the synthesis of cyclic carbonates¹⁰⁰ (Figure 1.14)

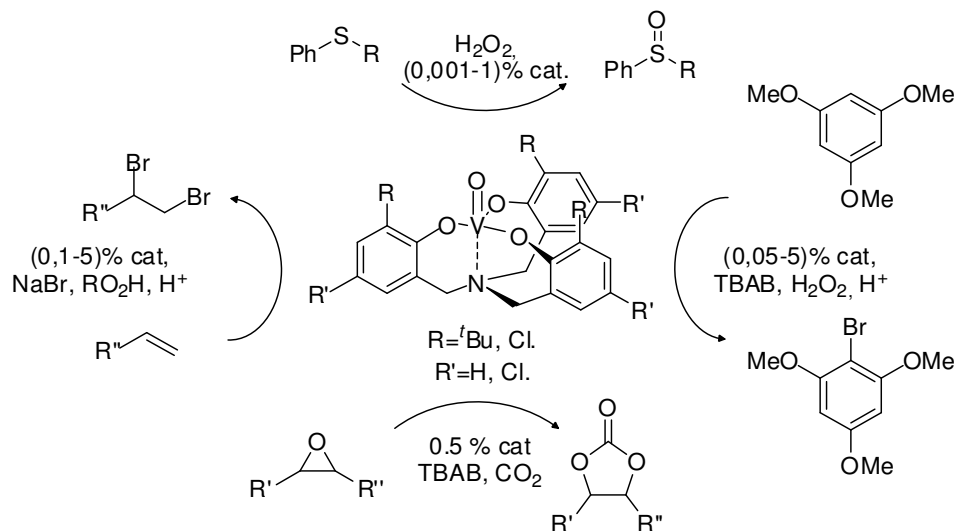


Figure 1.14: Catalytic applications of Vanadium aminotriphenolate complexes.

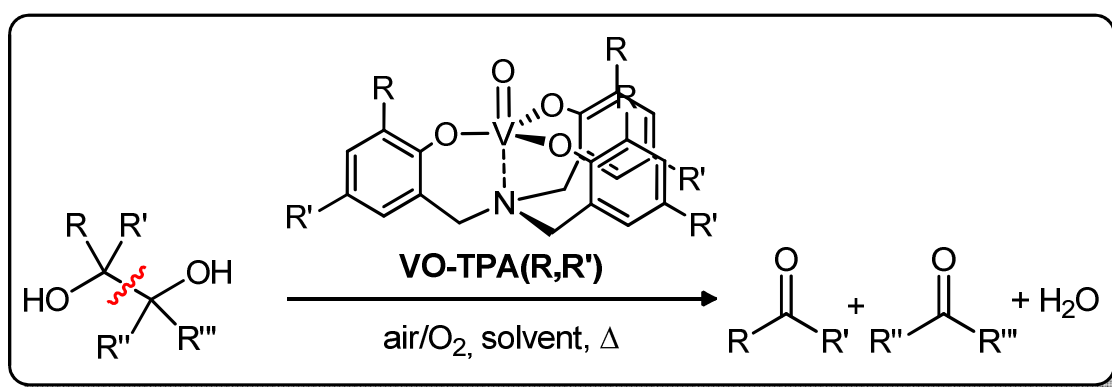
¹⁰⁰ Miceli, C.; Rintjema, J.; Martin, E.; Escudero-Adàn, E. C.; Zonta, C.; Licini, G.; Kleij, A. W.; *ACS Catal.* **2017**, *7*, 2367.

1.8 Aim of the Thesis

Lignin currently represents the most Earth-abundant and the cheapest renewable source of aromatic compounds. All these factors contribute to make lignin valorization by depolymerization a very appealing process. Among the several strategies developed up to now, oxidative depolymerization allows to obtain high valuable oxygenated aromatic molecules (aldehydes, carboxylic acids). It would be therefore desirable to develop a suitable oxidative depolymerization technique that employs a catalyst which allow to use mild non-toxic oxidants such as H₂O₂ or O₂. Inspired by Vanadium-based enzymes, a set of Vanadium (V) aminotriphenolate complexes **VO-TPA(R,R')** have been developed throughout the last few years. These compounds have been turned in useful catalysts for several oxidation reactions, with an impressive activity and selectivity. On the bases of what previously discussed, the aim of this thesis is to demonstrate the effectiveness of **VO-TPA(R,R')** as catalysts in aerobic oxidation of vicinal diols, which can be considered the simplest lignin models, and in the oxidative depolymerization of β -O-4 bond-bearing compounds and actual lignin. Moreover, we want to exploit the different stereoelectronic properties offered by suitable functionalization of *ortho*- and *para*- position of phenols in TPAs in order to choose the most appropriate complex as catalyst for a given reaction. *Chapter 2* describes the C-C oxidative cleavage of vicinal diols catalyzed by **VO-TPA(R,R')**. A complete screening of ligand, solvent and temperature effect, substrate concentration, catalyst loading, and oxidant has been performed using *meso*-hydrobenzoin as a standard substrate. We also extended of substrate scope to a wide variety of compounds, including benzylic diols and tertiary and secondary linear or cyclic aliphatic diols. We then proposed a reaction mechanism based on DFT calculations. Interestingly, by modulating reaction temperature and catalyst loading, we could trigger aldehyde oxidation to carboxylic acids. We therefore studied in more details this reaction, in presence of **VO-TPA(R,R')** complexes. We run preliminary trials devoted to find the best reaction conditions using benzaldehyde and undecanal as substrates. Finally, we reported first insights on the reaction mechanism. *Chapter 3* describes the aerobic oxidation of non-phenolic and phenolic β -O-4 lignin models, catalyzed by **VO-TPA(R,R')**. As in the case of vicinal diols, we carefully analyzed ligand, solvent and temperature effect, substrate concentration, catalyst loading, and oxidant in order to find the best reaction conditions for the highest selectivity towards C _{α} -C _{β} bond cleavage, which yields valuable aromatic aldehydes. We reported also preliminary elucidations of the reaction mechanism, by studying the importance of non-functionalized benzylic and primary -OH groups in the reactions. Since our purpose is to find an efficient lignin oxidative depolymerization procedure, *Chapter 4* is devoted to the oxidation of lignin samples, derived from wheat straw and sugarcane bagasse, in presence of **VO-TPA(R,R')**. A complete characterization of the samples by using 2D-HSQC-NMR, ³¹P-NMR (after derivatization to phosphite esters), FT-IR, GPC and MALDI-TOF-MS is reported. Those samples have been subjected to the action of **VO-TPA(R,R')**. A systematic analysis of the reaction was carried out using the above-mentioned techniques, demonstrating that our complexes are active also on actual lignin.

Chapter 2

Aerobic Oxidative C-C bond Cleavage of 1,2-Diols



*The results reported in Chapter have been partially published: Amadio, E.; González-Fabra, J.; Carraro, D.; Denis, W.; Gjoka, B.; Zonta, C.; Bartik, K.; Cavani, F.; Solmi, S.; Bo, C.; Licini, G.; Adv. Synth. Catal. **2018**, 360, 3286.*

A new catalytic method for aerobic oxidative C-C bond cleavage of vicinal diols catalyzed by vanadium aminotriphenolate complexes is described. Our results show that C-C bond cleavage can be efficiently performed in different solvents, under an air or oxygen atmosphere, with a large variety of glycols (cyclic or linear, with aromatic or aliphatic substituents) affording the corresponding carbonyl derivatives with high chemoselectivity. Reactions can be performed with as little as 10 ppm of catalyst loading, reaching TONs up to 81,000 and TOFs of up to 34,700 h⁻¹. A reaction mechanism, rationalized by DFT calculations, has been proposed. When lowering the catalyst loading to 0.2 mol %, a new reaction selectivity towards carboxylic acids is observed. We therefore studied in more detail aldehydes oxidation catalyzed by vanadium aminotriphenolate complexes, providing first insights into the reaction mechanism.

2.1 Introduction

In the view of lignin oxidative depolymerization and renewable feedstock transformation, vicinal diols can be considered the simplest models to be used in order to elucidate the activity of a catalyst and to understand the reaction mechanism¹. Oxidative carbon-carbon bond cleavage of vicinal diols yielding carbonyl compounds is a fundamental reaction in organic synthesis². Since the pioneering work of Malaprade in 1928³, 1,2-diols oxidative cleavage has been generally performed using stoichiometric high-valent inorganic oxidants, mainly periodates⁴, or lead tetracarboxylates⁵. Beside the intrinsic problems related to the use of stoichiometric amounts of oxidants, most of these reagents suffer from severe drawbacks in terms of product selectivity, toxicity, storage, handling, cost and solubility. More recently, catalytic procedures based on homogeneous manganese⁶, iron⁷, cobalt^{8,9}, copper¹⁰, molybdenum¹¹, ruthenium¹², palladium¹³, or polyoxometalates¹⁴ have been reported, although they suffer from the requirement of stoichiometric amounts of sacrificial organic or inorganic oxidants^{10,11,15}. When O₂ is used as primary oxidant, high pressures¹⁵ or activating sacrificial substrates^{5,6,8} are required or the scope of the substrate is limited to the more reactive tertiary or benzylic glycols^{15a}. Therefore, the design of more efficient and environmentally benign catalytic processes for the C-C bond cleavage of diols remains a topic of key importance. A recent example describes the use of CeCl₃ x 7 H₂O as photocatalyst and air as oxidant effective on a wide range of aryl- and alkyl-substituted diols, affording the corresponding carbonyl compounds in good yields¹⁶.

¹ a) Kärkäs, M. D.; Matsuura, B. S.; Monos, T. M.; Magallanes, G.; Stephenson, C. J.; *Org. Biomol. Chem.* **2016**, 14, 1853. b) Amadio, E.; Di Lorenzo, R.; Zonta, C.; Licini, G.; *Coord. Chem. Rev.* **2015**, 301-302, 147. c) Hanson, S. K.; Baker, R. T.; *Acc. Chem. Res.* **2015**, 48, 2037.

² Haines, A. H.; *Methods for the Oxidation of Organic Compounds: Alcohols, Alcohols Derivatives, Nitroalkanes, Alkyl Azides, Carbonyl Compounds, Hydroxyarenes and Aminoarenes*, Academic Press, London, **1988**, pp 277–304.

³ a) Malaprade, L.; Hebd, C. R.; *Seances Acad. Sci.* **1928**, 186, 382. b) Malaprade, L.; *Bull. Soc. Chim. Fr.* **1928**, 43, 683.

⁴ a) Sudalai, A.; Khenkin, A.; Neumann, R. *Org. Biomol. Chem.* **2015**, 13, 4374. b) Moorthy, J. N.; Singhal, N.; Senapati, K.; *Org. Biomol. Chem.* **2007**, 5, 767.

⁵ a) Baer, E.; Grosheintz, J. M.; Fischer, H. O. L.; *J. Am. Chem. Soc.* **1939**, 61, 2607. b) Lena, J. I. C. Sesenoglu, O.; Birlirakis, N.; Arseniyadis S.; *Tetrahedron Lett.* **2001**, 42, 21.

⁶ a) Escande, V.; Lam, C. H.; Grison, C.; Anastas, P. T.; *ACS Sust. Chem. Eng.* **2017**, 5, 3214. b) Escande, V.; Lam, C. H.; Coish, P.; Anastas, P. T.; *Angew. Chem. Int. Ed.* **2017**, 56, 9561.

⁷ Noack, H.; Georgiev, V.; Blomberg, M. R. A.; Siegbahn, P. E. M.; Johansson, A. J.; *Inorg. Chem.* **2011**, 50, 1194.

⁸ Santacesaria, E.; Sorrentino, A.; Rainone, F.; Di Serio, M.; Speranza, F.; *Ind. Eng. Chem. Res.* **2000**, 39, 2766.

⁹ Luo, H.; Wang, L.; Shang, S.; Niu, J.; Gao, S.; *Comms. Chem.* **2019**, 2, 17.

¹⁰ Sedai, B.; Diaz-Urrutia, C.; Baker, R. T.; Wu, R.; Silks, L. A. P.; Hanson, S. K.; *ACS Catal.* **2011**, 1, 794.

¹¹ Garcia, N.; Rubio-Presa, R.; Garcia-Garcia, P.; Fernandez-Rodriguez, M. A.; Pedrosa, M. R.; F. J. Arnaiz, Sanz, R.; *Green Chem.* **2016**, 18, 2335.

¹² Shiota, Y.; Herrera, J. M.; Juhász, G.; Abe, T.; Ohzu, S.; Ishizuka, T.; Kojima, T.; Yoshizawa, K.; *Inorg. Chem.* **2011**, 50, 6200.

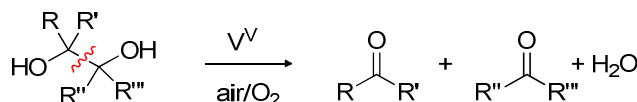
¹³ Wang, A.; Jiang, H.; *J. Org. Chem.* **2010**, 75, 2321.

¹⁴ Khenkin, A. M.; Neumann, R. *Adv. Synth. Catal.* **2002**, 344, 1017.

¹⁵ Shimizu, M.; Orita, H.; Suzuki, K.; Hayakawa, T.; Hamakawa, S.; Takehira, K. *J. Mol. Cat. A: Chem.* **1996**, 114, 217.

¹⁶ Schwarz, J.; König, B.; *Chem. Commun.* **2019**, 55, 486.

Recently, the use of vanadium complexes as catalysts for the aerobic oxidative C-C bond cleavage of vicinal diols has been reported (Eq. 2.1)¹. Vanadium complexes (VO_2^+ ,¹⁷ $\text{VO}(\text{acac})_2$,¹⁸ VOCl_3 , $\text{VO}(\text{OEt})\text{Cl}_2$, VOCl_2 ,¹⁹ $\text{H}_5[\text{PMo}_{10}\text{V}_2\text{O}_{40}]$ ²⁰) have been used with cyclic and acyclic *di*-tertiary diols providing the corresponding ketones in high yields. Unfortunately, the efficiency of these catalytic systems dramatically decreases with less substituted glycols.



Eq. 2.1: Aerobic C-C oxidative cleavage of diols to the corresponding carbonyl derivatives.

Only Vanadium-based polyoxometalates or $\text{Pt}/\text{C}-\text{V}_2\text{O}_5$ with high O_2 pressures and temperatures or strong acidic conditions could convert cyclohexane-1,2-diols, 1,2-ethanediol or monosaccharides forming mixtures of the corresponding aldehydes and over-oxidized products carboxylic acids²¹.

More recently Baker, Hanson and co-workers reported that vanadium complexes **V6-V8** (Figure 2.1) are able to oxidize pinacol under stoichiometric conditions to yield acetone²². Complex **V6**²³ is effective also under aerobic, catalytic conditions in pyridine or 1-methyl-2-pyrrolidinone. Under the best conditions, 97% yield of acetone was obtained using 5% of catalyst at 100°C and atmospheric pressure.

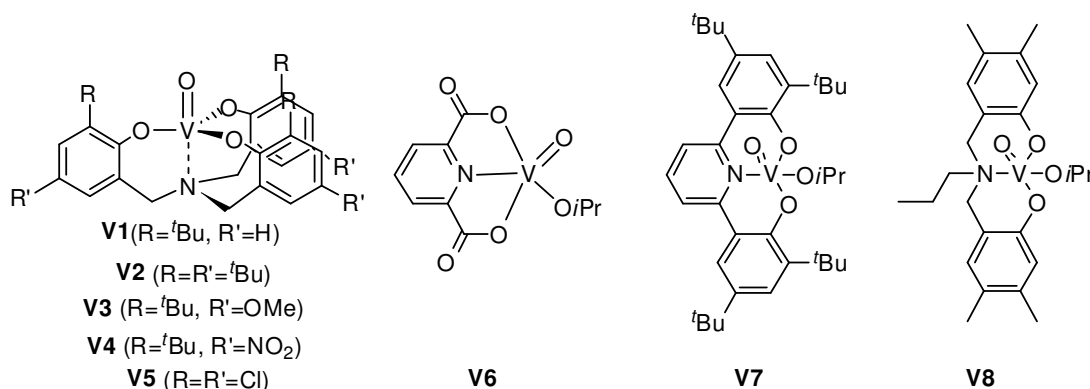


Figure 2.1. Vanadium complexes **V1-V8** as catalysts for the aerobic oxidative carbon-carbon cleavage of diols.

¹⁷ Littler, J. S.; Mallet, A. I.; Waters, W. A.; *J. Chem. Soc.* **1960**, 2761.

¹⁸ Zviely, M.; Goldman, A.; Kirson, I.; Glotter, E.; *J. Chem. Soc. Perkin Trans. I* **1986**, 229.

¹⁹ Kirihaara, M.; Yoshida, K.; Noguchi, T.; Naito, S.; Matsumoto, N.; Ema, Y.; Torii, M.; Ishizuka, Y.; Souta, I.; *Tetrahedron Lett.* **2010**, 51, 3619.

²⁰ Brègeault, J. M.; El Ali, B.; Mercier, J.; Martin, J.; Martin C. C. R.; *Acad. Sci. Paris, série II* **1989**, 309, 459.

²¹ a) Khenkin, A. M.; Neumann, R.; *J. Am. Chem. Soc.* **2008**, 130, 14474. b) Sarma, B. B.; Neumann R.; *Nat. Commun.* **2014**, 5, 4621. c) Rozhko, E.; Raabova, K.; Macchia, F.; Malmusi, A.; Righi, P.; Accorinti, P.; Alini, S.; Babini, P.; Cerrato, G.; Marzoli, M.; Cavani, F. *ChemCatChem* **2013**, 5, 1998. b) Obara, N.; Hirasawa, S.; Tamura, M.; Nakagawa, Y.; Tomishige K.; *ChemCatChem* **2016**, 8, 732.

²² a) Hanson, S. K.; Baker, R. T.; Gordon, J. C.; Scott, B. L.; Sutton, A. D.; Thorn, D. L.; *J. Am. Chem. Soc.* **2009**, 31, 428. b) Hanson, S. K.; Baker, R. T.; Gordon, J. C.; Scott, B. L.; Thorn, D. L.; *Inorg. Chem.* **2010**, 49, 5611. c) Zhang, G.; Scott, B. L.; Wu, R.; Silks, L. A. P.; Hanson, S. K.; *Inorg. Chem.* **2012**, 51, 7354.

²³ a) Crans, D. C.; Mahroof-Tahir, M. M.; Johnson, D.; Wilkins, P. C.; Yang, L.; Robbins, K.; Johnson, A.; Alfano, J. A.; Godzala, M. E.; Austin, L. T.; Willsky, G. R.; *Inorg. Chim. Acta* **2003**, 356, 365. c) Buglyo, P.; Crans, D. C.; Nagy, E. M.; Lindo, R. L.; Yang, L. Q.; Smee, J. J.; Jin, J. W. Z.; Chi, L. H.; Godzala, M. E.; Willsky, G. R.; *Inorg. Chem.* **2005**, 44, 5416.

While the capability of homogeneous vanadium complexes to catalyze the aerobic C-C bond cleavage of glycols has been explored to some detail, the development of an effective and sustainable vanadium-based catalytic process with broad substrate scope is still missing. In the next section, we report the catalytic activity of V(V) aminotriphenolate complexes **V1-V5** for the oxidative aerobic C-C bond cleavage of glycols. In particular, we examined a series of *ortho*-^tBu-substituted TPAs complexes bearing electron-donating **V2-V3** or electron-withdrawing **V4** groups in *para*-position with respect to the phenolic moiety, and the hexa-chloro derivative **V5**, not only using tertiary and benzylic diols as substrates, but also cyclic and linear aliphatic diols, both internal and terminal ones will be screened¹. The synthesis of **VO-TPA(R,R')** complexes **V1-V5** has already been described in *Chapter 1*.

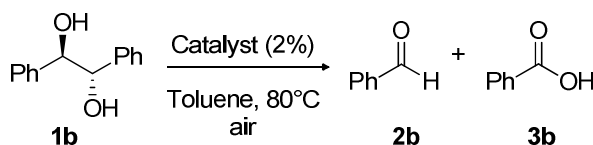
2.2 Aerobic Oxidative C-C Cleavage of Vicinal Diols: Reaction Conditions Optimization

The effectiveness of our catalytic system was first tested for the oxidation of pinacol **1a** [0.05M] (Eq. 2.1, R=R'=R''=R'''=Me), in the presence of 10% **V1** at 80°C under air and in different solvents (toluene, pyridine and NMP)²⁴. The course of the reaction was monitored via ¹H NMR. We were very pleased to observe that **V1** was effective, as complete conversion of the substrate into acetone occurred in only 2 hours.

A more detailed study was therefore carried out using *meso*-hydrobenzoin **1b** as a model system, in order to understand the catalytic ability of vanadium oxo aminotriphenolates **V1-V5**. Commercially available vanadium complexes (VO(OiPr)₃ and VO(acac)₂) and vanadium oxo bis-picolinate **V6**, used by Baker and Hanson, were examined by comparison as well (Table 2.1). Toluene was used as solvent, and reactions were carried out at 80° C under air. C-C cleavage of *meso*-hydrobenzoin **1b** afforded benzaldehyde **2b** and the relative overoxidation product benzoic acid **3b**.

²⁴ Gjoka, B.; Fe(III) and V(V) Aminotriphenolate complexes as catalysts for the conversion of renewable carbon feedstocks, *PhD thesis*, University of Padova, Italy, **2014**.

Table 2.1: Aerobic oxidative cleavage of *meso*-hydrobenzoin **1b** catalyzed by complexes **V1-V6**, VO(O*i*Pr)₃ or VO(acac)₂ (2%).^a Catalyst screening.



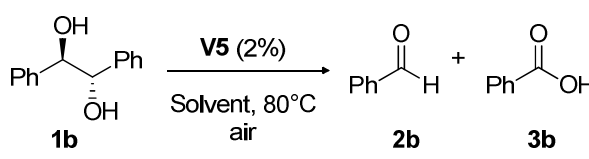
Entry	Cat.	Conv. (%) ^c	Time (h) ^b	Yield 2b:3b (%) ^c
1	V1	>99	4	98:2
2	V2	>99	5	97:3
3	V3	>99	10	94:6
4	V4	>99	0.7	>99:1
5	V5	>99	0.8	>99:1
6	VO(O <i>i</i> Pr) ₃	>99	6	98:2
7	V6	>99	6	99:1
9	VO(acac) ₂	>99	9	97:3
9	--	2	24	>99:1

^a Reaction conditions: [**1b**]₀=0.05 M, 2% of V-catalyst, toluene, 80 °C. ^b Time required for complete **1b** conversion. ^c Determined by quantitative HPLC, naphthalene as internal standard.

The results reported in Table 2.1 show that aminotriphenolate complexes **V1-V5** can catalyze the process. More importantly, it is evident that the reaction is strongly influenced by the ligand substitution, which affect the complex electronic properties. Indeed, **V4** (R = *t*Bu, R' = NO₂) and **V5** (R = R' = Cl), bearing EWG in the ligand backbone, are the most Lewis acidic complexes and are significantly more active than the **V1-V3** complexes (reaction fourteen-fold faster with respect to **V3**, bearing electron-donating substituents (*t*-Bu/MeO)), as well as the commercially available VO(O*i*Pr)₃, VO(acac)₂ and catalyst **V6** (Table 2.1, entries 5-7). Furthermore, the acceleration of the reaction was found to have a beneficial effect on its chemoselectivity: catalysts **V4** and **V5** afford exclusively two equivalents of benzaldehyde **2b** (Table 2.1, entry 4). The uncatalyzed reaction is negligible not occurring, giving negligible substrate conversion (2% after 24 h)²⁵. The effect of other parameters, like solvent (Table 2.2), temperature, substrate concentration, catalyst loading, and terminal oxidant has been explored as well (Table 2.3). Table 2.2 reports the results for the solvent screening, using **V5** as catalyst, due to the fact that it is the more active catalyst.

²⁵ The aerobic reactivity of **V5** with **1b** has been reported by Díaz-Urrutia, C. in Vanadium-Catalyzed Aerobic Oxidation of Diols and Lignin Models/Extracts, *PhD Thesis*, University of Ottawa, Canada, **2016**, chapter 6, 114-143.

Table 2.2: Aerobic oxidative cleavage of **1b** catalyzed by **V5** (2%)^a. Solvent screening.



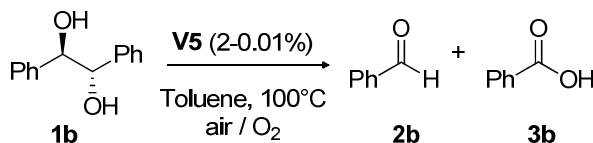
Entry	Solvent	Conv. (%)	Time (h) ^b	Yield 2b:3b (%) ^c
1	EtOH	50	2	>99:1
2	Pyridine	>99	6	99:1
3	DMSO	>99	4.5	99:1
4	DCE	>99	4	85:15
5	CH ₃ CN	>99	3	99:1
6	AcOEt	>99	0.7	99:1
7	Toluene	>99	0.7	>99:1

^a Reaction conditions: [**1b**]₀=0.05 M, **V5** (2%), 80 °C. ^b Time required for complete **1b** conversion. ^c Determined by quantitative HPLC, naphthalene as internal standard.

As far as the solvent is concerned, besides ethanol, all solvents examined gave complete conversions with 2% catalyst loading (1 mM). The best reaction performances were achieved using toluene and ethyl acetate: in both cases fast and exclusive formation of benzaldehyde was obtained in only 40 min (Table 2.2, entries 6 and 7). However, the use of toluene as solvent is more advantageous because it allows to increase the temperature up to 100 °C, thus accelerating the reaction (complete substrate conversion and same products selectivity after 20 min instead of 40 min), without affecting the catalyst stability.

Catalyst loading was examined as well: in toluene at 100°C [**1b**]₀ = 0.05 M catalyst loading could be decreased down to 0,1% (Table 2.3, entry 2 and Figure 2.2), reaching a TON = 1000 and a TOF of 1615 h⁻¹.

Table 2.3: Oxidative cleavage of *meso*-hydrobenzoin **1b** catalyzed by **V5** (2-0.001%) in toluene at 100°C in air or O₂. Catalyst loading.



Entry	Oxidant	[1b] ₀ (M)	V5 (%)	Time ^a (h)	Conv. (%) ^b	Yields 2b:3b (%) ^b	TON, TOF ^c (h ⁻¹)
1	Air	0.05	2	0.3	100	>99:1	50, 800
2	Air	0.05	0.1	2.5	100	99:1	1000, 1615
3	Air	0.5	0.2	6	56	96:4	280, 1000
4	O ₂	0.5	0.2	5	100	>99:1	500, 167
5	O ₂	0.5	0.01	48	82	98:2	8200, 870
6	O ₂	0.5	-	48	7	6:1	-
7	O ₂	0.05	-	24	2	2:0	-

^a Time required for complete **1b** conversion. ^b Determined by quantitative HPLC, naphthalene as internal standard. ^c See experimental section for TOF calculation method.

In order to perform the reaction at higher concentrations ([**1b**]₀ = 0.5M) the use of 0.2% catalyst loading did not allow complete substrate conversion (Table 2.3) (Figure 2.2). In order to improve the performance of the system and determine if the lower conversion observed at high substrate concentration could originate from rapid oxygen depletion in the reaction mixture, the reactions were carried out under an oxygen atmosphere (Table 2.3, entries 4-7). Under these new catalytic conditions, the reaction carried out with 0.2 % **V5** gave complete conversion into products in 5 hours (Table 2.3, entry 4).

Moreover, catalyst loading could be further decreased down to 0.01% (Table 2.3, entry 6 and Figure 2.1) obtaining 82% conversion of **1b** into benzaldehyde (and only 2% of benzoic acid), for a total TON of 8200 and a TOF of 870 h⁻¹. Control experiments gave a negligible conversion (>7 %) also under an O₂ atmosphere (Table 2.3, entries 6-7).

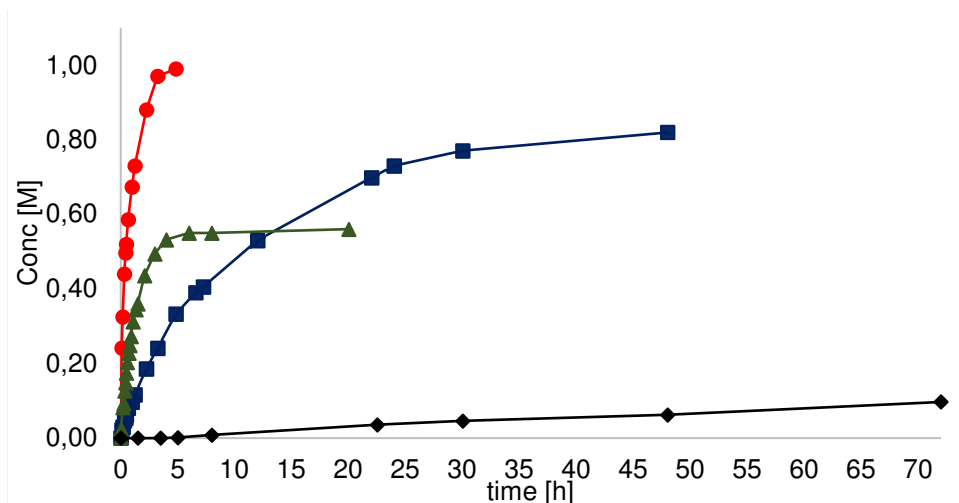


Figure 2.2: Reaction profiles for benzaldehyde **2b** formation for the oxidation of $[\mathbf{1b}]_0 = 0.5$ M in toluene, 100°C catalyzed by **V5**. \blacktriangle , **V5** = 0.2 mol%, reaction in air (TON = 280, TOF = 60 h⁻¹); \bullet , **V5** = 0.2 mol%; reaction in O₂ (balloon); \blacksquare , **V5** = 0.01 mol%, reaction in O₂ (balloon); \blacklozenge , uncatalyzed reaction.

A further improvement of the catalytic activity of **V5** was obtained when working with air at higher pressure. Unfortunately, oxygen/toluene mixtures are potentially explosive²⁶. Figure 2.3 indeed reports the UFLs of toluene/oxygen/CO₂ mixtures with different oxygen percentage (Y_{ox}) as function of pressure and temperature. As can be deduced from the curve at $Y_{ox} = 20$, at room pressure, toluene/air mixture is potentially flammable below 50 °C, which is defined as the upper flammable limit (UFL). Above 50 °C the mixture is under safety conditions, and therefore running the reactions at 100 °C is not hazardous.

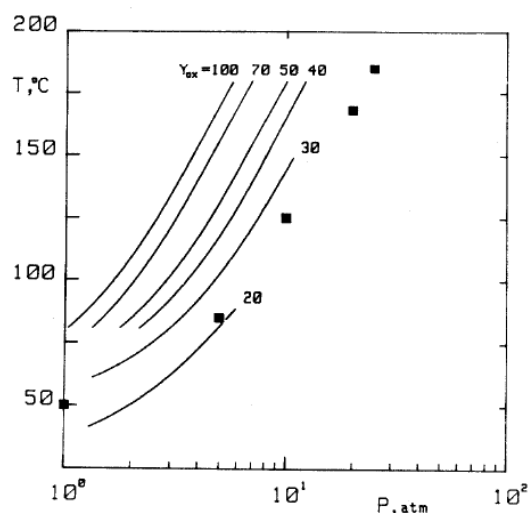


Figure 2.3: UFL of toluene/oxygen/CO₂ mixtures as a function of pressure and temperature.

Reproduced with permission from ref. 26a, Copyright 1982 Elsevier.

²⁶ Oxygen atmosphere cannot be used over 2 atm pressure at 100°C, while air can be used up to 8 atm. See: a) Crescitelli, S.; De Stefano, G.; Pistone, L.; Russo, G.; Tufano, V.; *J. Hazardous Materials* **1982**, 5, 189. b) Crescitelli, S.; Meli, S.; Russo, G.; Tufano, V.; *J. Hazardous Materials* **1980**, 3, 293.

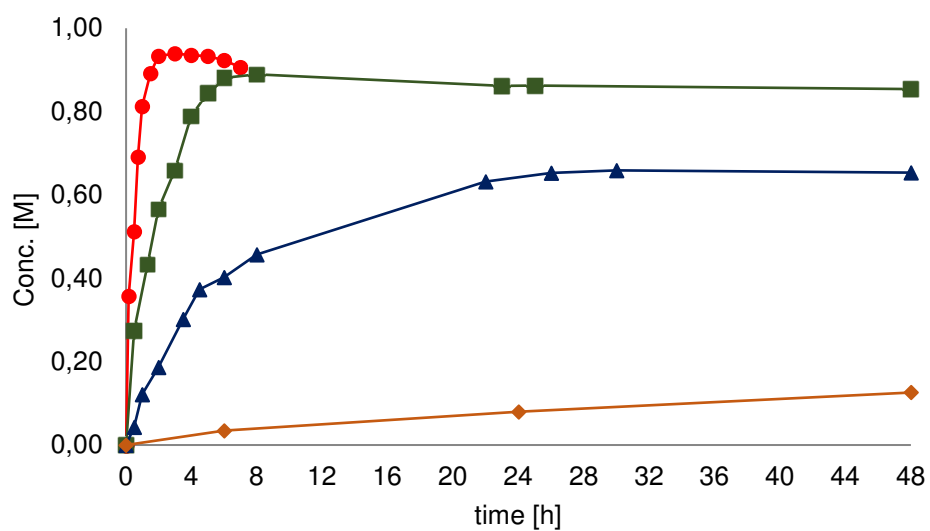
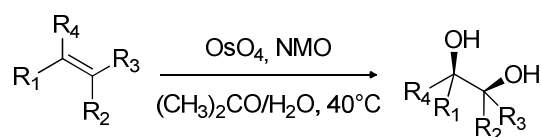


Figure 2.4: Reaction profiles for benzaldehyde **2b** formation for the oxidation of $[1b]_0 = 0.5$ M in toluene, 100°C catalyzed by **V5**: reaction in air (4 atm), semi-continuous reactor: ●, **V5** = 0.2 mol%; +, **V5** = 0.01 mol%; ▲, **V5** = 0.001 mol%. ◆ Uncatalyzed process gave 18% substrate conversion after 48 h.

2.3 Catalytic Activity Studies and Substrate Scope

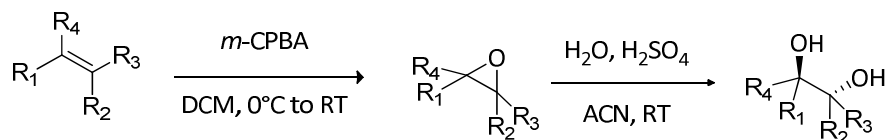
The generality of the oxidative method was explored with a large variety of vicinal diols, linear and cyclic, bearing different substituents: benzylic and aliphatic, with tertiary, secondary and even primary alcoholic functions. The reactions were carried out on 0.5 mmol concentration (10 ml), monitored by quantitative methods (HPLC or ^1H NMR), and the products were isolated via chromatography/distillation. Results are reported in Tables 2.5-2.7. Since many substrates were not commercially available, we synthesized them following two different procedures. *Syn*-diols **1d**, **1g-j**, **1o**, *syn*- + *anti*-**1v** were obtained by catalytic dihydroxylation according to Eq. 2.2



Eq. 2.2: Synthesis of *syn*-diols via dihydroxylation of respective alkenes.

As regards cyclododecanediol **1v**, a 1:1 mixture of *syn*- and *anti*-diols was obtained since we used a 1:1 mixture of *cis*- + *trans*-cyclododecene as starting material.

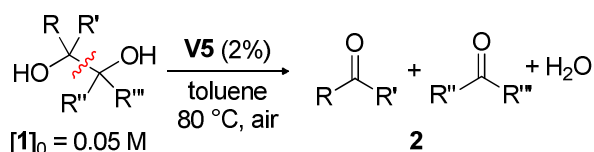
As regards *anti*-diols **1l**, **1n**, **1u**, **1v**, the synthesis was performed starting from the epoxidation of the relative alkene and the subsequent epoxide ring opening under acidic conditions in order to afford *anti*-diols, according to Scheme 2.1.

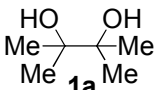
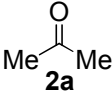
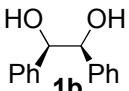
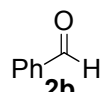
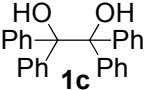
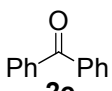
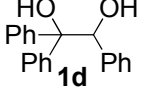
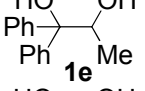
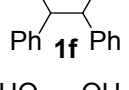
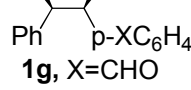
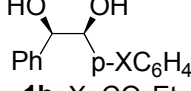
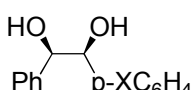
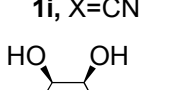
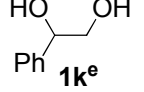


Scheme 2.1: Synthetic pathway to *anti*-diols, by epoxidation of respective alkenes and epoxide acid catalyzed ring opening.

In this case, we were able to obtain pure *anti*-cyclododecanediol **1v** by crystallization from hot MeOH of a mixture of *syn*- and *anti*-isomers obtained starting from a 1:1 mixture of *cis*- and *trans*-cyclododecene.

Table 2.5: oxidative cleavage of linear diols **1a-k** (0.05 M) catalyzed by **V5** (2%), at 80 °C, under air, toluene.



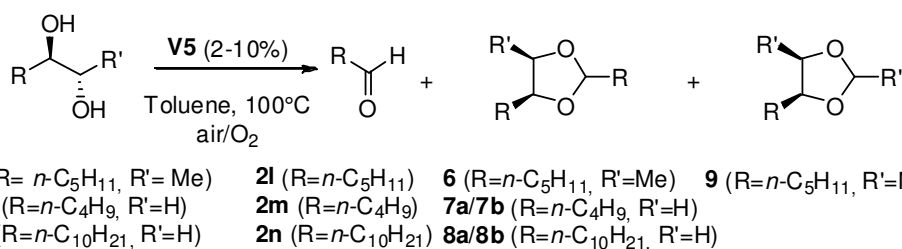
Substrate	Conv. (%)	Time (h)	Products	Yields (%)	Isolated Yields ^c (%)
 1a	>99	1	 2a	98 ^b	
 1b	>99	0.7	 2b	>99 ^a	90
 1c	98	4.0	 2c	98 ^a	82
	98 ^d	0.4		98 ^a	
 1d	>99	0.3	2b + 2c	99 ^a	2b=72, 2c=88
 1e	>99	0.6	2c	99 ^a	96
 1f	>99	0.5	2b	>99 ^a	92
 1g, X=CHO	>99	0.3	2b + C₆H₄p-X-C(=O)H 2g, X=CHO	99 ^a	2b=81, 2g=87
 1h, X=CO₂Et	>99	0.3	2b + C₆H₄p-X-C(=O)H 2h, X=CO₂Et	99 ^a	2b=87, 2h=90
 1i, X=CN	>99	0.3	2b + C₆H₄p-X-C(=O)H 2i, X=CN	99 ^a	2b=75, 2i=84
 1j, X=Br	>99	0.3	2b + C₆H₄p-X-C(=O)H 2j, X=Br	99 ^a	2b=76, 2j=85
 1ke	>99	4.0	2b	>99 ^a	85

^a Determined by HPLC using naphthalene as internal standard. ^b Determined by ¹H NMR using 1,3,5-trimethoxybenzene as internal standard. ^c Isolated yields after chromatography on silica gel and solvent removal (DCM). ^d Reaction run in xylenes, 130 °C, under O₂. ^e Reaction run at 100 °C under O₂.

With tertiary diols **1a**, **1c-e** (2% catalyst, 80°C), quantitative conversion into the corresponding ketones (acetone or benzophenone) was obtained (Table 2.5). Acetone and acetaldehyde could not be isolated, due to their volatility. Secondary benzylic glycols, **1b**, **1f-k**, afforded the corresponding aromatic aldehydes quantitatively as the only products. Remarkably, non-symmetric *p*-substituted *dl*-hydrobenzoin derivatives **1f-j** furnished benzaldehyde and the corresponding *p*-substituted benzaldehydes in a 1:1 ratio, without any further over-oxidation or decomposition. For **1b** the reaction has been also carried out also on larger scale (2.5 mmol) and **2b** was isolated in 85% yield. 1-Phenyl-1,2-ethandiol **1k**, bearing a primary alcoholic function, was converted quantitatively into **2b**.

It is worth noting that **V5** is also effective for internal and terminal linear aliphatic diols (Table 2.6). In this case, we explored two reaction conditions: the first one with 0.05 M substrate concentration and 10% catalyst loading (diluted conditions), whereas the second one higher substrate concentration were used (0.25 M) with 2% catalyst loading (concentrated conditions).

Table 2.6: Aerobic oxidative C-C cleavage of linear aliphatic diols (0.05-0.25M) catalyzed by **V5** in toluene, air/O₂. Substrate scope.



Entry	[1] ₀ (M)		V5 (mol%)	Time (h)	Products (%) ^a	Yields (%) ^{b,c}	Isolated Yields (%) ^d
1l							
2l: 6: 9							
1	0.05	Air	10	3	91:5:4	92	80
2	0.25	O ₂	2	7	60:29:11	72	
1m							
2m:7a:7b							
3	0.05	O ₂	10	0.5	96:4:0	96	86
4	0.25	O ₂	2	8	70:26:4	77	
1n							
2n:8a:8b							
5	0.05	O ₂	10	0.5	99:1:0	99	96
6	0.25	O ₂	2	8	60:33:7	71	

^a Determined via ¹H NMR/quantitative GC analysis of the reaction crude, 1,3,5-trimethoxybenzene as internal standard. ^b Yields considering aldehyde **2** + acetals. ^c Yields determined via GC, TMB used as internal standard; ^d Isolated yields after chromatography on silica gel and distillation at reduced pressure.

As can be seen from Table 2.6, oxidation of diols **1l-n** in presence of **V5** furnished an unprecedented high degree of C-C cleavage, affording the corresponding aldehyde **2l-n** in yields up to 99 % (catalyst loading down to 10 %). Under concentrated conditions, concomitant *in-situ* formation of acetals **6-9**, deriving from condensation of the starting diols and product aldehydes appeared, hampering quantitative transformation of the substrates. Taking into account this product distribution, the overall yield in aldehydes is given considering also the amount transformed in acetals (Table 2.5, second-last column)²⁷. The *in-situ* acetal formation was observed also with other catalytic processes²⁸, and becomes favored at higher substrate concentrations and longer reaction times (concentrated conditions).

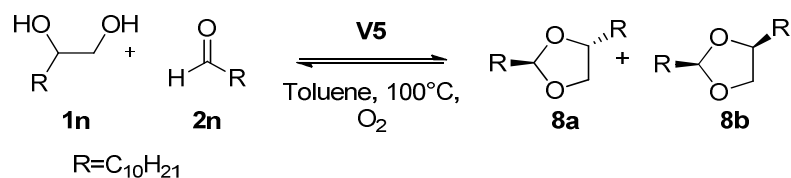
Diol **1l** afforded hexanal **2l**, acetaldehyde and the corresponding acetals **6** and **7**. Under diluted conditions (Table 2.5, entries 1,2), complete substrate conversion was achieved in 3 h with 92 % yield in **2l**, 80 % after purification. By lowering the catalyst loading to 2%, the reaction afforded 72% yield in **2l** together with the formation of acetals **6** and **7** (30%). The reaction proceeds even more effectively with terminal diols. Reaction of hexane-1,2-diol **1m** and dedecane-1,2-diol **1n** (Table 2.5, entries 3 and 5 respectively), under O₂ atmosphere, produces the corresponding aldehydes, pentanal **2m** and undecanal **2n**, in yields up to 99% in only 30 min (86 and 96%, respectively, after chromatography). The formation of acetals **8** and **9**, as a mixture of *cis/trans* diastereoisomers, was also observed, especially in the reactions carried out under more concentrated conditions (Table 2.5, entries 4 and 6). Noticeably, we detected only the acetals deriving from the condensation of heavier aldehydes **2m**, **2n** with the starting diols in the reaction mixture, whereas no acetals originating from formaldehyde were observed.

The catalytic activity of a simpler Vanadium complex VO(acac)₂ was also tested, using the optimized reaction conditions ([substrate]₀ = 0.25 M, 2 mol% catalyst, toluene, O₂ (balloon), 100°C) with three aliphatic 1,2-diols: *syn*-1,2-cyclopentanediol *syn*-**1r**, *exo,exo*-2,3-camphanediol **1m** and hexan-1,2-diol **1m**. In all cases no significant substrate conversion was observed (see for comparison Tables 2.7-2.9). Only after 24 h some substrate conversion was detected (10-60%), but only traces of the desired products were obtained, in complex reaction mixtures.

Considering that in certain conditions we could obtain a discrete amount of acetals from the reaction between linear diols and the corresponding aldehydes, we investigated whether by tuning the reaction conditions, we could also modulate reaction selectivity towards acetals formation. Another trial was therefore performed using a 1:1 mixture of **1n** and **2n**, which reacted in the presence of **V5** (10%), in order to afford acetals **8a-b** (Eq. 2.3).

²⁷ Due to reversibility of the acetalization reaction the aldehyde present in the acetals can be retrieved and the unreacted diol can be recycled.

²⁸ a) Khenkin, A. M.; Neumann, R.; *J. Am. Chem. Soc.* **2008**, 130, 14474. b) Sarma, B. B.; Neumann, R.; *Nat. Commun.* **2014**, 5, 4621.



Eq. 2.3: Acetals **8a,b** formation from reaction between diol **1n** and aldehyde **2n**. Reaction conditions: [**1n**] = [**2n**] = 0.25 M, 10 mol % **V5**, toluene, 100 °C, O₂.

The reaction indeed afforded high yields of acetals **8a/8b** (83%) in an 81:19 ratio with a 17 % of undecanal **2n** in 4h. The quantitative conversion into products was hampered by a residual activity of **V5** as C-C cleavage catalyst.

This catalytic system was also tested with secondary bicyclic aliphatic diols **1o-r**, (O₂ atmosphere, 100°C and higher catalyst loadings or substrate concentrations, Table 2.7).

Table 2.7: Oxidative C-C cleavage of cyclic diols **1o-r** (0.05 – 0.25 M) catalyzed by **V5** in toluene, air/O₂ as oxidant. Substrate scope.

Substrate	[1] (M) (oxidant)	V5 (%)	Time (h)	Products	Yields ^c (%)	Isolated Yields ^d (%)
 1o^a	0.05M (air)	10	0.5	 2o	99	90
 1p^b	0.05M (air)	10	4.0	 2p	50	46
 1q	0.25M (O ₂)	2	0.5	 2q	99	46
 1r	0.25M (O ₂)	2	1.5	 2r	98	72

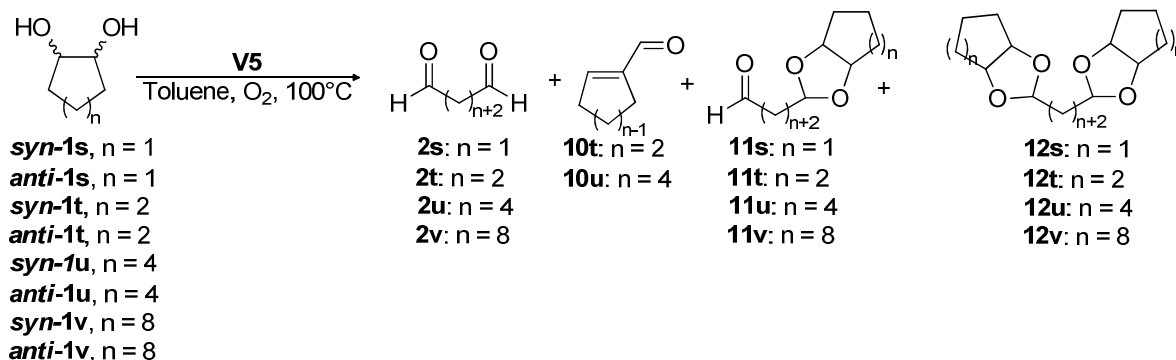
^a Reaction carried out at 80 °C in ACN. ^b Reaction carried out at 80 °C. ^c Yield determined by ¹H NMR using 1,3,5-trimethoxybenzene (TMB) as internal standard. ^d Isolated yields after chromatography on silica gel and solvent removal (DCM).

As can be seen from Table 2.7, bicyclic diols gave, in less than 1 h complete and clean conversion into the corresponding cyclic carbonyl compounds, except from aldehyde **2p**, which is unstable and degrades during the reaction. The cleavage of norbornanediol **1o** was run in ACN since in toluene, as soon as the catalyst is inserted into reaction system, the solution turns from deep blue to bright yellow, and by ESI-MS we see the presence of free ligand, which is an index of catalyst degradation. We suppose that in toluene the reaction is too fast and even under O₂ atmosphere, the reoxidation of metal center to V(V) does not occur before catalyst degradation.

The catalytic system was also explored with aliphatic cyclic diols **1s-v** (Table 2.8). These derivatives are quite interesting because they produce α,ω linear *bis*-aldehydes or *bis*-acids, which can be used

in polymer industry. We tested a series of *syn*- and *anti*- cyclic diols with cycles of different size, in order to see whether the geometry affects the catalytic activity of our complexes. The reactions were tested with both diluted and concentrated catalytic conditions.

Table 2.8: Aerobic C-C cleavage of cyclic aliphatic vicinal diols under O₂, [1]₀ = 0.05 M or 0.25 M, 100°C, 10%-2% **V5**.



Entry	Substrate	[Sub] ₀ M	V5%	time (h)	Conv. ^a (%)	Yield 2 ^a (%)	Yield 10 ^a (%)	Yield 11 ^{b,29} (%)	Yield 12 ^{b,29} (%)	Mass Balance (%)
1	<i>syn</i> - 1s	0.05	10	0.75	>99	>99	-	-	-	>99
2		0.25	2	0.75	>99	95	-	-	-	95
3	<i>anti</i> - 1s	0.05	10	1.5	>99	>99	-	-	-	>99
4		0.25	2	24	11	10	-	-	-	99
5	<i>syn</i> - 1t	0.05	10	1.5	>99	45	5	19	1	70
6		0.25	2	1	98	7	6	12	35	62
7	<i>anti</i> - 1t	0.05	10	2.5	>99	12	8	6	-	26
8		0.25	2	1	79	24	3	19	6	73
9	<i>syn</i> - 1u	0.05	10	0.08	>99	>99	-	-	-	>99
10		0.25	2	3	96	24	3	19	6	56
11	<i>anti</i> - 1u	0.05	10	0.5	>99	82	9	5	2	98
12		0.25	2	4	91	30	4	22	6	71
13	<i>syn</i> -and <i>anti</i> - (1:1) 1v	0.05	10	0.5	>99	>99	-	-	-	>99
14		0.25	2	1.5	98	72	-	21	2	95
15	<i>anti</i> - 1v	0.05	10	0.67	>99	>99	-	-	-	>99
16		0.25	2	20	98	72	-	14	12	98

^aYield determined by GC using naphthalene as internal standard. ^bYield determined by ¹H-NMR using naphthalene as internal standard.

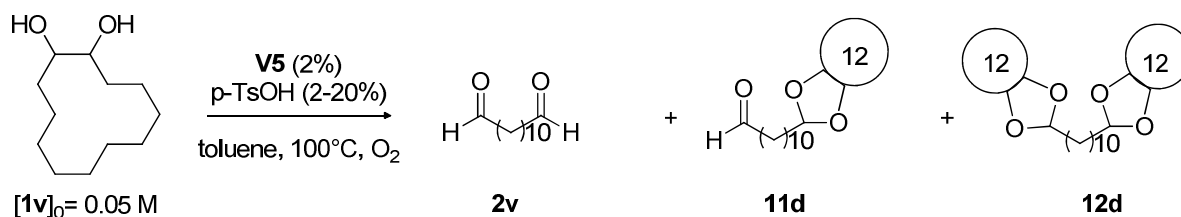
²⁹ Yield of **11t-v** was determined considering that this product is formed from two equivalents of diol **1t-v**. Yield of **12t-v** was determined considering that this product is formed from three equivalents of diol **1t-v**.

In all cases, the reaction occurs with almost complete conversion of the substrates. However, the size and stereochemistry of the diols have a significant impact on yields and chemoselectivity of the reaction. *Bis*-aldehydes originating from C-C oxidative cleavage are always the major products **2s-v**. As regards cyclohexanediol **1t** and cyclooctanediol **1u**, the self-condensation products **10a-b** were also observed. Moreover, the formation of mono and bis acetals **11a-d** and **12a-d**, originating from the aldehydes and unreacted diols have been observed as well. The product distribution has been quantified by ¹H-NMR (**10a-b**, **11a-d**, **12a-d**) and by GC analysis (**2s-v**).

As can be seen from Table 2.8, the best reaction conditions in terms of reaction time and selectivity were achieved using diluted conditions ($[1]_0 = 0.05$ M, 10% **V5**), indeed in most cases we obtained 80 - 100 % of *bis*-aldehydes. For cyclohexanediol **1t** and cyclooctanediol **1u**, a discrete amount of self-condensation products **10a-b** (up to 9%) were also obtained. When working under more concentrated conditions and with lower catalyst loadings ($[1]_0 = 0.25$ M, 2% **V5**) a general slow-down of the reaction was observed, yielding into a higher mono- and bis- acetal formation **11a-d**, **12a-d**. Another trend that clearly emerges from these data is a much higher reactivity of *syn*-compounds than the corresponding *anti*-isomers. This can be attributed to their ring strain. Indeed, in order to have catalysis, the substrate must coordinate with both hydroxyl groups to vanadium center, and for *syn*- compounds, this is easier than *anti*-compounds.

Both *syn*- and *anti*- cyclopentanediol **1s** were converted into glutaraldehyde **2s** under diluted conditions. *syn*-**1s** is quantitatively converted in only 40 min, while *anti*-**1s** requires 1.5 h for reaction completeness. Under more concentrated conditions, only the more reactive *syn*-**1s** underwent C-C cleavage, while *anti*-**1s** gave only 20 % conversion. Both *syn*- and *anti*-cyclohexanediol **1t** under more and less concentrated conditions afforded a complex reaction mixture with only a little amount of adipaldehyde **2t** (7-45 %). Attempts to identify the other reaction products were not successful till now. Diols of larger cycles **1u**, **1v** reacted easily affording only the corresponding *bis*-aldehydes (under more diluted conditions). Worth of mention is that the reaction of *syn*-**1u** gave *bis*-aldehyde **2u** in only 5 minutes. In all the cases the reactions carried out under more concentrated conditions afforded also the *mono*- and *bis*- acetals **11** and **12** together with the aldol condensation product (only for *syn*- and *anti*-**1t,u**). Considering the significant amount of acetals obtained working under more concentrated conditions for *syn*- + *anti*-cyclododecanediol **1v** the reaction was carried out in the presence of *p*-TsOH (Table 2.9). In this case, substrate concentration and catalyst loading were lowered respectively to 0.05 M and 2 mol % in order to slow down the cleavage reaction (Table 2.8, entry 13 vs Table 2.9, entry 1) and favor the acetal formation.

Table 2.9: Aerobic C-C cleavage of **1v** under O₂, [1v]₀ = 0.05 M, 100°C, 2% **V5**, 2-20 % *p*-TsOH x H₂O.



Entry	<i>p</i> -TsOH H ₂ O (%)	x	Time (h)	Conv. (%) ^a	Yield 2v (%) ^a	Yield 11d (%) ^{b,29}	Yield 12d (%) ^{b,29}	Mass Balance (%)
1	0		4	96	92	4	0	100
2	2		4	>99	79	10	10	99
3	10		2.5	>99	51	24	23	98
4	20		4	0	0	0	0	100

^a Yield determined by GC using naphthalene as internal standard. ^b Yield determined by ¹H-NMR using naphthalene as internal standard.

While the reaction without additive affords almost completely the bis-aldehyde **2v**, the addition of 2 mol % of *p*-TsOH enhances the amount of acetals up to 20 %, without affecting reaction time. The addition of 10 % acid, instead, not only increases reaction speed, but also the yield of acetals. A further increase of the amount of *p*-TsOH x H₂O to 20 mol % leads to catalyst degradation and therefore no reaction is observed. We can therefore conclude that a catalytic amount of *p*-TsOH (10 %) not only act as a catalyst for acetal formation, but it could also accelerate C-C cleavage reaction exerting a positive effect on the reaction rate.

The chemoselectivity of the reaction was also explored. When looking at the scope of substrate (Table 2.5) we verified the inertness of other functional groups like formyl, bromo, cyano, or ethyl-ester **1g-j**. We also run a series of reactions using different substrates like benzylic alcohol, thioanisole, dioctyl and diisopropylamine, styrene and cyclooctene ([1] = 0.05 M, toluene, 100°C, **V5** (10 mol %)). In all cases we didn't detect any substrate conversion as well as the formation of oxidation products, even after 48 h of reaction. Moreover, we didn't observe any catalyst degradation during the reaction. However, strong acidic substituents, such as sulfonic groups are not compatible with **VO-TPA(R,R')** complexes, since they're able to protonate the phenolate groups leading to complex disruption and the release of TPA ligands.

2.4 Catalyst Stability under Turnover Conditions

The stability of catalyst **V5** under turn-over conditions has been monitored by NMR (Figure 2.5) and ESI-MS experiments (Figure 2.6). It is known that Vanadium complexes with tripodal ligands like TPAs undergo temperature-dependent structural equilibria between TBP geometry and OCT geometry in solution, based on the coordination of monodentate Lewis bases (H_2O , sulfoxides)¹⁸. Therefore, the experiment was carried out in a coordinating solvent, namely ACN in order to have a single species in solution which leads to have a single set of ^1H and ^{51}V NMR signals for **V5**. The reaction was performed directly in an NMR tube ($[\text{V5}]_0 = 5.0 \times 10^{-3} \text{ M}$, $[\text{1b}]_0 = 0.05 \text{ M}$; 80°C , air, CD_3CN). The course of the reaction was also monitored during time by ESI-MS.

Complete substrate conversion into **2b** was obtained in 1h. Moreover, no change in color of the solution (which remained dark blue) was observed during the overall process. The presence of catalyst **V5** could be clearly detected at the beginning and at the end of the reaction via all analytical techniques. In Figure 2.5 ^{51}V NMR spectra are reported where a singlet at -429.6 ppm can be detected at the beginning and at the end of the reaction (spectra A and D).

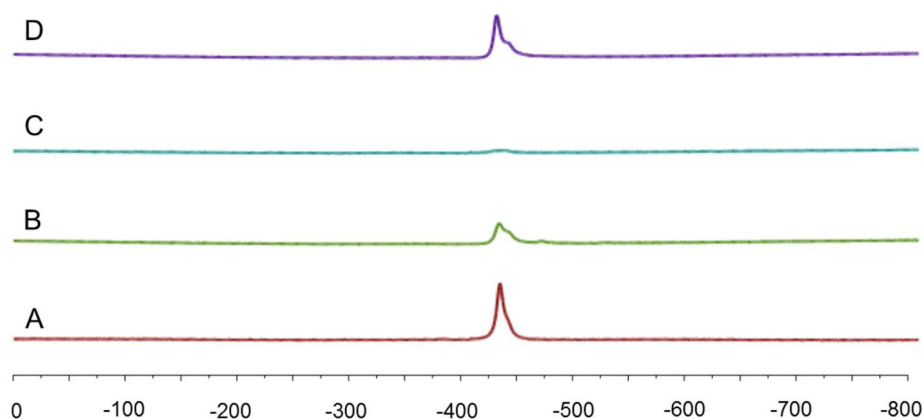


Figure 2.5: ^{51}V NMR spectra for the monitoring of aerobic oxidative cleavage of **1b** catalyzed by **V5** (10%) in CD_3CN at 80°C under air (1 atm): $[\text{V5}] = 5.0 \times 10^{-3} \text{ M}$, RT (A).; after **1b** addition: $[\text{V5}] = 5.0 \times 10^{-3} \text{ M} + 10 \text{ equiv. 1b}$, RT, (B); after 30 min at 80°C , (C), after 60 min at 80°C , (D).

Also ESI-MS (Figure 2.6) showed the presence of complex **V5** as a chloride ($[\text{V5} + \text{Cl}^-]$ $m/z = 637.8$) or a formate adduct ($[\text{V5} + \text{HCO}_2^-]$, $m/z = 647.8$) both in the beginning and at the end of the reaction, in negative mode. Noticeably, after the addition of **1b** (10 equiv.) a peak assignable to the **V5-1b** deprotonated adduct can be observed ($m/z = 817.9$). It is generally accepted that the initial step for the vanadium catalyzed C-C bond cleavage mechanism is the coordination of the diol to the vanadium complex²². This substrate/catalyst adduct, after C-C bond cleavage of the diol, will produce a vanadium reduced species that is finally re-oxidized back to **V5** by dioxygen.

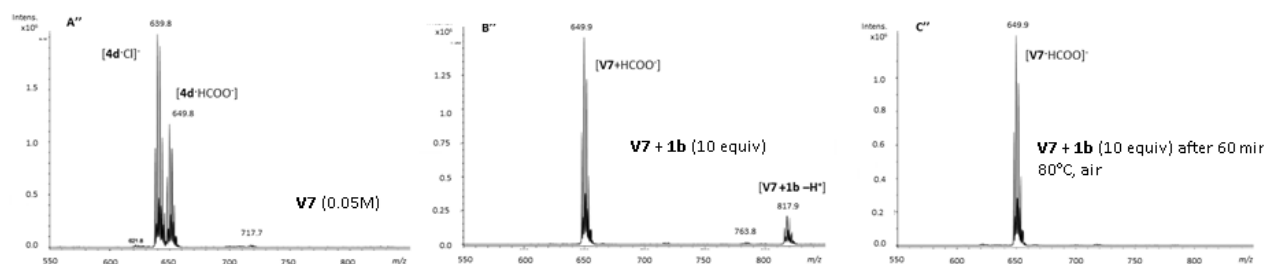


Figure 2.6: ESI-MS spectra for the oxidative cleavage of **1b** catalyzed by **V5** (10%) in CD₃CN at 80°C under air (1 atm): A'': [**V5**] = 5.0×10⁻³ M, RT; B'': [**V5**] = 5.0×10⁻³ M + [**1b**] = 10 equiv., RT; C'': [**V5**] = 5.0×10⁻³ M + [**1b**] = 10 equiv. after 60 min at 80°C, complete **1b** conversion into benzaldehyde **2b**.

2.5 Proposed Reaction Mechanism

In order to have some information about the reaction mechanism, a computational study using DFT calculations of the C-C oxidative cleavage of ethylene glycol **1w** and pinacol **1a** catalyzed by **V5** both in toluene and in water was performed (Figure 2.7).

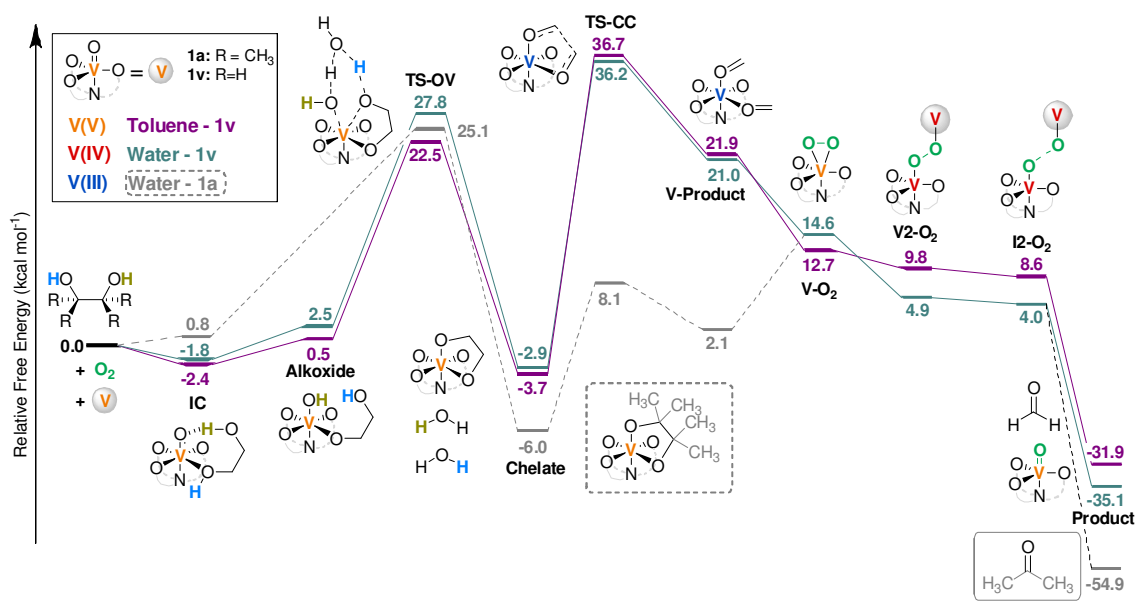


Figure 2.7: Gibbs free-energy profile (kcal·mol⁻¹) of the oxidative carbon-carbon (C-C) cleavage of ethylene glycol **1w** in water (green line) and in toluene (purple line) and of pinacol **1a** in water (grey line), catalyzed by **V5** using O₂ as oxidant.

The reaction mechanism can be divided into three main steps: in the first one, **1v** is deprotonated and a water molecule is formed; in the second step, C-C bond cleavage of the diol and reduction of V^V to V^{III} occur; finally, the last step is devoted to the recovery of the catalytic active species by O₂ mediated oxidation of V^{III} to V^V.

The initial coordination of **1w** to **V5** was studied in detail by exploring the different interaction modes of the acidic protons of **1w** with the oxygen atoms of the complex (in both ligand and Vanadium *axial* oxo sites). The most stable situation presents a hydrogen bond between one of the alcoholic protons

of **1w** (yellow in Figure 2.7) and the oxo atom. The initial coordination intermediate **IC** presents a relative Gibbs free-energy of $-1.8 \text{ kcal}\cdot\text{mol}^{-1}$ in water ($-2.4 \text{ kcal}\cdot\text{mol}^{-1}$ in toluene). This first deprotonation step leads to an **Alkoxide** intermediate and formation of a hydroxyl-group in the *axial* position of the complex³⁰. After that, the second proton of the diol (labeled in blue in Figure 2.7) is transferred to the hydroxyl group through **TS-OV** leading to the formation of a non-oxo intermediate **Chelate**, ($-2.9/-3.7 \text{ kcal}\cdot\text{mol}^{-1}$) with the concomitant formation of a water molecule. The relative Gibbs free-energy barrier of this process, computed from **IC** as the most stable intermediate previous to **TS-OV**, is $27.8 \text{ kcal}\cdot\text{mol}^{-1}$ in water, and $24.9 \text{ kcal}\cdot\text{mol}^{-1}$ in toluene. Non-oxido V^V complexes are rare, even if the natural product Amavidine³¹ bears such structure and in literature³², several other examples, especially for systems bearing multidentate ligands, have been reported.

Consecutively, the C-C bond cleavage takes place in a two-fold, one-electron reduction step, and the metal complex V^V is formally reduced to V^{III} with the oxidation of the two alkoxide groups to carbonyl compounds, thus breaking the C-C bond. The **TS-CC** is a V^{III} complex (triplet state) and presents an associated relative Gibbs free energy of 36.2 (water) or 36.7 (toluene) $\text{kcal}\cdot\text{mol}^{-1}$, constituting a relative barrier of 39.1 (water) or 40.4 (toluene) $\text{kcal}\cdot\text{mol}^{-1}$. The obtained intermediate (**V-Product**) is less energetically stable than the intermediates previously reported (21.0 (water), 21.9 (toluene) $\text{kcal}\cdot\text{mol}^{-1}$), which indicates that the reaction proceeds rapidly to the reoxidation of the catalyst to V^V just after the C-C cleavage step³³.

The reoxidation from V^{III} to V^V occurs through the reaction of one O_2 molecule with two **V-Product** intermediates. This two-step process occurs through a peroxo intermediate (**V-O₂**), which is a singlet state species and is located energetically between **V-Product** and **V₂-O₂** intermediates. The singlet state of **V-O₂** complex is best described as a V^V -peroxo species, while its triplet state (lying 15 kcal mol^{-1} above) is a V^{IV} -superoxo. After this peroxovanadate is formed an extra $V(III)$ entity is required to break the O-O bond via a bimetallic intermediate (**V₂-O₂**) formed by assembling one **V-O₂** complex and one V^{III} , which is much more stable than the previous intermediates ($4.9 \text{ kcal}\cdot\text{mol}^{-1}$). It is worth mentioning that **V₂-O₂** and **I₂-O₂** display triplet state character. The corresponding singlet configuration of the second intermediate **I₂-O₂** is less stable than the triplet by only $3.5 \text{ kcal}\cdot\text{mol}^{-1}$. Therefore, the reoxidation of the Vanadium complex and recovery of the catalyst, although spin-forbidden, are very fast processes that lead to the initial complex **V5**.

The rapid and spontaneous oxidation of V^{III} aminotriphenolates complexes ($R=R'=\text{Me}$, *t*-Bu), prepared from $VCl_3(\text{THF})_3$ to the corresponding V^V oxo-derivatives, by atmospheric oxygen, was

³⁰ An experimental evidence of the formation of this adduct comes from ESI-MS experiments (Figure 2.2)

³¹ Armstrong, E. M.; Beddoes, R. L.; Calviou, L. J.; Charnock, J. M.; Collison, D.; Ertok, N.; Naismith, J. H.; Garner, C. D.; *J. Am. Chem. Soc.* **1993**, 115, 807.

³² For recent examples see a) Parker, B. F.; Zhang, Z.; Leggett, C.; Arnold, J.; Rao, L.; *Dalton Trans.*, **2017**, 46, 11084. b) Galindo, A.; *Inorg. Chem.* **2016**, 55, 2284 and references therein.

³³ Experimental evidence of the formation of a $V(III)$ -aminotriphenolate complex upon oxidation of **1b** with **V5** under anaerobic conditions has been reported by Diaz-Urrutia, C. in Vanadium-Catalyzed Aerobic Oxidation of Diols and Lignin Models/Extracts, *PhD Thesis*, University of Ottawa, Canada, **2016**.

reported by Kol et al.³⁴ In the case of the hexachloro derivative, the isolated V^{III} complex has been only partially characterized and the re-oxidation after exposition to O₂ did not afford **V5** but a blue paramagnetic species which hasn't been characterized in more detail.

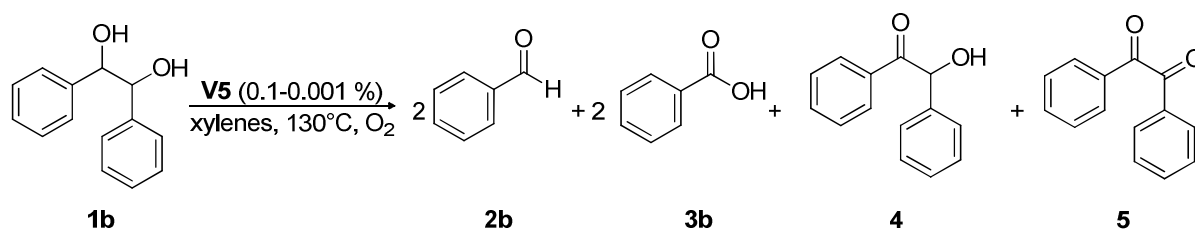
The computed Gibbs free-energy of the complete reaction is -35.1 (water) or -31.9 kcal·mol⁻¹ (toluene), therefore an exergonic process. The global Gibbs free-energy barrier is high but taking into account that the reaction is run at 80°-100°C, and that the aliphatic diols such as **1o-v** are the least reactive diols, the proposed reaction mechanism is feasible. However, when we considered a more reactive substrate like pinacol **1a**, the more stable **Chelate** (-6 kcal mol⁻¹) can be transformed into the **V-product** via a **TS-CC** with a much lower relative Gibbs free energy (8.1 kcal·mol⁻¹), for a global relative barrier of only 25.1 kcal·mol⁻¹. The computed Gibbs free-energy of the reaction for **1a** oxidation is -54.9 kcal·mol⁻¹, almost double the free-energy determined for the reaction with **1w**.

³⁴ Groysman, S.; Goldberg, I.; Goldschmidt, Z.; Kol, M.; *Inorg. Chem.* **2005**, 44, 5073.

2.6 C-C Cleavage of *meso*-hydrobenzoin in Xylene

In order to increase the reaction rate, the use of aromatic solvents with higher boiling point was explored. The oxidative cleavage of **1b** (0.5 M) was carried out in xylenes (a mixture of *ortho*-, *meta*- and *para*-isomers) at 130°C, exploring different catalyst loadings of **V5** (0.1 – 0.001 %) or of the commercially available VO(acac)₂ (Table 2.10 and Figure 2.8).

Table 2.10: Aerobic oxidative carbon-carbon bond cleavage of **1b** under O₂, [1b]₀ = 0.5 M, xylenes, 130°C, **V5** as catalyst, catalyst loadings 0.1 – 0.001 %.



Entry	V5 (%)	Time (h) ^a	Conv. (%) ^b	Yield 2b (%) ^b	Yield 3b (%) ^b	Yield 4 (%) ^b	Yield 5 (%) ^b	Mass Balance (%)	TON	TOF ^c (h ⁻¹)
1	0.2	0.67	>99	79	12	1	3	96	455	1250
		4		-	90	-	4	94		
2 ^d	0.2	0.5	>99	90	2	-	4	96	460	2120
		24		84	4	-	4	92		
3 ^e	0.2	1.5	>99	80	13	3	4	100	465	725
4	0.1	1.5	>99	78	18	1	3	100	960	2340
		24		8	83	-	7	98		
5	0.01	2.5	>99	70	17	2	9	98	8600	5130
		24		3	82	-	8	93		
6 ^e	0.01	4	>99	60	29	0	11	100	8900	4430
7	0.001	3	>99	51	30	10	9	100	81000	34700
		24		12	65	6	13	96		
8	-	24	21	14	-	6	-	99	-	-

^a Time required to get a complete **1b** conversion. ^b Determined by HPLC using biphenyl as internal standard.

^c See experimental section for TOF calculation method. ^d Reaction run in presence of TEMPO (1 equiv.).

^e Reaction run using VO(acac)₂ as catalyst.

The results reported in Table 2.10 clearly show that, in addition to the C-C cleavage (products **2b** and **3b**), also the benzylic oxidation to give products **4** and **5** occurs. This is in line with previous observations (see Table 2.4, reaction under air at 4 atm). However, in this case, the higher reaction temperature has a remarkable effect on the reaction rate. Notably, even at lower catalyst loadings and longer reaction times with respect to the same reactions run in toluene (Table 2.4), the chemoselectivity increases to give **3b**, **4** and **5** in up to 49 % HPLC yield (Table 2.10, entry 7). The

reactions could be performed at very low catalyst loadings (down to 10 ppm), obtaining in all cases a complete substrate conversion and good selectivity towards the C-C bond cleavage. The spontaneous cleavage of **1b** in the absence of catalyst (background reaction) was found to occur, yet at a very slow rate (about 20 % conversion after 1 day in xylenes at 130°C under O₂). Thus, compared to toluene (Table 2.4), we observe that in xylenes our system is more efficient in terms of TOFs and, more importantly, over-oxidation to the carboxylic acid can be accessed for longer reaction times. In other words, this catalytic system can be employed under different conditions to afford a chemodivergent cleavage of diols.

From the profiles of the reaction with 0.1 % **V5** (Figure 2.8), and those of **2b** and **2c** in the reactions with 0.1 % and 0.01 % **V5** (Figure 2.9, see also Table 2.10 entries 3-4), the presence of a consecutive reaction kinetics can be observed. The first transformation is the V-catalyzed C-C bond cleavage of **1b** affording benzaldehyde **2b**, which is subsequently oxidized to benzoic acid **3b**. Even with low catalyst loading (0.1 % of **V5**), the first reaction step proceeds smoothly (complete conversion after 1.25 h, see Figure 2.8), whereas the second oxidation reaction ends in about 8 h. Interestingly, the aldehyde oxidation was found not to proceed to completion, yet stopped at about 83 % yield. This could be due to catalyst decomposition. In fact, we found that the use of 0.1 % **V5** allows faster benzaldehyde oxidation when compared to the reaction with 0.01 % loading, suggesting the involvement of the catalyst in the oxidation of **2b**.

Parallel to C-C cleavage, benzylic oxidation occurs from the beginning of the reaction (Figure 2.8), with benzoin **4** being formed as an intermediate species. Throughout the reaction, benzoin **4** is completely oxidized within 4 h to benzil **5**, whose amount remains then constant until the end of the reaction. The extent of benzylic oxidation was found to increase when the catalyst amount was lowered (Table 2.10, entry 5 and 7).

VO(acac)₂, a commercially available complex, was also found to be a suitable catalyst for the cleavage of **1b** even at low catalyst loadings (100 ppm). In this context, **V5** and VO(acac)₂ afforded similar selectivity at all of the investigated concentrations (Table 2.10). Nevertheless, **V5** provided higher TOF values with loading 0.2 %, thus exhibiting faster substrate conversion. At lower catalyst loadings (0.01 %) the differences in reactivity become negligible at the beginning, even though **V5** is more efficient near complete substrate consumption (Figure 2.10).

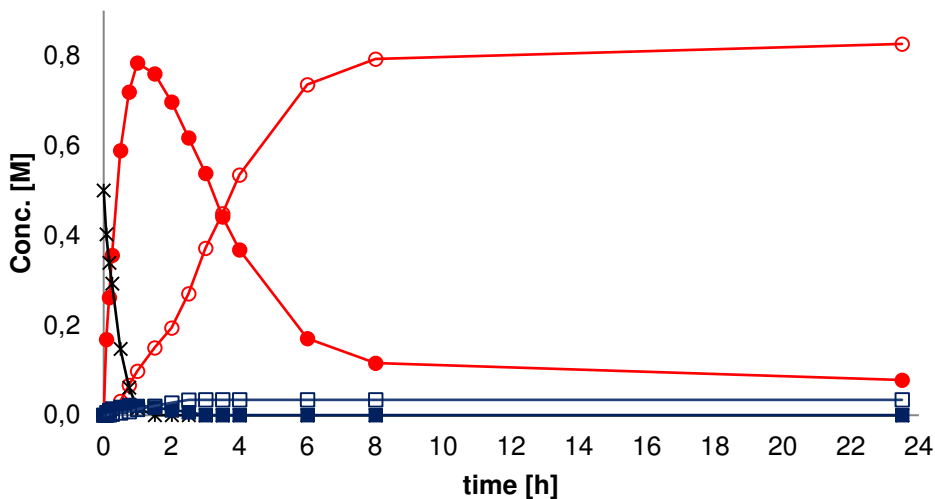


Figure 2.8: Reaction profiles for *meso*-hydrobenzoin **1b** consumption, $[1b]_0 = 0.5$ M in xylenes, 130°C catalyzed by **V5** (0.1 mol %): reaction in O₂ (balloon): *, *meso*-hydrobenzoin, **1b**; ●, benzaldehyde, **2b**; ○, benzoic acid, **3b**; ■, benzoin, **4**; □, benzil, **5**.

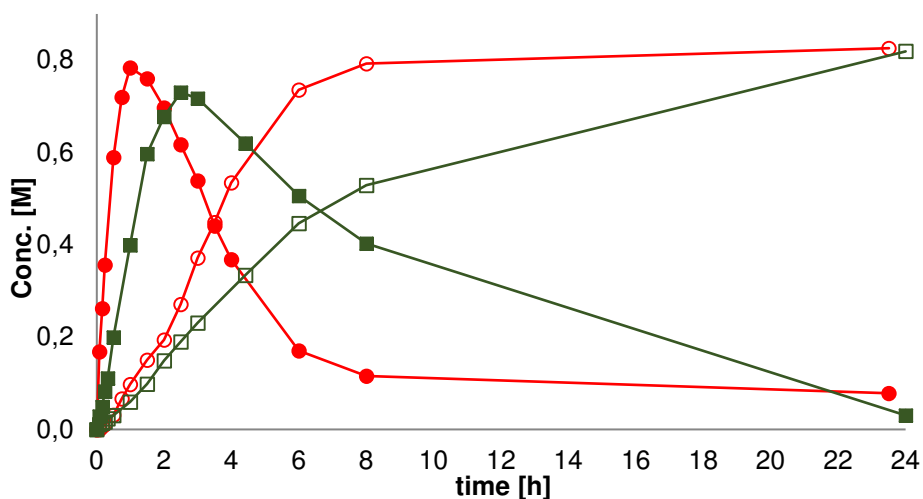


Figure 2.9: kinetic profiles for **2b** oxidation in xylenes, 130°C catalyzed by **V5**. ●, benzaldehyde, **2b**, **V5** = 0.1 mol %; ○, benzoic acid, **2c**, **V5** = 0.1 mol %; ■, benzaldehyde, **2b**, **V5** = 0.01 mol %; □, benzoic acid, **2c**, **V5** = 0.01 mol %.

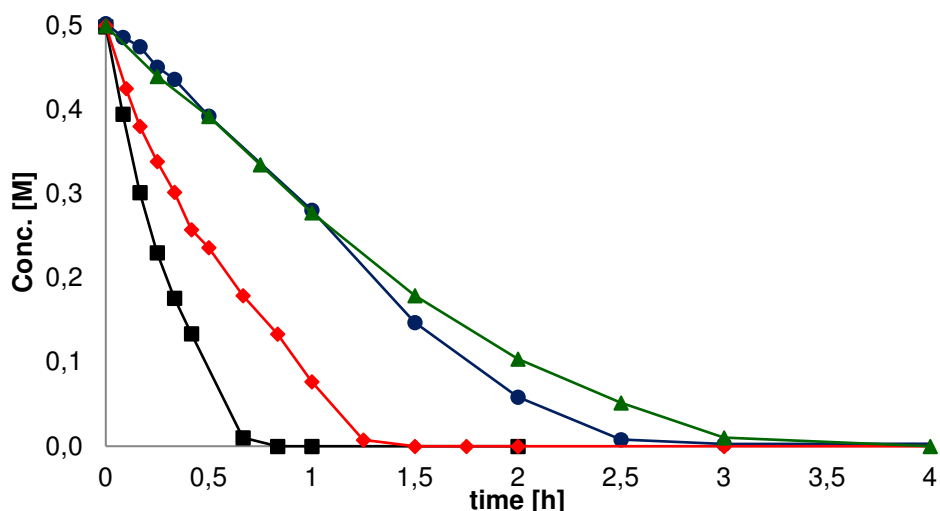


Figure 2.10: Reaction profiles for *meso*-hydrobenzoin **1b** consumption, $[1b]_0 = 0.5$ M in xylenes, 130°C catalyzed by **V5** or $VO(acac)_2$, reaction in O_2 (balloon): ■, **V5** = 0.2 mol%; ♦, $VO(acac)_2$ = 0.2 mol%; ●, **V5** = 0.01 mol %; ▲, $VO(acac)_2$ = 0.01 mol%.

In order to gain more insights into the possible radical nature of the mechanism of **2b** oxidation, the reaction was carried out with 0.2 % **V5** in the presence of a radical trap (TEMPO) in stoichiometric amount. Under these conditions **1b** was completely converted into **2b** without affecting the reaction time. However, the overoxidation process leading to the formation of benzoic acid **3b** was strongly inhibited (Table 2.10, entry 2). This suggests the involvement of a radical pathway for this second reaction step.

In conclusion, these results show that we simply by modulating solvent, reaction time and temperature we could induce chemodivergency to the reaction directing the selectivity either towards aldehyde **2b** or acid **3b**. This makes **VO-TPA(R,R')** complexes versatile catalysts for such reactions.

2.7 Oxidation of Aldehydes to Carboxylic Acids

In the last section, we showed that using xylenes as solvent at 130 °C under O₂, **V5** was able to oxidize benzaldehyde **2b** into benzoic acid **3b**. Therefore, in order to gain more information on the oxidation of aldehydes to carboxylic acids (not usually observed in toluene), the reactivity of benzaldehyde **2b** and undecanal **2n** was studied in more detail.

Oxidation of aldehydes to carboxylic acids is a fundamental transformation for functional group conversion³⁵. Although carboxylic acids can be readily obtained from oxidation of the corresponding aldehydes, highly efficient and environmentally friendly processes still remain a challenge³⁶. Established methods for such reaction include the use of stoichiometric amounts of toxic and hazardous oxidants such as KMnO₄³⁷, CrO₃³⁸, KHSO₅³⁹, KIO₄⁴⁰, Ag(I)⁴¹ (Tollens reagent), Cu(II) (Fehling reagent)⁴², often used in harmful solvents such as chlorinated hydrocarbons. Therefore, greener and more sustainable strategies are required. In this context, the development of oxidation processes involving molecular oxygen as terminal oxidant would be desirable. Although aldehydes are commonly known to be prone to oxidation, sometimes they are rather stable and inert. For these reasons, catalytic methods based on the use of molecular oxygen are limited and often require rare and expensive noble metal catalysts⁴³. For example, in 2000, Sheldon and co-workers developed a homogeneous aerobic catalytic procedure for the aldehyde oxidation in water using Pd as catalyst and oxygen pressures up to 30 bar^{43a,b}. In 2008, Sha et al. reported a heterogeneous catalytic in-water procedure for the oxidation of aldehydes using Cu(II) / Ag(I) oxides, however, this method requires high catalyst loadings and presents a limited substrate scope^{43e}. In 2009, Yoshida et al. reported a N-heterocyclic carbene-catalyzed oxidation process under O₂, in which a mixture of water and DMF 1:10 was used as solvent⁴⁴. Recently, several catalytic systems for the aerobic oxidation of aldehydes to carboxylic acids under greener and milder conditions have been developed. In particular, a catalytic version of Tollens reaction has been developed by Li et al., employing a catalytic amount of Ag(I), using O₂ as terminal oxidant in water³⁵. However, since silver is an expensive and toxic element, and its availability is decreasing⁴⁵ it would be highly desirable to switch the catalytic system to more earth-abundant and cheap metals. A first example of a catalytic Fehling

³⁵ Liu, M.; Wang, H.; Zeng, H.; Li, C. *Sci. Adv.* **2015**, 1(2), e1500020.

³⁶ Yu, H.; Ru, S.; Dai, G.; Zhai, Y.; Lin, H.; Han, S.; Wei, Y.; *Angew. Chem. Int. Ed.* **2017**, 56, 3867.

³⁷ Mahmood, A.; Robinson, G. E.; Powell, L.; *Org. Process Res. Dev.* **1999**, 3, 363.

³⁸ Thottathil, J. K.; Moniot, J. L.; Mueller, R. H.; Wong, M. K. Y.; Kissick, P. T.; *J. Org. Chem.* **1986**, 51, 3140.

³⁹ Travis, B. R.; Sivakumar, M. G.; Hollist, O.; Borhan, B.; *Org. Lett.* **2003**, 5, 1031.

⁴⁰ Hunsen, M.; *Synthesis* **2005**, 2487.

⁴¹ Oshima, K.; Tollens, B.; *Ber. Dtsch. Chem. Ges.* **1901**, 34, 1425.

⁴² Fehling, H.; *Ann. Chem. Pharm.* **1849**, 72, 106.

⁴³ a) ten Brink, G. J.; Arends, I. W.; Sheldon, R. A.; *Science* **2000**, 287, 1636. b) Stahl, S. S.; *Science* **2005**, 309, 1824. c) Besson, M.; Gallezot, P.; *Catal. Today* **2000**, 57, 127 d) Mallat, T.; Baiker, A.; *Chem. Rev.* **2004**, 104, 3037; e) Tian, Q.; Shi, D.; Sha, Y.; *Molecules* **2008**, 13, 948 f) Shapiro, N.; Vigalok, A.; *Angew. Chem. Int. Ed.* **2008**, 47, 2849.

⁴⁴ Yoshida, M.; Katagiri, Y.; Zhu, W. B.; Shishido, K.; *Org. Biomol. Chem.* **2009**, 7, 4062.

⁴⁵ Atwood, D. A.; *The Rare Earth Elements: Fundamentals and Applications*, Wiley, Chichester, **2012**.

reaction, based on Cu(II) under O₂ and mild reaction conditions, has been reported by the same research group⁴⁶. Nevertheless, the organic ligands used in these reactions are susceptible to self-degradation, which limits their usefulness. Wei et al. therefore developed a Fe-Mo-Polyoxometalate system, which is able to catalyze the oxidation of several aldehydes under aerobic conditions, in water at 50°C and in presence of a catalytic amount of base (Na₂CO₃, 10 mol %)³⁶. As regards Vanadium, it has been reported that V₂O₅ can oxidize aldehydes to the corresponding esters, using H₂O₂ as terminal oxidant⁴⁷. More recently, Thakur et al. reported that commercially available VO(acac)₂ could oxidize aldehydes in presence of an excess of H₂O₂ (3 equiv.), used as terminal oxidant. Both aromatic and aliphatic aldehydes were tested as substrates, with aromatic aldehydes giving faster reactions thanks to the greater electrophilicity of the carbonyl carbon⁴⁸. It is worth noting that in the last three years, other metal-free methods for aldehyde oxidation have been developed. Kang and co-workers reported that N-hydroxyphthalimide can be used as an organocatalyst affording a number of carboxylic acids starting from the corresponding aldehydes at RT under oxygen (1 atm)⁴⁹. He et al. reported a catalyst-free process which employs dipropylene glycol dimethylether as solvent, under ambient air, obtaining very high conversion of aldehydes into carboxylic acids and of substituted phthalic aldehydes into cyclic anhydrides⁵⁰. Wang and collaborators reported that O₂ (1 atm) was sufficient to oxidize aldehydes at RT in water at neutral pH⁵¹, even though only few substrates were studied and the operative substrate concentration was very low, making the process less appealing from a synthetic point of view, especially when large amounts of product are needed.

Conscious of the preliminary results obtained in xylenes (Table 2.10), we decided to examine the benzaldehyde oxidation, investigating substrate concentration and catalyst loading (Table 2.11 and Figure 2.11).

⁴⁶ Liu, M.; Li, C. J.; *Angew. Chem. Int. Ed.* **2016**, 55, 10806.

⁴⁷ a) Gopinath, R.; Barkataki, B.; Talukdar, B.; Patel, B. K.; *J. Org. Chem.* **2003**, 68, 2944. b) Gopinath, R.; Patel, B. K.; *Org. Lett.* **2000**, 2, 577.

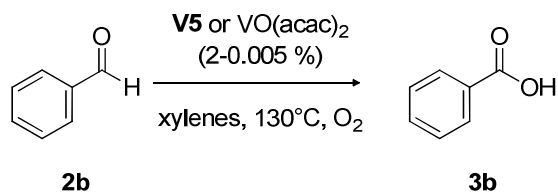
⁴⁸ Talukdar, D.; Sharma, K.; Bharadwaj, S. K.; Thakur, A. J.; *Synlett.* **2013**, 24, 963.

⁴⁹ Dai, P. F.; Qu, J. P.; Kang, Y. B.; *Org. Lett.* **2019**, 21, 1393.

⁵⁰ Liu, K. J.; Fu, Y. L.; Xie, L. Y.; Wu, C.; He, W. B.; Peng, S.; Wang, Z.; Bao, W. H.; Cao, Z.; Xu, X.; He, W. M.; *ACS Sust. Chem. Eng.* **2018**, 6, 4916.

⁵¹ Zhang, Y.; Cheng, Y.; Cai, H.; He, S.; Shan, Q.; Zhao, H.; Chena, Y.; Wang, B.; *Green Chem.* **2017**, 19, 5708.

Table 2.11: Aerobic oxidation of benzaldehyde **2b**, 100°C, **V4-5** or VO(acac)₂ as catalyst, toluene, 100°C, O₂, or xylenes, 130°C, O₂.



Entry	[2b] ₀ (M)	Solvent	cat. (mol %)	T(°C)	Time (h)	Conv. (%) ^a	Yield 3b (%) ^a	Mass Balance (%)
1	0.25	Toluene	V5 (2)	100	24	0	0	100
2	0.25	Xylenes	V5 (2)	130	24	83	82	99
3	0.25	Xylenes	V5 (1)	130	6	70	69	99
					24	>99	98	98
4	0.25	Xylenes	V5 (0.1)	130	6	97	88	91
					24	>99	92	91
5	0.25	Xylenes	V4 (0.1)	130	6	92	92	100
					24	97	97	100
6	0.25	Xylenes	VO(acac) ₂ (0.1)	130	6	94	94	100
					24	95	95	100
7 ^b	0.25	Xylenes	V5 (0.1)	130	6	2	2	100
					24	8	8	100
8	0.25	Xylenes	-	130	6	55	54	99
					24	92	91	99
9	0.5	Xylenes	V5 (0.1)	130	6	76	75	99
					24	95	87	92
10	1	Xylenes	V5 (1)	130	4	49	48	99
					6	61	60	99
					24	94	91	97
11 ^c	1	Xylenes	V5 (1)	130	4	56	56	100
					6	60	60	100
					24	73	69	96
12 ^d	1	Xylenes	V5 (0.1)	130	4	83	78	95
13 ^d	1	Xylenes	VO(acac) ₂ (0.1)	130	4	79	79	100
14	1	Xylenes	V5 (0.005)	130	4	86	85	99
					6	88	87	99
					24	93	92	99
15	1	Xylenes	-	130	4	70	69	99
					6	74	73	99
					24	87	86	99

^a Determined by HPLC using biphenyl as internal standard. ^b Reaction run in presence of 100 mol % TEMPO. ^c Reaction run in presence of 1 mol % TEMPO. ^d Reaction stops after 4 h.

In analogy to what we observed with **1b** (Tables 2.3 and 2.10), benzaldehyde does not undergo oxidation in toluene (Table 2.11, entry 1), whereas in xylenes it is converted to benzoic acid (Table 2.11, entry 2). This indicates that solvent and temperature are crucial parameters in order to activate the process for this substrate. Since it has been demonstrated that reactions are favored at lower substrate concentrations⁵¹, we decided to start our investigation working at a concentration of **[2b]** = 0.25 M.

Surprisingly, when lowering the catalyst amount to 1 mol% and to 0.1 mol% (Table 2.11, entries 3 and 4), we could obtain complete substrate conversion after 24 h (1 mol% **V5**) or 6 h (0.1 mol% **V5**, 97 % conversion, 88 % yield). The uncatalyzed reaction is also occurring, with 91 % yield after 24 h (Table 2.11, entry 8). Increasing the substrate concentration to 0.5 M (Table 2.11, entry 9), we were able to obtain the desired product in 87 % yield after 24 h. A further increase in the substrate concentration to 1 M and catalyst loading to 1 mol% (Table 2.11, entries 10-11), led to a lower yield of **3b** than when using 0.1 mol % **V5** (Table 2.11, entry 12). Therefore, we further decreased the catalyst amount to 0.005 mol% and obtained 92 % yield after 24 h, a lower amount than the one obtained with **[2b]₀** = 0.25 M (Table 2.11, entries 4 and 14). From the reaction profiles reported in Figure 2.11, we can note that the reaction performed with 1 mol% **V5** is slower compared to reaction performed with lower loadings, even though afforded >90 % yield of **3b** after 24 h. Finally, complex **V4** showed a slightly less activity with respect to **V5** (Table 2.11, entries 4-5), whereas VO(acac)₂ (0.1 mol %, both for **[2b]₀** = 0.25 M and **[2b]₀** = 1 M) afforded benzoic acid **3b** in an analogous manner with respect to **V5** (Table 2.11 entries 4-6, 10-11), indicating that actually Vanadium(V) aminotriphenolate complexes are not necessary in order to have catalysis for benzaldehyde oxidation, although they are for C-C cleavage of **1b** (Tables 2.1 and 2.10).

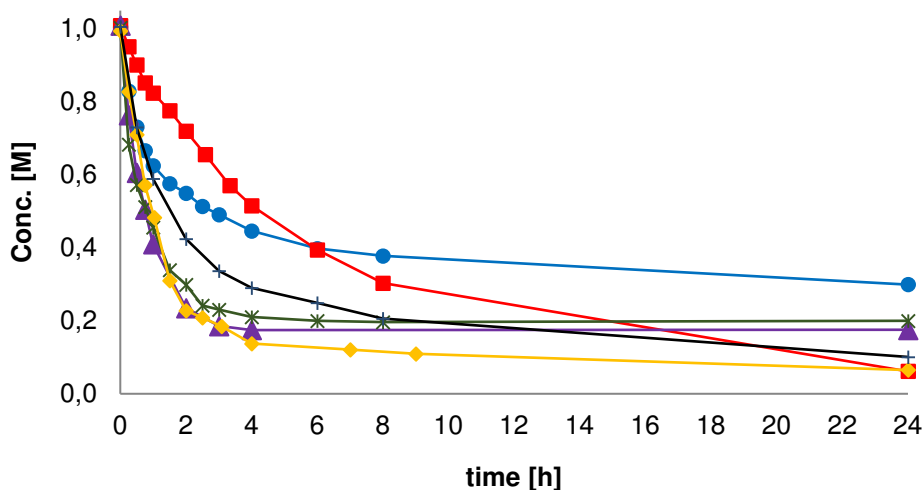
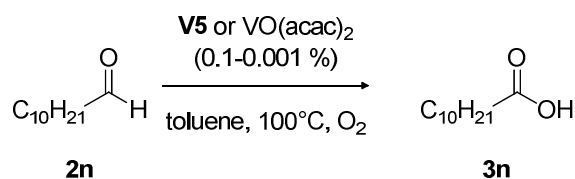


Figure 2.11: Reaction profiles for benzaldehyde **2b** oxidation, $[2b]_0 = 1$ M in xylenes, 130°C catalyzed by **V5** or VO(acac)₂: reaction in O₂ (balloon): ■, **V5** = 1 mol%; ●, **V5** = 1 mol% + 1 % TEMPO; +, uncatalyzed reaction; *, VO(acac)₂ = 0.1 mol%. ▲, **V5** = 0.1 mol%; ◆, **V5** = 0.005 mol%.

Aldehyde oxidation was also tested using aliphatic undecanal **2n** as substrate. Oxidation to the corresponding undecanoic acid **3n** occurred even in toluene at 100°C (Table 2.12 and Figure 2.12). In analogy to what obtained for benzaldehyde (Table 2.11), the decrease of **V5** loading from 5 mol% to 0.1 mol% allowed obtaining faster reactions, complete substrate conversion and quantitative yield (Table 2.12, entries 1-10). In toluene, the difference between **V5** and VO(acac)₂ was even more evident, with the latter providing lower activity (Table 2.12, entries 3 and 7). The uncatalyzed reaction also occurred spontaneously and afforded 95 % yield of **3n** after 24 h (Table 2.12, entry 11). Thus, we showed that **V5** is a suitable catalyst for aldehyde oxidation, being effective both on an aromatic and an aliphatic substrate, affording complete conversion in few hours with low loadings (<1 mol%). The increase of substrate concentration to 0.5 M only partly affects the reaction process (Table 2.12, entries 12-13), whereas the reaction with $[2n]_0 = 1$ M afforded almost complete conversion after 24 h (Table 2.12, entry 14). These trends are in line with the previously reported data for benzaldehyde in xylenes (Table 2.11).

Table 2.12: aerobic oxidation of undecanal **2n**, 100°C, **V4-5** or VO(acac)₂ as catalyst, toluene, 100°C, O₂.



Entry	[2n] ₀ (M)	cat. (mol%)	Time (h)	Conv. (%) ^a	Yield 3n (%) ^a	Mass Balance (%)
1	0.25	V5 (5)	2	56	56	100
			6	84	84	100
2 ^{b,c}	0.25	V5 (2)	2	92	88	96
3	0.25	V5 (2)	2	76	74	98
			6	83	80	97
4 ^d	0.25	V5 (2)	2	11	11	100
			24	66	64	98
5 ^e	0.25	V5 (2)	2	25	20	95
			24	96	87	91
6 ^f	0.25	V5 (2)	24	21	10	89
7 ^b	0.25	VO(acac) ₂ (2)	2	72	72	100
8 ^b	0.25	V4 (2)	2	82	82	100
9	0.25	V5 (1)	2	85	84	99
			6	95	94	99
			24	>99	98	98
10	0.25	V5 (0.1)	2	89	88	99
			6	97	95	98
			24	>99	96	96
11	0.25	-	2	82	82	100
			6	91	90	99
			24	96	95	99
12 ^b	0.5	V5 (1)	2	95	93	98
13	0.5	V5 (0.1)	6	94	93	99
			24	98	97	99
14	1	V5 (1)	6	90	90	100
			24	97	97	100

^a Determined by GC-FID using biphenyl as internal standard. ^b Reaction stops after 2 h. ^c Reaction run in presence of TEMPO (2 mol %). ^d Reaction run in presence of TEMPO (10 mol %). ^e Reaction run in presence of BHT (10 mol %). ^f Reaction run in presence of TEMPO (100 mol %).

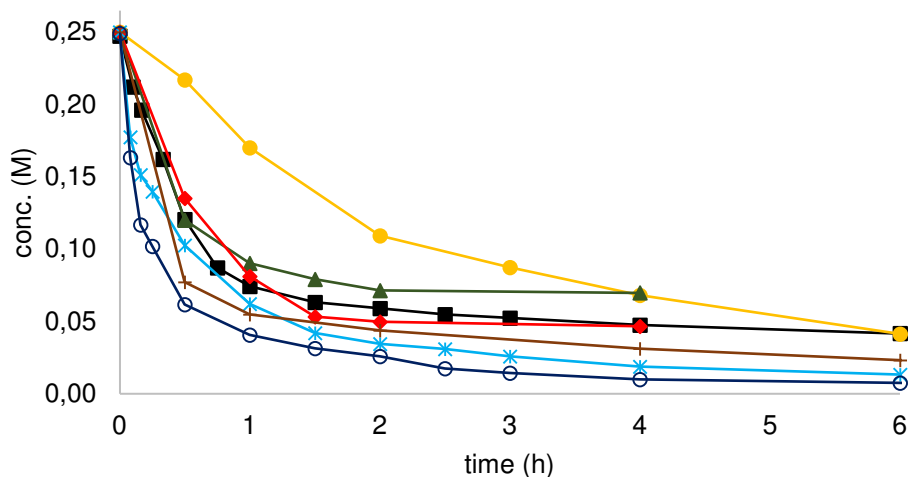


Figure 2.12: Reaction profiles for undecanal **2n** oxidation, $[2n]_0 = 0.25$ M in toluene, 100°C catalyzed by **V5** or **V4** or $\text{VO}(\text{acac})_2$: reaction in O_2 (balloon): ●, **V5** = 5 mol %; ■, **V5** = 2 mol %; ▲, $\text{VO}(\text{acac})_2$ = 2 mol %; ◆, **V4** = 2 mol %; +, uncatalyzed reaction; *, **V5** = 1 mol %; ○, **V5** = 0.1 mol%.

In order to gain insights about the reaction mechanism, we added a radical trap, namely TEMPO (100-10 mol%), which inhibited the reaction with both **2b** (Table 2.11, entry 7) and **2n** (Table 2.12, entries 4 and 6 and Figure 2.13). This indicates that the reaction proceeds through a radical pathway (as showed also in *Section 2.6*). Surprisingly, contrary to what found for **2b** (Table 2.11, entry 11) where the addition to 1 % TEMPO did not afford any improvement to the reactivity, the addition of 2 mol% of TEMPO to **2n** led to an increase in the reaction rate and to a better yield (Table 2.12, entries 2 and 3). An additional experiment was performed running the reaction in the presence of BHT as radical trap, which proved less effective than TEMPO in inhibiting the reaction (Table 2.12, entry 5).

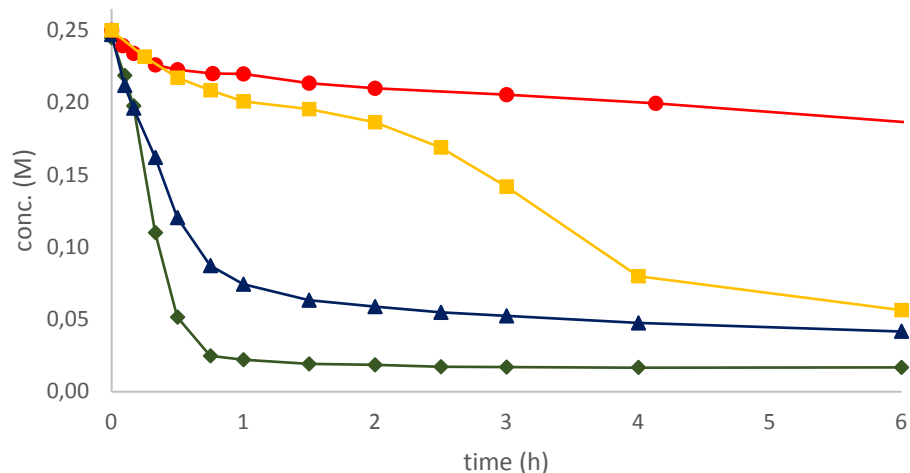


Figure 2.13: Reaction profiles for undecanal **2n** oxidation, $[2n]_0 = 0.25$ M in toluene, 100°C catalyzed by **V5**: reaction in O_2 (balloon): ●, **V5** = 2 mol% + 10 mol% TEMPO; ■, **V5** = 2 mol% + 10 % BHT; ▲, **V5** = 2 mol%; ◆, **V5** = 2 mol% + 2 mol% TEMPO.

2.8 Conclusions

In this chapter we showed that aminotriphenolate complexes **V4-V5** are effective catalyst for the aerobic oxidative C-C bond cleavage of vicinal diols, from tertiary and benzylic ones to linear and cyclic aliphatic glycols. In particular, **V5** was found to be the most active, since it works under mild conditions (air or O₂ as oxidants, 80-130°C), in different solvents. In almost all cases the reactions afforded quantitatively the relative aldehydes with low reaction time and very little overoxidation to the corresponding acids, also in the presence of different functional groups. The high TONs (up to 81,000) and TOFs (up to 34,700 h⁻¹) of the system, together with the ability to transform terminal and cyclic aliphatic glycols make this complex the most general and effective homogeneous catalyst reported up to now for this kind of reaction. The stability of the catalyst was verified during the reaction by ⁵¹V NMR and ESI-MS. Preliminary experiments together with DFT calculations suggest a pre-association of the substrate to the metal center followed by a two-electron oxidation mechanism, yielding a reduced V^{III} metal complex and the carbonyl derivatives. Fast re-oxidation by O₂ finally regenerates the catalyst closing the cycle. Interestingly, when performing the oxidation of *meso*-hydrobenzoin lowering the catalyst amount below 0.2 mol %, in xylenes at 130°C, we could switch the reaction selectivity towards carboxylic acids rather than aldehydes. We therefore studied in more details the aerobic oxidation of aldehydes to carboxylic acids, catalyzed by **VO-TPA(R,R')** complexes. Preliminary trials devote to finding the best conditions have been run using benzaldehyde and undecanal as substrates. In both cases, fastest conversion to carboxylic acids were achieved with a substrate concentration of 0.25 M and 0.1 mol % catalyst. Finally, the addition of a radical trap (TEMPO) resulted in a complete oxidation inhibition indicating that the reactions could proceed through a radical mechanism. Currently, we are extending the substrate scope towards a series of *p*-substituted benzaldehydes and naturally occurring aldehydes (citral, perillaldehyde, HMF) in order to study the influence of other functional groups in the reactions.

2.9 Experimental

General Remarks

All chemicals and dry solvents were purchased from Sigma-Aldrich and used without further purification. Deuterated solvents (Sigma-Aldrich) were used without further purification. Other organic solvents, (Sigma-Aldrich) were used without further purification.

MilliQ Water: Deionized water was purified with a Millipore system, constituted by ion exchange resins and activated-carbon resins.

^1H -NMR, $^{13}\text{C}\{^1\text{H}\}$ -NMR, DEPT-135 and ^{51}V NMR spectra have been recorded at 301 K with a Bruker spectrometer AC-200 MHz (^1H : 200.13 MHz; ^{13}C : 50.3 MHz) or Avance Bruker DRX-300 (^1H : 300.13 MHz; ^{13}C : 75.5 MHz, ^{51}V : 78.28 MHz). Chemical shifts (δ) have been reported in parts per million (ppm) relative to the residual undeuterated solvent as an internal reference (CDCl_3 : 7.26 ppm for ^1H -NMR and 77.0 ppm for ^{13}C NMR; CD_3CN : 1.94 ppm for ^1H -NMR and 118.26 ppm for ^{13}C NMR). For ^{51}V NMR spectra was referred to $\text{VO}(\text{O}_2)\text{picolinate}$ (5×10^{-3} M, water, pH = 1) used as external standard. The multiplicity of the signals is indicated in the following way: s: singlet, d: doublet, t: triplet, q: quartet, dd: doublet of doublets, m: multiplet, br: broad.

GC-MS spectra have been recorded with an Agilent 6850 Series GC System interfaced with an Agilent 5973 Network Mass Selective Detector. Carrier gas He (1 mL/min), phase HP-5MS, column 30mt I.D. 0,25, film 0,25 μm , 5% diphenyl / 95% dimethylsiloxane. Injector temperature has been set to 250 $^\circ\text{C}$, detector temperature has been set to 280 $^\circ\text{C}$. ESI-MS spectra were recorded on an Agilent 1100 LC/MSD IonTrap spectrometer, in positive/negative modes, by direct flow injection using acetonitrile or methanol (both with 0.1 % v/v of HCOOH for analysis in positive mode) as mobile phase. TLC: Silica gel PET plates Macherey-Nagel POLYGRAM[®] SIL G/UV₂₅₄ have been used; detection by UV-Vis and treatment with PMA staining reagent (10 % w/w in ethanol) or KMnO_4 . Flash Chromatography was performed as described in literature using Macherey-Nagel silica gel 60 (0.04-0.63 mm, 230-400 mesh)⁵². Reactions that required an N_2 inert atmosphere were carried out in a glove-box MBRAUN MB 200MOD, equipped with a regulation and recycling inert gas system MB 150 G-1 (nitrogen working pressure: 6 bar). Each substance introduced in the glove-box has been previously subjected to repeated vacuum / N_2 cycles into a pre-chamber. Water level inside the box was real-time monitored by MBraun moisture analyzer. FT-IR spectra has been recorded in the range (4000-600) cm^{-1} and resolution 4 cm^{-1} , on a Nicolet 5700 FT-IR instrument, using KBr pellets. HPLC analyses were performed on a Shimadzu HPLC equipped with a Knauer Eurospher II 100-5 C18 (5 μm of active phase, 250 x 4,6 mm column) operating at room temperature, eluent water /acetonitrile gradient, naphthalene/biphenyl as internal standard. The UV detector was set at $\lambda = 210$ nm. The concentration of both reagents and products was estimated from the calibration curves. GC-FID analyses were performed on a Shimadzu GC-2010, equipped with a Supelco column

⁵² Still, C. W.; Khan, Mitra, A.; *J. Org. Chem.* **1978**, 43, 2923.

(phase: SPB^T-1, length: 15 m, ID: 0.1 mm, 0.1 μ m Film, 100% dimethylsiloxane). Carrier gas He (69 ml/min). Injector temperature has been set to 280 °C, detector temperature has been set to 330 °C. The concentration of both reagents and products was estimated from the calibration curves.

Turnover numbers (TONs) were calculated as the maximum moles of desired product over the amount (in moles) of catalyst used. Turnover frequencies (TOFs) were calculated as amount in moles of substrate consumed at 20 % conversion over the moles of catalyst used over the time required to reach 20 % conversion.

All reactions were performed in: i) 10-20 mL Schlenk reactors, equipped with an air/oxygen balloon and a condenser, or ii) in a semi-continuous stirred autoclave reactor (100 mL volume), made out of glass and equipped with a condenser, at an operating pressure of 4 atm (BuchiMiniclave) with an air flow rate of 150 mL/min⁵³. TPAs were prepared according to previously reported procedures⁵⁴.

Synthesis of Complexes V1-V5

In a glove box, a solution of V(O)(O*i*Pr)₃ (0.2 mmol) in dry THF or CH₂Cl₂ (1 mL) was added dropwise to a colorless solution of the corresponding ligand (0.2 mmol) in dry THF or CH₂Cl₂ (3 mL). The color of the solution turned immediately to dark-red (**V1** and **V2**), dark-violet (**V3**) or dark-blue (for **V4** and **V5**). The mixture was stirred for 3 h at RT and then the solvent was evaporated under vacuum leading to a dark-colored crude product, which was recrystallized from CH₂Cl₂/hexane (for **V1-V4**) or CH₂Cl₂/ether (for **V5**). Yields: 81-92%. The following characterizations are in agreement with those reported in literature.

Complex V1⁵⁵: ¹H-NMR (300 MHz, CDCl₃): δ (ppm): 7.23 (d, *J* = 7.3 Hz, 3H), 7.01 (d, *J* = 7.3 Hz, 3H), 6.88 (t, *J* = 7.3 Hz, 3H), 3.76 (bs, 3H), 2.86 (bs, 3H), 1.55 (s, 27H). ¹³C{¹H}-NMR (50 MHz, CDCl₃): δ (ppm): 143.9 (C), 136.5 (C), 128.1 (CH), 126.8 (C), 125.7 (CH), 123.3 (CH), 57.6 (CH₂), 35.3 (C), 29.9 (CH₃). ⁵¹V-NMR (78.28 MHz, CDCl₃): δ -389.21. MS (ESI): *m/z* calc. 568.26 [M+H⁺], found 568.25.

Complex V2³⁴: ¹H-NMR (300 MHz, CDCl₃): δ (ppm): 7.25 (d, *J* = 2.4 Hz, 3H), 7.03 (d, *J* = 2.4 Hz, 3H), 3.86 (d, *J* = 13.1 Hz 3H), 2.88 (d, *J* = 13.1 Hz 3H), 1.56 (s, 27H), 1.30 (s, 27H). ¹³C{¹H}-NMR (75 MHz, CDCl₃): δ 168.67 (C), 147.01 (C), 136.75 (C), 127.50 (C), 125.89 (CH), 123.60 (CH), 59.43 (CH₂), 36.67 (C), 36.06 (C), 33.06 (CH₃), 31.24 (CH₃). ⁵¹V-NMR (78.28 MHz, CDCl₃): δ (ppm): -365.27 ppm. MS (ESI): *m/z* calc. 735.95 [M+H⁺], found 736.00.

⁵³ Rozhko, E.; Raabova, K.; Macchia, F.; Malmusi, A.; Righi, P.; Accorinti, P.; Alini, S.; Babini, P.; Cerrato, G.; Manzoli, M.; Cavani, F. *ChemCatChem* **2013**, 5 (7), 1998.

⁵⁴ Licini, G.; Mba, M.; Zonta, C.; *Dalton Trans.* **2009**, 5265.

⁵⁵ Mba, M.; Pontini, M.; Lovat, S.; Zonta, C.; Bernardinelli, G.; Kündig, E.P.; Licini, G.; *Inorg. Chem.* **2008**, 47, 8616.

Complex V3³⁴: ¹H-NMR (300 MHz, CDCl₃): δ (ppm): 6.78 (d, *J* = 2,8 Hz, 3H), 6.54 (d, *J* = 2.8 Hz, 3H), 3.77 (br s, 3H), 3.77 (s, 3H), 2.83 (br s, 3H), 1.54 (s, 27H). ¹³C{¹H}-NMR (75 MHz, CDCl₃): δ 165.09 (C), 154.93 (C), 138.34 (C), 127.80 (C), 112.15 (CH), 111.64 (CH), 58.07 (CH₂), 55.95(OCH₃), 35.61 (C), 29.93 (CH₃). ⁵¹V-NMR (78.28 MHz, CDCl₃): δ (ppm): -329.94 ppm. MS (ESI): *m/z* calc. 658,71 [M+H⁺], found 657,70.

Complex V4⁵⁶: ¹H-NMR (300 MHz, CDCl₃): δ (ppm): 8.24 (d, *J* = 2,9 Hz, 3H), 8.04 (d, *J* = 2.8 Hz, 3H), 3.48 (s, 3H), 1.60 (s, 27H). ¹³C{¹H}-NMR (75 MHz, CDCl₃): δ 142.81 (C), 126.59 (C), 123.89 (CH), 122.85 (CH), 57.07 (CH₂), 35.75 (C), 29.47 (CH₃). Two quaternary carbons were not detected. ⁵¹V-NMR (78.28 MHz, CDCl₃): δ (ppm): -407.45 ppm. MS (ESI): *m/z* calc. 747.2 [M+HCOO⁻], found 747.0.

Complex V5^{34,57}: ¹H-NMR (300 MHz, ACN-*d*₃): δ (ppm): 7.30 (d, *J* = 2.6 Hz, 3H), 7.03 (d, ³*J*_{HH} = 2.6 Hz, 3H), 3.54 (s, 6H). ⁵¹V-NMR (78.28 MHz, ACN-*d*₃): δ (ppm): -431.09. ⁵¹V-NMR (78.28 MHz, CD₃CN): MS (ESI): *m/z* calc. 637.8 [M+Cl⁻], found 637.8; *m/z* calc. 647.8 [M+HCOO⁻], found 647.9.

Synthesis of Complex V6

Complex V6 was prepared accordingly to literature⁵⁸. In a glove box a solution of V(O)(O*i*Pr)₃ (122 mg, 0.5 mmol) in dry CH₃CN (2 mL) was added dropwise to a suspension of pyridine-2,6-dicarboxylic acid (83.6 mg, 0.5 mmol) in dry CH₃CN (5 mL). The yellow solution formed was stirred at RT overnight. The solvent was evaporated under vacuum leading to a yellow solid, which was recrystallized from CH₂Cl₂/*n*-hexane. Yield: 80 mg, 28%. ¹H-NMR (300 MHz, ACN-*d*₃): δ (ppm): 8.56 (d, *J* = 7.6 Hz, 1H), 8.22 (d, *J* = 7.6 Hz, 2H), 6.33 (sept, *J* = 6.1 Hz, 1H), 1.66 (d, *J* = 6.1 Hz, 6H). ⁵¹V-NMR (78.28 MHz, CDCl₃): δ (ppm): -568.25 ppm.

Synthesis of substrates 1g-j and substrates 1o, 1v

Solution of (*E*)-stilbenes (**1g-j**), norbornene (**1o**) and (*E+Z*)-cyclododecene (**1v**) in ACN/H₂O = 9/1 were treated with *N*-methyl-morpholine-*N*-oxide (NMO) (50% w/w water solution) and OsO₄ (0.2 M in toluene). The reaction was stirred at RT and was monitored by TLC and ¹H NMR. After consumption of the substrate, the mixture was diluted with aq. NaSO₃, extracted with CH₂Cl₂, and the organic layers washed with brine. The organic phase, dried over Na₂SO₄, was then concentrated under vacuum. The crude products were purified by column chromatography on silica gel or by crystallization.

⁵⁶ Zardi, P.; Wurst, K.; Licini, G.; Zonta, C.; *J. Am. Chem. Soc.* **2017**, 139, 15616.

⁵⁷ Miceli, C.; Rintjema, J.; Martin, E.; Escudero-Adàn, E. C.; Zonta, C.; Licini, G.; Kleij, A. W.; *ACS Catal.* **2017**, 7, 2367.

⁵⁸ Thorn, D. L.; Harlow, R. L.; Herron, N.; *Inorg. Chem.* **1996**, 35, 547.

4-((1*R,2*R**)-1,2-dihydroxy-2-phenylethyl)benzaldehyde (±)-1g**

According to the general procedure, (±)-**1g** was synthesized starting from (*E*)-4-styrylbenzaldehyde (1.5 g, 7.21 mmol) using 1% of OsO₄ and NMO (10.82 mmol) in 100 ml of ACN/H₂O = 9/1 solution. After 3 h of at RT the reaction was extracted and the product **1g** purified by column chromatography on silica gel (*n*-hexane/ethyl acetate 8:2), as a colorless oil (350 mg, 20% yield). ¹H NMR (200 MHz, CDCl₃) δ (ppm): 9.83 (s, 1H), 7.64 (d, *J* = 8.0 Hz, 2H), 7.26 – 6.99 (m, 7H), 4.70 (d, *J* = 7.6 Hz, 1H), 4.58 (d, *J* = 7.6 Hz, 1H), 4.03 (s, 1H). ¹³C{¹H}-NMR (50 MHz, CDCl₃) δ (ppm): 192.63, 147.29, 139.67, 135.82, 129.65, 128.45, 127.87, 127.19, 79.18, 78.87. ¹H and ¹³C spectra in CDCl₃ are in agreement with those reported in literature⁵⁹.

Ethyl 4-((1*R,2*R**)-1,2-dihydroxy-2-phenylethyl)benzoate (±)-1h**

According to the general procedure, (±)-**1h** was synthesized from ethyl (*E*)-4-styrylbenzoate (0.5 g, 1.98 mmol) in 80 ml of ACN/H₂O = 9/1 solution using 1% of OsO₄ and NMO (2.98 mmol). After stirring overnight at rt, (±)-**1h** was purified as a white solid by crystallization from *n*-hexane/CH₂Cl₂ (410 mg, 72% yield). ¹H-NMR (200 MHz, CDCl₃) δ (ppm): 7.93 (d, *J* = 8.4 Hz, 2H), 7.36 – 4.40 (m, 7H), 4.81 (d, *J* = 7.4 Hz, 1H), 4.71 (d, *J* = 7.4 Hz, 1H), 4.38 (q, *J* = 7.1 Hz, 2H), 3.96 (brs, 2H), 1.41 (t, *J* = 7.1 Hz, 3H). ¹³C{¹H}-NMR (50 MHz, CDCl₃) δ (ppm): 166.66, 144.98, 139.66, 130.20, 129.52, 128.51, 128.42, 127.14, 79.34, 79.02, 61.18, 14.49. MS (ESI): *m/z* calc. 309.2; exp. 309.11 [M + Na]⁺. Elemental analysis calcd (%) for C₁₇H₁₈O₄: C, 71.31; H, 6.34; found: C 71.76; H 6.32. Mp: 85.7–87.5 °C.

4-((1*R,2*R**)-1,2-dihydroxy-2-phenylethyl)benzotrile (±)-1i**

According to the general procedure, (±)-**1i** was synthesized from (*E*)-4-styrylbenzotrile (0.5 g, 2.44 mmol) using 1% of OsO₄ and NMO (3.66 mmol) in 80 ml of ACN/H₂O = 9/1 solution. After stirring overnight at RT, (±)-**1i** was purified by column chromatography on silica gel (*n*-hexane/ethyl acetate 7:3), affording (±)-**1i** as a white solid (64%). ¹H-NMR (200 MHz, CDCl₃) δ (ppm): 7.43 (d, *J* = 8.1 Hz, 2H), 7.26-7.01 (m, 7H), 4.68 (d, *J* = 8.0 Hz, 1H), 4.53 (d, *J* = 8.0 Hz, 1H), 3.73 (brs, 2H). ¹³C{¹H}-NMR (50 MHz, CDCl₃) δ (ppm): 145.66, 139.42, 131.94, 128.56, 127.96, 127.17, 118.97, 111.41, 79.15, 78.59. Elemental analysis calcd (%) for C₁₅H₁₃NO₂: C 75.30; H 5.48; N 5.85; found: C 75.12; H 5.34, N 5.64. Mp: 89.5-91.5 °C

(1*R,2*R**)-1-(4-bromophenyl)-2-phenylethane-1,2-diol (±)-1j**

According to the general procedure, (±)-**1j** has been synthesized from (*E*)-1-bromo-4-styrylbenzene (0.5 g, 1.93 mmol) using 1% of OsO₄ and NMO (2.89 mmol) in 50 ml of ACN/H₂O = 9/1 solution. After stirring overnight at RT (±)-**1j** was purified by crystallization from *n*-hexane/CH₂Cl₂ (402 mg,

⁵⁹ Lee, B. S.; Mahajan, S.; Janda, K. D.; Tetrahedron Letters **2005**, 46, 4491.

72% yield) as a white solid. ^1H NMR (300 MHz, CDCl_3) δ (ppm): 7.33 (d, $J = 8.3$ Hz, 2H), 7.26 – 6.94 (m, 7H), 4.64 (d, $J = 7.5$ Hz, 2H), 4.59 (d, $J = 7.4$ Hz, 2H), 2.90 (brs, 2H). $^{13}\text{C}\{^1\text{H}\}$ -NMR (75 MHz, CDCl_3) δ (ppm): 141.00, 140.28, 132.66, 130.16, 129.77, 129.66, 128.45, 123.27, 80.58, 79.99. Mp: 100.0-102.5 °C. ^1H and ^{13}C spectra in CDCl_3 are in agreement with those reported in literature⁶⁰.

(1R*,2S*,3R*,4S*)-bicyclo[2.2.1]heptane-2,3-diol 1o

According to the general procedure, **1o** has been synthesized from norbornene (2.076 g, 22.05 mmol) using 1% of OsO_4 and NMO (25.56 mmol) in 50 ml of $\text{ACN}/\text{H}_2\text{O} = 9/1$ solution. After stirring overnight at RT **1o** was purified by crystallization from hot toluene (2.022g, 72% yield) as a white solid. ^1H NMR (300 MHz, CDCl_3) δ (ppm): 3.67 (s, 2H), 2.91 (d, $J = 4.5$ Hz, 2H), 2.13 (s, 2H), 1.75 (d, $J = 10.3$ Hz, 1H), 1.45 (d, $J = 7.9$ Hz, 1H), 1.07 (dd, $J = 13.9, 9.3$ Hz, 1H). $^{13}\text{C}\{^1\text{H}\}$ -NMR (75 MHz, CDCl_3) δ (ppm): 74.96, 43.21, 31.71, 24.65. ^1H and ^{13}C spectra in CDCl_3 are in agreement with those reported in literature⁶¹.

syn-cyclododecane-1,2-diol (\pm)-syn-1v + anti-cyclododecane-1,2-diol (\pm)-anti-1v

According to the general procedure, **1v** has been synthesized from (*E* + *Z*)-cyclododecene (2.064 g, 12.41 mmol) using 1% of OsO_4 and NMO (19.29 mmol) in 90 ml of $\text{ACN}/\text{H}_2\text{O} = 9/1$ solution. After stirring overnight at RT **1o** was purified by column chromatography on silica gel (*n*-hexane/ethyl Acetate 1:1) (2.036g, 82% yield) as a white solid (anti/syn = 65/35). ^1H NMR (200 MHz, CDCl_3 , *syn*) δ (ppm): 3.79 (t, $J = 5.1$ Hz, 2H), 2.53 (s, br, 2H), 1.61-1.51 (m, 2H), 1.42-1.33 (m, 18 H). $^{13}\text{C}\{^1\text{H}\}$ -NMR (50 MHz, CDCl_3) δ (ppm): 73.12, 28.08, 24.56, 24.24, 22.05, 21.89. ^1H NMR (200 MHz, CDCl_3 , *anti*) δ (ppm): 3.67 (s, 2H), 2.62 (s, br, 2H), 1.71-1.68 (m, 2H), 1.42-1.33 (m, 18 H). $^{13}\text{C}\{^1\text{H}\}$ -NMR (50 MHz, CDCl_3) δ (ppm): 71.74, 29.87, 24.10, 23.82, 23.00, 20.75. ^1H and ^{13}C spectra in CDCl_3 are in agreement with those reported in literature⁶².

General Procedure for the synthesis of (2S*,3R*)-octane-2,3-diol ((\pm)-1l) dodecane-1,2-diol ((\pm)-1n), anti-cyclooctane-1,2-diol ((\pm)-anti-1u) and anti-cyclododecane-1,2-diol ((\pm)-anti-1v)

Diols (\pm)-1l, (\pm)-1n, (\pm)-anti-1u and (\pm)-anti-1v were prepared by a two-step procedure based on epoxidation of the commercially available alkenes followed by acid-catalyzed hydrolysis.

To a solution of (*E*)-2-octene, 1-dodecene, (*Z*)-1-cyclooctene and (*E+Z*)-1-cyclododecene in CH_2Cl_2 , *m*-CPBA was added at 0 °C under nitrogen atmosphere. The reactions were warmed to room temperature overnight under stirring and monitored by TLC and GC-MS. After starting material

⁶⁰ Zhang, H.; Feng, D.; Sheng, H.; Ma, X.; Wan, J.; Tang, Q.; *RSC Adv.* **2014**, 4, 6417.

⁶¹ Wu, F.; Mandadapu, V.; Day, A. I.; *Tetrahedron*, **2013**, 69, 9957.

⁶² Minato, M.; Yamamoto, K.; Tsuji, J.; *J. Org. Chem.* **1990**, 55, 766.

consumption, the reaction mixtures were then carefully quenched by dropwise and sequential addition of aqueous NaHCO₃ solution. The residues were extracted with CH₂Cl₂. The organic phase was washed with brine and water, dried over anhydrous NaSO₄ and evaporated in vacuum. The crude was purified either by distillation using the Kugelrohr apparatus or by column chromatography on silica gel affording the title compound.

(±)-*trans*-2,3-octene-oxide

According to the general procedure, (±)-*trans*-2,3-octene-oxide has been synthesized from *trans*-2,3-octene (1,0 g, 8.9 mmol) using *m*-CPBA (2.3 g, 13.4 mmol), in CH₂Cl₂ (60 mL). After stirring at RT overnight, (±)-*trans*-2,3-octene-oxide was purified by distillation using the Kugelrohr apparatus (b.p. 79 °C at 15 torr) a colorless oil in 35 % yield (400 mg). ¹H-NMR (200 MHz, CDCl₃), δ (ppm) = 2.72 (m, 1H), 2.62 (m, 1H), 6.44 (t, *J* = 2.3 Hz, 1H), 1.50-1.27 (m, 11H), 0.89 (t, *J* = 4.0 Hz, 3H). ¹³C{¹H} NMR (50.32 MHz, CDCl₃), δ (ppm) = 60.06, 54.80, 32.20, 31.83, 25.86, 22.77, 17.87, 14.17. GC-MS (IE) = *m/z*: 56(100), 71(50), 85(65), 99(11), 113(8), 127([M-H]⁺, 3). All spectra data are in agreement with those reported in literature⁶³.

1,2-dodecene-oxide

According to the general procedure, (±)-1,2-dodecene-oxide has been synthesized from 1-dodecene (2.274 g, 13.51 mmol) using *m*-CPBA (3.426 g, 19.85 mmol), in CH₂Cl₂ (50 mL). After stirring at RT overnight, (±)-1,2-dodecene-oxide was obtained as a yellowish oil and used without further purification. ¹H-NMR (200 MHz, CDCl₃), δ (ppm) = 2.94-2.85 (m, 1H), 2.74 (t, *J* = 4.5 Hz, 1H), 2.46 (dd, *J* = 5.1, 2.7 Hz, 1H), 1.59-1.45 (m, 2H), 1.27 (s, 16H), 0.88 (t, *J* = 6.4 Hz, 3H). ¹³C{¹H} NMR (50.32 MHz, CDCl₃), δ (ppm) = 58.34, 52.75, 47.44, 32.46, 29.80, 29.70, 29.55, 26.29, 22.92, 14.34. All spectra data are in agreement with those reported in literature⁶⁴.

cys-cyclooctene-oxide

According to the general procedure, cys-cyclooctene-oxide has been synthesized from 1,2-cyclooctene (1.692 g, 15.35 mmol) using *m*-CPBA (3.987 g, 23.10 mmol), in CH₂Cl₂ (50 mL). After stirring at RT overnight, Cyclooctene-oxide was obtained as a yellowish oil and used without further purification (1.289 g, 67% yield). ¹H-NMR (200 MHz, CDCl₃), δ (ppm) = 2.91-2.87 (m, 2H), 2.16-2.11 (m, 2H), 1.63-1.22 (m, 10H). ¹³C{¹H} NMR (50.32 MHz, CDCl₃), δ (ppm) = 55.73, 26.66, 26.40, 25.70. All spectra data are in agreement with those reported in literature⁶⁵.

⁶³ Prat, I.; Font, D.; Company, A.; Junge, K.; Ribas, X.; Beller, M.; Costas, M. *Adv. Synth. Catal.* **2013**, 355, 947.

⁶⁴ Hao, E.; Wang, Z.; Jiao, L.; Wang, S.; *Dalton Trans.* **2010**, 39, 2660.

⁶⁵ Shea, K. J.; Kim, J. S.; *J. Am. Chem. Soc.* **1992**, 114, 3051.

***cys+trans*-1,2-cyclododecene-oxide**

According to the general procedure, *cys+trans*-1,2-cyclododecene-oxide has been synthesized from cyclo1-dodecene (2.589 g, 15.57 mmol) using *m*-CPBA (3.287g, 19.05 mmol), in CH₂Cl₂ (50 mL). After stirring at RT overnight, *cys+trans*-1,2-cyclododecene-oxide was obtained as a yellowish oil and used without further purification (2.467 g, 87 % yield, *cys/trans* = 70/30). ¹H-NMR (200 MHz, CDCl₃, *cys*), δ (ppm) = 2.70 (m, 2H), 2.17 (ddd, *J* = 13.3, 7.2, 2.9 Hz, 2H), 1.63-1.23 (m, 16H), 1.04 (ddt, *J* = 14.9, 10.0, 4.8 Hz, 2H). ¹³C{¹H} NMR (50.32 MHz, CDCl₃), δ (ppm) = 60.02, 31.52, 26.80, 25.69, 24.14, 24.00. ¹H-NMR (200 MHz, CDCl₃, *trans*), δ (ppm) = 2.88 (d, *J* = 9.8 Hz, 2H), 1.81 (dt, *J* = 14.1, 7.2 Hz, 2H), 1.63-1.23 (m, 18H). ¹³C{¹H} NMR (50.32 MHz, CDCl₃), δ (ppm) = 58.26, 26.06, 25.18, 24.21, 23.76, 22.57. All spectra data are in agreement with those reported in literature⁶⁶.

To solutions of *trans*-2-octene-oxide, 1,2-dodecene-oxide, *cys*-1,2-cyclooctene-oxide, *cys+trans*-1,2-cyclododecene-oxide in CH₃CN/H₂O (3:1 v/v), H₂SO₄ was added and the reaction was stirred overnight at room temperature. The reaction course was monitored by TLC and GC-MS. After starting material consumption, an aqueous NaHCO₃ solution was added and the solution was extracted with CH₂Cl₂. The organic phase was washed with brine and water, dried over anhydrous NaSO₄ and evaporated in vacuum. The resulting product was used without any further purification or by purification after column chromatography on silica gel (*n*-hexane/ethyl acetate 1:1).

(2S*, 3R*)-octane-2,3-diol (±)-1l

According to the general procedure, (±)-**1l** has been synthesized from *trans*-2-octene-oxide using H₂SO₄ (125 μL, 2.34 mmol) in ACN/H₂O (3:1 v/v, 6 mL). After stirring at RT overnight, title compound was obtained as a yellowish oil without any further purification (300 mg, 88%). ¹H-NMR (200 MHz, CDCl₃), δ (ppm) = 3.85 (m, 1H), 3.66 (m, 1H), 2.26 (m, 2H), 1.79-1.26 (m, 8H), 1.18 (d, *J* = 6.2 Hz, 3H), 0.93 (t, *J* = 6.2 Hz, 3H). ¹³C{¹H} NMR (50.3 MHz, CDCl₃), δ (ppm) = 74.97, 70.46, 31.87, 31.78, 25.69, 22.68, 16.61, 14.03. GC-MS (EI) = *m/z*: 131(M⁺-CH₃, 9), 101(40), 83(100), 55(80). All spectra data are in agreement with those reported in literature⁶³.

Dodecane-1,2-diol (±)-1n

According to the general procedure, (±)-**1n** has been synthesized from 1,2-dodecene-oxide (2.099 g, 11.39 mmol) using H₂SO₄ (1.127 g, 11.49 mmol) in ACN/H₂O (3:1 v/v, 30 mL). After stirring at RT overnight, title compound was obtained as a white solid (1.870 g, 98%) after purification by column chromatography on silica gel (*n*-hexane/ethyl acetate 1:1). ¹H-NMR (200 MHz, CDCl₃), δ (ppm) = 3.72-3.59 (m, 2H), 3.47-3.35 (m, 1H), 2.91 (s, br, 2H), 1.42-1.39 (m, 2H), 1.25 (s, 16H), 0.87 (t, *J* = 6.2 Hz, 3H). ¹³C{¹H} NMR (50.3 MHz, CDCl₃), δ (ppm) = 72.50, 67.00, 33.36, 32.05, 29.80, 29.74,

⁶⁶ Altinis Chiraz, C. I.; Mora, L.; Jimenez, L. S.; *Synthesis* **2007**, 1, 92.

29.69, 29.47, 25.69, 22.82, 14.24. All spectra data are in agreement with those reported in literature⁶⁷.

Anti-cyclooctane-1,2-diol (\pm)-1u

According to the general procedure, (\pm)-**1u** has been synthesized from *cis*-1,2-cyclooctene-oxide (1.289 g, 10.22 mmol) using H₂SO₄ (1.082 g, 11.03 mmol) in ACN/H₂O (3:1 v/v, 30 mL). After stirring at RT overnight, title compound was obtained as a yellowish oil (0.799 g, 54%) after purification by column chromatography on silica gel (*n*-hexane/ethyl acetate 1:1). ¹H-NMR (200 MHz, CDCl₃), δ (ppm) = 3.59 (m, 2H), 2.14 (s, 2H), 1.85-1.82 (m, 2H), 1.71-1.53 (m, 10H) ¹³C{¹H} NMR (50.3 MHz, CDCl₃), δ (ppm) = 76.24, 31.98, 26.28, 23.85. All spectra data are in agreement with those reported in literature⁶⁸.

Anti-cyclododecane-1,2-diol (\pm)-1v

According to the general procedure, (\pm)-**1v** has been synthesized from *cis+trans*-1,2-cyclododecene-oxide (2.467 g, 13.53 mmol) using H₂SO₄ (1.262 g, 12.87 mmol) in ACN/H₂O (3:1 v/v, 30 mL). After stirring at RT overnight, title compound was obtained as colorless needles (0.496 g, 18%) after purification by crystallization from hot MeOH. ¹H-NMR (200 MHz, CDCl₃), δ (ppm) = 3.80-3.79 (m, 2H), 1.73-1.45 (m, 6 H), 1.44 (s, 4H), 1.33 (s, 12H). ¹³C{¹H} NMR (50.3 MHz, CDCl₃), δ (ppm) = 73.15, 28.12, 24.58, 24.26, 22.07, 21.89. Mp: 106-108 °C, literature reports Mp: 105-107 °C⁶⁹.

Synthesis of acetals 7a-b and 8a-b

2,4-dibutyl-1,3-dioxolane (7a-b) (mixture of *cis/trans* diastereoisomers)

To a mixture of hexane-1,2-diol (1.122 g, 9.50 mmol) and pentanal (0.810 g, 9.40 mmol), *p*-TsOH (19 mg, 0.1 mmol) was added and the mixture was heated at 80°C under a N₂ atmosphere ON. After reaction completion (GC-MS and TLC), the mixture was evaporated to dryness and the crude was purified by column chromatography (*n*-hexane/ethyl acetate 19:1). Title compound was obtained as a colorless oil (0.548 g, 29 % yield). ¹H-NMR (300 MHz, CDCl₃), δ (ppm) = 4.96 (t, 1H, *J* = 4.8 Hz, *minor diastereoisomer*), 4.88 (t, 1H, *J* = 4.7 Hz, *major diastereoisomer*), 4.09-3.88 (m, 2H), 3.50-3.40 (m, 1H), 1.67-1.34 (m, 12H), 0.91 (t, 6H, *J* = 6.7 Hz). ¹³C{¹H}-NMR (50.3 MHz, CDCl₃), δ (ppm) = 104.80 (CH) (*major diastereoisomer*), 104.07 (CH) (*minor diastereoisomer*), 76.92 (CH) (*major diastereoisomer*), 76.16 (CH) (*minor diastereoisomer*), 70.70 (CH₂) (*minor diastereoisomer*), 69.78 (CH₂) (*major diastereoisomer*), 34.16 (CH₂) (*minor diastereoisomer*), 34.04 (CH₂) (*major diastereoisomer*), 33.37 (CH₂) (*major diastereoisomer*), 33.18 (CH₂) (*minor diastereoisomer*), 28.03

⁶⁷ Wu, X.; Cruz, F. A.; Lu, A.; Dong, V. M.; *J. Am. Chem. Soc.* **2018**, 140, 10126.

⁶⁸ Rosatella, A. A.; Afonso, C. A. M.; *Adv. Synth. Catal.* **2011**, 353, 2920.

⁶⁹ Svoboda, M.; Sicher, J.; *Collection Czechoslov. Chem. Commun.* **1957**, 1540.

(CH₂), 26.32 (CH₂), 22.82 (CH₂), 14.11 (CH₃). GC-MS (EI): 129 (M⁺-C₄H₉, 100), 83 (74), 71 (17), 55 (57).

2,4-di-*n*-decyl-1,3-dioxolane (8a-b) (mixture of *cis/trans* diastereoisomers)

To a solution of dodecane-1,2-diol (214.58 mg, 1.06 mmol) and undecanal (180.59 mg, 1.06 mmol), in dry toluene (10 mL), *p*-TsOH (1.90 mg, 0.01 mmol) was added and the mixture was refluxed under a N₂ atmosphere using a Dean-Stark apparatus ON. After reaction completion (GC-MS and TLC), the mixture was evaporated to dryness and the crude was purified by column chromatography (n-hexane/ethyl acetate 9:1). Title compound was obtained as a colorless oil (188 mg, 50 % yield). ¹H-NMR (300 MHz, CDCl₃): 4.95 (t, *J* = 4.8 Hz, 1H, *minor diastereoisomer*), 4.87 (t, *J* = 4.7 Hz, 1H, *major diastereoisomer*), 4.09-3.88 (m, 2H), 3.49-3.40 (m, 1H), 1.66-1.59 (m, 4H), 1.41-1.26 (m, 32H), 0.88 (t, 6H, *J* = 6.6 Hz). ¹³C{¹H}-NMR (50.3 MHz, CDCl₃), δ (ppm) = 104.80 (CH) (*major diastereoisomer*), 104.07 (CH) (*minor diastereoisomer*), 76.92 (CH) (*major diastereoisomer*), 76.17 (CH) (*minor diastereoisomer*), 70.69 (CH₂) (*minor diastereoisomer*), 69.78 (CH₂) (*major diastereoisomer*), 34.47 (CH₂) (*minor diastereoisomer*), 34.34 (CH₂) (*major diastereoisomer*), 33.69 (CH₂) (*major diastereoisomer*), 33.48 (CH₂) (*minor diastereoisomer*), 32.05 (CH₂), 29.72 (CH₂), 29.47 (CH₂), 25.88 (CH₂), 24.19 (CH₂), 22.82 (CH₂), 14.24 (CH₃). GC-MS: 213 (M⁺-C₁₀H₂₁, 100), 111 (18), 97 (31), 83 (26), 69 (26), 55 (21).

General Procedure for catalytic aerobic C-C oxidative cleavage of 1,2-diols 1a-s

Catalytic aerobic oxidation of *meso*-hydrobenzoin (1b) for catalyst, solvents, catalyst loading and solvent screening, (Tables 2.1-2.5)

Procedure at atmospheric pressure: In a 2 ml volumetric flask, *meso*-hydrobenzoin **1b** (1.0-0.1 mmol), vanadium catalyst (**V1-V5**, **V6**, VO(OiPr)₃, VO(acac)₂) and naphthalene or biphenyl as internal standard, taken from stock solutions, were added in a 1 ml solution of the solvent of choice. The solution was made up to a 2.0 ml volume and transferred into a 20 mL reactor equipped with a stirring bar, condenser, in an air or oxygen atmosphere (balloon). The reactor was heated (silicon oil bath with a temperature control) under magnetic stirring to the desired temperature (80°C, 100°C or 130°C). The reaction course was monitored *via* quantitative HPLC analysis. All compounds were identified by comparison of their retention time with pure standards.

Procedure under high pressure: In a 100 mL glassy reactor-vessel (BuchiMiniclave), equipped with stirring bar, condenser and an air/N₂ inlet and outlet line with bubbling septum, *meso*-hydrobenzoin **1b** (15 mmol, 3,210 g) and naphthalene as internal standard were added in toluene (25 mL). The reactor was heated (silicon oil bath with temperature control) to 100°C under N₂ atmosphere. At 100°C N₂ was then substituted by an air flow. **V5** was injected (0.1-0.001% in 5 mL of toluene) and

the resulting solution was pressurized at 4 atm of air. The reactor was continuously fed with an air flow (150 mL/min). The reaction course was monitored via quantitative HPLC analysis by sampling the solution during time. At the end of the reaction, the solution was cooled at RT, under inert atmosphere.

WARNING: oxygen-toluene mixture flammability range should be taken into account when performing the reactions at high pressure²⁶

Aerobic oxidative carbon-carbon bond cleavage of diols 1a-v. Scope of the reaction (Tables 2.6-2.10)

In a 10 ml volumetric flask, substrate (**1a-v**) (0.5 or 2.5 mmol), **V5** or VO(acac)₂ (2 or 10 mol %) and, eventually an internal standard (naphthalene or 1,3,5-trimethoxybenzene), were added in 5 ml of solvent solution. The solution was made up to 10 ml volume and transferred into a 20 mL reactor, equipped with a stirring bar, condenser under air or oxygen atmosphere (balloon). After heating under stirring to 80°C or 100°C, the reaction course was monitored by quantitative HPLC or ¹H NMR analysis or GC. Conversions and chemical yields were determined on the crude of the reaction by quantitative HPLC or GC or ¹H NMR. After complete substrate conversion, the reaction mixtures were concentrated under vacuum and purified over a silica gel column to remove the catalyst and impurities. More volatile products were separated by distillation.

According to the general procedure, **2b** was obtained from the cleavage of **1b** (107.13 mg, 0.5 mmol) using **V5** (6.06 mg, 0.01 mmol, 2 mol%). After complete conversion, product **2b** was purified by column chromatography on silica gel (*n*-pentane: CH₂Cl₂ = 4:1 to CH₂Cl₂ only), and obtained as a colorless oil (96.52 mg, 90 % yield).

Aerobic oxidative carbon-carbon bond cleavage of diol 1b: example on preparative scale

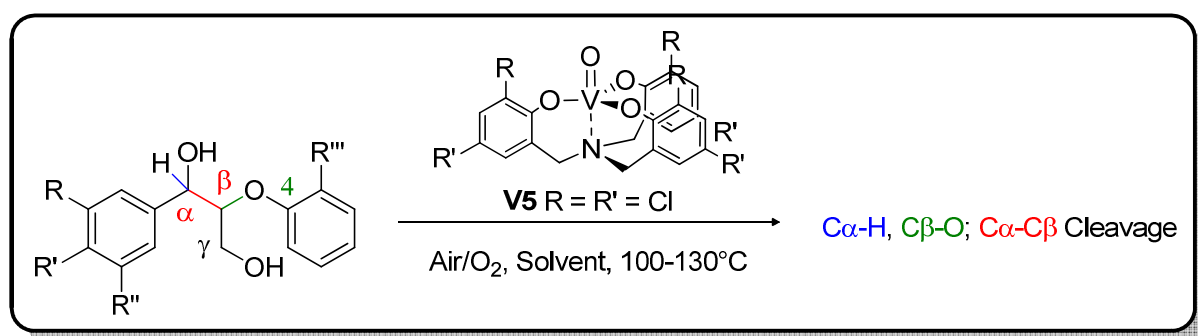
According to general procedure, **1b** (535,65 mg, 2,5 mmol) and **V5** (30,30 mg, 0.05 mmol, 2 mol %) were mixed in a 10 mL volumetric flask and added to 5 mL of toluene. The solution was made up to 10 ml volume and transferred into a 20 mL reactor, equipped with a stirring bar, condenser under oxygen atmosphere (balloon). After heating under stirring 100°C, the reaction course was monitored by GC-MS. After complete substrate conversion, the reaction mixture was purified over a silica column (*n*-pentane: CH₂Cl₂ = 4:1 to CH₂Cl₂ only) to remove the catalyst and impurities, and to afford **2b** as a colorless oil (450.83 mg, 85 % yield).

General Procedure for catalytic aerobic oxidation of aldehydes 2b, 2n

In a 2 ml volumetric flask, benzaldehyde **2b** or undecanal (2.0-0.5 mmol), vanadium catalyst (**V4-V5**, VO(acac)₂) and naphthalene or biphenyl as internal standard, taken from stock solutions, were added in a 1 ml solution of the solvent of choice. The solution was made up to a 2.0 ml volume and transferred into a 20 mL reactor equipped with a stirring bar, condenser, in an air or oxygen atmosphere (balloon). The reactor was heated (silicon oil bath with a temperature control) under magnetic stirring to the desired temperature (100°C or 130°C). The reaction course was monitored *via* quantitative HPLC or GC analyses. All compounds were identified by comparison of their retention time with pure standards.

Chapter 3

Selective Aerobic Oxidation of β -O-4 Lignin Models catalyzed by Vanadium Complexes

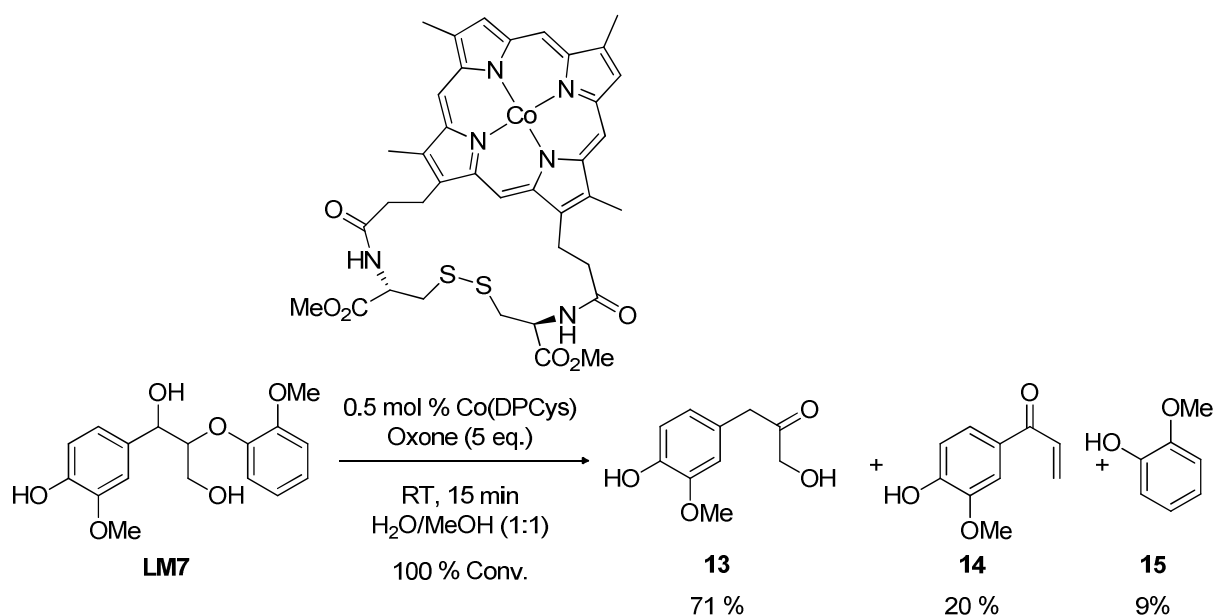


A selective aerobic catalytic degradation method based on Vanadium(V) aminotriphenolate complexes **VO-TPA(R,R')** for dimeric and trimeric β -O-4 Lignin model compounds has been developed. Among all the catalysts investigated, **V5** showed the best performances and its reactivity has been studied in more detail. Effects of solvent, temperature, substrate concentration, catalyst loading and oxidant (air or O₂) have also been examined, showing that in toluene at 100°C under oxygen we were able to obtain faster reactions. In every case the selectivity was strongly directed towards benzylic oxidation (C α -H cleavage, 50-85 % selectivity), but when lowering catalyst loading to 1 mol % and rising substrate concentration to 0.25 M we could obtain an unprecedented high selectivity towards C α -C β cleavage (up to 32 %). The activity of **V5** was also tested with a non-phenolic trimeric β -O-4 model, showing results in line with those obtained for dimeric models (selectivity for C α -H cleavage, 51-70 %, C α -C β cleavage, 12-20 % and C β -O cleavage, 15-30 %). Phenolic β -O-4 lignin models were also tested, affording mainly C α -H cleavage products (16-32 %). Finally, aerobic oxidation of model analogues have been performed in order to clarify the importance of α -OH groups or γ -OH groups in the benzylic oxidation.

3.1: Introduction

3.1.1 Lignin Oxidative Depolymerization

Among the several techniques for lignin valorization, oxidative depolymerization is particularly interesting because it leads to the formation of highly valuable aromatic carbonyl compounds. Moreover, reactions are more robust and do not require the use of inert atmosphere or low pressures, since only inexpensive oxidants such as peroxides, oxygen or air are typically used as oxidants. Catalytic approaches in this field can draw inspiration from nature, since it has been discovered that oxidative depolymerization is the election technique chosen by living organisms which are able to digest lignin. For example, several white-rot fungi are capable of degrading lignin through lignin peroxidase¹, manganese peroxidase² or laccase enzymes. Early reports on lignin models oxidative degradation were therefore devoted to the use of biomimetic catalysts such as iron, cobalt and manganese porphyrins. Although these examples resulted in an unselective degradation of β -O-4 models and low yields of desired products¹ Ying and co-workers were able to employ Co-based deuteroporphyrins as biomimetic catalysts for oxidative depolymerization of **LM7**, in presence of Oxone[®] ($2 \text{ KHSO}_5 \times \text{KHSO}_4 \times \text{K}_2\text{SO}_4$) (Eq. 3.1)³.



Eq. 3.1: Oxidative degradation of phenolic lignin models by Co deuteroporphyrin catalyst.

Analogous to metalloporphyrins, Co-Salen complexes are well-known to activate O_2 to form Co-superoxo species that could be used in oxidative degradation of lignin-like models⁴. In particular,

¹ a) Tien, M.; Kirk, T. K.; *Proc. Natl. Acad. Sci. U.S.A.* **1984**, 81, 2280. b) Kuwahara, M.; Glenn, J. K.; Morgan, M. A.; Gold, M. H.; *FEBS Lett.* **1984**, 169, 247.

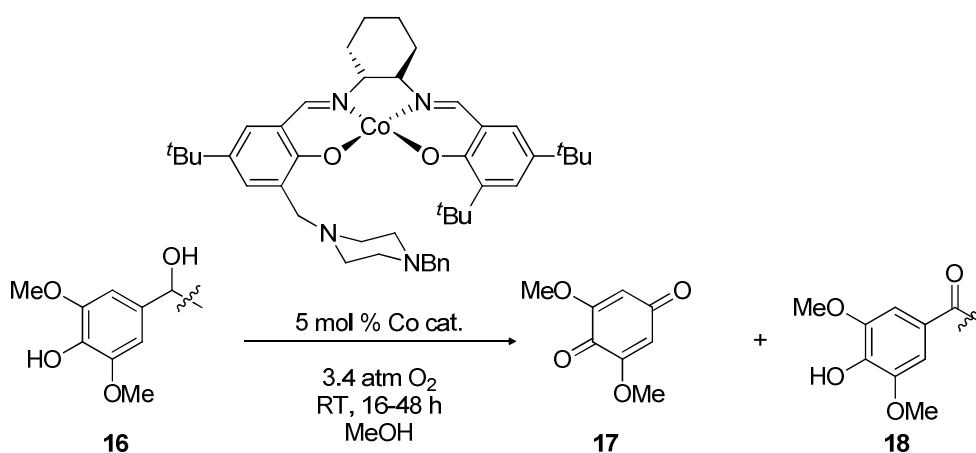
² a) Gasser, C. A.; Hommes, G.; Schäffer, A.; Corvini, P. F-X.; *Appl. Microbiol. Biotechnol.* **2012**, 95, 1115.

b) Hofrichter, M.; *Enzyme Microb. Technol.* **2002**, 30, 454.

³ Zhu, C.; Ding, W.; Shen, T.; Tang, C.; Sun, C.; Xu, S.; Chen, Y.; Wu, J.; Ying, H.; *ChemSusChem* **2015**, 8, 1768.

⁴ Drago, R. S.; Corden, B. B.; Barnes, C. W.; *J. Am. Chem. Soc.* **1986**, 108, 2453.

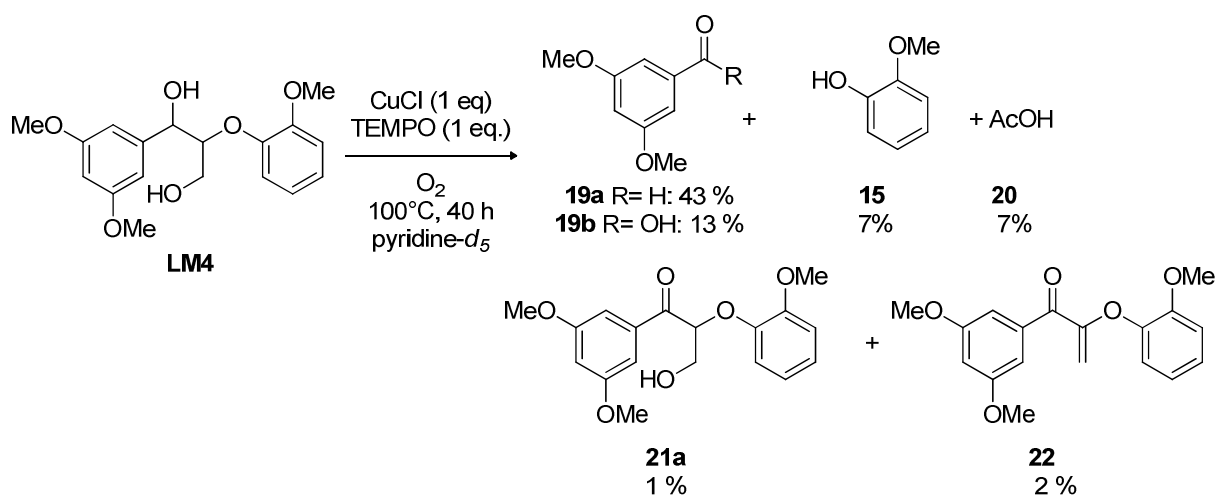
Bozell et al. designed a new class of unsymmetrical Co Salen complexes bearing a sterically encumbered base within the ligand scaffold⁵. These systems were able to afford benzoquinones in high yields from the oxidation of phenolic β -O-4 lignin models (Eq.3.2)



Eq. 3.2: Co-Schiff base catalyzed aerobic oxidation of phenolic β -O-4 bond models.

This system was also employed on organosolv lignin, but the yields of monomeric species derived from depolymerization were rather low (3.5 %)^{5a}.

Considering that the primary pathway for lignin oxidative degradation in nature involves a single electron transfer⁶, several TEMPO-mediated oxidation reactions have been developed in order to find an efficient lignin depolymerization strategy. Another step of such strategy was the coupling with O₂ as terminal oxidant, since it's abundant, inexpensive and environmentally benign. Originally, a Cu/TEMPO system was developed by Hanson et al. for the degradation of **LM4** (Eq. 3.3). In this catalytic system, Cu is believed to activate O₂, whereas TEMPO promotes alcohol oxidation⁷.



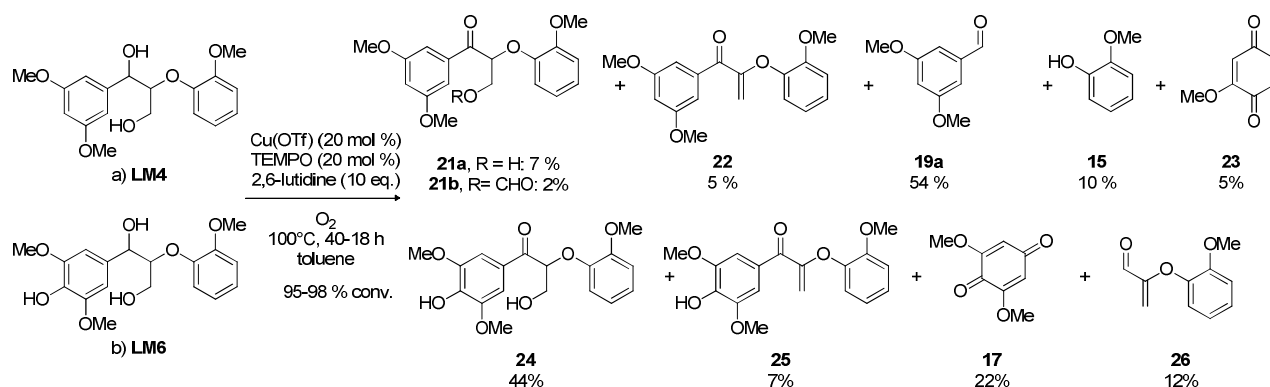
Eq 3.3: Stoichiometric oxidation of **LM4** with CuCl/TEMPO.

⁵ a) Biannic, B.; Bozell, J. J.; *Org. Lett.* **2013**, 15, 2730. b) Biannic, B.; Bozell, J. J.; Elder, T.; *Green Chem.* **2014**, 16, 3635.

⁶ a) Schoemaker, H. E.; Harvey, P. J.; Bowen, R. M.; Palmer, J. M.; *FEBS Lett.* **1985**, 183, 7. b) Tien, M.; Kirk, T. K.; *Science*, **1983**, 221, 661.

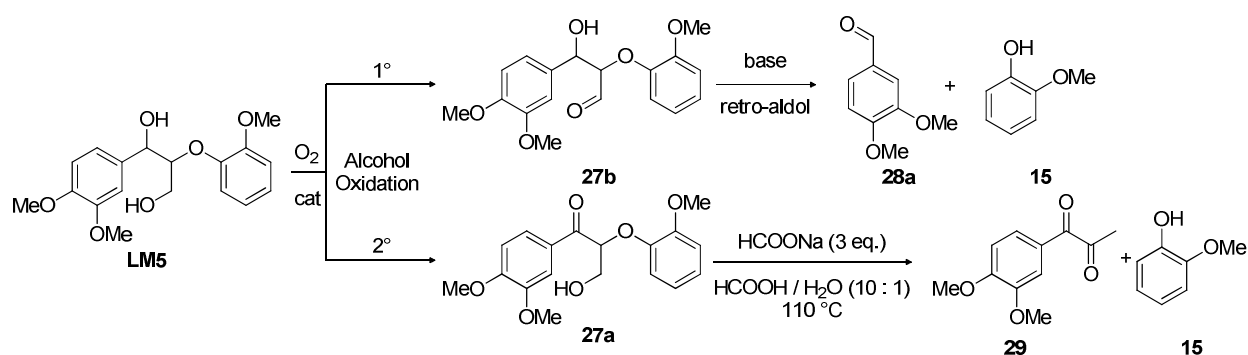
⁷ Sedai, B.; Diaz-Urrutia, C.; Baker, R. T.; Wu, E.; Silks, L. A. P.; Hanson, S. K.; *ACS Catal.* **2011**, 1, 794.

However, the yields were poor with low selectivity and several side products were originated from the reaction mixture. Baker and co-workers subsequently optimized the system, using a Cu(OTf) / TEMPO system in presence of 2,6-lutidine (10 equiv.) in toluene. The reaction yielded 54 % of 3,5-dimethoxybenzaldehyde **19a**⁸ (Eq. 3.4a). This system is also active on the phenolic model **LM6**, affording in this case a selectivity directed towards benzylic oxidation, rather than C_α-C_β cleavage (Eq 3.4 b).



Eq 3.4: Catalytic oxidation of **LM4** (a) and **LM6** (b) by Cu(OTf)/TEMPO/2,6-lutidine system.

Stahl and co-workers developed a metal-free strategy for a two-step oxidation and depolymerization of **LM5** and aspen lignin (Scheme 3.1)⁹. Indeed, oxidation of β-O-4 bonds can occur either on primary hydroxy groups (γ-OH) or secondary hydroxy groups (α-OH), leading to different subsequent cleavage mechanisms and quite different aromatic products. When the γ-OH was oxidized to an aldehydic group, C-C cleavage could be induced via retro-aldol reaction, producing guaiacol and aromatic aldehydes. On the other hand, if the oxidation takes place in α-OH, the corresponding ketone could be degraded to monomeric compounds by HCOOH / HCOONa in an almost quantitative yield¹⁰ (Scheme 3.1).



Scheme 3.1: Chemoselective alcohol oxidation strategies for lignin models⁹.

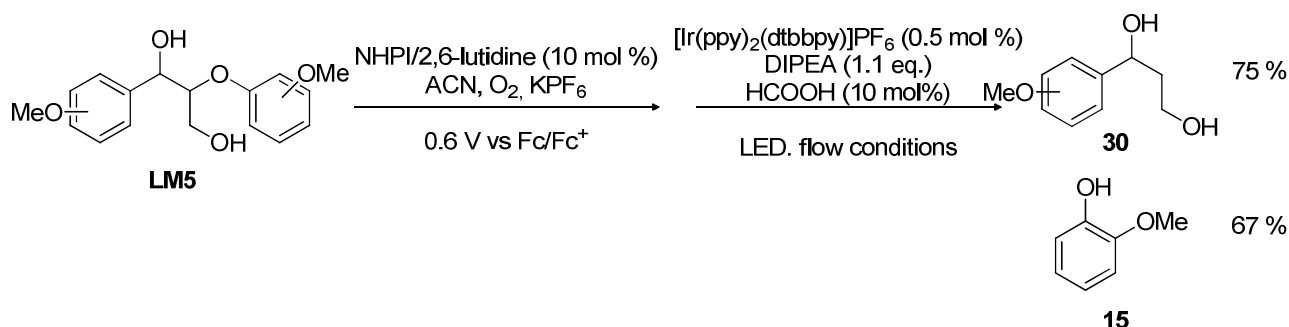
More recently, other approaches based on photoredox catalysis have been developed. As an example, Stephenson et al. reported a combined electro / photoredox catalyzed process using a

⁸ Sedai, B.; Baker, R. T.; *Adv. Synth. Catal.* **2014**, 356, 3563.

⁹ Rahimi, A.; Azarpira, A.; Kim, H.; Ralph, J.; Stahl, S. S.; *J. Am. Chem. Soc.* **2013**, 135, 6415.

¹⁰ Rahimi, A.; Ulbrich, A.; Coon, J. J.; Stahl, S.S.; *Nature* **2014**, 515, 249.

dual wavelength switching strategy for oxidation of α -OH followed by cleavage of β -O-4 bonds at room temperature with a very good yield (Scheme 3.2)¹¹.



Scheme 3.2: One-pot electrocatalytic oxidation and photocatalytic cleavage of β -O-4 lignin models.

A similar procedure developed by the same research group required $\text{Pd}(\text{OAc})_2$ / DMSO in the benzylic oxidation step, and afforded higher overall product yields¹².

3.1.2 Vanadium (V) Complexes in Lignin Oxidative Depolymerization

Currently, Vanadium-based catalysts are the most extensively investigated for lignin oxidation¹³. Moreover, throughout the last few years the studies regarding Vanadium complexes showed that their reactivity is variable, depending on the substrate, ligand stereoelectronic properties, activation conditions (thermal or photoinduced), and anaerobic or aerobic conditions¹⁴. These features provide opportunities for enlarging the ligand library in order to optimize both the activity and the selectivity for lignin oxidative depolymerization. One of first examples of an oxovanadium tridentate salen catalyst **V9** for aerobic oxidation of β -O-4 model **LM5a** was reported by Toste and co-workers¹⁵. This system afforded mainly products **30** and guaiacol **15** deriving from non-oxidative C_β -O bond cleavage (Eq. 3.5) with good overall yields. A discrete amount of ketone **31** formed by C_α -H Cleavage (benzylic oxidation) was also detected.

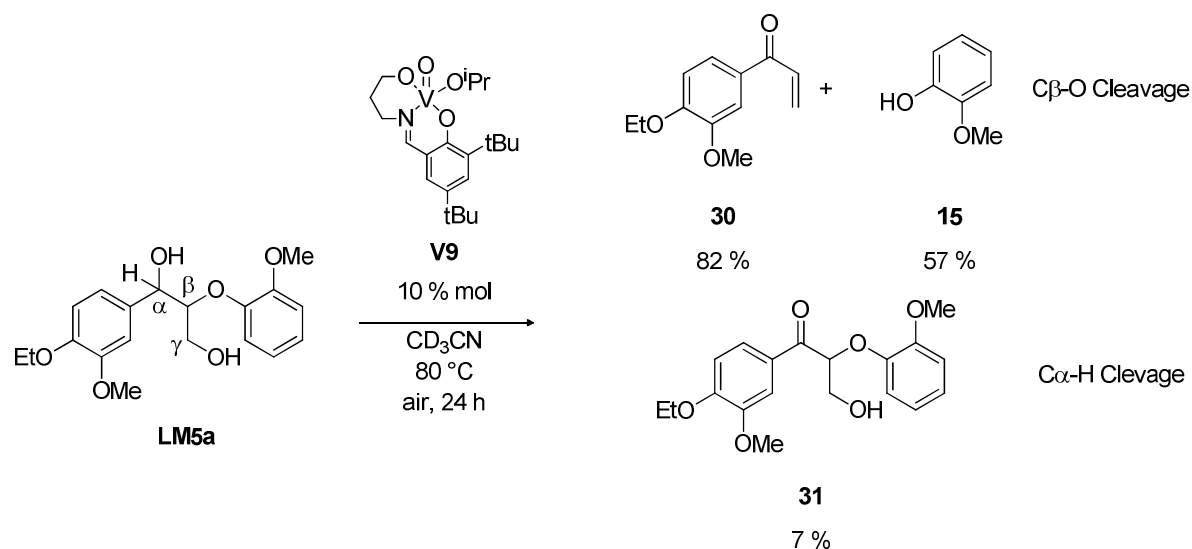
¹¹ a) Kärkäs, M. D.; Bosque, I.; Matsuura, B. S.; Stephenson, C. R. J.; *Org. Lett.* **2016**, 18, 5166. b) Bosque, I.; Magallanes, G.; Rigoulet, M.; Kärkäs, M. D.; Stephenson, C. R. J.; *ACS Cent. Sci.* **2017**, 3, 621.

¹² Magallanes, G.; Kärkäs, M. D.; Bosque, I.; Lee, S.; Maldonado, S.; Stephenson, C. R. J.; *ACS Catal.* **2019**, 9, 2252.

¹³ Wang, M.; Ma, J.; Liu, H.; Luo, N.; Zhao, Z.; Wang, F.; *ACS Catal.* **2018**, 8, 2129.

¹⁴ a) da Silva, J. A. L.; Fraústo da Silva, J. J. R.; Pombeiro, A. J. L.; *Coord. Chem. Rev.* **2011**, 255, 2232. b) Hirao, T.; *Coord. Chem. Rev.* **2003**, 237, 271.

¹⁵ Son, S.; Toste, F. D.; *Angew. Chem. Int. Ed.* **2010**, 49, 3791.



Eq. 3.5: Vanadium Catalyzed C_β-O bond cleavage reaction. Adapted from ref. 16.

This model was also subjected to the action of several other Vanadium complex **V10-V12** and commercially available Vanadium salts and complexes (VO(OⁱPr)₃, VOSO₄ x n H₂O, VO(acac)₂)¹⁷ under the same reaction conditions (Table 3.1).

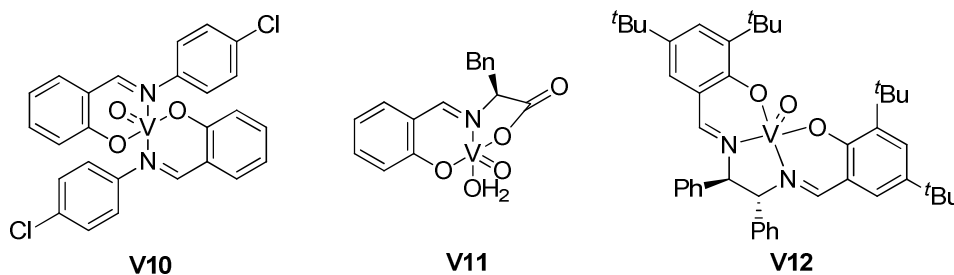


Table 3.1: Aerobic oxidation of **LM5a** catalyzed by Vanadium complexes. Product distribution.

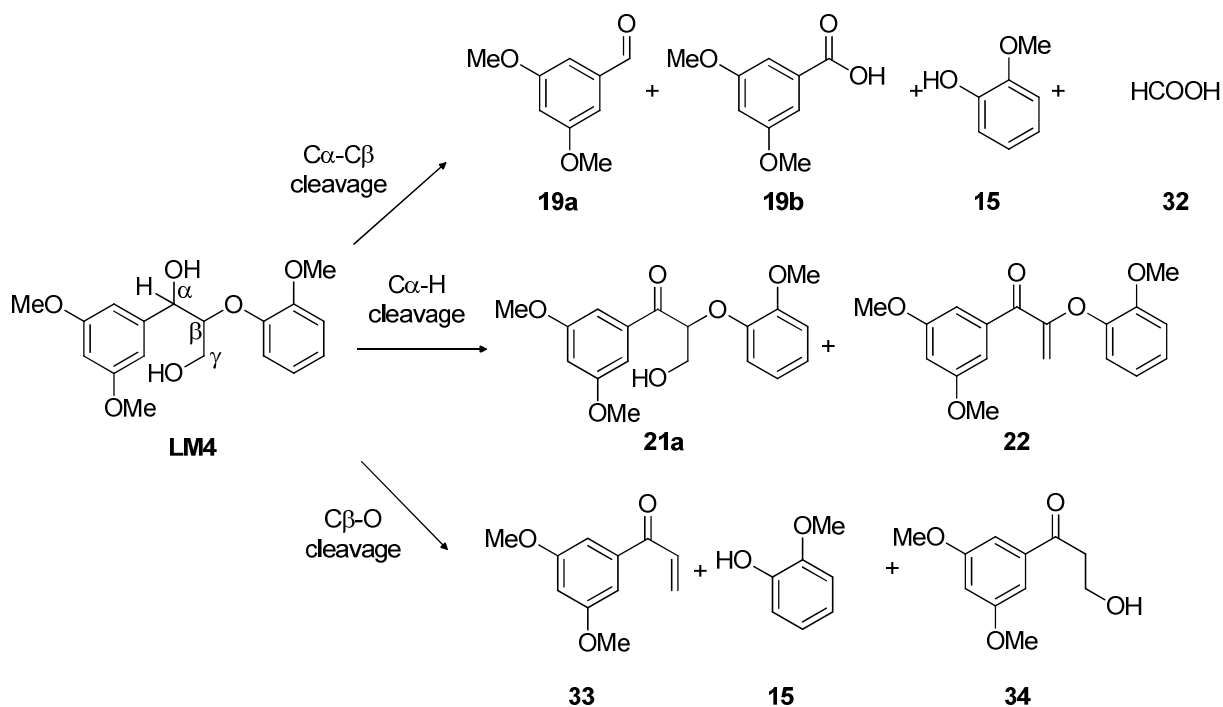
Entry	Catalyst	Conv. (%)	Yield (%)		
			C _α -H Cleavage	C _β -O Cleavage	
			31	30	15
1	VO(O ⁱ Pr) ₃	82	45	5	11
2	VOSO ₄ x n H ₂ O	34	6	2	2
3	VO(acac) ₂	79	31	13	22
4	V9	>95	7	82	57
5	V10	86	59	6	6
6	V11	66	41	13	14
7	V12	55	37	3	0

Conditions: [**LM5a**]₀ = 0.1 M, 10 % mol catalyst, 80 °C, 24 h, CD₃CN, under air.

¹⁶ Hanson, S. K.; Baker, R. T.; *Acc. Chem. Res.* **2015**, 48, 2037.

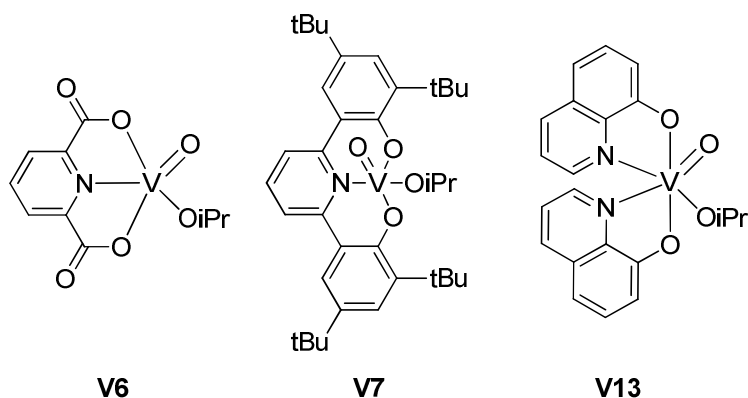
¹⁷ Chan, J. M. W.; Bauer, S.; Sorek, H.; Sreekumar, S.; Wang, K.; Toste, F. D. *ACS Catal.* **2013**, 3, 1369.

It is interesting to note that all complexes except **V9** yielded ketone **31** as the major product, and only little amounts of products coming from C_β-O cleavage **30** and **15** were detected in the reaction mixture. Also, no amount of C_α-C_β cleavage deriving products (aldehydes or carboxylic acids) were detected. Parallel to this study, Hanson and co-workers^{7,18,19} reported that when using **LM4**, also products coming from C-C cleavage were formed, according to Eq. 3.6.



Eq 3.6: Products obtained by aerobic oxidation of model **LM4**, catalyzed by Vanadium Complexes²⁰.

In this case, several Vanadium complexes have been tested, namely VO(OⁱPr)₃, **V6**, **V7** and **V13**, under several reaction conditions (Table 3.2).



¹⁸Zhang, G.; Scott, B. L.; Wu, R.; Silks, L. A.; Hanson, S. K. *Inorg. Chem.* **2012**, 51, 7354.

¹⁹Hanson, S. K.; Wu, R.; Silks, L. A. P.; *Angew. Chem. Int. Ed.* **2012**, 51, 3410.

²⁰Amadio, E.; Di Lorenzo, R.; Zonta, C.; Licini, G.; *Coord. Chem. Rev.* **2015**, 301-302, 147.

Table 3.2: Aerobic oxidation of **LM4** catalyzed by Vanadium complexes. Product distribution.

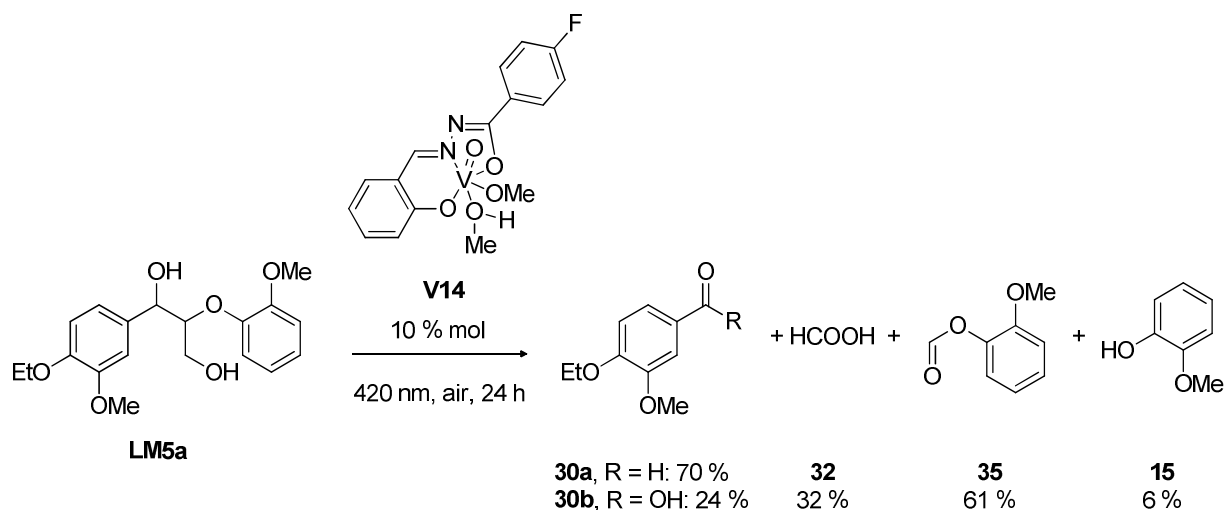
Entry	Catalyst	Solvent	Conv. (%)	Yield (%)						
				C _α -C _β Cleavage			C _α -H Cleavage		C _β -O Cleavage	
				19a	19b	32	21a	22	33	34
1	VO(O ⁱ Pr) ₃	DMSO- <i>d</i> ₆	75	7	12	7	39	-	16	-
2	V6	DMSO- <i>d</i> ₆	>95	2	11	4	65	5	14	-
3	V6	Pyridine- <i>d</i> ₅	85	4	6	<1	27	14	29	-
4	V7	Toluene- <i>d</i> ₈	84	4	6	4	27	-	26	14
5	V13^a	Pyridine- <i>d</i> ₅	65	-	-	-	55	10	-	-

Conditions: [**LM4**]₀ = 0.104-0.086 M, 10 % mol catalyst, 100 °C, 48 h, under air. ^a [**LM4**]₀ = 0.67 M, 10 % mol catalyst, 100 °C, 48 h, under air.

Unlike **LM5a**, in this case, depending on the Vanadium complex used, both C_α-C_β, C_α-H and C_β-O cleavage were obtained. Table 3.2 shows also that different complexes shows a different selectivity as already pointed out, and in all cases the selectivity was directed towards benzylic oxidation (27-70 %). C_α-C_β cleavage was seen in all cases except for **V13**, which afforded only benzylic oxidation products, even if in only a tiny amount (2-18 %). Moreover, a change in solvent from DMSO to pyridine led to a different selectivity, with a higher yield of product **33** coming from C_β-O cleavage. One last thing that is worth noting is that in all cases quite harsh reaction conditions are required: pyridine or DMSO as solvents, high temperatures, high catalyst loading (10%), and complete substrate conversion can be obtained only after long reaction times (up to a week). Therefore, an effective catalyst for oxidative degradation of lignin/lignin models is a goal that is still far from being reached.

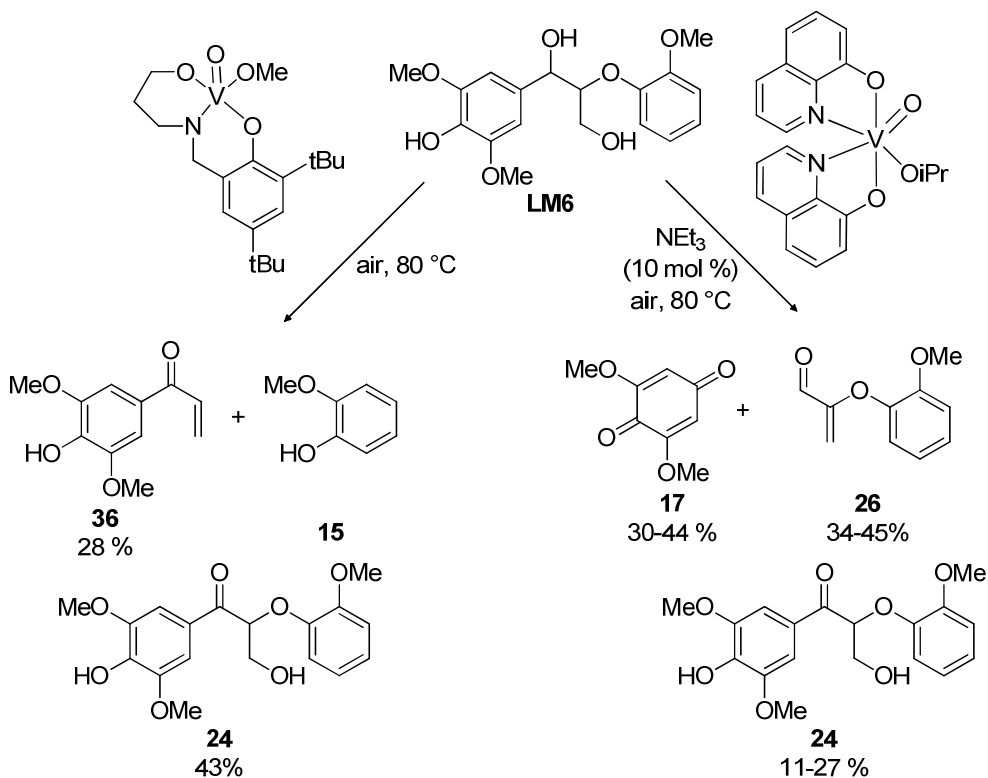
Besides thermal activation, also photocatalysis based on Vanadium complexes has been explored so far in order to efficiently depolymerize β-O-4 linkages. Hirao and co-workers reported for a Vanadium (V) species **V14** that effectively realized chemoselective cleavage of C_α-C_β bonds under visible light (>420 nm) (Eq. 3.7). After 24 h of reaction, aromatic aldehydes and aromatic acids were obtained in a high yield.²¹

²¹ Gazi, S.; Ng, W. K. H.; Ganguly, R.; Moeljadi, A. M. P.; Hirao, H.; Soo, H. S.; *Chem Sci.* **2015**, *6*, 7130.



Eq. 3.7: Photocatalytic degradation of β -O-4 lignin model.

From these studies, it emerged that i) the nature of the ligand, ii) the substrates and iii) the reaction conditions (thermal or photochemical activation) play a fundamental role in determining the selectivity of the depolymerization process. This can be appreciated also when considering a phenolic model **LM7**, whose oxidation based on different Vanadium complexes afforded different products (Scheme 3.3)

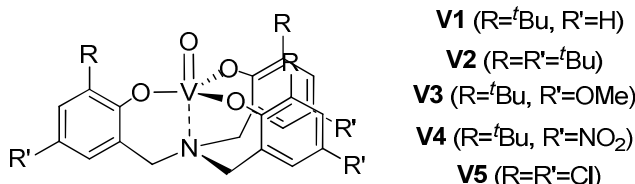


Scheme 3.3: Oxidation of the phenolic β -O-4 model **LM6** by **V9** (left) and **V13** (right)¹⁹.

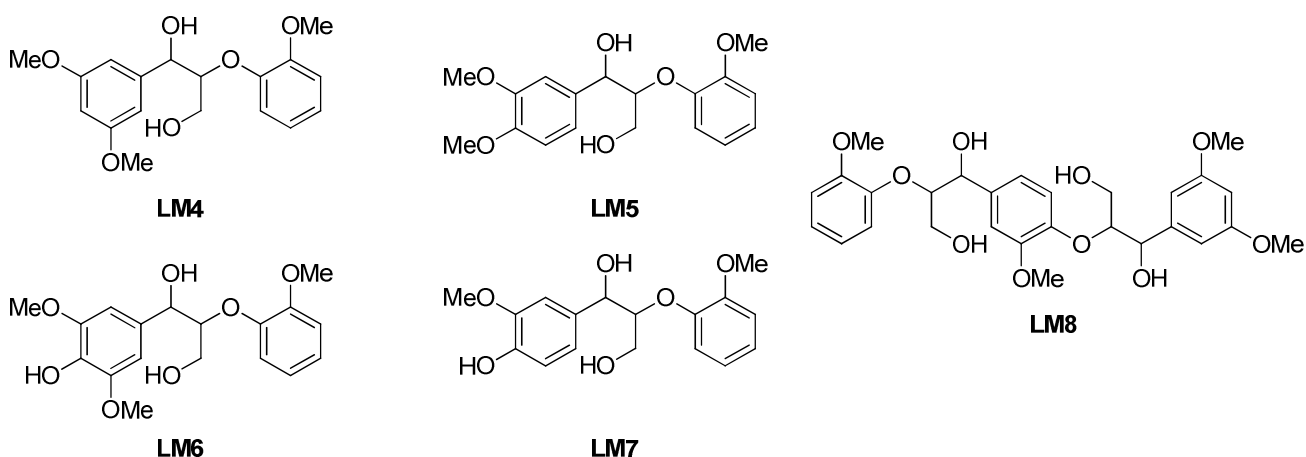
In particular, complex **V13** initially deprotonates the phenolic -OH to generate a phenoxyl radical, leading to cleavage of $\text{C}_{(\text{alkyl})}-\text{C}_{(\text{phenyl})}$ bond, affording quinone **17** and acrolein derivative **26**.

Complex **V9** instead favors the breaking of C β -O bond and benzylic oxidation, affording ketones and guaiacol¹⁹.

In this context, we have recently shown that aminotriphenolate complexes are easily tunable Lewis acids that are able to efficiently activate dioxygen and hydrogen peroxides exhibiting an excellent catalytic oxidative reactivity²². Among them, **V5** is one of the most active homogeneous catalysts for the aerobic C-C oxidative cleavage of diols²³.



Encouraged by these results, the aim of this chapter is to extend the catalytic investigation into the oxidation of lignin-related substrates to the more complicated aryl ethers **LM4**, **LM5** and **LM8**, considered as the typical non-phenolic β -O-4 lignin models, and also to two phenolic β -O-4 lignin models **LM6** and **LM7**. Indeed, β -arylethers represent approximately 50% of the linkages occurring in the natural polymer (see *Chapter 1*).

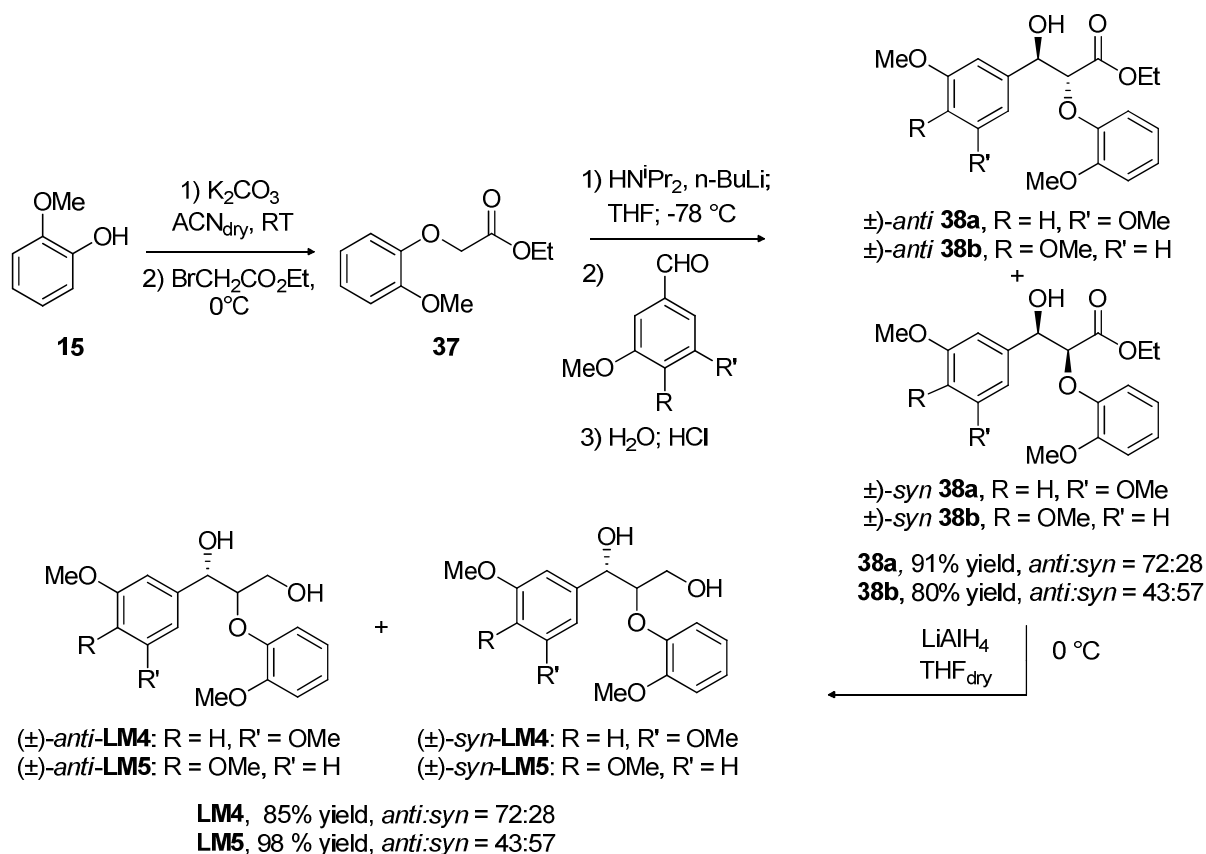


3.2 Synthesis of β -O-4 Lignin Models

Lignin β -O-4 model 1-(3,5-dimethoxyphenyl)-2-(methoxyphenoxy)-propane-1,3-diol **LM4** and 1-(3,4-dimethoxyphenyl)-2-(methoxyphenoxy)-propane-1,3-diol **LM5** were synthesized according to procedures reported in literature (scheme 3.4)¹⁵, from an aldol condensation of a properly functionalized guaiacol and 3,5-dimethoxybenzaldehyde **19a** or 3,4-dimethoxybenzaldehyde **28a**, and a subsequent ester reduction with LiAlH₄, as a mixture of *syn*- and *anti*- diastereomers 70:30 for both models **LM4** and **LM5**. The diastereomeric ratio was determined by ¹H-NMR.

²² Mba, M.; Pontini, M.; Lovat, S.; Zonta, C.; Bernardinelli, G.; Kündig, E.P.; Licini, G.; *Inorg. Chem.* **2008**, 47, 8616.

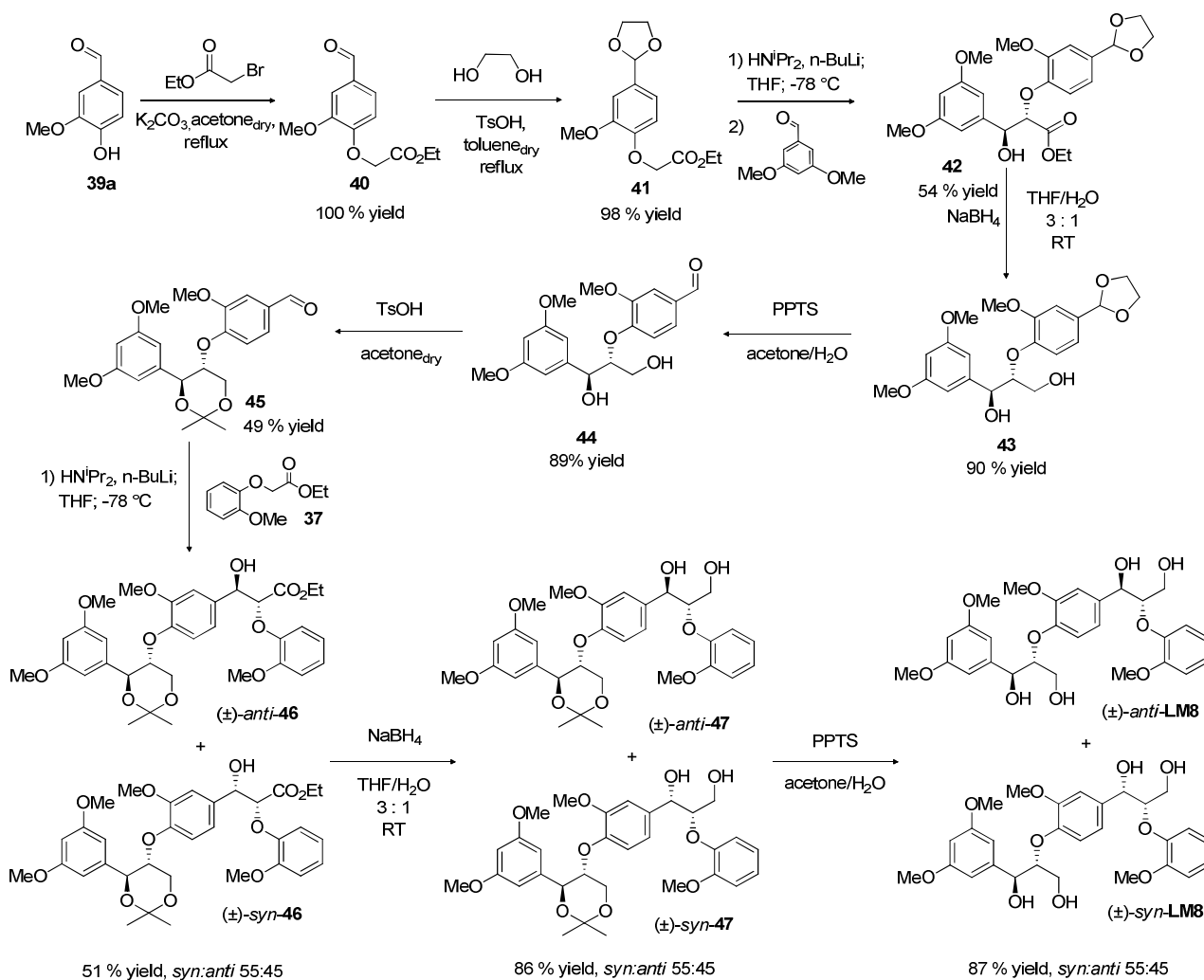
²³ Amadio, E.; González-Fabra, J.; Carraro, D.; Denis, W.; Gjoka, B.; Zonta, C.; Bartik, K.; Cavani, F.; Solmi, S.; Bo, C.; Licini, G.; *Adv. Synth. Catal.* **2018**, 360, 3286.



Scheme 3.4: Synthesis of models **LM4** and **LM5**.

As regards the trimeric model compound 2-(4-(1,3-dihydroxy-2-(2-methoxyphenoxy)propyl)-2-methoxyphenoxy)-1-(3,5-dimethoxyphenyl)propan-1,3-diol **LM8**, this substrate was obtained adapting the procedure reported in literature for the synthesis of a similar compound (Scheme 3.5)²⁴ We chose to use vanillin **39a** and 3,5-dimethoxybenzaldehyde **19a** as starting monomers since our goal is to develop a catalytic system that is capable to maximize the yield of vanillin from lignin depolymerization and because their HPLC calibration curves were already available.

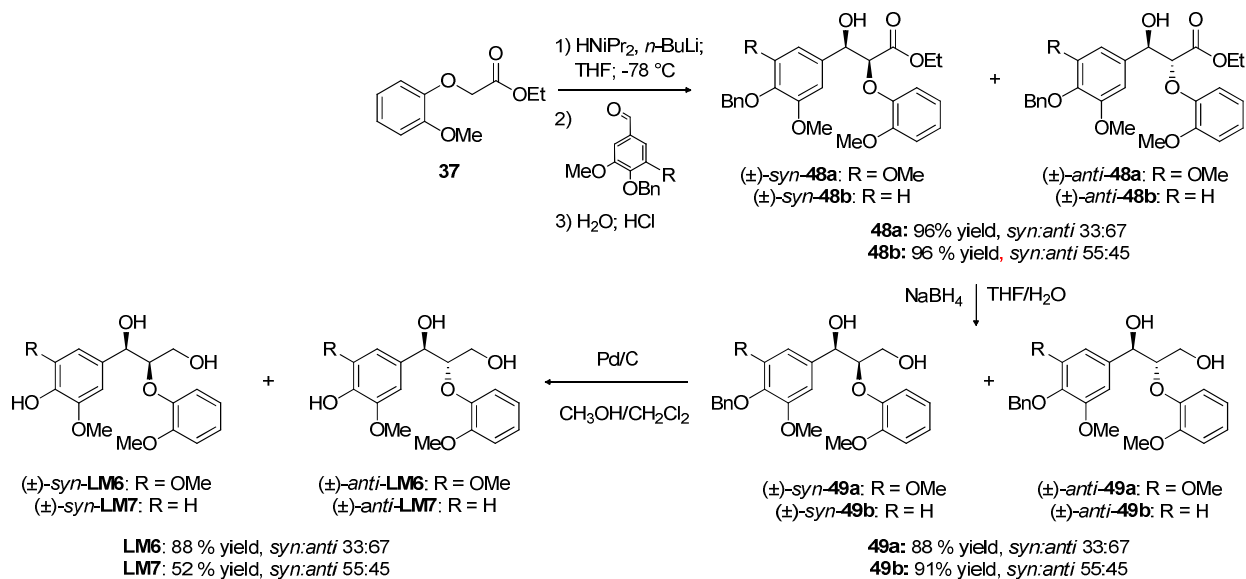
²⁴ a) Ciofi-Baffoni, S.; Banci, L.; Brandi, A. *J. Chem. Soc. Perkin Trans.* **1998**, 1, 3207. b) Baciocchi, E.; Fabbri, C.; Lanzalunga, O.; *J. Org. Chem.* **2003**, 68, 9061.



Scheme 3.5: Synthesis of **LM8**.

The synthesis starts from **39a**, which is functionalized in order to obtain a suitable enolate that reacts with **19a** through an aldol condensation to yield intermediate **42**. This intermediate is present in two diastereomeric forms that have been separated from each other by column chromatography. The one that formed with higher yield (*anti*-diastereomer) was then further functionalized and, with a further aldol condensation, a properly functionalized guaiacol **37** was inserted. At this point, the two diastereomers that has formed were used without a separation. After other two final synthetic steps, it was possible to obtain the trimeric model **LM8**, in a *syn*- / *anti*- ratio of 55/45 (*syn*- / *anti*- ratio was determined by $^1\text{H-NMR}$).

Phenolic lignin models have been synthesized according to the procedure reported by Bolm et al., similar to that of models **LM4** and **LM5**, based on an aldolic condensation between benzyl ether OH-protected vanillin and a properly functionalized guaiacol, which afford diastereoisomeric models in a ratio *syn*- / *anti*- = 33/67 for **48a** and 55/45 for **48b** (determined by $^1\text{H-NMR}$). Compounds **LM6** and **LM7** are finally obtained by reduction of ester functionality with NaBH_4 and deprotection of benzylic -OH group by hydrogenation (Scheme 3.6).

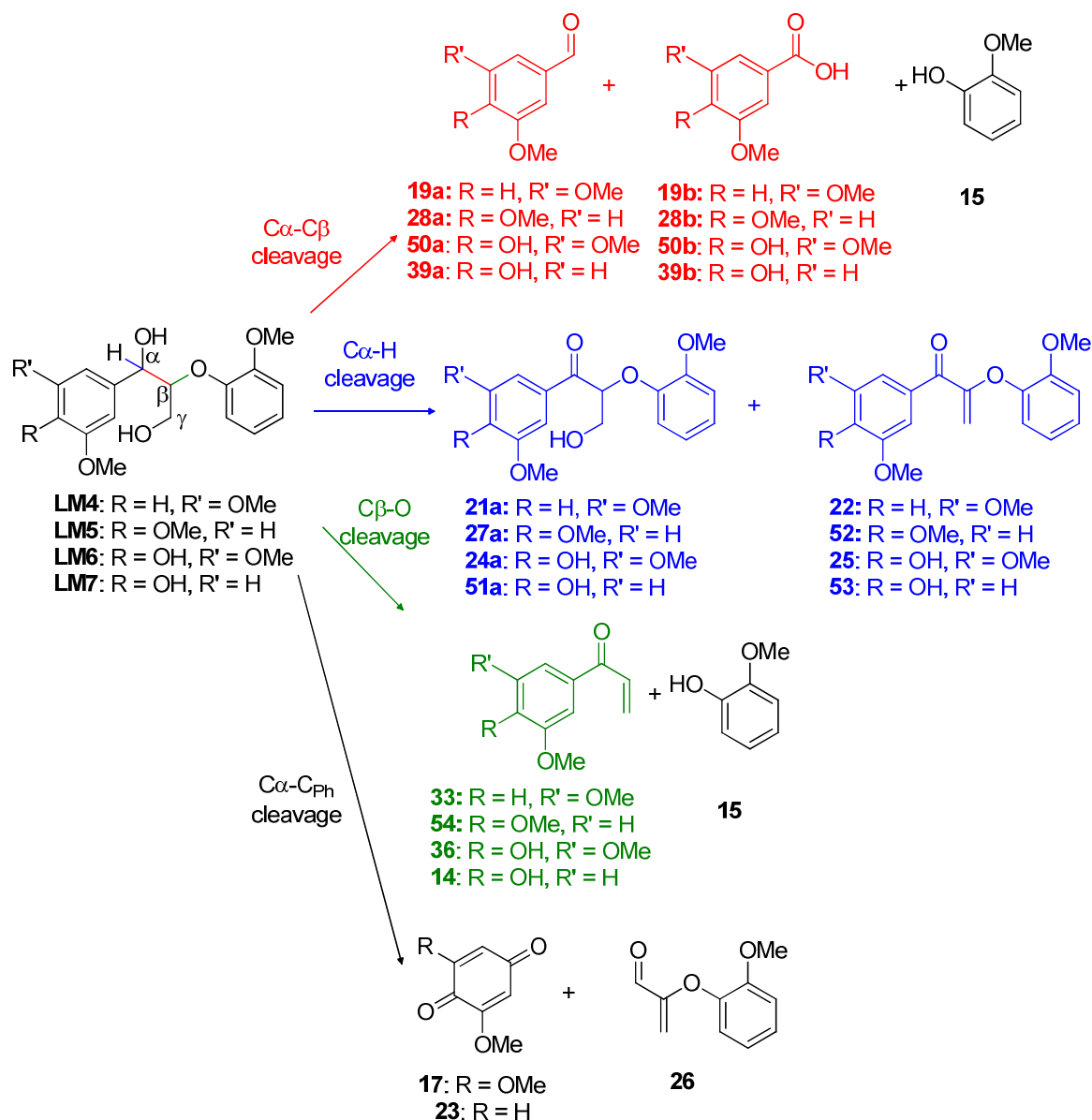


Scheme 3.6: Synthesis of phenolic models **LM6** and **LM7**.

3.3 V^{V} Catalyzed Aerobic Oxidative Cleavage of non-phenolic Dimeric $\beta\text{-O-4}$ Lignin

Models

When non-phenolic lignin model **LM4** was oxidized under air using our Vanadium (V) aminotriphenolate complexes as catalysts (**V1-5**), three different reactivities occurred in the reaction mixture, leading to the formation of different products listed in Eq. 3.8. The first one is benzylic alcohol oxidation generally called as $\text{C}_\alpha\text{-H}$ cleavage, which affords ketone **21a** and the corresponding dehydrated compound **22** (Eq. 3.8, blue path). The second mechanism is $\text{C}_\alpha\text{-C}_\beta$ cleavage (Eq. 3.8, red path), which yields 3,5-dimethoxy benzaldehyde **19a** and the relative overoxidation products 3,5-dimethoxybenzoic acid **19b**. The third mechanism is $\text{C}_\beta\text{-O}$ cleavage (Eq. 3.8, green path) and affords (1-(3,5-dimethoxyphenyl)prop-2-en-1-one **33**. Guaiacol **15** has also been detected and quantified even if its amount cannot be assigned unequivocally to a reactivity since derives from both $\text{C}_\alpha\text{-C}_\beta$ and $\text{C}_\beta\text{-O}$ cleavages. All the possible products were identified by combining LC-MS, ESI-MS, GC/MS and ^1H NMR analyses, and synthesized if not commercially available, in order to set up quantitative HPLC methods.



Eq. 3.8: Main mechanisms of Vanadium catalyzed oxidative cleavage of models **LM4** and **LM5**.

As in the case of vicinal diols (*Chapter 2*), we began our investigation by screening the ligand effect of **VO-TPA(R,R')** complexes in the aerobic catalytic oxidation of model **LM4**, using toluene as solvent. We tested also commercially available $\text{VO}(\text{acac})_2$ and complex **V5**, under the same reaction conditions. Results are summarized in Table 3.3.

Table 3.3: Aerobic oxidation of **LM4**, under air, $[\text{LM4}]_0 = 0.05 \text{ M}$, toluene, 80°C , 10% catalyst, ligand effect.

Entry	Cat.	Time (h)	Conv. (%)	Yield	Yield	Yield	Yield	Yield	Mass	Selectivity (%) (C-H/C-C/C-O)
				19a (%) (C-C)	19b (%) (C-C)	21a (%) (C-H)	22 (%) (C-H)	33 (%) (C-O)	Balance (%)	
1	V5	8	93	8.8	0.8	81	0.6	1	100	
		22	>99	9.9	1	84	3	2	100	87/13/1
2	V4	24	41	4	1	32	0	4	100	78/12/10
3	V1	24	2	1	0	1	0	0	100	-
4	V2	24	2	1	0	1	0	0	100	-
5	V3	24	25	5	0	14	0	1	95	70/25/5
6	V6	24	20	2	2	12	3	1	93	75/20/5
7	$\text{VO}(\text{acac})_2$	24	92	9	3	41	10	8	79	72/17/11

^a: Determined by HPLC using biphenyl as internal standard.

First of all, we noted that complex **V5** was the most active in performing oxidative degradation of **LM4**, since in 8 h conversion was above 90 % and complete after 22 h (Table 3.3, entry 1). As regards the product distribution, ketone **21a** was found to be the most abundant product, meaning that the principal degradation mechanism is benzylic oxidation ($\text{C}_\alpha\text{-H}$ cleavage). Besides, we detected about 10 % of **19a**, coming from $\text{C}_\alpha\text{-C}_\beta$ cleavage. Finally, negligible extent of $\text{C}_\beta\text{-O}$ cleavage was observed. As regards *ortho*-^tBu-substituted complexes **V1-4**, the most active one was found to be **V4**, bearing electron-withdrawing $-\text{NO}_2$ substituents in *para*- positions with respect to the hydroxyl groups (Table 3.3, entry 2), even if its activity is considerably lower than complex **V5** (only 41 % conversion after 24 h). Looking at the reaction selectivity, both complexes afford a higher extent of benzylic oxidation, and a similar selectivity with respect to the other two cleavage mechanisms. Other Vanadium (V) aminotriphenolate complexes **V1-3** were significantly less active, with oxidation starting only several hours of induction. It's interesting to note that for complex **V6**, the activity towards **LM4** in toluene (Table 3.3, entry 6) is significantly depleted with respect to pyridine/DMSO (Table 3.2. entries 2-3), and this highlights the importance of choosing the right solvent for this reaction. Finally, commercially available $\text{VO}(\text{acac})_2$ showed a discrete activity (92 % conversion after 24 h, Table 3.3, entry 7), even if lower with respect to **V5**. Moreover, this system is also less selective, since besides benzylic oxidation which still remains the most occurring mechanism, discrete and comparable amounts of $\text{C}_\alpha\text{-C}_\beta$ cleavage products and $\text{C}_\beta\text{-O}$ cleavage products were obtained.

Due to its high catalytic activity, the effect of other reaction parameters like solvent (Table 3.4), temperature (Table 3.5) and catalyst loading (Table 3.6) has been therefore explored using the best catalyst **V5**. The reaction proceeds rapidly only in toluene, which in analogy to the results obtained in the case of vicinal diols afforded the best catalytic performances (Table 3.4, entry 1). In DCE, AcOEt, ACN and dioxane a very high to almost full conversion of the reagent were observed but

within 48-96 h (Table 3.4, Entry 1-5). Only modest rates were instead observed in acetone, THF or pyridine (Table 3.4, Entry 6-8). The catalytic performance definitively slows down using DMF, DMSO and EtOH (Table 3.4, Entry 9-10). As far as the reaction's selectivity is concerned, we can notice that this parameter is not strongly influenced by the solvent used being the C α -H cleavage the main reactivity (with ketone **21a** as the major product). The C α -C β breaking occurs in the range between 10-17 % while only little amount of products coming from C β -O cleavage have been detected (1-6 %). Interestingly, only in acetone the solvent influenced the catalyst's reactivity increasing respectively the amount of dehydrated ketone **22** or the amount of **33**, this last due to the C β -O cleavage reaction.

Table 3.4. Aerobic oxidation of **LM4** catalyzed by vanadium complex **V5** under air, [**LM4**]₀ = 0.05 M, toluene, 80°C, 10% catalyst. Influence of solvents.

Entry	Solvent	Time (h)	Conv. (%)	Yield 19a (%) (C-C)	Yield 19b (%) (C-C)	Yield 21a (%) (C-H)	Yield 22 (%) (C-H)	Yield 33 (%) (C-O)	Mass Balance (%)	Selectivity (%) (C-H/C-C/C-O)
1	Toluene	8	93	9	1	81	1	1	100	89/10/1
		22	>99	10	1	84	3	2	100	87/11/2
2	DCE	23	83	10	0	69	0	2	97	86/12/2
		48	98	11	4	73	2	2	95	83/16/1
3	AcOEt	23	66	9	0	53	0	4	100	81/14/6
		96	96	11	2	62	2	6	87	77/16/7
4	ACN	23	61	7	0	51	0	2	98	85/12/3
		96	95	10	2	74	1	3	94	84/13/3
5	Dioxane	23	58	9	1	45	0	3	97	78/17/5
		96	91	11	2	66	1	6	95	78/15/7
6	THF	23	46	4	1	13	0	2	73	68/22/10
		96	70	7	1	29	0	6	72	68/18/14
7	Acetone	23	40	2	0	10	28	1	100	92/6/2
		96	72	3	0	20	49	3	100	92/5/3
8	Pyridine	23	19	4	1	13	0	0	98	73/27/0
		96	77	10	7	52	8	0	100	80/20/0
9	DMF	96	24	7	0	14	2	1	100	-
10	EtOH	96	4	1	0	2	0	0	99	-
11	DMSO	96	7	2	0	5	0	0	100	-

^aConversions and Yields determined by HPLC using biphenyl as internal standard.

Further investigations have been carried out exploring the influence of temperature on the selectivity and reactivity (Table 3.5). Also in this case, the most active catalyst **V5** was used.

Table 3.5: Aerobic oxidation of **LM4** catalyzed by vanadium complex **V5**. Influence of temperature.

Entry	T(°C)	Time (h)	Conv. (%)	Yield	Yield	Yield	Yield	Yield	Mass Balance (%)	Selectivity (%) (C-H/C-C/C-O)
				19a (%) (C-C)	18b (%) (C-C)	21a (%) (C-H)	22 (%) (C-H)	33 (%) (C-O)		
1	80	8	93	8.8	0.8	81	0.6	1	100	
		22	>99	9.9	1	84	3	2	100	87/13/1
2	100	8	>99	10	6	75	6	3	100	78/12/10
		22	>99	10	12	24	24	2	72	
3 ^b	80	96	0	0	0	0	0	0	100	-

Conditions: $[\text{LM4}]_0 = 0.05 \text{ M}$, $\text{VO}(\text{Cl}, \text{Cl}) = 10\% \text{ mol}$, under air, toluene as a solvent; ^a Conversion and Yield determined by HPLC using biphenyl as internal standard. ^b Reaction performed without catalyst.

From the data reported in Table 3.5 it is evident that faster oxidation occurred when increasing the reaction temperature to 100 °C as expected. In comparison with the reaction at 80 °C, at 100 °C the yields of the dehydrated ketone **22** and acid **33** slightly increase while the amount of aldehyde **19a** remains unchanged and always around 10% (9.9 % at 22 h for 80 °C and 10 % at 8 h for 100 °C). Therefore, the C_α-H cleavage is again the principal oxidation mechanism even if a slight increment of the C_α-C_β cleavage selectivity can be pointed out with increasing the temperature (10.9 % in total at 22h for 80 °C and 16.2 % at 8 h for 100 °C). The C_β-O still occurred but in trace amount. From a deeper investigation of the reaction profile (Figure 3.1), it is evident that the aldehyde **19a** is formed in the initial steps of the reaction, within the first hour, and it remains constant till the end of the reaction (10.4 % after 8 h) even if the corresponding acid **19b** (revealed after the third hour) gradually increases to 5.8 % after 8 h. Without complex **V5**, no substrate conversion was observed even after 96 h.

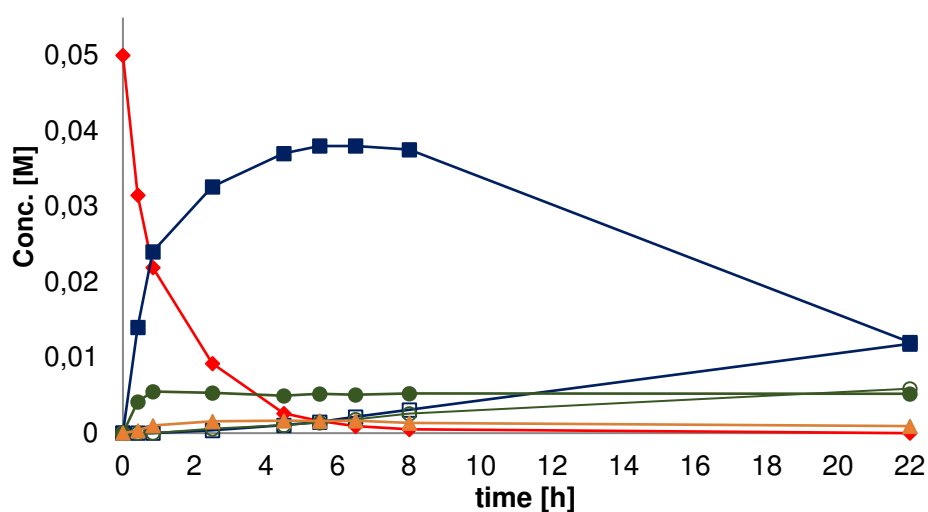


Figure 3.1: Kinetic profiles for the aerobic oxidation of **LM4**, $[\text{LM4}]_0 = 0.05 \text{ M}$, **V5** = 10% mol, under air, toluene, 100 °C. \blacklozenge , substrate **LM4**, \blacksquare , ketone **21a**, \square , dehydrated ketone **22**, \bullet , 3,5-dimethoxybenzaldehyde **19a**, \circ , 3,5-dimethoxybenzoic acid **19b**, \blacktriangle , C_β-O cleavage product **33**.

As a next step, we moved to the analysis of the catalyst loading and the oxidant. In particular, we tested a substrate concentration of 0.05 M, 0.15 M and 0.25 M, a catalyst loading in a range from 20 to 1 %, and the use of air or O₂ as terminal oxidant. Results are reported in table 3.6 and in Figure 3.2.

Table 3.6: Aerobic oxidation of **LM4** catalyzed by vanadium complex **V5**. Catalyst loading and oxygen effect.

Entry	[LM4] ₀	cat. (%)	Oxidant	Time (h)	Conv. (%)	Yield 19a (%) (C-C)	Yield 19b (%) (C-C)	Yield 21a (%) (C-H)	Yield 22 (%) (C-H)	Yield 33 (%) (C-O)	Mass Balance (%)	Selectivity (%) (C-H/C-C/C-O)
1	0.05	20	Air	5.5	>99	11	4	73	4	1	93	84/15/1
2	0.05	10	Air	8	>99	10	6	75	6	3	100	81/16/3
3	0.15	10	Air	7.5	>99	10	4	68	9	2	93	84/14/2
4	0.25	10	Air	6.5	>99	12	3	70	11	1	97	84/15/1
5	0.25	5	Air	8	99	11	3	64	3	5	86	78/17/5
6	0.25	1	Air	48	99	14	3	61	6	11	96	71/18/10
7	0.05	10	O ₂	3.5	99	10	7	70	6	6	99	77/17/6
8	0.05	10 ^b	O ₂	24	96	11	9	14	20	9	67	55/32/13
9	0.05	10 ^c	O ₂	24	95	11	6	50	17	10	99	71/18/11
10	0.25	10	O ₂	1.5	99	12	5	82	-	2	100	82/17/2
11	0.25	10 ^b	O ₂	8	98	10	3	16	8	6	45	57/30/13
12	0.25	5	O ₂	7	99	15	5	65	8	7	100	73/20/7
13	0.25	1	O ₂	24	99	18	7	52	9	10	99	64/27/11
14	0.25	1 ^b	O ₂	24	97	9	2	32	3	4	53	69/23/8
15 ^d	0.25	1	O ₂	9	>99	15	5	32	10	8	70	60/28/12
16	0.25	1	Air (4 atm)	24	>99	10	10	30	0	0	50	-
17	0.05	-	O ₂	96	-	-	-	-	-	-	-	-

Conditions: toluene, 100 °C. ^aConversion and Yield determined by HPLC using biphenyl as internal standard.

^b VO(acac)₂ used as catalyst. ^c **V4** used as catalyst. ^d Reaction run in xylenes, at 130 °C.

When using 20 % of catalyst, under air, substrate **LM4** (0.05 M), (Table 3.6, entry 1) could be converted in 5.5 h, affording ketone **21a** as the major product (73 % + 4% of dehydrated compound **22**). We detected also 11 % of **19a** and 4 % of the corresponding acid **19b**. The amount of product derived from C_β-O cleavage was negligible (1 %). A decrease of the catalyst amount to 10 % and an increase of the substrate concentration (Table 3.6, entries 3-4), with the same amount of **V5**, affect only the reaction time (6.5 h), without affecting the reaction selectivity (mainly directed towards C_α-H cleavage). A further decrease of the catalyst loading down to 1 % (Table 3.6, entries 5-6), leads to a slowdown of the reaction down to 48 h, and an increase of the reaction selectivity as regards

both C_α-C_β and C_β-O cleavage (respectively 18 % and 10 %, with 1 % **V5**) (Figure 3.2). Significant changes in the reaction speed are conveyed by the use of O₂ as terminal oxidant (Table 3.6, entries 7-15). Indeed, when using 10 % catalyst, both for substrate concentration of 0.05 M (Table 3.6, entries 2 and 7) and 0.25 M (Table 3.6, entries 4 and 10), a remarkable gain in time required to get a complete substrate conversion is obtained (3.5 h vs 8 h and 1.5 h vs 6.5 h respectively). The same reaction conditions (0.05 M of substrate, 10 % catalyst loading) were tested also for VO(acac)₂ (Table 3.6, entry 8) and **V4** (Table 3.6, entry 8). Both complexes showed a less pronounced activity than **V5**, but although **V4** showed also a comparable selectivity, with VO(acac)₂ a loss in mass balance was detected, index of formation of other unidentified species. Interestingly, when we decreased the amount of catalyst down to 1 % (Table 3.6, entries 13-15), besides the deceleration seen in analogy with reactions run under air, a considerable increase in C_α-C_β cleavage (up to 27 %) was observed. This is a very interesting result, because it's the first example of a homogeneous thermal-activated Vanadium (V) complex that displays such a high degree of selectivity for aromatic aldehydes / benzoic acids. The same reaction run in xylenes at 130°C (Table 3.6, entry 14) gave complete substrate conversion after 9 h instead of 24 h required in toluene (Table 3.6, entry 13), and a comparable selectivity with respect to the kind of cleavage occurred in the reaction mixture, even if these conditions suffer from a discrete loss in the yield of ketone **21a**, result seen also when employing VO(acac)₂ as catalyst (Table 3.6, entries 9,11 and 14). Finally, use of air at 4 atm under the same reaction conditions (Table 3.6, entry 16) was explored, and a control experiment (without catalyst) (Table 3.6, entry 17) didn't afford any substrate conversion even after 96 h.

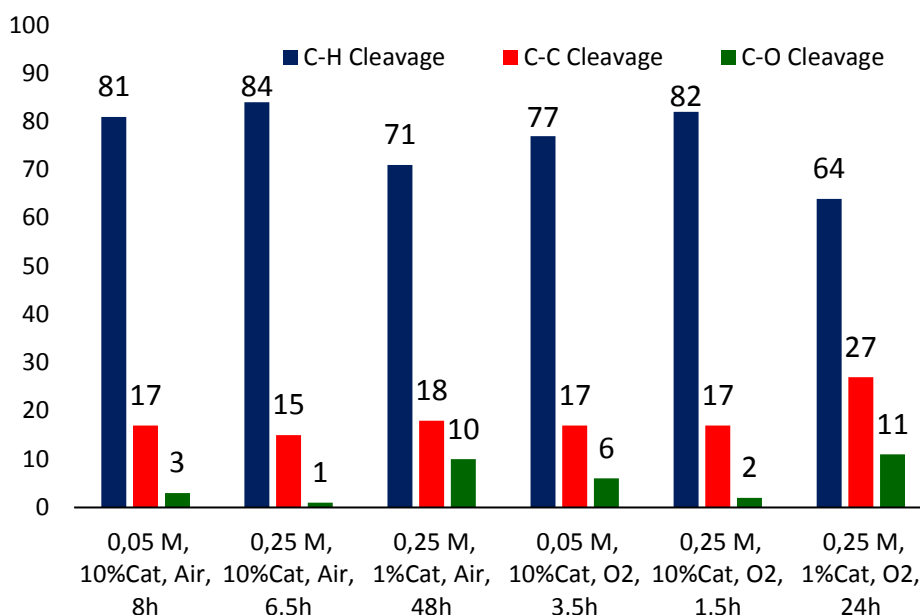
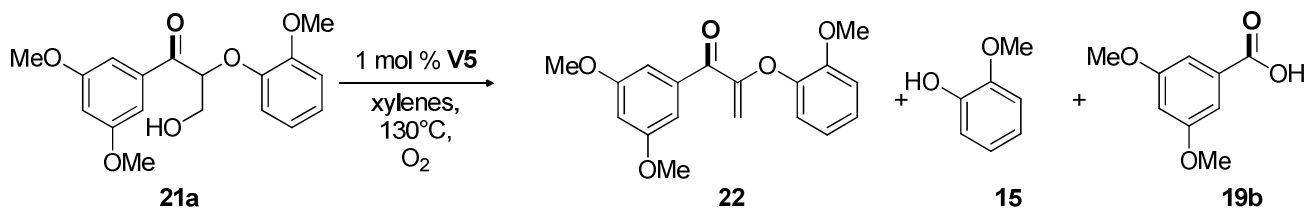


Figure 3.2: Aerobic oxidation of **LM4** catalyzed by **V5** in Toluene at 100°C. Below each bar are listed: substrate concentration (M), catalyst loading (mol %), oxidant and time required to obtain a complete substrate conversion (h). “C_α-H Cleavage” takes into account the sum of determined amounts of products **21a** + **22**. “C_α-C_β Cleavage” takes into account the sum of determined amounts of products **19a** + **19b**.

In order to better understand the loss in ketone **21a** seen when using xylene as solvent, we verified the behaviour of this compound under the optimized reaction conditions ($[\mathbf{21a}]_0 = 0.25 \text{ M}$, 1 % **V5**) (Table 3.7). Besides the expected dehydration product **22** we also detected in the reaction mixture compounds **15** and **19b**, index of an instability of compound with respect to C_α - C_β cleavage.

Table 3.7: Investigation of reactivity of ketone **1c** in xylenes, 130 °C, O_2 .



Entry	time (h)	Conv. (%) ^a	Yield 22 (%) ^a	Yield 15 (%)	Yield 19b (C-C)	Mass Balance (%)
1	8	49	6	5	12	69
	24	79	7	10	16	44

Conditions: $[\mathbf{21a}]_0 = 0.25 \text{ M}$, **V5** = 1% mol, under O_2 , xylenes, 130 °C; ^aConversion and Yield determined by HPLC using biphenyl as internal standard.

After 24 h of reaction (Table 3.7), 79 % of substrate was converted, affording 7 % of dehydration product **22**, 10 % of guaiacol **15** and 16 % of 3,5-dimethoxybenzoic acid **19b**. We could not identify any other reaction product, also by NMR and GC-MS, therefore, our hypothesis is that some repolymerization occurred under such reaction conditions. These results are in agreement to what found by Diaz-Urrutia when subjecting ^{13}C -labelled ketone **21a** to the action of complex **V5** (10 mol %) in $\text{DMSO-}d_6$ at 100 °C under air. Indeed, after 48 h, approximately 40 % of the substrate was converted, yielding ^{13}C -labelled **22** (14 %), **19b** (19 %) and **15**, together with the presence of ^{13}C -labelled formic acid (7 %), detected by ^{13}C -NMR²⁵.

With the optimal reaction conditions in order to maximize the amount of C_α - C_β cleavage, we performed a solvent screening with the aim to verify that such high degree of selectivity was achievable over a wide range of solvents and not only in toluene (Table 3.8).

²⁵ Diaz-Urrutia, C. in Vanadium-Catalyzed Aerobic Oxidation of Diols and Lignin Models/Extracts, *PhD Thesis*, University of Ottawa, Canada, **2016**.

Table 3.8: Aerobic oxidation of **LM4**, under O₂, [LM4]₀ = 0.25 M, 100°C, 1% **V5**, solvent screening.

Entry	Solvent	Time (h)	Conv. (%)	Yield ^a	Yield ^a	Yield ^a	Yield ^a	Yield ^a	Mass Balance (%)	Selectivity (%) (C-H/C-C/C-O)
				19a (%) (C-C)	19b (%) (C-C)	21a (%) (C-H)	22 (%) (C-H)	33 (%) (C-O)		
1	Toluene	24	99	18	7	52	9	10	97	64/26/10
2	Dioxane	96	98	10	6	52	14	8	92	73/18/9
3	ACN	96	96	8	12	31	12	8	75	60/28/12
4	Pyridine	96	68	7	15	24	17	1	96	66/33/1
5	AcOEt	96	64	7	2	37	5	12	99	67/14/19
6	DMSO	96	7	2	0	5	0	0	100	-

^a Determined by HPLC using biphenyl as internal standard.

From the results obtained it emerged that only in toluene **LM4** could be completely converted into products after 24 h (Table 3.8, entry 1), whereas other solvents required at least 96 h in order to afford a complete substrate conversion. Indeed, dioxane and ACN gave an almost total reagent consumption after 96 h (Table 3.8, entries 2 and 3), whereas in Pyridine and AcOEt, substrate conversion was about 64-68 % (Table 3.8, entries 4 and 5). Finally, parallel to what we noted for diluted conditions (Table 3.4), in DMSO our system is not effective, with less than 7 % substrate conversion even after 96 h (Table 3.8, entry 6). As far as the reaction selectivity is concerned, we can note that despite the solvent used, selectivity is always oriented towards benzylic oxidation (60 - 73 %) and the amount of C-C cleavage is maintained at about 14-33 %. This result is very promising if we consider that the solubility of lignin oligomers in toluene decreases with the increase in the number of residues (trimeric compounds are less soluble than dimers) and therefore, we will be forced to change solvent when employing actual lignin samples.

We tested also a second β -O-4 lignin model **LM5** under the same reaction conditions (Table 3.9 and Figure 3.3). Reaction products are listed in Eq.3.8.

Table 3.9: Aerobic oxidation of **LM5** catalyzed by vanadium complexes **V5**. Catalyst loading and oxygen effect.

Entry	[LM5] ₀	cat. (%)	Oxidant	Time (h)	Conv. (%)	Yield 28a (%) (C-C)	Yield 28b (%) (C-C)	Yield 27a (%) (C-H)	Yield 52 (%) (C-H)	Yield 54 (%) (C-O)	Mass Balance (%)	Selectivity (%) (C-H/C-C/C-O)
1	0.05	10	Air	3.5	99	7	3	60	4	2	78	85/13/2
2 ^b	0.05	10	Air	9	98	18	3	68	4	1	94	76/22/1
3	0.25	10	O ₂	2.5	99	13	5	60	8	13	99	68/18/14
4	0.25	5	O ₂	3.5	99	12	4	57	10	15	99	69/16/15
5	0.25	1	O ₂	32	99	15	4	49	7	16	92	62/21/17
6 ^c	0.25	1	O ₂	9	99	13	6	26	9	17	72	50/27/23

^a Conversion and Yield determined by HPLC using biphenyl as internal standard. ^b Reaction run at 80 °C. ^c Reaction run in xylenes at 130 °C.

The obtained data show that the complex **V5** effectively catalyzes the oxidation. With [**LM5**]₀ = 0.05 after 3.5 hours of reaction at 100 °C full conversion of **LM5** (Table 3.9, entry 1) is observed. The oxidation gives mainly the C_α-H cleavage (**27a**+**52** = 85 % of selectivity) and only few selectivity of C_α-C_β (**28a**+**28b** = 13 %) or C_β-O (**54** = 2 %) bonds breaking. Similarly to what is observed for **LM4**, when using 0.25 M of reagent and under pure oxygen the C_α-H cleavage decreased in favour of both C_α-C_β and C_β-O cleavages which incremented up to 27 % in selectivity (Table 3.9, entries 3-6). However, with **LM5**, despite the reaction time, the amount of catalyst used does not affect the products distribution that much (Table 3.9, entries 4 and 5). When switching the solvent to xylenes and rising the temperature to 130 °C (Table 3.9, entry 6), the same behaviour for **LM4** is observed (Table 3.6), that is an acceleration of the reaction and a loss in yield of ketone **27a**.

In summary, the oxidation of non-phenolic β-O-4 lignin models **LM4** and **LM5** gives mainly C_α-H oxidation. However, despite the influence on reaction times, the increase of substrate concentration or lowering the catalyst amount can surprisingly have a positive effect on the relative reactivity C_α-C_β / C_β-O / C_α-H in favor of C_α-C_β cleavage. These effects are more pronounced if we use pure oxygen as oxidant. These results are very promising if we compare it with the most efficient Vanadium-based homogeneous catalyst present in literature up to now, which was reported by S. Hanson **V6**^{7,18,19}. These complex, in order to obtain a complete substrate conversion, requires the use of DMSO/pyridine mixtures as solvent and reaction times up to 48 h. Moreover, the selectivity towards C_α-C_β cleavage is dramatically lower compared to our system, because with **V5**, C_β-O cleavage is preferred. This makes evident that the selectivity towards the kind of cleavage is strongly influenced by the electronic properties of the ligands in V(V) complexes, with more electron-withdrawing ones directing the system to undergo a higher degree of C_α-C_β cleavage.

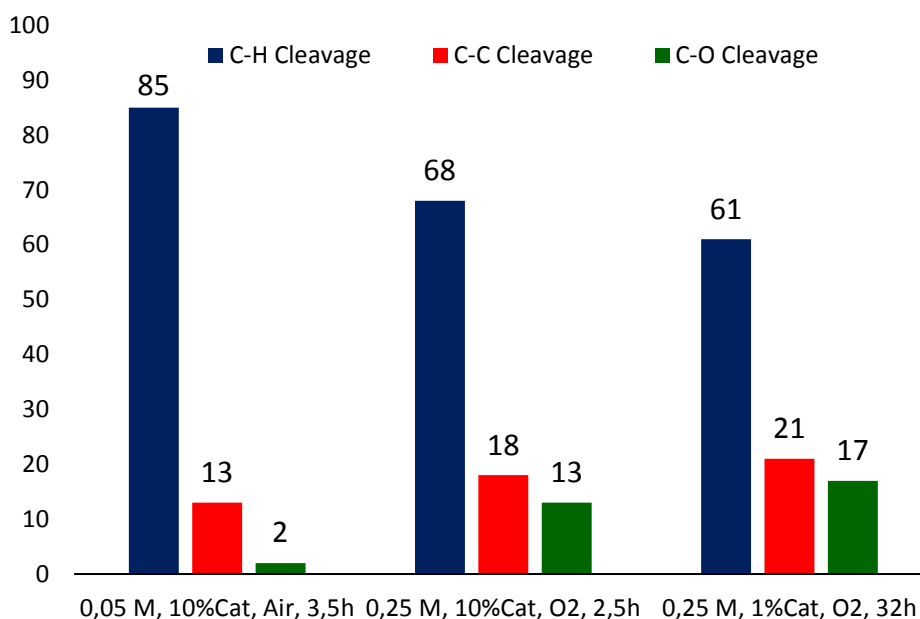


Figure 3.3: Aerobic oxidation of **LM5** catalyzed by **V5** in Toluene at 100°C. Below each bar are listed: substrate concentration (M), catalyst loading (mol %), oxidant and time required to obtain a complete substrate conversion (h). “C_α-H Cleavage” takes into account the sum of determined amounts of products **27a** + **52**. “C_α-C_β Cleavage” takes into account the sum of determined amounts of products **28a** + **28b**.

3.4 Aerobic Oxidation of Phenolic β-O-4 Lignin Models

In the reactivity of compounds **LM4** and **LM5**, the catalytic performance of **V5** significantly differs from the previously reported catalysts of Hanson and Toste. Specifically, it showed high selectivity towards the C_α-H and C_α-C_β bond cleavage and catalyzed the C_β-O degradation only at a lower extent^{15,19}. Therefore, we investigated the catalytic behavior of this complex also with phenolic lignin models **LM6** and **LM7**. In this case, besides the three different cleavage mechanisms that occur also in non-phenolic β-O-4 lignin models (namely, C_α-H, C_α-C_β and C_β-O cleavage), also the C_{Ph}-C_α cleavage could occur (black path in Eq. 3.8), affording quinones **17**, **23**, and acrolein derivative **26**. We began the investigation with **LM6** (0.05 M), employing 10 mol% **V5** under air, with toluene or ethyl acetate as solvent at 80 °C or 100 °C. The results are reported in Table 3.10.

Table 3.10: Aerobic oxidation of **LM6**, product distribution.

Entry	Solvent	T (°C)	Time (h)	Conv. (%) ^a	Yield	Yield	Yield	Yield	Yield	Yield	Yield	Mass Balance (%)	
					50a (%) ^a (C-C)	50b (%) ^a (C-C)	24a (%) ^a (C-H)	25 (%) ^a (C-H)	36 (%) ^a (C-O)	17 (%) ^a (C _{Ph} -C _α)	26 (%) ^a (C _{Ph} -C _α)		15 (%) ^a
1	Toluene	100	5	>99	3	1	25	-	-	10	-	16	39
2	AcOEt	80	24	98	4	1	30	-	-	11	-	20	46

Conditions: [**LM6**]₀ = 0.05 M, **V5** = 10% mol, under air; ^a Conversion and yield determined by HPLC using biphenyl as internal standard.

As can be seen from table 3.10 (entry 1), in toluene **LM6** is completely converted in 5 h, affording 25 % of ketone **24a**. A discrete amount of products deriving from C_α-C_β cleavage has also been detected, whereas no C_β-O cleavage seemed to occur. Finally, 10 % of quinone **17** was detected, suggesting that our complexes was able to catalyze C_{Ph}-C_α cleavage as well, in analogy with complex **V13** reported by Hanson et al.¹⁹. Conversely, we found 16-20 % guaiacol **15** in the reaction crude, which is more than expected based on the detected amounts of the reaction counterparts. Additionally, a rather low mass balance was observed, which led us to hypothesize that some of the cleavage products could re-polymerize under the reaction conditions leading to high molecular weight byproducts not detectable by standard HPLC techniques, as already reported¹⁹. Using AcOEt as solvent (Table 3.10, entry 2) gave similar results, though a slightly higher mass balance was obtained (46 % vs 39 %) likely due to the lower reaction temperature.

Additional studies were undertaken using a similar model **LM7** in toluene at 100°C using different reaction conditions (Table 3.11).

Table 3.11: Aerobic oxidation of **LM7** catalyzed by vanadium complex **V5**. Products distribution.

Entry	[LM7] ₀ (M)	Oxidant	Time (h)	Conv (%) ^a	Yield	Yield	Yield	Yield	Yield	Yield	Yield	Mass Balance (%)	
					39a (%) ^a (C-C)	39b (%) ^a (C-C)	51a (%) ^a (C-H)	53 (%) ^a (C-H)	14 (%) ^a (C-O)	23 (%) ^a (C _{Ph} -C _α)	26 (%) ^a (C _{Ph} -C _α)		15 (%) ^a
1	0.05	Air	1.5	>99	1	1	16	-	-	-	-	24	18
2	0.05	O ₂	3	>99	2	1	29	4	-	-	-	21	35
3	0.25	O ₂	1.25	>99	2	0	16	2	-	-	-	15	20

Conditions: [**LM7**]₀ = 0.05 M, **V5** = 10% mol, under air or O₂; ^a Conversion and Yield determined by HPLC using biphenyl as internal standard.

The results obtained with **LM7** are in agreement with those for **LM6**. The reaction selectivity was directed towards the benzylic oxidation **51a** and **53**, and little amounts of aldehydes and carboxylic acids coming from C_α-C_β cleavage **39a,b** were observed. Moreover, also in this case, a higher amount of **15** was found with respect to the other expected reaction products. Differently from the previous case, we did not detect any product deriving from C_{Ph}-C_α cleavage. However, during the

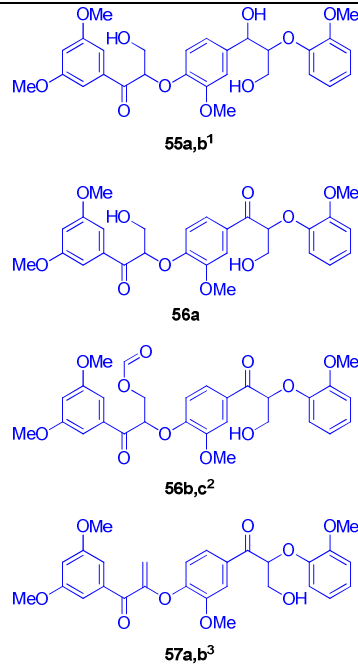
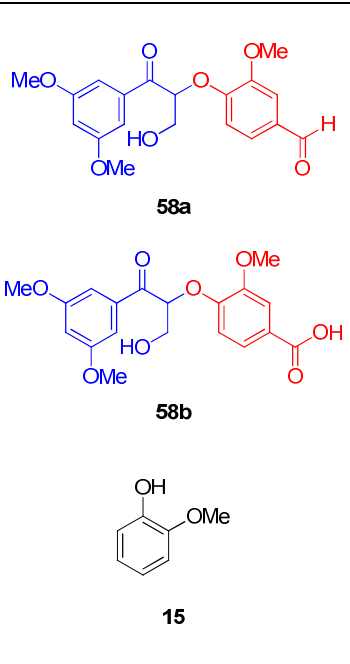
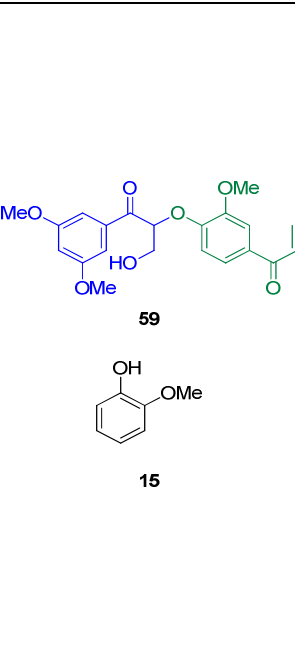
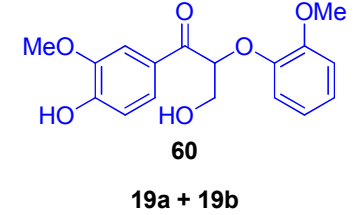
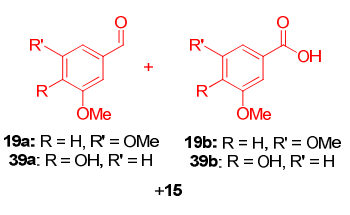
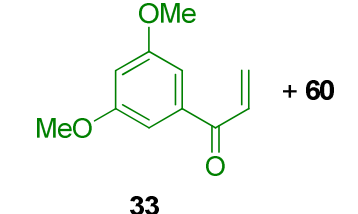
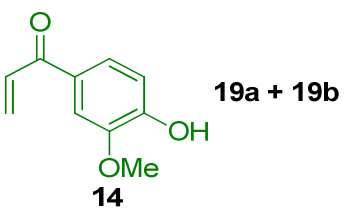
reaction, a precipitate accounting for about 10 % of the mass balance was formed. This precipitate is an intractable mixture insoluble in most organic solvents, in analogy to what obtained also by Hanson and co-workers¹⁹. Thus, the reactivity of phenolic β -O-4 lignin models with **V5** seems to be more complicated and less selective than the one of non-phenolic β -O-4 lignin models. Indeed, under our reaction conditions, radical reactions leading to polymeric compounds could be triggered.

3.5 V^V Catalyzed Aerobic Oxidative Cleavage of a Trimeric β -O-4 Lignin Model

Next, the reactivity of **V5** was also tested on the trimeric lignin model **LM8** bearing a vanillyl residue **39a** connected to other two aromatic moieties (3,5-dimethoxybenzaldehyde **19a** and guaiacol **15**). By means of GC-MS and LC-MS, we were able to identify the majority of products coming from the reaction with **V5**. The possible reaction pathways that can occur are also in this case the C $_{\alpha}$ -C $_{\beta}$ cleavage, C $_{\beta}$ -O cleavage and benzylic oxidation (C $_{\alpha}$ -H cleavage, Chart 3.1). However, in **LM8** we have the presence of two distinct β -O-4 bonds in the same molecule. Hence, products coming from different pathways acting on either or both these positions can be formed, leading to a number of products (see Chart 3.1). All of the products reported in the chart were identified by combining LC-MS, ESI-MS, GC/MS and ¹H NMR analyses. When not commercially available, they were synthesized in order to set up an HPLC method as quantitative as possible. Products **55a,b**, **56a-c**, **57a,b** and **59** were identified in the reaction mixture only qualitatively, due to the excessive synthetic efforts required for their synthesis. Therefore, their quantitation was performed assuming the same response factor of similar species (the response factor of ketone **56a** was assigned to compounds **55a,b**, **56b,c** and **57a,b**, whereas the response factor of product **58a** was assigned to compound **59**).

Two reaction conditions have been tested. One with [LM8]₀ = 0.05 M, 10 mol% **V5** in toluene at 100 °C under O₂, and one with [LM8]₀ = 0.20 M, 1 mol% **V5** in toluene at 100 °C under O₂. It is worth mentioning that 0.20 M is the maximum substrate concentration in toluene due to solubility issues.

Chart 3.1: Possible products generated from the cleavage of two β -O-4 bonds of **LM8** with **V5**.

	C-H Cleavage	C-C Cleavage	C-O Cleavage
C-H Cleavage	 <p>55a,b¹</p> <p>56a</p> <p>56b,c²</p> <p>57a,b³</p>	 <p>58a</p> <p>58b</p> <p>15</p>	 <p>59</p> <p>15</p>
C-C Cleavage	 <p>60</p> <p>19a + 19b</p>	 <p>19a: R = H, R' = OMe 19b: R = H, R' = OMe 39a: R = OH, R' = H 39b: R = OH, R' = H</p> <p>+15</p>	<p>33 + 39a + 39b + 15</p>
C-O Cleavage	 <p>33</p> <p>+ 60</p>	 <p>19a + 19b</p> <p>14</p>	<p>33 + 14 + 15</p>

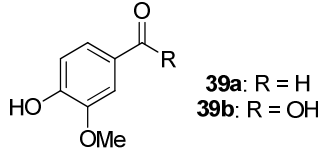
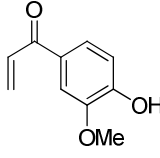
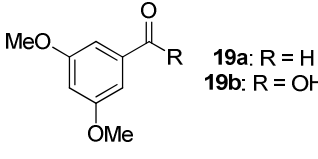
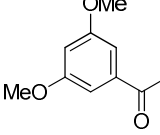
¹ **a** and **b** defined depending on the carbonyl group being on the first (**a**) or the second (**b**) β -O-4 bond. ² **b** and **c** defined depending on the formate group being on the first (**b**) or the second β -O-4 bond (**c**). ³ **a** and **b** defined depending on the alkene group being on the first (**a**) or the second β -O-4 bond (**b**).

Looking in more details at the product distribution, benzylic oxidation of **LM8** afforded mostly monoketones **55a,b**, which over time were further oxidized to diketone **56a**. In analogy to what found for **LM4** and **LM5** (Eq. 3.8), ketone **56a** can undergo dehydration to yield compounds **57a,b**. Quite surprisingly, the product corresponding to the dehydration of both β -O-4 bonds was not detected in our crude mixture. C_{α} - C_{β} cleavage of both β -O-4 bonds affords 3,5-dimethoxybenzaldehyde **19a** and the corresponding benzoic acid **19b**, vanillin **39a** and the over-oxidation product vanillic acid **39b**. C_{β} -O cleavage of both bonds afforded the α,β -unsaturated compounds **33** and **14**. Products deriving from the combination of different reaction pathways were also detected. For instance, C_{α} -H cleavage of the first β -O-4 bond and C_{α} - C_{β} cleavage of the other afforded compound **58a**, the corresponding acid **58b**, and guaiacol **15**. Product **59** was formed via C_{β} -O cleavage of the second β -O-4 bond,

while C_α-H cleavage on the second β-O-4 bond gave product **60**. More generally, as for the remaining products, C_α-C_β cleavage occurred affording benzaldehydes and benzoic acids whereas C_β-O cleavage afforded α,β-unsaturated compounds. Yields and selectivity are listed in Table 3.12 and in Figure 3.4.

Table 3.12: Aerobic oxidation of **LM8**, in toluene at 100 °C, under O₂. Catalyst loading and product distribution.

Entry	1	2	3
[LM8] ₀ (M)	0.05	0.05	0.20
Cat. (mol %)	V5 (10)	V4 (10)	V5 (1)
time (h)	9	24	24
Conv. (%) ^a	>99	>99	>99
15 (%) ^a	2	19	4
55a,b (%) ^{a,b}	7	13	1
56a (%) ^a	38	14	31
56b,c (%) ^{a,b}	5	2	9
57a,b (%) ^{a,b}	6	5	10
58a,b (%) ^a	3 / 2	3 / 1	3 / 7
59 (%) ^{a,c}	3	6	3
60 (%) ^a	8	14	10

39a,b (%) ^a	 39a: R = H 39b: R = OH	1 / 2	1 / 2	1 / 1
17 (%) ^a		6	1	4
19a,b (%) ^a	 19a: R = H 19b: R = OH	1 / 2	2 / 6	2 / 6
33 (%) ^a		9	19	10

Reaction conditions: toluene, 100 °C, O₂ as oxidant. ^a Conv. and yields determined by HPLC, naphthalene used as internal standard. ^b Identified from the reaction mixture; quantification performed assuming the response factor of **56b**. ^c Identified from the reaction mixture; quantification performed assuming the response factor of **58a**.

These data show that **V5** is effective also for the depolymerization of **LM8**. In fact, in every case we obtained complete substrate conversion in few hours (9-24). All of the conditions tested, gave results in agreement with those of **LM4** and **LM5** (Tables 3.6 and 3.9). Indeed, the selectivity of the reaction is once again directed towards C_α-H cleavage, with more than 30 % yield of diketone **56a** (Table 3.12, entries 1 and 3). Another trend observed in analogy with **LM4** and **LM5**, is the increase of the amount of C_α-C_β cleavage products when lowering the catalyst loading to 1 % and increasing the substrate concentration to 0.20 M, reaching 20 % selectivity. However, C_α-C_β cleavage occurred mainly in combination with C_α-H cleavage on the other β-O-4 bond, affording aldehyde **16a** and the overoxidation product **16b**. C_β-O cleavage occurred in the reaction mixture with 15-18 % selectivity. The major product coming from this pathway is product **33** (up to 9%, accounting for about 50% of the C_β-O cleavage), while compounds **14** and **17** were obtained in even lower yield (Table 3.12). Complex **V4** was tested in diluted conditions (Table 3.12, entry 2). Compared to **V5** (Table 3.12, entry 1), this complex exhibited lower activity, converting quantitatively the substrate only after 24 h. The selectivity was directed towards the benzylic oxidation. However, with **V4**, C_β-O cleavage seemed to be more important than with **V5** (30 % vs 18 %), even though this is likely due to the low recovery of diketone **56a** (14 % vs 31 %), which decreased the selectivity towards C_α-H cleavage.

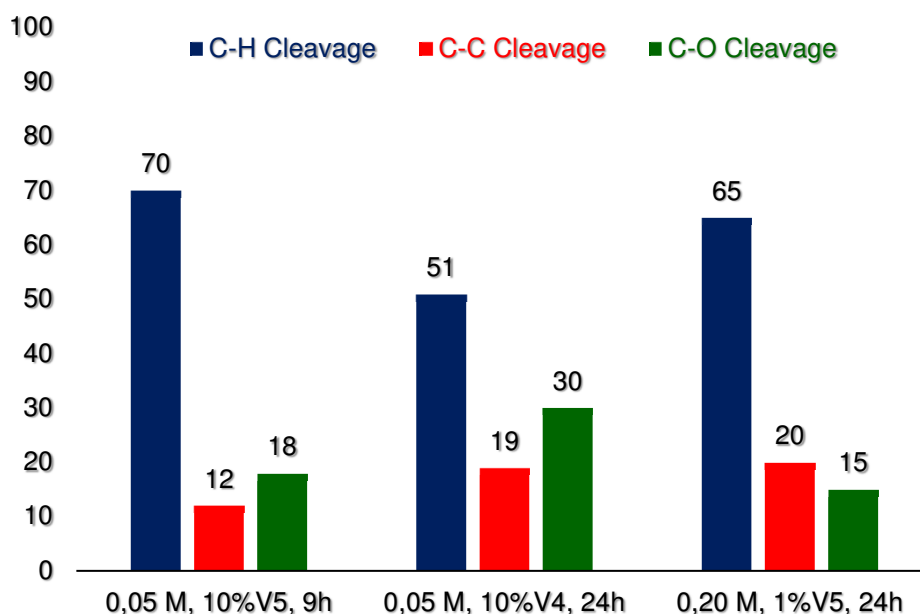
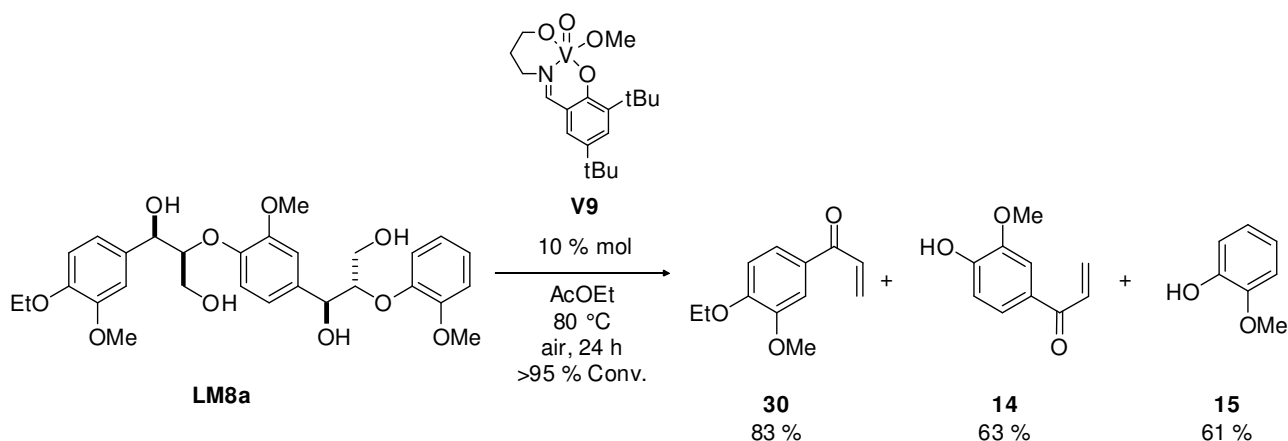


Figure 3.4: Aerobic oxidation of **LM8** catalyzed by **V4** or **V5** in toluene at 100°C. Below each bar are listed: substrate concentration (M), catalyst loading (mol %) and time required to obtain a complete substrate conversion (h). “C_α-H Cleavage”, “C_α-C_β Cleavage” and “C_β-O Cleavage” take into account the sum of determined amounts of products deriving from those mechanisms.

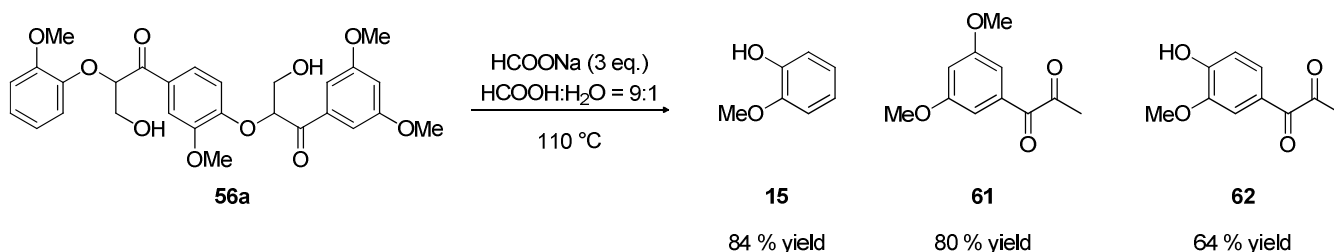
Comparing these results with the literature data, the only example regarding the degradation of a similar trimeric β-O-4 lignin model **LM8a** was reported in literature by Toste and co-workers (Eq. 3.9)¹⁵. They used catalyst **V9**, obtaining exclusively redox-neutral C_β-O cleavage after 24 h at 80°C in ethyl acetate, yielding α,β-unsaturated compounds and guaiacol.



Eq. 3.9: Redox-neutral degradation of model compound **LM8a**.

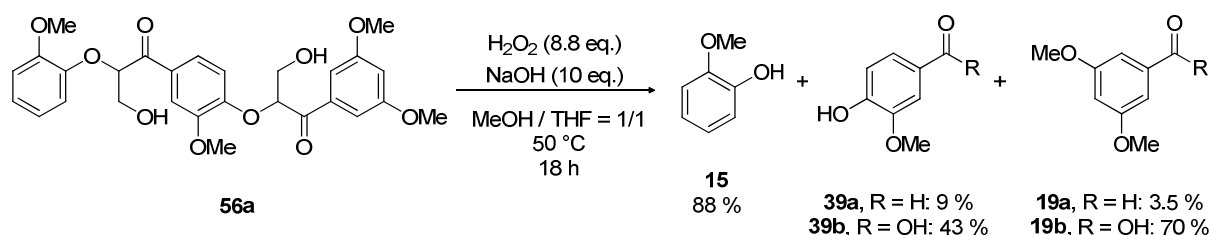
Conversely, with complexes **V5** and **V4** we were able to direct the selectivity of the reaction towards the benzylic oxidation. This should be seen as an advantage rather than a limitation. In fact, the major presence of oxidized products of high molecular weight such as diketone **56a** or compounds **56b,c-57a,b** is not a reaction “sink”. Indeed, several degradation procedures have been reported for these kinds of compounds. For instance, the Baeyer-Villiger Oxidation and subsequent ester hydrolysis⁹, and the formic acid treatment both developed by Stahl et al.¹⁰, allow to obtain valuable

aromatic compounds starting from these compounds. To prove this point, we treated diketone **56a** with 3 eq. of sodium formate in formic acid / H₂O = 9.1, according to the conditions employed by Stahl et al. Interestingly, the depolymerization occurred smoothly affording guaiacol **15** and the α,β -diketones **61** and **62**, respectively in 80 % and 64 % yields (Eq. 3.10).



Eq. 3.10: Formic acid treatment of diketone **56a**. Yields were determined by ¹H NMR using HMDSO as internal standard.

Moreover, we applied also the aforementioned procedure for Baeyer-Villiger Oxidation and subsequent ester hydrolysis⁹ on the crude mixture obtained by the reaction in Table 3.12 entry 3, which was mainly composed by diketone **56a**, and related compounds **56b,c** and **57a,b** (Table 3.12, entry 3) (Eq. 3.11).

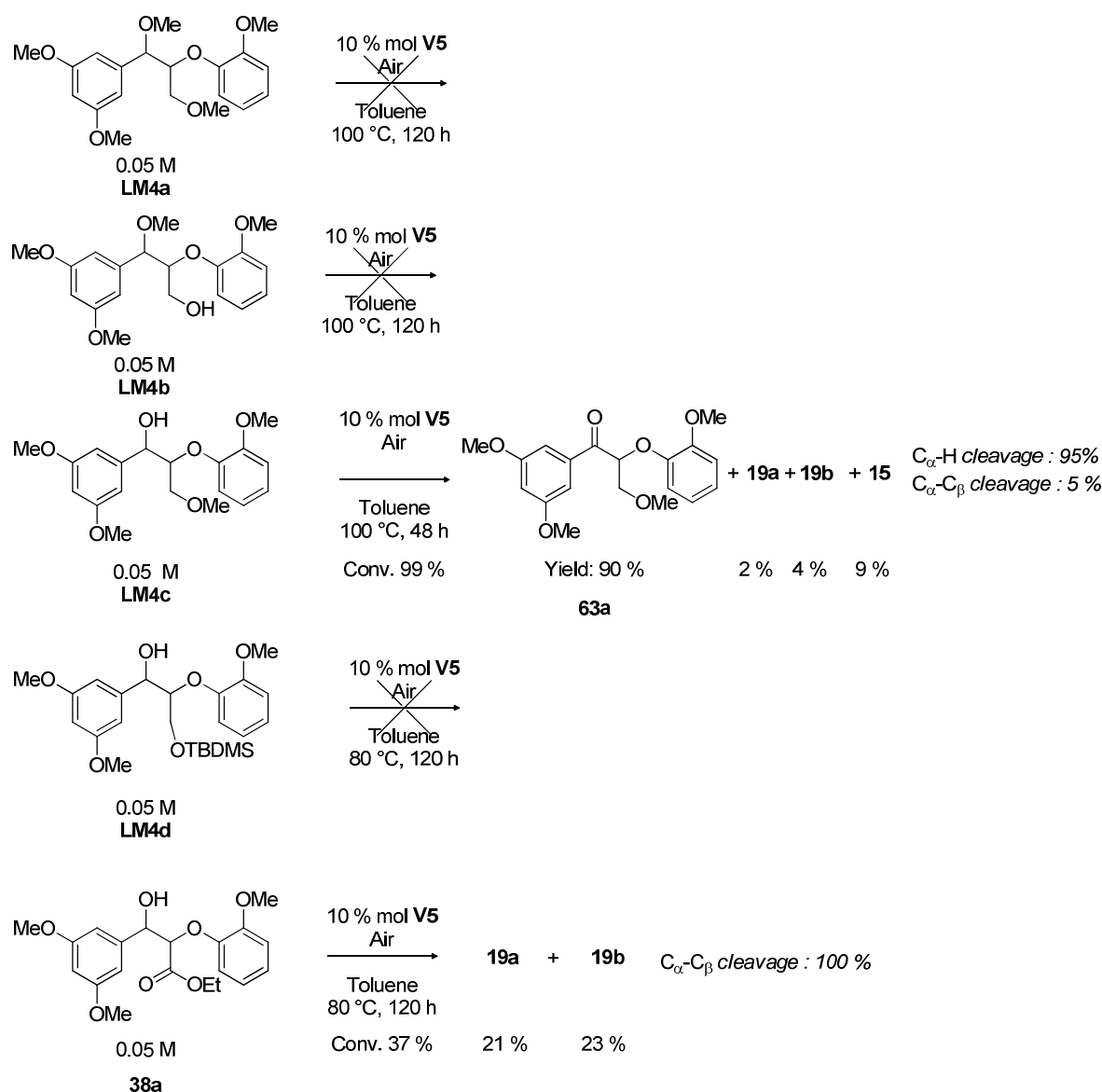


Eq. 3.11: Selective C-C bond cleavage of reaction mixture oxidized β -O-4 trimeric model **56a**. Yields were determined either by ¹H NMR using HMDSO as external standard or by quantitative HPLC using naphthalene as internal standard, considering the amount of oxidized β -O-4 model compounds present in the reaction mixture (**56a-c** + **57a,b** + **58a,b** + **59** + **60**).

After 18 h, we noticed complete substrate disappearance, together with the formation of **15** (88 % yield), **19a** and its corresponding benzoic acid **19b** (3.5 % and 70 % yield respectively), and vanillin **39a** and vanillic acid **39b** (9 % and 43 % yield respectively). Although these reaction conditions are not optimized for this application, they provide a strong support for the development of a tandem process for aerobic catalytic oxidation/oxidative C _{α} -C _{β} cleavage of β -O-4 lignin models. This led us to conclude that, by combination of our system and the above-mentioned procedures, we could improve the yield of aromatic monomers in the oxidation of model **LM8**, making this strategy more appealing.

3.6 Structure-Reactivity Relationship: Aerobic Oxidation of Lignin Model Derivatives

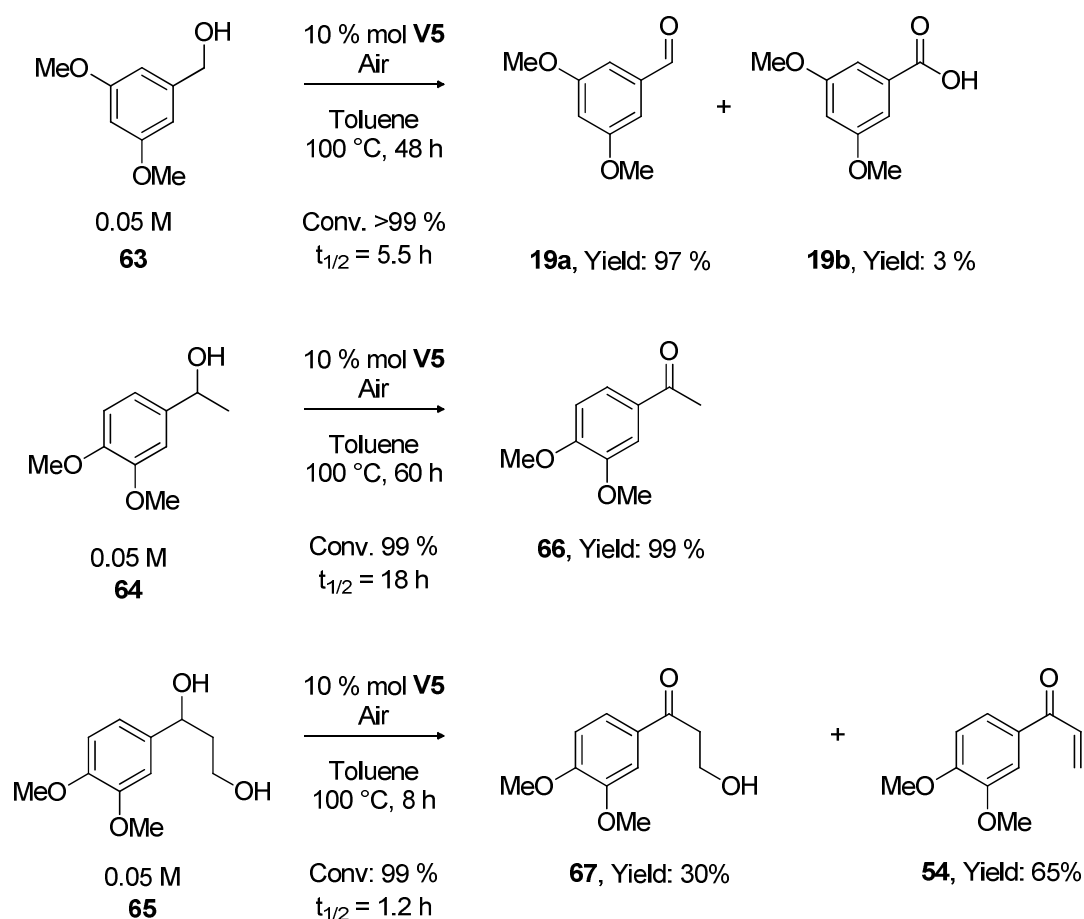
Having identified and quantified most of the products coming from the aerobic catalytic oxidation of models **LM4**, **LM5** and **LM8**, we observed that the selectivity was mainly directed towards the C α -H oxidation (and not towards the C α -C β cleavage as in the case of vicinal diols, see *Chapter 2*). This difference prompted us to explore how the molecular structure of substrate **LM4** affects the reaction selectivity. Therefore, a variety of derivatives of model **LM4** have been synthesized and subjected to the standard reaction conditions in the presence of **V5** (Scheme 3.5).



Scheme 3.5: Aerobic oxidation of **LM4** analogous compounds.

When the bis(methyl ether) substrate **LM4a** or the secondary methyl ether derivative **LM4b** were used, the oxidation reaction was not observed even upon heating at 100 °C for long reaction times (up 120 hours) in toluene. This indicates towards the importance of the coordination of the benzylic hydroxyl group to the metal center of **V5** as a requirement. In contrast, methyl ether **LM4c** was mainly

converted to ketone **63a** (88% of yield, 95 % of selectivity) and only partially underwent C $_{\alpha}$ -C $_{\beta}$ cleavage yielding products **19a** and **19b** (2 and 4% respectively). Importantly, the C $_{\alpha}$ -C $_{\beta}$ cleavage of **LM4c** occurred with a lower rate than **LM4** (48 h instead of 8 h, see Table 3.6 entry 2). C $_{\beta}$ -O cleavage product was not detected with **LM4c**. The low reactivity observed for model **LM4c** suggests that despite the γ -OH group is not fundamental for the oxidation, its presence facilitate the reaction. For a deeper investigation on the role of the primary hydroxyl group, substrates **LM4d** and **38a** were tested, which present either a silyl ether functionality or an ester group. As regards **LM4d**, no substrate conversion was observed after longer reaction times probably due to the high steric hindrance of the TBDMS-protecting group. On the other hand, the oxidation of **38a** proceeded slowly (with only 37 % of conversion after 120 h at 80 °C) but with high selectivity towards the C $_{\alpha}$ -C $_{\beta}$ cleavage. However, this C $_{\alpha}$ -C $_{\beta}$ bond-breaking can be access also via retro-aldol reaction as demonstrated by Stahl and co-workers⁹. To finally prove the involvement of the primary alcohol group in the reactivity, a study of the oxidation of several benzyl alcohols **63-65** was undertaken (Scheme 3.6).



Scheme 3.6: Aerobic oxidation of benzylic alcohols **63-65** catalyzed by **V5**.

The alcohol oxidation was investigated at a concentration of 0.05 M in toluene at 100 °C with **V5** (10 mol %). The reaction with (3,5-dimethoxyphenyl)methanol **63** yielded 97 % of the corresponding aldehyde **19a** with only few traces of 3,5-dimethoxybenzoic acid **19b** after 48 h at 100 °C. Secondary

alcohol **64** showed slower reactivity likely due to steric hindrance, and longer reaction times (up to 60 hours) were required for observe full conversion of the reagent. On the contrary, substrate **65** is completely oxidized after only 8 hours. The reaction in this case yields the corresponding ketone **67** which is further dehydrated to afford the α,β -unsaturated compound **54**. Despite the subsequent transformation of **67**, it is clear that the presence of the peripheral primary alcohol notably accelerates the reaction. The reactivity of our catalyst towards models **63-65** indicates that hydroxyl groups present in lignin models affect the reactivity and the selectivity of the aerobic oxidation. In particular, the benzylic OH group is crucial in order to access oxidation, whereas the γ -OH group exclusively assists the benzylic oxidation, leading to an enhancement of the selectivity towards ketone formation.

3.7 Conclusions

In this chapter, we have demonstrated that Vanadium V aminotriphenolate complex **V5** is an effective catalyst for the aerobic oxidation of non-phenolic β -O-4 lignin model compounds **LM4** and **LM5**. As in the case of vicinal diols (*Chapter 2*), toluene gave the best effects in terms of reaction speed and product yields, with faster reactions run at 100 °C. Moreover, in every condition studied, the selectivity was strongly directed to benzylic oxidation (50-85 %), but an unprecedented high value with respect to C_α - C_β cleavage was observed when decreasing the catalyst amount to 1 % and increasing substrate concentration to 0.25 M (up to 32 %). We tested also two phenolic lignin models **LM6** and **LM7**, obtaining products coming from both benzylic oxidation (16-32 % yield) and C_α - C_{Ph} cleavage (10-11 % yield), with low amounts of products coming from C_α - C_β cleavage (2-5 % yield). A non-phenolic trimeric β -O-4 lignin model **LM8** was subjected to **V5**, showing a selectivity directed towards benzylic oxidation on both linkages (51-70 %), together with a discrete amount of products deriving from C_α - C_β cleavage (12-20 % selectivity) and C_β -O cleavage (15-30 % selectivity). We have also demonstrated also that ketone **56a** coming from C_α -H cleavage of **LM8** can be further degraded to afford monomeric aromatic compounds (70 % yield of 3,5-dimethoxybenzoic acid **19b** and 43 % yield of vanillic acid **39b**), thus paving the way to an effective tandem procedure for β -O-4 oligomers oxidative depolymerization. Finally, in order to understand the reaction mechanism, α - and γ -functionalized lignin model derivatives have been synthesized and analyzed, discovering that an α -OH group is essential for oxidation, whereas a γ -OH group only exerts catalytic effects on benzylic oxidation.

3.8 Experimental

General Remarks

All chemicals and dry solvents were purchased from Sigma-Aldrich and used without further purification. Deuterated solvents (Sigma-Aldrich) were used without further purification. Other organic solvents, (Sigma-Aldrich) were used without further purification. MilliQ Water: Deionized water was purified with a Millipore system, constituted by ion exchange resins and activated-carbon resins. ^1H -NMR, $^{13}\text{C}\{^1\text{H}\}$ -NMR, DEPT-135 and ^{51}V NMR spectra have been recorded at 301 K with a Bruker spectrometer AC-200 MHz (^1H : 200.13 MHz; ^{13}C : 50.3 MHz) or Avance Bruker DRX-300 (^1H : 300.13 MHz; ^{13}C : 75.5 MHz, ^{51}V : 78.28 MHz). Chemical shifts (δ) have been reported in parts per million (ppm) relative to the residual undeuterated solvent as an internal reference (CDCl_3 : 7.26 ppm for ^1H -NMR and 77.0 ppm for ^{13}C NMR; CD_3CN : 1.94 ppm for ^1H -NMR and 118.26 ppm for ^{13}C NMR). For ^{51}V NMR spectra was referred to $\text{VO}(\text{O}_2)\text{picolinate}$ (5×10^{-3} M, water, pH = 1) used as external standard. The multiplicity of the signals is indicated in the following way: s: singlet, d: doublet, t: triplet, q: quartet, dd: doublet of doublets, m: multiplet, br: broad. GC-MS spectra have been recorded with an Agilent 6850 Series GC System interfaced with an Agilent 5973 Network Mass Selective Detector. Carrier gas He, phase HP-5MS, column 30mt I.D. 0,25, film 0,25 μm , 5% diphenyl 95% dimethylsiloxane. Injector temperature has been set to 250 $^\circ\text{C}$, detector temperature has been set to 280 $^\circ\text{C}$ and the carrier gas is He (1 mL/min) with a HP-5MS column. ESI-MS spectra were recorded on an Agilent 1100 LC/MSD IonTrap spectrometer, in positive/negative modes, by direct flow injection using acetonitrile or methanol (both with 0.1 % v/v of HCOOH for analysis in positive mode) as mobile phase or an ESI-TOF MarinerTM BiospectrometryTM Workstation (Applied Biosystems) by flow injection, using acetonitrile or methanol/formic acid 0.1% as mobile phase. TLC: Silica gel PET plates Macherey-Nagel POLYGRAM[®] SIL G/UV₂₅₄ have been used; detection by UV-Vis and treatment with PMA staining reagent (10 % w/w in ethanol) or KMnO_4 . Flash Chromatography was performed as described in literature using Macherey-Nagel silica gel 60 (0.04-0.63 mm, 230-400 mesh)²⁶. Reactions that required an N_2 inert atmosphere were carried out in a glove-box MBRAUN MB 200MOD, equipped with a regulation and recycling inert gas system MB 150 G-1 (nitrogen working pressure: 6 bar). Each substance introduced in the glove-box has been previously subjected to repeated vacuum / N_2 cycles into a pre-chamber. Water level inside the box was real-time monitored by MBraun moisture analyzer. FT-IR spectra has been recorded in the range (4000-600) cm^{-1} and resolution 4 cm^{-1} , on a Nicolet 5700 FT-IR instrument, using KBr pellets. HPLC analyses were performed on a Shimadzu HPLC equipped with a Knauer Eurospher II 100-5 C18 (5 μm of active phase, 250 x 4,6 mm column) operating at room temperature, eluent water /acetonitrile gradient, naphthalene/biphenyl as internal standard. The UV detector was set at $\lambda = 210$ nm. The concentration of both reagents and products was estimated from the calibration curves.

²⁶ Still, C. W.; Khan, Mitra, A.; *J. Org. Chem.* **1978**, 43, 2923.

GC-FID analyses were performed on a Shimadzu GC-2010, equipped with a Supelco column (phase: SPB^{T1}-1, length: 15 m, ID: 0.1 mm, 0.1 μ m Film, 100% dimethylsiloxane). Carrier gas He (69 ml/min). Injector temperature has been set to 280 °C, detector temperature has been set to 330 °C. The concentration of both reagents and products was estimated from the calibration curves.

Synthesis of Arylglycerol β -Aryl Ether Lignin Models LM4-LM7

The dimeric lignin model compounds (mixture of *erythro(anti)*/*threo(syn)* distereoisomers) were prepared by a three-step procedure, based on an aldol condensation reaction, following previously reported procedures²⁷. Hereafter, the characterization data of the main compounds are reported.

Ethyl-(2-methoxyphenoxy)-acetate 37

To a solution of triethylamine (10.889 g, 107.6 mmol) in dry acetonitrile (80 mL), 2-methoxyphenol (10.161 g, 81.9 mmol) was added and the mixture was stirred at room temperature for 1 h, and then it was cooled at 0 °C. Ethyl bromoacetate (18.069 g, 108.2 mmol) was added dropwise in 30 min and the reaction was allowed to reach room temperature overnight. Then the mixture was evaporated under reduced pressure until almost dryness and diluted in ethyl acetate (100 mL). The organic phase was washed with a solution of HCl_{aq} 0.1 M (2 x 30 mL), sat. NaHCO₃ aq. (2 x 30 mL), water and then dried over anhydrous Na₂SO₄. The solvent was evaporated obtaining the product, a yellowish oil, which was used without any further purification (97 %, 16.70 g). ¹H-NMR (300 MHz, CDCl₃), δ (ppm) = 6.99-6.84 (m, 4H), 4.68 (s, 2H), 4.26 (q, J = 7.2 Hz, 2H), 3.88 (s, 3H), 1.28 (t, J = 7.2 Hz, 3H). ¹³C NMR (75 MHz, CDCl₃), δ (ppm) = 170.43, 151.18, 148.81, 122.95, 122.15, 116.09, 113.68, 68.01, 62.55, 57.25, 15.55. GC-MS (EI) = m/z : 52(8), 65(8), 77(50), 92(15), 95(23), 109(16), 121(12), 122(60), 123(47), 124(9), 137(45), 210(M⁺, 100). All spectra data are in agreement with those reported in the literature²⁷.

Preparation of the β -hydroxy esters

Typical procedure: Synthesis of ethyl 3-(3,5-dimethoxyphenyl)-3-hydroxy-2-(2-methoxyphenoxy)propanoate 38a

To a cooled solution (-78 °C) of freshly distilled diisopropylamine (4.2 mL, 30.0 mmol) in dry THF (30 mL), was added dropwise a solution of *n*BuLi (2.5 M in hexane, 13.0 mL, 32.6 mmol) in 15 min under nitrogen atmosphere. After stirring for 30 min at -78°C, to this mixture a solution of Ethyl-(2-methyl phenoxy)-acetate (3.616 g, 21.8 mmol) in 20 mL of dry THF was added dropwise over a period of 1 h. Then the 3,5 dimethoxybenzaldehyde (3.616 g, 21.8 mmol) in dry THF (10 mL) was added dropwise in 20 min and the stirring was continued for 2-3 h at -78°C. The disappearance of the aldehyde was monitored by TLC and ¹H-NMR. At the end of the reaction, the mixture was warmed

²⁷ Buendia, J.; Mottweiler, J.; Bolm, C.; *Chem. Eur. J.* **2011**, *17*, 13877.

up at 0°C (it was observed a changing of color from yellowish to brilliant red) and quenched with distilled water (60 mL). A solution of HCl_{aq} 4 N was added till PH = 7 was reached. The residue was extracted with Ethyl Acetate (2 x 100 mL). The organic phase was washed with brine and water, dried over anhydrous NaSO₄ and evaporated in vacuum. The crude was purified by column chromatography on silica gel (*n*-hexane/ethyl acetate from 4/1 to 1/4) affording **38a** (yellow-brown oil) as a mixture of diastereoisomers (*erythro* (*anti*) / *threo* (*syn*) = 72/28) with an overall yield of 91 % (7.47 g). The major diastereoisomer is assigned as the *erythro* (*anti*) form based on a comparison with the closely related labelled ¹³C-**38a**⁷ and the 3-hydroxy-3-(3,4-dimethoxyphenyl)-2-(2-methoxyphenoxy)-propanoate²⁸ compounds. ¹H-NMR (300 MHz, CDCl₃), δ (ppm) = 7.07-6.80 (m, 4H, *syn-anti*), 6.63 (d, *J* = 2.1 Hz, 2H, *anti*), 6.59 (d, *J* = 2.1 Hz, 2H, *syn*), 6.39 (t, *J* = 2.1 Hz, 1H, *syn-anti*), 5.15 (d, *J* = 4.8 Hz, 1H, *anti*), 5.05 (d, *J* = 6.8 Hz, 1H, *syn*), 4.74 (d, *J* = 4.8 Hz, 1H, *anti*), 4.50 (d, *J* = 6.8 Hz, 1H, *syn*), 4.17 (q, *J* = 7.2 Hz, 2H, *anti*), 4.11 (q, *J* = 7.2 Hz, 2H, *syn*), 3.87 (s, 3H, *syn-anti*), 3.78 (s, 6H, *anti*), 3.77 (s, 6H, *syn*) 1.26 (t, *J* = 7.2 Hz, 3H, *anti*), 1.15 (t, *J* = 7.2 Hz, 3H, *syn*). ¹³C NMR (75 MHz, CDCl₃), δ (ppm) = 170.86, 170.66, 162.24, 162.10, 152.09, 148.64, 142.99, 142.11, 125.39, 125.31, 122.59, 120.33, 119.64, 113.88, 106.42, 106.33, 102.07, 101.72, 86.60, 85.21, 76.54, 75.52, 62.69, 57.35, 56.78, 15.50, 15.39. ESI-MS = *m/z* calcd for C₂₀H₂₄O₇+Na⁺, [M + Na⁺]: 399.1, found: 399.1.

Ethyl 3-(3,4-dimethoxyphenyl)-3-hydroxy-2-(2 methoxyphenoxy)propanoate 38b

Following the here above reported procedure, compound **38b** was prepared (yellow-brown oil) as a mixture of diastereoisomers (*erythro* (*anti*) / *threo* (*syn*) = 43/57) with overall yield of 80 %. ¹H-NMR (300 MHz, CDCl₃), δ (ppm) = 7.07-6.79 (m, 7H, *syn-anti*), 5.15 (d, *J* = 5.0 Hz, 1H, *anti*), 5.06 (d, *J* = 7.1 Hz, 1H, *syn*), 4.74 (d, *J* = 5.0 Hz, 1H, *anti*), 4.48 (d, *J* = 7.1 Hz, 1H, *syn*), 4.12 (m, 2H, *anti-syn*), 3.88 (s, 3H *syn-anti*), 3.78 (s, 9H, *anti-syn*), 1.24 (t, *J* = 7.2 Hz, 3H, *anti*), 1.10 (t, *J* = 7.2 Hz, 3H, *syn*). ¹³C NMR (75 MHz, CDCl₃), δ (ppm) = 169.3, 150.6, 148.8, 148.7, 147.2, 131.7, 123.9, 121.1, 119.3, 119.0, 112.3, 110.7, 110.1, 83.9, 73.8, 61.2, 55.9, 55.8, 55.8, 14.1. ESI-MS = *m/z* calcd for C₂₀H₂₄O₇+Na⁺, [M + Na⁺]: 399.1, found: 399.1. All spectra data are in agreement with those reported in the literature²⁷. Pure samples of the two diastereoisomers can be obtained by crystallization of the yellow-brown oil in ethyl acetate/*n*-hexane leading to *erythro* (*anti*) as a white solid while *threo* (*syn*) as a yellowish oil.

Ethyl 3-(4-(benzyloxy)-3,5-dimethoxyphenyl)-3-hydroxy-2-(2-methoxyphenoxy) propanoate 48a

Following the here above reported procedure, compound **48a** was prepared (white solid) as a mixture of diastereoisomers (*erythro* (*anti*) / *threo* (*syn*) = 63/37) with overall yield of 96% after

²⁸ Cho, D. W.; Parthasarathi, R.; Pimentel, A. S.; Maestas, G. D.; Park, H. J.; Yoon, U. C.; Dunaway-Mariano, D.; Gnanakaran, S.; Langan, P.; Mariano, P. S. *J. Org. Chem.* **2010**, 75, 6549.

purification of the crude by column chromatography on silica gel (*n*-hexane/Ethyl Acetate from 8/2 to 1/1). ¹H-NMR (300 MHz, CDCl₃), δ (ppm) = 7.54-7.30 (m, 5H), 7.03-6.89 (m, 4H), 6.75 (s, 2H, *anti*), 6.69 (s, 2H, *syn*), 5.19 (m, 1H, *J* = 4.5 Hz, *anti*), 5.09 (d, 1H, *J* = 6.9 Hz, *syn*), 5.02 (s, 2H), 4.24-4.04 (m, 2H), 3.89 (s, 3H, *syn*), 3.88 (s, 3H, *anti*), 3.86 (s, 6H, *anti*), 3.85 (s, 6H, *syn*), 1.19 (t, 3H, *J* = 7.1 Hz, *anti*), 1.11 (t, 3H, *J* = 7.1 Hz, *syn*). ¹³C NMR (75 MHz, CDCl₃), δ (ppm) = 169.41, 169.32, 153.47, 153.31, 150.54, 150, 35, 137.86, 134.80, 133.77, 128.47, 128.11, 127.78, 124.01, 123.92, 121.09, 118.67, 118.43, 112.31, 104.10, 85.48, 83.62, 75.20, 74.99, 74.09, 61.25, 56.09, 55.82, 14.08, 13.97. ESI-MS = *m/z* calcd for C₂₇H₃₀O₈Na⁺: 505.2, found: 505.2. All spectra data are in agreement with those reported in the literature²⁷.

Ethyl 3-(4-(benzyloxy)-3-methoxyphenyl)-3-hydroxy-2-(2-methoxyphenoxy) propanoate 48b

Following the here above reported procedure, compound **48b** was prepared (white solid) as a mixture of diastereoisomers (*erythro anti* / *threo syn*) = 40/60) with overall yield of 96% after purification of the crude by column chromatography on silica gel (*n*-hexane/Ethyl Acetate from 9/1 to 2/8). ¹H-NMR (300 MHz, CDCl₃), δ (ppm) = 7.42-7.39 (m, 2 H), 7.36-7.27 (m, 3 H), 7.08 (d, *J* = 1.8 Hz, 1H, *anti*), 7.01 (d, *J* = 1.5 Hz, 1 H, *syn*), 6.99-6.97 (m, 1 H), 6.91-6.90 (m, 1 H), 6.89-6.86 (m, 2 H), 6.84-6.81 (m, 2 H), 5.13 (m, 3 H), 5.04 (d, *J* = 7.0 Hz, 1H, *syn*), 4.71 (d, *J* = 5.1 Hz, 1 H *anti*), 4.47 (d, *J* = 7.0 Hz, 1 H, *syn*), 4.02 (q, *J* = 7.2 Hz, 2H *anti*), 4.01 (d, *J* = 7.2 Hz, 2H, *syn*), 3.87 (s, 3H), 3.84 (s, 3 H *anti*), 3.82 (s, 3H, *syn*), 1.11 (t, *J* = 7.2 Hz, 3H *anti*), 1.02 (t, *J* = 7.2 Hz, 3H, *syn*). ¹³C NMR (75 MHz, CDCl₃), δ (ppm) = 170.91, 152.08, 151.88, 151.19, 150.97, 149.68, 149.42, 148.84, 148.77, 138.71, 138.60, 130.00, 129.29, 128.73, 125.36, 122.55, 121.06, 120.26, 119.771, 115.23, 115.17, 113.88, 113.83, 112.32, 112.19, 86.90, 85.32, 76.37, 75.33, 72.47, 62.66, 57.49, 57.31, 15.56, 15.42. ESI-MS = *m/z* calcd for C₂₆H₂₈O₇Na⁺: 475.17, found: 475.2. All spectra data are in agreement with those reported in the literature²⁷.

Preparation of the β-hydroxy-1,3-propanediols LM4-LM5

Typical procedure: Synthesis of **1-(3,5-dimethoxyphenyl)-2-(2-methoxyphenoxy)propane-1,3-diol LM4**

To a cooled solution (0 °C) of the diastereoisomers ethyl 3-(3,5-dimethoxyphenyl)-3-hydroxy-2-(2-methoxyphenoxy)propanoate **38a** (mixture of *erythro anti* / *threo syn*) = 72/28) (6.352 g, 16.9 mmol) in dry THF (45 mL), was slowly added a solution of LiAlH₄ (1.0 M in THF, 20.0 mL, 20.0 mmol) under nitrogen atmosphere. The reaction was allowed to reach room temperature overnight under stirring, until TLC and NMR analysis indicated the absence of starting material. The mixture was then carefully quenched by dropwise and sequential addition of water (10 mL). A solution of HCl_{aq} 4 N was added till PH = 7 was reached. The residue was extracted with CH₂Cl₂ (3 x 100 mL). The organic phase was washed with brine and water, dried over anhydrous NaSO₄ and evaporated under vacuum. The resulting amber oil was used without any further purification (4.80 g, 85 % yield, *erythro*

(*anti*) / *threo* (*syn*) = 72/28). The major diastereoisomer is assigned as the *erythro* (*anti*) form based on a comparison with the already reported *erythro* and *threo* product⁷. ¹H-NMR (300 MHz, CDCl₃), δ (ppm) = 7.16-6.92 (m, 4H, *syn-anti*), 6.65 (d, *J* = 2.3 Hz, 2H, *syn*), 6.58 (d, *J* = 2.3 Hz, 2H, *anti*), 6.44 (t, *J* = 2.3 Hz, 1H, *syn*), 6.41 (t, *J* = 2.3 Hz, 1H, *anti*), 5.01 (d, *J* = 4.3 Hz, 1H, *anti*), 4.99 (d, *J* = 8.0 Hz, 1H, *syn*), 4.18 (m, 1H, *anti*), 4.08 (m, 1H, *syn*), 3.96-3.88 (m, 1H, *syn-anti*), 3.94 (s, 3H, *syn*), 3.93 (s, 3H, *anti*), 3.82 (s, 6H, *syn*), 3.81 (s, 6H, *anti*), 3.66 (dd, *J* = 3.4, 12.2 Hz, 1H, *anti*), 3.62 (dd, *J* = 4.0, 13.0 Hz, 1H, *syn*). ¹³C NMR (75 MHz, CDCl₃), *anti* diastereoisomer, δ (ppm) = 156.88, 148.50, 143.97, 139.81, 123.54, 121.18, 120.72, 112.60, 106.02, 105.03, 101.15, 89.88, 78.77, 65.63, 60.85. ¹³C NMR (75 MHz, CDCl₃), *syn* diastereoisomer, δ (ppm) = 156.44, 148.13, 143.93, 139.68, 123.61, 121.18, 120.64, 112.54, 105.62, 105.03, 101.79, 94.67, 78.00, 66.11, 61.35. ESI-MS = *m/z* calcd for C₁₈H₂₂O₆+Na⁺, [M + Na⁺]: 357.0, found: 357.0. All spectra data are in agreement with those reported in the literature⁷.

1-(3,4-dimethoxyphenyl)-2-(2-methoxyphenoxy)propane-1,3-diol LM5

Following the here above reported procedure and using pure compound *anti*-**38b** (0.623 g), **LM5** in the *erythro* (*anti*) pure diastereoisomer was prepared (0.546 g, 98 %) as a yellowish solid. ¹H-NMR (300 MHz, CDCl₃), δ (ppm) = 7.15-6.86 (m, 7H), 5.03 (d, *J* = 4.7 Hz, 1H), 4.19 (m, 1H), 4.0 (m 1H), 3.93 (s, 3H), 3.92 (s, 3H), 3.91 (s, 3H), 3.70 (m, 1H). ¹³C NMR (75 MHz, CDCl₃) δ (ppm) = 153.21, 150.58, 150.03, 148.40, 133.87, 126.78, 125.82, 123.16, 122.69, 119.88, 113.71, 112.58, 110.72, 89.05, 74.17, 62.23, 57.42. ESI-MS = *m/z* calcd for C₁₈H₂₂O₆Na⁺, [M + Na⁺]: 357.1, found: 357.3. All spectra data are in agreement with those reported in the literature²⁷.

1-(4-(benzyloxy)-3,5-dimethoxyphenyl)-2-(2-methoxyphenoxy)propane-1,3-diol 49a

Following the here above reported procedure, and using compound **48a** (3.00 g, 4.14 mmol), **49a** was prepared (colorless syrup) as a mixture of diastereoisomers (*erythro* (*anti*) / *threo* (*syn*) = 60/40) with overall yield of 88% (2.4 g). The crude was used without any purification. ¹H-NMR (300 MHz, CDCl₃), δ (ppm) = 7.52-7.28 (m, 5H), 7.16-6.93 (m, 4H), 6.71 (s, 2H, *syn*), 6.64 (s, 2H, *anti*), 5.03 (s, 2H), 5.00 (m, 1H), 4.23-3.51 (m, 3H), 3.96 (s, 3H, *syn*), 3.93 (s, 3H, *anti*), 3.86 (s, 3H, *syn*), 3.84 (s, 3H, *anti*), 2.86 (s, 1H). ¹³C NMR (75 MHz, CDCl₃) δ (ppm) = 153.9, 152.0, 147.3, 138.2, 137.0, 135.8, 128.6, 128.3, 127.9, 124.4, 121.9, 121.2, 112.7, 103.9, 87.5, 75.2, 73.3, 61.1, 56.5, 56.2. ESI-MS = *m/z* calcd for C₂₅H₂₈O₇Na⁺, [M + Na⁺]: 463.2, found: 463.4. All spectra data are in agreement with those reported in the literature^{11a}.

1-(4-(benzyloxy)-3-methoxyphenyl)-2-(2-methoxyphenoxy)propane-1,3-diol 49b

Following the here above reported procedure, and using compound **48b** (6.00 g, 13 mmol), **49b** was prepared (colorless syrup) as a mixture of diastereoisomers (*erythro* (*anti*) / *threo* (*syn*) = 46/56) with overall yield of 91% (5 g). The crude was used without any purification. ¹H-NMR (300 MHz, CDCl₃),

δ (ppm) = 7.43-7.40 (m, 2 H), 7.37-7.27 (m, 3 H), 7.09 (d, J = 7.8 Hz, 2 H, *anti*), 7.01 (d, J = 5.7 Hz, 2 H, *syn*), 6.91-6.81 (m, 5 H), 5.11 (s, 2 H), 4.96-4.93 (m, 1 H), 4.15 (m, 1 H, *anti*), 4.02 (m, 1 H, *syn*), 3.92 (d, J = 5.7 Hz, 1 H, *anti*), 3.88 (d, J = 5.7 Hz, 1 H, *syn*), 3.85 (s, 3 H, *syn*), 3.84 (s, 3 H), 3.80 (s, 3 H, *syn*), 3.69 (d, J = 3.3 Hz, 1 H, *anti*), 3.65 (m, 1 H), 3.60 (d, J = 3 Hz, 1 H, *syn*), 3.49 (d, J = 3.9 Hz, 1 H, *syn*), 3.45 (d, J = 4.2 Hz, 1 H, *anti*), 3.37 (bs, 1 H). ^{13}C NMR (75 MHz, CDCl_3), δ (ppm) = 152.87, 152.64, 151.28, 151.21, 149.49, 149.19, 149.07, 148.52, 138.68, 138.64, 135.02, 134.48, 130.01, 129.32, 128.80, 125.51, 123.14, 122.18, 121.00, 115.47, 113.68, 112.12, 111.57, 90.45, 88.40, 75.29, 74.29, 72.54, 62.98, 62.37, 57.52, 57.34. ESI-MS = m/z calcd for $\text{C}_{24}\text{H}_{26}\text{O}_6\text{Na}^+$: 433.16, found: 433.2. All spectra data are in agreement with those reported in the literature²⁷.

Preparation of the β -hydroxyl 1, 3-propanediols LM6-LM7

1-(4-hydroxy-3,5-dimethoxyphenyl)-2-(2-methoxyphenoxy)propane-1,3-diol LM6

To a solution of **49a** (1.40 g, 3.18 mol) in 20 ml of MeOH, Pd/C (140 mg, 10 w/w %) was added. The mixture was subjected to one cycle of vacuum/ N_2 to exclude air and then hydrogenated with a hydrogen balloon at room temperature overnight. The catalyst was removed by filtration and washed with MeOH, and then the filtrate was concentrated and purified on silica gel using ethyl acetate/*n*-hexane (7/3 to 9/1) to provide 980 mg (88%) of pure product as a mixture of diastereoisomers (*erythro (anti) / threo (syn)* = 67/33). ^1H -NMR (300 MHz, CDCl_3), δ (ppm) = 7.18-6.95 (m, 4H), 6.69 (s, 2H, *syn*), 6.63 (s, 2H, *anti*), 5.68 (brs, 1H), 4.98 (m, 1H), 4.19 (m, 1H, *anti*), 4.05 (m, 1H, *syn*), 3.99-3.48 (m, 2H), 3.92 (s, 3H, *syn*), 3.89 (s, 3H, *anti*), 3.89 (s, 6H, *syn*), 3.88 (s, 6H, *anti*). ^{13}C NMR (75 MHz, CDCl_3), δ (ppm) = 147.33, 147.14, 134.37, 131.33, 124.32, 121.84, 121.07, 120.91, 112.40, 104.02, 103.12, 89.44, 87.35, 74.38, 73.16, 63.99, 61.22, 61.00, 56.53, 56.08. ESI-MS = m/z calcd for $\text{C}_{18}\text{H}_{22}\text{O}_7\text{Na}^+$: 373.13, found: 373.1. All spectra data are in agreement with those reported in the literature²⁷.

1-(4-hydroxy-3-methoxyphenyl)-2-(2-methoxyphenoxy)propane-1,3-diol LM7

Following the here above reported procedure, and using compound **49b** (4.55 g, 11 mmol), **LM7** was prepared (white solid) as a mixture of diastereoisomers (*erythro (anti) / threo (syn)* = 45/55) with overall yield of 52% (1.86 g). ^1H -NMR (300 MHz, CDCl_3), δ (ppm) = 7.14 - 7.03 (m, 1 H), 6.99-6.80 (m, 6 H), 5.60 (s, br), 4.96 (d, J = 7.5 Hz, 1 H, *syn*), 4.96 (d, J = 4.8 Hz, 1 H, *anti*), 4.15 (m, 1 H, *anti*), 4.01 (m, 1 H, *syn*), 3.91 (s, 3 H, *syn*), 3.88 (s, 3 H, *anti*), 3.88 (s, 3 H), 3.94-3.46 (m, 2 H), 2.62 (s, br). ^{13}C NMR (75 MHz, CDCl_3), δ (ppm) = 152.02, 151.72, 148.03, 147.30, 147.06, 147.02, 145.99, 145.52, 132.20, 131.90, 124.66, 124.63, 122.10, 122.14, 121.47, 121.44, 120.67, 119.43, 114.72, 114.66, 112.6, 112.59, 109.82, 109.07, 89.95, 87.83, 74.41, 73.17, 61.46, 61.15, 56.38, 56.29. ESI-MS = m/z calcd for $\text{C}_{17}\text{H}_{20}\text{O}_6\text{Na}^+$: 343.13, found: 343.2. All spectra data are in agreement with those reported in the literature²⁷.

Synthesis of Trimeric Lignin Model 2-(4-(1,3-dihydroxy-2-(2-methoxyphenoxy)propyl)-2-methoxyphenoxy)-1-(3,5-dimethoxyphenyl)propane-1,3-diol LM8

The trimeric lignin model compound (mixture of *erythro(anti)/threo(syn)* diastereoisomers) was prepared by a nine-step procedure (Scheme 1S), based on aldol condensation reactions, following previously reported procedures for a similar compound. Hereafter, the characterization data of the main compounds are reported²⁴.

Ethyl-2-(4-formyl-2-methoxyphenoxy)acetate 40

To a stirred solution of vanillin (18.723 g, 123.06 mmol) in dry acetone under N₂, oven-dried K₂CO₃ (25.587 g, 185.14 mmol) and ethyl bromoacetate (15 mL, 135 mmol) were added. The mixture was stirred under reflux for 3h (TLC, AcOEt/*n*-hexane = 3:2). The mixture was then filtered through celite and solvent removed under vacuum. The product was obtained as a white solid and used without further purification (29.73 g, 99 % yield). Mp: 94-96 °C (lett. 94.5-95.5 °C) ¹H NMR (300 MHz, CDCl₃) δ (ppm) = 9.84 (s, 1H), 7.40-7.37 (m, 2H), 6.85 (d, J = 8.1 Hz, 1H), 4.75 (s, 2H), 4.24 (q, J = 7.2 Hz, 2H), 3.92 (s, 3H), 1.26 (t, J = 7.2 Hz, 3H). ¹³C NMR (75 MHz, CDCl₃) δ (ppm) = 192.3, 169.5, 154.0, 151.5, 132.6, 127.6, 113.9, 111.4, 67.4, 63.1, 57.6, 15.6. ESI-MS: *m/z* calcd for C₁₂H₁₄O₅ + H⁺, [M + H⁺]: 239.09, for C₁₂H₁₄O₅ + Na⁺, [M + Na⁺]: 261.07; found: 239.0, [M + H⁺], 261.0, [M + Na⁺]. GC-MS (EI, 70 eV) *m/z* (%): 238 (M⁺, 100). All spectra data are in agreement with those reported in the literature²⁴.

Ethyl-2-(4-(1,3-dioxolan-2-yl)-2-methoxyphenoxy)acetate 41

To a solution of **40** (29.73 g, 124.79 mmol) in dry toluene, dry ethylene glycol (10.5 mL, 188.28 mmol) and *p*-toluenesulfonic acid x H₂O (11.87 mg, 0.06 mmol) were added. Dean-Stark apparatus was set, and the mixture was stirred under reflux overnight. After substrate consumption, the mixture was allowed to cool at RT and washed with NaHCO_{3, aq}, dried with Na₂SO₄ and evaporated to dryness. The product was obtained as a yellow-orange oil and used without further purification (35.23 g, 96 % yield). ¹H NMR (200 MHz, CDCl₃) δ (ppm) = 7.07 (dd, J = 6 and 1.8 Hz, 1H), 7.02 (d, J = 1.8 Hz, 1H), 6.86 (d, J = 8.2 Hz, 1H), 5.79 (s, 1H), 4.72 (s, 2H), 4.29 (q, J = 7.2 Hz, 2H), 4.22-4.02 (m, 4H), 3.95 (s, 3H), 1.32 (t, J = 7.2 Hz, 3H). ¹³C NMR (75 MHz, CDCl₃) δ (ppm) = 170.4, 151.2, 149.5, 133.5, 120.6, 115.4, 111.4, 105.0, 68.1, 66.7, 62.8, 57.4, 15.6. ESI-MS: *m/z* calcd. for C₁₄H₁₈O₆+H⁺, [M + H⁺]: 283.12; found: 283.1, [M + H⁺]. GC-MS (EI) = *m/z*: 281 (M⁺, 100). All spectra data are in agreement with those reported in the literature²⁴.

Ethyl-2-(4-(1,3-dioxolan-2-yl)-2-methoxyphenoxy)-3-(3,5-dimethoxyphenyl)-3-hydroxypropanoate 42

To a cooled solution (-78 °C) of freshly distilled diisopropylamine (8.4 mL, 60.0 mmol) in dry THF (60 mL), was added dropwise a solution of *n*BuLi (2.5 M in hexane, 30 mL, 75 mmol) in 15 min under nitrogen atmosphere. After stirring for 30 min at -78°C, to this mixture a solution of **41** (14.101 g, 50.0 mmol) in 50 mL of dry THF was added dropwise over a period of 1 h. Then the 3,5 dimethoxybenzaldehyde (8.308 g, 50.0 mmol) in dry THF (50 mL) was added dropwise in 20 min and the stirring was continued for 2-3 h at -78°C. The disappearance of the aldehyde was monitored by TLC and ¹H-NMR. At the end of the reaction, the mixture was warmed up at 0°C (it was observed a changing of color from yellowish to brilliant red) and quenched with distilled water (60 mL). A solution of HCl_{aq} 4 N was added till PH = 7 was reached. The residue was extracted with Ethyl Acetate (2 x 100 mL). The organic phase was washed with brine and water, dried over anhydrous NaSO₄ and evaporated in vacuum. The crude was purified by column chromatography on silica gel (*n*-hexane/ethyl acetate 1/1) affording **42** as pure anti-diastereoisomer (yellow-brown oil, 3.64 g, 16% yield) ¹H NMR (300 MHz, CDCl₃) δ (ppm) (*anti*) = 7.08 (d, J = 1.6 Hz, 1H), 6.97 – 6.88 (m, 2H), 6.61 (d, J = 2.2 Hz, 2H), 6.38 (t, J = 2.3 Hz, 1H), 5.72 (s, 1H), 5.13 (t, J = 5.3 Hz, 1H), 4.71 (d, J = 4.8 Hz, 1H), 4.16-3.98 (m, 6H), 3.87 (s, 3H), 3.76 (s, 6H), 3.63 (d, J = 5.7 Hz, 1H), 1.14 (t, J = 7.2 Hz, 3H). ¹³C NMR (75 MHz, CDCl₃) δ (ppm) (*anti*) = 170.5, 162.1, 152.1, 149.2, 142.8, 134.9, 120.9, 119.8, 111.7, 106.3, 104.8, 101.8, 85.1, 75.5, 66.7, 62.8, 57.4, 56.8, 15.5. ESI-MS: *m/z* calcd for C₂₃H₂₈O₉+H⁺, [M + H⁺]: 449.18, for C₂₃H₂₈O₉+Na⁺, [M + Na⁺]: 471.16; found: 449.2, [M + H⁺], 471.1, [M + Na⁺]. All spectra data are in agreement with those reported in the literature for a similar compound²⁴.

2-(4-(1,3-dioxolan-2-yl)-2-methoxyphenoxy)-1-(3,5-dimethoxyphenyl)propane-1,3-diol 43

To a solution of **42** (3.64 g, 8.1 mmol) in THF:H₂O = 3:1 (82 mL), NaBH₄ (1.576 g, 41.7 mmol) was added in portions along 6 h. The mixture was stirred at RT for an additional 1 h. After complete substrate conversion (¹H-NMR), H₂O (20 mL) was added in order to quench NaBH₄, and the mixture was extracted with Et₂O, dried with Na₂SO₄ and evaporated to dryness. The product was obtained as a pale-yellow oil and used without further purifications (2.97 g, 90 % yield). ¹H NMR (300 MHz, CDCl₃) δ (ppm) = 7.06-6.96 (m, 3H), 6.52 (d, J = 1.9 Hz, 2 H), 6.35 (t, J= 2.2 Hz, 1H), 5.74 (s, 1H), 4.94 (t, J = 3.6 Hz, 1H), 4.17-3.96 (m, 5H), 3.88 (s, 3H), 3.75 (s, 6H), 3.67-3.65 (m, 2H), 2.76 (t, J = 6.0 Hz 1H). ¹³C NMR (75 MHz, CDCl₃) δ (ppm) = 162.4, 153.1, 149.0, 143.7, 135.2, 122.0, 121.4, 111.6, 105.4, 104.8, 101.2, 88.6, 74.4, 66.8, 62.1, 57.4, 56.8. ESI-MS: *m/z* calcd. for C₂₁H₂₆O₈+H⁺, [M + H⁺]: 407.17, for C₂₁H₂₆O₈+Na⁺, [M + Na⁺]: 429.15; found: 407.2, [M + H⁺], 429.2, [M + Na⁺]. All spectra data are in agreement with those reported in the literature for a similar compound²⁴.

4-((1-(3,5-dimethoxyphenyl)-1,3-dihydroxypropane-2-yl)oxy)-3-methoxybenzaldehyde 44

Compound **43** (2.90 g, 7.1 mmol) was dissolved in acetone/H₂O = 4:1, 40 mL and PPTS (0.398 g, 1.6 mmol) was added. The mixture was stirred under reflux ON until complete substrate consumption (¹H-NMR). Then, acetone was evaporated under reduced pressure and NaHCO_{3,aq} and Et₂O were added. The organic layer was washed with water, dried with Na₂SO₄ and evaporated to dryness. The product was obtained as a pale-yellow oil and used without further purification (2.30 g, 89 % yield). ¹H NMR (300 MHz, CDCl₃) δ (ppm) = 7.06-6.96 (m, 3H), 6.52 (d, J = 1.9 Hz, 2 H), 6.35 (t, J = 2.2 Hz, 1H), 5.74 (s, 1H), 4.94 (t, J = 3.6 Hz, 1H), 4.17-3.96 (m, 5H), 3.88 (s, 3H), 3.75 (s, 6H), 3.67-3.65 (m, 2H), 2.76 (t, J = 6.0 Hz 1H). ¹³C NMR (75 MHz, CDCl₃) δ (ppm) = 162.4, 153.1, 149.0, 143.7, 135.2, 122.0, 121.4, 111.6, 105.4, 104.8, 101.2, 88.6, 74.4, 66.8, 62.1, 57.4, 56.8. ESI-MS: *m/z* calcd. for C₂₁H₂₆O₈+H⁺, [M + H⁺]: 407.17, for C₂₁H₂₆O₈+Na⁺, [M + Na⁺]: 429.15; found: 407.2, [M + H⁺], 429.2, [M + Na⁺]. All spectra data are in agreement with those reported in the literature for a similar compound²⁴.

4-((4-(3,5-dimethoxyphenyl)-2,2-dimethyl-1,3-dioxane-5-yl)oxy)-3-methoxybenzaldehyde 45:

To a solution of **44** (2.29 g, 6.3 mmol) in dry acetone, under N₂, anhydrous *p*-TsOH (114 mg, 0.6 mmol) was added and the mixture was stirred at RT for 1 h. Then, 4 Å molecular sieves were added and the mixture stirred for a further 16 h. Then, the solution was neutralized with Na₂CO₃, filtered through celite and the solvent evaporated to dryness. The residue was dissolved in Et₂O, washed with H₂O, dried with Na₂SO₄ and evaporated to dryness. The crude product was purified by column chromatography (ethyl acetate/*n*-hexane) to afford pure **45** as a pale-yellow oil (1.244 g, 49 % yield). ¹H NMR (300 MHz, CDCl₃) δ (ppm) = 9.85 (s, 1H), 7.41–7.38 (m, 1H), 7.05 (d, J = 8.0 Hz, 1H), 6.57 (d, J = 2.0 Hz, 1H), 6.36 (t, J = 2.2 Hz, 1H), 4.99 (d, J = 4.9 Hz, 1H), 4.41 (dd, J = 8.7, 5.0 Hz, 1H), 3.91 (s, 3H), 3.87–3.76 (m, 2H), 3.76 (s, 6H), 2.54 (bs, 2H). ¹³C NMR (75 MHz, CDCl₃) δ (ppm) = 192.3, 162.5, 154.2, 152.9, 143.7, 133.3, 127.7, 119.3, 111.7, 105.7, 101.3, 86.9, 75.0, 62.6, 57.5, 56.8. ESI-MS = *m/z* calcd. for C₁₉H₂₂O₇+Na⁺, [M + Na⁺]: 385.13; found: 385.1, [M + Na⁺]. All spectra data are in agreement with those reported in the literature for a similar compound²⁴.

Ethyl-3-(4-((4-(3,5-dimethoxyphenyl)-2,2-dimethyl-1,3-dioxane-5-yl)oxy)-3-methoxyphenyl)-3-hydroxy-2-(2-methoxyphenoxy)propanoate 46

Following the same synthetic procedure for **42**, starting from **45** (1.198 g, 3.0 mmol) product **46** was obtained using **37** (0.631 g, 3.0 mmol) from purification by column chromatography as a pale yellow oil (0.964 g, 51 % yield) ¹H NMR (300 MHz, CDCl₃) δ (ppm) (*syn*) = 7.07 – 6.76 (m, 6H), 6.68 (s, br, 2H), 6.50 – 6.46 (m, 1H), 6.35 (s, br, 1H), 4.98 (dd, J = 6.3, 2.7 Hz, 1H), 4.90 (d, J = 8.5 Hz, 1H), 4.42 (dd, J = 6.0, 1.5 Hz, 1H), 4.19 – 3.93 (m, 5H), 3.82-3.73 (m, 12H), 3.66 (d, J = 5.7 Hz, 1H), 1.61 (s, 3H), 1.50 (s, 3H), 1.03-0.95 (m, 1H). ¹H NMR (300 MHz, CDCl₃) δ (ppm) (*anti*) = 7.07 – 6.76 (m, 6H), 6.68 (s, br, 2H), 6.50 – 6.46 (m, 1H), 6.35 (s, br, 1H), 5.06 (t, J = 5.0 Hz, 1H), 4.90 (d, J = 8.5

Hz, 1H), 4.67 (d, J = 4.8 Hz, 1H), 4.19 – 3.93 (m, 5H), 3.82-3.73 (m, 12H), 3.66 (d, J = 5.7 Hz, 1H), 1.61 (s, 3H), 1.50 (s, 3H), 1.09-1.06 (m, 3H). ¹³C NMR (75 MHz, CDCl₃) δ (ppm) = 170.8, 170.7, 162.1, 152.0, 151.9, 151.8, 151.6, 148.8, 148.7, 148.3, 143.1, 135.0, 134.0, 125.5, 122.6, 121.0, 120.8, 120.8, 120.4, 119.8, 119.7, 118.0, 117.9, 113.8, 112.5, 106.7, 101.8, 101.0, 86.6, 85.3, 76.2, 75.9, 75.2, 64.3, 62.7, 57.3, 57.2, 56.8, 29.8, 21.3, 15.5. ESI-MS: *m/z* calcd for C₃₃H₄₀O₁₁+Na⁺, [M + Na⁺]: 635.25; found: 635.2, [M + Na⁺]. All spectra data are in agreement with those reported in the literature for a similar compound²⁴.

1-(4-((4-(3,5-dimethoxyphenyl)-2,2-dimethyl-1,3-dioxane-5-yl)oxy)-3-methoxyphenyl)-2-(2-methoxyphenoxy)propane-1,3-diol 47:

Following the same synthetic procedure for **43**, starting from **46** (0.964 g, 1.6 mmol) product **47** was obtained from purification by column chromatography as a white solid (0.77 g, 86 % yield). ¹H NMR (300 MHz, CDCl₃) δ (ppm) = 7.11-6.66 (m, 8H), 6.51-6.46 (m, 1H), 6.34 (s, 1H), 4.90-4.87 (m, 2H), 4.20-3.91 (m, 4H), 3.90-3.73 (m, 12H), 3.60-3.38 (m, 3H), 2.65 (m, 1H), 1.62 (s, 3H), 1.50 (s, 3H). ¹³C NMR (75 MHz, CDCl₃) δ (ppm) = 162.1, 153.2, 152.8, 151.9, 148.4, 148.3, 148.0, 142.9, 135.7, 135.5, 125.8, 123.2, 123.1, 122.6, 121.0, 120.9, 119.8, 118.6, 118.5, 113.7, 112.3, 112.2, 111.5, 111.4, 106.8, 101.8, 101.0, 91.0, 88.8, 76.1, 75.2, 74.1, 64.3, 62.5, 62.2, 57.4, 56.8, 29.8, 21.3. ESI-MS: *m/z* calcd for C₃₁H₃₈O₁₀+Na⁺, [M + Na⁺]: 593.24, found: 593.2, [M + Na⁺]. All spectra data are in agreement with those reported in the literature for a similar compound²⁴.

2-(4-(1,3-dihydroxy-2-(2-methoxyphenoxy)propyl)-2-methoxyphenoxy)-1-(3,5-dimethoxyphenyl)propane-1,3-diol LM8:

Following the same synthetic procedure for **44**, starting from **47** (0.77 g, 1.3 mmol) **LM8** was obtained from purification by column chromatography as a white solid (0.621 g, 87 % yield). ¹H NMR (300 MHz, CDCl₃) δ (ppm) = 7.09-6.87 (m, 7 H), 6.53-6.52 (m, 2 H), 6.36 (t, J= 2.2 Hz, 1 H), 5.02-4.94 (m, 2 H), 4.16-3.99 (m, 2 H), 3.91-3.77 (m, 14 H), 3.65-3.55 (m, 4 H), 2.76-2.70 (m, 2 H). ¹³C NMR (75 MHz, CDCl₃) δ (ppm) = 162.4, 153.2, 153.1, 152.8, 148.9, 148.3, 148.0, 148.0, 147.6, 143.7, 137.7, 137.4, 125.9, 125.8, 123.2, 123.2, 122.5, 122.5, 122.3, 122.2, 121.9, 121.8, 120.7, 113.7, 112.4, 112.3, 111.6, 105.4, 101.2, 90.7, 88.7, 88.7, 75.3, 74.4, 74.1, 62.5, 62.2, 62.2, 57.5, 57.4, 56.8. ESI-MS: *m/z* calcd. for C₂₈H₃₄O₁₀+Na⁺, [M + Na⁺]: 553.20; found: 553.2, [M + Na⁺]. All spectra data are in agreement with those reported in the literature for a similar compound²⁴.

Synthesis of Protected Lignin Models LM4a-d

Protected lignin models were prepared following an already reported procedures developed for similar lignin model compounds^{15,29}. Hereafter the characterization data of all the intermediate are reported.

²⁹ Kleine, T.; Buendia, J.; Bolm, C.; *Green Chem.* **2013**, 15, 160.

1-(1,3-dimethoxy-2-(2-methoxyphenoxy)propyl)-3,5-dimethoxybenzene LM4a

To a cooled solution (0 °C) of **LM4** (334 mg, 1 mmol) in dry THF (5 mL), NaH (88 mg, 60% w/w in oil, 2.2 mmol) followed by MeI (137 μ L, 312 mg, 2.2 mmol) were added under nitrogen atmosphere. The reaction mixture was stirred at room temperature overnight, concentrated, and purified by column chromatography with *n*-hexane/EtOAc (9:1) yielding pure product as a colorless oil (239 mg, Yield 66%, *erythro (anti) / threo (syn)* = 77/23). The major diastereoisomer is assigned as the *erythro (anti)* form based on a comparison with the already reported **LM4** and with *erythro* and *threo* products reported in literature⁷. ¹H NMR (200 MHz, CDCl₃) δ (ppm) = 6.94-6.89 (m, 4H), 6.65 (d, *J* = 2.3 Hz, 2H, *syn*), 6.58 (d, *J* = 2.3 Hz, 2H, *anti*), 6.43 (t, *J* = 2.3 Hz, 1H, *syn*), 6.39 (t, *J* = 2.3 Hz, 1H, *anti*), 4.53 (m, 2H, *anti* and *syn*), 3.86-3.70 (m, 11 H), 3.40-3.33 (s, 6H, *syn* and *anti*). ¹³C NMR (50 MHz, CDCl₃) δ (ppm) = 160.66, 150.92, 150.67, 147.83, 141.10, 141.03, 122.40, 122.22, 120.85, 118.41, 117.98, 112.39, 112.25, 105.60, 105.45, 100.04, 99.85, 83.28, 82.86, 82.66, 77.80, 77.16, 76.52, 71.35, 71.21, 59.20, 57.46, 55.77, 55.26. ESI-MS = *m/z* calcd for C₂₀H₂₆O₆+Na⁺, [M + Na⁺]: 385.16, found: 385.2.

3-(3,5-dimethoxyphenyl)-3-methoxy-2-(2-methoxyphenoxy)propane-1-ol LM4b

To a solution of **LM4d** (600 mg, 1.34 mmol) in dry THF was added NaH (59 mg, 60% w/w oil, 1.47 mmol) followed by MeI (92 μ L, 1.47 mmol) in 5 min. The reaction mixture was stirred overnight and quenched by addition of a saturated aqueous solution of NH₄Cl. The mixture was extracted with EtOAc, and the combined organic layers were dried over Na₂SO₄, filtered, and concentrated. To a solution of the TBS-ether (360 mg, 0.778 mmol) in THF (5.0 mL) was added a solution of TBAF in THF (1.0 M, 933 μ L, 0.93 mmol). The reaction mixture was stirred for 30 min and concentrated. The primary alcohol **LM4b** was purified by flash column chromatography with *n*-hexane/EtOAc (from 9:1 to 1:1) yielding pure product as a colorless oil (236 mg, Yield 88%, *erythro (anti) / threo (syn)* = 76/24). ¹H NMR (200 MHz, CDCl₃) δ (ppm) = 7.30-6.58 (m, 4H), 6.59 (m, 2H), 6.44 (m, 1H), 4.47 (m, 1H *anti* and *syn*), 4.25-3.80 (m, 12 H), 3.36 (s, 3H, *anti*), 3.35 (s, 3H, *syn*). ¹³C NMR (50 MHz, CDCl₃) δ (ppm) = 161.22, 161.07, 151.46, 151.31, 148.67, 147.73, 141.66, 140.78, 123.78, 121.71, 121.53, 121.04, 120.59, 112.31, 112.23, 105.70, 100.49, 100.14, 92.00, 87.60, 86.58, 84.39, 83.33, 62.01, 61.58, 60.57, 57.63, 57.38, 55.99, 55.54, 14.40. ESI-MS = *m/z* calcd for C₁₉H₂₄O₆Na⁺, [M + Na⁺]: 371.38, found: 371.2.

1-(3,5-dimethoxyphenyl)-3-methoxy-2-(2-methoxyphenoxy)propane-1-ol LM4c

Following the procedure reported for the synthesis of **LM4b**, the crude benzylic alcohol **LM4c** was purified by flash column chromatography with hexanes/EtOAc (from 8:2 to 1:1) yielding pure product as a colorless oil (176 mg, Yield 80%, *erythro (anti) / threo (syn)* = 76/24). ¹H NMR (200 MHz, CDCl₃) δ (ppm) = 7.18-6.88 (m, 4H), 6.60 (m, 2H, *syn* and *anti*), 4.93 (m, 2H, *anti* and *syn*), 4.43 (m, 1H, *anti* and *syn*), 3.90 (s, 3H, *anti*), 3.85 (s, 3H, *syn*), 3.81 (s, 9H, *anti* and *syn*), 3.75-3.43 (m, 2 H), 3.37

(s, 3H, *syn* and *anti*). ^{13}C NMR (50 MHz, CDCl_3) δ (ppm) = 160.97, 151.77, 147.36, 142.67, 141.66, 124.00, 121.65, 120.91, 112.43, 105.70, 105.25, 104.44, 100.14, 99.71, 85.23, 77.94, 77.33, 76.68, 73.24, 71.44, 59.49, 56.07, 55.52. ESI-MS = m/z calcd for $\text{C}_{20}\text{H}_{26}\text{O}_6^+\text{Na}^+$, $[\text{M} + \text{Na}^+]$: 385.16, found: 385.2.

3-((tert-butyldimethylsilyl)oxy)-3-(3,5-dimethoxyphenyl)-2-(2-methoxyphenoxy)propane-1-ol LM4d

To a solution of **LM4** (668 mg, 2.0 mmol) and imidazole (449 mg, 6.6 mmol) in dry CH_2Cl_2 (10.0 mL) was added TBSCl (813 mg, 5.3 mmol) at room temperature. The reaction mixture was stirred at room temperature overnight, concentrated, and purified by column chromatography with *n*-hexane/EtOAc (9:1) yielding the bis-TBS ether as a colorless oil (945 mg, Yield 84%). To a solution of this TBS ether (900 mg, 1.6 mmol) in DCM/MeOH (1:1, 10 mL) at 0 °C was added CSA (122 mg, 0.527 mmol). The reaction mixture was stirred at 0 °C for 1 hour then quenched with saturated aqueous solution of NaHCO_3 (20 mL). The aqueous layer was extracted with CH_2Cl_2 , and the combined organic layers were dried over Na_2SO_4 concentrated, and purified by column chromatography with *n*-hexane/EtOAc (8:2) to give the mono-TBS ether **LM4d** (586 mg, Yield 82%, *erythro* (*anti*) / *threo* (*syn*) = 76/24). ^1H NMR (200 MHz, CDCl_3) δ (ppm) = 7.06-6.77 (m, 4H), 6.65-6.58 (m, 2H), 6.41 (m, 1H), 4.96 (m, 1H *anti* and *syn*), 4.25-3.47 (m, 13 H), 0.90 (s, 9H), 0.10 (s, 3H), 0.95 (s, 9H, *anti*), 0.90 (s, 9H, *syn*), 0.15 (s, 3H, *anti*), 0.07 (s, 3H, *syn*), -0.01 (s, 3H, *syn*), -0.05 (s, 3H, *anti*). ^{13}C NMR (50 MHz, CDCl_3) δ (ppm) = 210.86, 160.78, 151.27, 148.01, 144.91, 143.53, 123.48, 123.29, 121.54, 120.03, 112.23, 105.17, 100.01, 99.88, 88.27, 87.88, 75.37, 75.05, 61.80, 61.47, 55.94, 55.54, 25.98, 18.36, -4.52, -4.69, -4.96. ESI-MS = m/z calcd for $\text{C}_{24}\text{H}_{36}\text{O}_6\text{SiNa}^+$, $[\text{M} + \text{Na}^+]$: 471.22 found: 471.2.

Synthesis of ketone 21a via isolation from the reaction mixture

Typical procedure: Aerobic Oxidation of 1-(3,5-dimethoxyphenyl)-2-(2-methoxyphenoxy)propane-1,3-diol **LM4** catalyzed by **V5**.

In a 100 mL two-neck round-bottom flask equipped with a reflux condenser, an air inlet (air balloon) and a septum was charged with lignin model **LM4** (334.4 mg, 1.0 mmol), **V5** (60.5 mg, 0.1 mmol) dissolved in 20 mL of toluene. The solution was heated with stirring at 80 °C till complete conversion of the reagent (about 10 h). The reaction was periodically monitored by HPLC (by transferring 10 μL of the reaction mixture to a 1 mL of ACN/water (50% v/v), TLC and NMR (by evaporating 0.25 mL of the reaction mixture and dissolving the residue in CDCl_3). The reaction mixture was cooled to room temperature and the solvent removed under vacuum. The residue was purified by column chromatography on silica gel (petroleum ether/ethyl acetate from 7:3 to 3:7) affording ketone 1-(3,5-dimethoxyphenyl)-3-hydroxy-2-(2-methoxyphenoxy)propan-1-one **21a**, 3,5-dimethoxybenzaldehyde and 2-methoxyphenol (110 mg, 33 % of yield). The above reported procedure was followed for the

oxidation of the other non-phenolic lignin model 1-(3,4-dimethoxyphenyl)-3-hydroxy-2-(2-methoxyphenoxy)propane-1-one **LM5** to isolate the corresponding ketone **27a** (82 mg, 25 % of yield).

Alternative synthesis of ketone 21a

Alternatively to the isolation from the mixture reaction, the non-phenolic Ketones **21a**, **27a** and **56a** can be prepared *via* a selective benzylic oxidation of the corresponding β -O-4 model compounds using of 2,3-dichloro-5,6-dicyano-1,4-benzoquinone (DDQ) as a stoichiometric oxidant following the procedure reported by Westwood et al³⁰. The procedure failed in the synthesis of the ketone **24a**.

1-(3,5-dimethoxyphenyl)-3-hydroxy-2-(2-methoxyphenoxy)propane-1-one 21a

To a solution of **LM4** (100 mg, 0.300 mmol) in dichloromethane (5 mL) was added DDQ (72 mg, 0.315 mmol) and the reaction mixture stirred overnight at room temperature. The reaction mixture was then filtered, and the organic layer was washed with sat. NaHCO₃, dried over Na₂SO₄ and concentrated. The crude was purified by preparative TLC using *n*-hexane/ethyl acetate (3/7) as eluent to yield the title compound as a white solid (51 mg, 51 % yield). ¹H-NMR (200 MHz, CDCl₃), δ (ppm): 7.18 (d, *J* = 2.3 Hz, 2H), 7.02-6.83 (m, 4H), 6.67 (t, *J* = 2.3 Hz, 1H), 5.40 (t, *J* = 5.1 Hz, 1H), 4.05 (d, *J* = 5.1 Hz, 2H), 3.85 (s, 3H), 3.82 (s, 6H). ¹³C NMR (50 MHz, CDCl₃) δ (ppm): 196.2, 161.1, 150.8, 147.0, 136.9, 124.0, 121.3, 119.1, 112.5, 106.6, 106.3, 84.8, 63.6, 55.9, 55.8. ESI-MS = *m/z* calcd for C₁₈H₂₁O₆⁺: 333.3, [M + H⁺], found: 333.2; C₁₈H₂₀O₆+Na⁺, [M + Na⁺]: 355.1, found: 355.0. All spectra data are in agreement with those reported in the literature⁷.

1-(3,4-dimethoxyphenyl)-3-hydroxy-2-(2-methoxyphenoxy)propane-1-one 27a

Following the above reported procedure **27a** was synthesized as a pure white solid (52 mg, 52% yield). ¹H-NMR (200 MHz, CDCl₃), δ (ppm): 7.79 (dd, *J* = 8.4, 2.0 Hz, 1H), 7.65 (d, *J* = 2.0 Hz, 1H), 7.07-6.80 (m, 5H), 5.44 (t, *J* = 5.2 Hz, 1H), 4.11 (m, 2H), 4.00 (s, 3H), 3.97 (s, 3H), 3.84 (s, 3H), 2.81 (s, br, 1H). ¹³C NMR (50 MHz, CDCl₃) δ (ppm): δ 195.24, 154.17, 150.58, 149.42, 147.17, 128.29, 123.85, 123.72, 121.38, 118.39, 112.52, 111.20, 110.35, 84.62, 63.94, 56.31, 56.18, 56.01. ESI-MS = *m/z* calcd for C₁₈H₂₁O₆⁺: 333.3, [M + H⁺], found: 333.2; C₁₈H₂₀O₆+Na⁺, [M + Na⁺]: 355.1, found: 355.0. All spectra data are in agreement with those reported in the literature³¹.

1-(4-hydroxy-3-methoxyphenyl)-3-hydroxy-2-(2-methoxyphenoxy)propane-1-one 51a

Following the above reported procedure **51a** was synthesized as a pure brown solid (237 mg, 75% yield). ¹H-NMR (300 MHz, CDCl₃), δ (ppm) = 7.72 (dd, 1H, *J* = 8.3, 1.9 Hz), 7.63 (d, 1H, *J* = 1.9 Hz), 7.08-6.73 (m, 5H), 6.55 (s, br, 1H), 5.45 (t, 1H, *J* = 5.1 Hz), 4.11 (m, 2H, *J* = 5.1 Hz), 3.92 (s, 3H),

³⁰ Lancefield, C. S.; Ojo, O. S.; Tran, F.; Westwood, N. J.; *Angew. Chem. Int. Ed.* **2015**, 54, 258.

³¹ Wu, A.; Lauzon, J. M.; James, B. R.; *Catal. Letter* **2015**, 145, 511.

3.87 (s, 3H), 3.45 (s, br, 1H). ¹³C NMR (50 MHz, CDCl₃) δ 194.90, 151.23, 150.28, 146.92, 127.73, 127.47, 124.19, 123.41, 121.16, 117.95, 114.15, 112.34, 110.83, 84.13, 63.71, 56.03, 55.81. ESI-MS = *m/z* calcd for C₁₇H₁₈O₆Na⁺: 341.31, found: 341.3.

2-(4-(3-hydroxy-2-(2-methoxyphenoxy)-1-one-propyl)-2-methoxyphenoxy)-1-(3,5-dimethoxyphenyl)-3-hydroxy-propane-1-one 56a

LM8 (104.14 mg, 0.20 mmol) was dissolved in CH₂Cl₂ and DDQ (93.63 mg, 0.41 mmol) was added. The reaction mixture was stirred on at RT. After complete substrate consumption (NMR), the mixture was filtered through celite and washed with NaHCO₃ aq. The organic layer was dried with Na₂SO₄ and the solvent was removed under vacuum. The crude product was purified by column chromatography (AcOEt/*n*-hexane 70/30 to AcOEt) to afford **56a** as a white solid (61.71 mg, 60 % yield). ¹H NMR (400 MHz, CDCl₃) δ (ppm): 7.60-7.58 (m, 2H), 7.16 (d, *J* = 1.9 Hz, 2H), 6.99-6.94 (m, 1H), 6.88-6.75 (m, 4H), 6.68 (t, *J* = 2.3 Hz, 1H), 5.61 (t, *J* = 4.2 Hz, 1H), 5.35 (t, *J* = 5.1 Hz, 1H) 4.18-4.08 (m, 2H), 4.04-4.02 (m, 2H), 3.84 (d, *J* = 2.4 Hz, 3H), 3.80 (s, 9H), 3.03 (s, br, 2H). ¹³C NMR (100 MHz, CDCl₃) δ (ppm): 195.10, 195.06, 194.98, 161.09, 151.51, 150.39, 150.35, 149.85, 145.84, 136.25, 136.24, 129.63, 129.59, 123.60, 123.58, 123.27, 123.26, 121.17, 128.28, 128.22, 114.98, 114.87, 112.33, 112.32, 112.16, 112.13, 106.38, 106.36, 84.35, 83.06, 63.61, 63.55, 63.49, 55.96, 55.95, 55.79, 55.64. ESI-MS = *m/z* calcd for C₂₈H₃₁O₁₀, [M + H⁺]: 527.2; found 527.2 [M + H⁺].

4-((1-(3,5-dimethoxyphenyl)-3-hydroxypropane-1-one-2-yl)oxy)-3-methoxybenzaldehyde 58a

Following the above reported procedure **58a** was synthesized from **44** (105.49 mg, 0.29 mmol) and DDQ (70.71 mg, 0.31 mmol) in DCM (10 mL). The crude was purified by column chromatography on silica gel (AcOEt/*n*-hexane 70/30 to AcOEt) to afford DC072 as a yellowish oil (104.90 mg, 54 % yield). ¹H NMR (400 MHz, CDCl₃) δ (ppm): 9.80 (s, 1H), 7.40 (s, 1H), 7.31 (dd, *J* = 8.1, 1.9 Hz, 1H), 6.84 (d, *J* = 8.2 Hz, 1H), 7.16 (s, 2H), 6.68 (t, *J* = 2.3 Hz, 1H) 5.63 (dd, *J* = 6.0, 3.6 Hz, 1H), 4.25 – 4.00 (m, 2H), 3.88 (s, 3H), 3.80 (s, 6H), 3.17 (s, br, 1H). ¹³C NMR (75 MHz, CDCl₃) δ (ppm) = 195.02, 190.89, 161.26, 152.22, 150.54, 136.38, 131.73, 126.33, 115.52, 110.38, 106.54, 83.28, 63.66, 56.12, 55.79. ESI MS: *m/z* calcd for C₁₉H₂₀O₇+H⁺, [M + H⁺]: 361.12, found: 361.2 [M + H⁺].

3-hydroxy-(4-hydroxy-3-methoxyphenyl)-2-(2-methoxyphenoxy)-propane-1-one 60

Following the above reported procedure **60** was synthesized from **LM7** (484,3 mg, 1.51 mmol) and DDQ (363.2 mg, 1.60 mmol) as a colorless oil (319.0 mg, 66% yield). ¹H NMR (300 MHz, CDCl₃) δ (ppm) = 7.68 (dd, *J* = 1.8, 8.4 Hz, 1H), 7.60 (d, *J* = 1.8 Hz, 1H), 7.00-6.77 (m, 5H), 6.34 (bs), 5.40 (t, *J* = 5.2 Hz, 1H), 4.06 (d, *J* = 5.1 Hz, 2H), 3.89 (s, 3H), 3.83 (s, 3H), 3.03 (s, br, 1H). ¹³C NMR (75 MHz, CDCl₃) δ (ppm) = 195.3, 151.6, 150.6, 147.3, 128.1, 124.6, 123.8, 121.6, 118.3, 114.6, 112.7, 111.2, 84.5, 64.1, 56.4, 56.2. ESI MS: *m/z* calcd for C₁₇H₁₈O₆+H⁺, [M + H⁺]: 319.12, calcd for

$C_{17}H_{18}O_6+Na^+$, $[M + Na^+]$: 341.10, found: 319.2 $[M + H^+]$, 341.2 $[M + Na^+]$. All spectra data are in agreement with those reported in the literature⁹.

Synthesis of dehydrated ketones

The dehydrated ketone **22** can be prepared from the correspondent ketone **21a** *via* a selective primary alcohol dehydration following the procedure reported by James et al³¹.

1-(3,5-dimethoxyphenyl)-2-(2-methoxyphenoxy)prop-2-en-1-one **22**

To a solution of **21a** (50 mg, 0.144 mmol) in CH_2Cl_2 (5 mL) NEt_3 (45 μ L, 0.303 mmol) was added and the solution was stirred for 10 min at room temperature. After addition of tosyl chloride (32.9, mg, 0.173 mmol), the mixture was stirred overnight, and then diluted with 10 mL CH_2Cl_2 , washed with 15 mL of H_2O , dried with Na_2SO_4 , and concentrated in vacuo to give a yellow oil. The crude was purified by preparative TLC using *n*-hexane/ethyl acetate (6/4) as eluent to yield the title compound as a colorless oil (20 mg, 43 % yield). 1H -NMR (200 MHz, $CDCl_3$) δ (ppm) = 7.49 (d, J = 2.9 Hz, 2H), 7.45-7.13 (m, 4H), 6.82 (t, J = 2.9 Hz, 1H), 5.06 (d, J = 3.1 Hz, 1H), 4.48 (d, J = 3.1 Hz, 1H), 3.33 (s, 3H), 3.29 (s, 6H). ^{13}C NMR (50 MHz, $CDCl_3$) δ (ppm) = 190.50, 160.66, 157.70, 151.19, 143.50, 138.35, 125.99, 121.93, 121.38, 113.08, 107.93, 107.85, 107.80, 107.78, 105.67, 101.47, 56.00, 55.76. ESI-MS = m/z calcd for $C_{18}H_{19}O_5^+$: 315.12, $[M + H^+]$, found: 315.1. All spectra data are in agreement with those reported in the literature⁷.

1-(3,4-dimethoxyphenyl)-2-(2-methoxyphenoxy)prop-2-en-1-one **52**

Following the above reported procedure **52** was synthesized from **27a** (100 mg, 0.30 mmol) as a colorless oil (80 mg, 84% yield). 1H -NMR (300 MHz, $CDCl_3$) δ (ppm) = 7.82 (dd, J = 8.4, 1.7 Hz, 1H), 7.64 (d, J = 1.7 Hz, 1H), 7.16-7.68 (m, 5H), 5.20 (d, J = 2.2 Hz, 1H), 4.70 (d, J = 2.2 Hz, 1H), 3.94 (s, 3H), 3.93 (s, 3H), 3.84 (s, 3H). ^{13}C NMR (75 MHz, $CDCl_3$) δ (ppm) = 190.53, 159.48, 154.83, 152.45, 150.19, 144.81, 130.58, 127.19, 126.50, 123.12, 122.69, 114.34, 113.79, 111.40, 101.29, 57.53, 57.45, 57.32. ESI-MS = m/z calcd for $C_{18}H_{19}O_5^+$: 315.12, $[M + H^+]$, found: 315.1. All spectra data are in agreement with those reported in the literature³¹.

Synthesis of alkenes coming from C_β -O cleavage

The alkenes coming from C_β -O cleavage can be prepared from the corresponding aldehyde *via* a two steps vinylation and benzylic alcohol oxidation procedure.

To a solution of 3,5-dimethoxybenzaldehyde or 3,4-dimethoxybenzaldehyde (2.0 g, 12.05 mmol) in dry Et_2O (20 mL) was dropwise added vinylmagnesium bromide (1.0 M in THF, 12.5 mL, 12.5 mmol) at 0 °C. The solution was allowed to warm to room temperature and stirred overnight. The reaction mixture was quenched with saturated aqueous NH_4Cl and extracted with CH_2Cl_2 . The combined

organic layer was washed with H₂O, dried with Na₂SO₄, and concentrated under vacuum. The crude was purified by flash chromatography using *n*-hexane/ethyl acetate (7/3) as eluent to yield products.

1-(3,5-dimethoxyphenyl)-1-hydroxyprop-2-ene

According to the general procedure, title compound was obtained as a brownish oil (1.200 g, 50 % yield). ¹H-NMR (200 MHz, CDCl₃) δ (ppm) = 6.58 (d, *J* = 2.3 Hz, 2H), 6.42 (t, *J* = 2.3 Hz, 1H), 6.07 (ddd, *J* = 17.1, 10.2, 6.0 Hz, 1H), 5.40 (dt, *J* = 17.1, 1.4 Hz, 1H), 5.24 (dt, *J* = 10.2, 1.4 Hz, 1H), 5.17 (m, 1H), 3.83 (s, 6H). ¹³C NMR (50 MHz, CDCl₃) δ (ppm) = 161.20, 145.36, 140.16, 115.52, 104.37, 99.95, 75.57, 55.57. ESI-MS = *m/z* calcd for C₁₁H₁₄O₃Na⁺, [M + Na⁺]: 217.08, found: 217.1.

All spectra data are in agreement with those reported in the literature³².

1-(3,4-dimethoxyphenyl)-1-hydroxyprop-2-ene

According to the general procedure, title compound was obtained as a brownish oil (700 mg, 30 % yield). ¹H-NMR (300 MHz, CDCl₃) δ (ppm) = 6.97-6.82 (m, 3H), 6.06 (ddd, *J* = 17.1, 10.2, 5.9 Hz, 1H), 5.35 (dt, *J* = 17.1, 1.4 Hz, 1H), 5.25 – 5.11 (m, 2H), 3.89 (s, 3H), 3.87 (s, 3H). ¹³C NMR (75 MHz, CDCl₃) δ (ppm) = 149.5, 149.0, 140.7, 135.7, 119.1, 115.3, 111.5, 110.0, 75.5, 56.4, 56.3. ESI-MS = *m/z* calcd for C₁₁H₁₄O₃Na⁺, [M + Na⁺]: 217.08, found: 217.1. All spectra data are in agreement with those reported in the literature³³.

To a solution of the above alcohols (230 mg, 1.20 mmol) in CH₂Cl₂ (5 mL) was added DDQ (285 mg, 1.26 mmol) and the reaction mixture stirred overnight at room temperature. The reaction mixture was then filtered, and the organic layer was washed with sat. NaHCO₃, dried over Na₂SO₄ and concentrated. The crude was purified by flash chromatography using *n*-hexane/ethyl acetate (8/2) as eluent to yield alkenes as yellow oils.

1-(3,5-dimethoxyphenyl)prop-2-en-1-one **53**

According to the general procedure, compound **33** was obtained as a brownish oil (190 mg, 83 % yield). ¹H NMR (200 MHz, CDCl₃) δ (ppm) = 7.11 (dd, *J* = 17.1, 10.5 Hz, 5H), 7.07 (d, *J* = 2.3 Hz, 1H), 6.65 (t, *J* = 2.3 Hz, 1H), 6.43 (dd, *J* = 17.1, 1.8 Hz, 1H), 5.91 (dd, *J* = 10.5, 1.8 Hz, 1H), 3.83 (s, 2H). ¹³C NMR (50 MHz, CDCl₃) δ (ppm) = 190.69, 161.08, 139.36, 132.55, 130.34, 106.66, 105.48, 55.72. ESI-MS = *m/z* calcd for C₁₁H₁₃O₃⁺, [M + H⁺]: 193.09, found: 193.2. All spectra are in agreement with those of a closely related labelled model reported in literature⁷.

³² Cristol, S. J.; Ali, M. B.; Sankar, I. V.; *J. Am. Chem. Soc.* **1989**, 111, 8207.

³³ Swain, N. A.; Brown, R. C. D.; Bruton, G. D.; *J. Org. Chem.* **2004**, 69, 122.

1-(3,4-dimethoxyphenyl)prop-2-en-1-one **54**

According to the general procedure, compound **54** was obtained as a brownish oil (196 mg, 86 % yield). ^1H NMR (200 MHz, CDCl_3) δ (ppm) = 7.60 (d, J = 8.4 Hz, 1H), 7.57 (s, 1H), 7.20 (dd, J = 17.1, 10.5 Hz, 1H), 6.94 (dd, J = 15.0, 8.1 Hz, 1H), 6.43 (dd, J = 17.1, 1.9 Hz, 1H), 5.87 (dd, J = 10.5, 1.9 Hz, 1H), 3.97 (s, 3H), 3.95 (s, 3H); ^{13}C NMR (50 MHz, CDCl_3) δ (ppm) = 191.06, 132.09, 129.40, 127.03, 123.58, 110.95, 110.55, 110.14, 109.13, 56.24, 56.17. ESI-MS = m/z calcd for $\text{C}_{11}\text{H}_{13}\text{O}_3^+$, $[\text{M} + \text{H}^+]$: 193.09, found: 193.2. All spectra data are in agreement with those reported in the literature³⁴.

General procedure for Catalytic Oxidation of β -O-4 Lignin Models

HPLC analysis: In a 2 ml volumetric flask, **LM4-8** (0.1 or 0.5 mmol), catalyst (1 or 10 mol %) and, eventually an internal standard (naphthalene or biphenyl, 20 % mol/substrate), were added in 1 ml of solvent solution. The solution was made up to 2 ml volume and transferred into a 10 mL reactor, equipped with a stirring bar, and a condenser under air or oxygen atmosphere (balloon). The reactor was heated under magnetic stirring at the desired temperature (80°, 100°C or 130 °C), and the reaction course was monitored by quantitative HPLC. Conversions and chemical yields were determined on the crude of the reaction by quantitative HPLC. All compounds were identified by comparison of their retention time with pure standards. After complete substrate conversion, the reaction mixtures were concentrated under vacuum and purified over a silica gel column to remove the catalyst and impurities. More volatile products were separated by distillation.

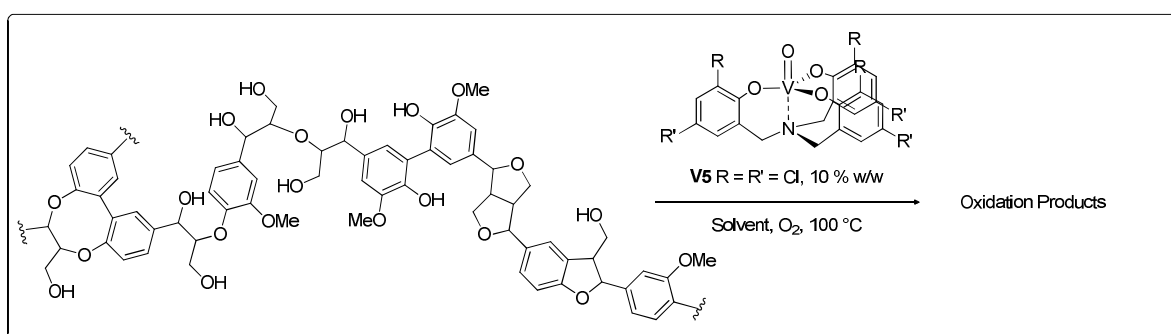
NMR analysis: In a 5-mL screw-cap vial, diol (0.1 mmol) and 10 mol% of **V5** (6.0 mg, 0.005 mmol) were dissolved in toluene- d_8 (2 mL) containing silicon oil (2 μL) as an internal standard. An initial ^1H -NMR spectrum was recorded, then the solution was heated at the desired temperature with stirring and monitored periodically by ^1H NMR (by transferring 0,25 mL of the reaction mixture to a 0,3 mL of toluene- d_8). The conversion and the yield were determined by integration against the internal standard.

Carrying out the reaction on a larger scale in a Schlenk reactor equipped with an air balloon and using non deuterated solvent, allowed for isolation of the products. The reaction mixture was cooled to room temperature and the solvent removed under vacuum. The residue was purified by column chromatography on silica gel (petroleum ether/ethyl acetate 8:2 or CH_2Cl_2 / diethyl ether 9:1).

³⁴ Verma, F.; Shukla, P.; Bhardiya, S. R.; Singh, M.; Rai, A.; Rai, V. K.; *Adv. Synth. Catal.* **2019**, 361, 1247.

Chapter 4

Aerobic Oxidation of Organosolv Wheat Straw and Steam Exploded Sugarcane Bagasse Lignin



The development of an efficient aerobic catalytic lignin oxidative depolymerization process is still a major challenge, despite the progresses made in this field throughout the last years. In this *Chapter*, the catalytic behavior of **V5** in aerobic oxidation of wheat straw organosolv and steam exploded sugarcane bagasse lignin has been investigated. Lignin samples were firstly characterized by 2D-HSQC-NMR, ³¹P-NMR, FT-IR GPC and MALDI-TOF-MS, showing a significant amount of β-O-4 bond associated with the almost total absence of other recurring linkages (β-5, β-β and dibenzodioxocin) in the case of sugarcane bagasse lignin. Those samples were then treated with **V5** (10 % w/w) at a lignin concentration of 20 mg/mL, using 1,4-dioxane or toluene as solvents at 100 °C under O₂ (1 atm). In both cases, a significative disappearance of β-O-4 linkages was observed. The reaction of SCB lignin with **V5** yielded the formation of the corresponding β-O-4 ketones (benzylic oxidation), whereas with WS lignin, our catalyst demonstrated the highest degree of depolymerization.

4.1 Introduction

As stated in *Chapter 1*, currently the main fate of lignin is to be burnt as an energy source¹. Even if lignin starts to be employed in the synthesis of low-value products such as epoxy resins, foams, dispersant etc., its complicated structure and the lack of an efficient valorization technique render the production of high-value fine chemicals still a challenge. However, with the decline of fossil fuels from which many aromatic compounds are obtained, scientific interest has moved throughout the last few years on the investigation of suitable strategies in order to transform lignin, which is the only renewable source of aromatic molecules, in valuable compounds. Up to now, due to the high complexity and variability of lignin structure, catalytic degradation studies have been based mainly on models containing β -O-4 bonds. Several depolymerization strategies have also been explored, namely reductive approaches², redox neutral C-O bond cleavage³, benzylic oxidation⁴ and tandem approaches⁵. In *Chapter 3* we have shown that currently, several homogeneous transition-metal catalyzed processes for lignin oxidative depolymerization have been developed and effectively employed in β -O-4 model compounds¹. Oxidative depolymerization allows to obtain aromatic compounds with oxygen-containing functionalities, a value-added process. Many of these compounds indeed serve as target chemicals or platform chemicals for further functionalization⁶. Recently, many of these strategies were also applied in actual lignin samples, giving very promising results. As regards transition metal catalyzed lignin oxidative depolymerization, Bozell and co-workers employed a Co(III) salen complex as a catalyst in aerobic oxidation of tulip poplar organosolv lignin, obtaining a series of quinones with an overall yield of 3.5 % with respect to the initial weight of lignin. MTO was also used in the oxidation of sugar cane or red spruce lignin, in presence of H₂O₂ and AcOH, with an acid content of 0.81 – 1.76 g/mmol⁷. Another example which employs a Co/Mn/Br catalyst in AcOH for lignin aerobic oxidation has been developed by Partenheimer. The products were a very complex mixture of aromatic molecules, with an overall

¹ Kärkäs, M. D.; Matsuura, B. S.; Monos, T. M.; Magallanes, G.; Stephenson, C. J.; *Org. Biomol. Chem.* **2016**, 14, 1853.

² a) Sergeev, A. G.; Hartwig, J. F.; *Science* **2011**, 332, 439. b) Sergeev, A. G.; Webb, J. D.; Hartwig, J. F.; *J. Am. Chem. Soc.* **2012**, 134, 20226. c) Ren, Y.; Yan, M.; Wang, J.; Zhang, Z. C.; Yao, K. *Angew. Chem. Int. Ed.* **2013**, 52, 12674. d) Nichols, J. M.; Bishop, L. M.; Bergman, R. G.; Ellman, J. A.; *J. Am. Chem. Soc.* **2010**, 132, 12554. e) Wu, A.; Patrick, B. O.; Chung, E.; James, B. R.; *Dalton Trans.* **2012**, 41, 11093; f) vom Stein, T.; Weigand, T.; Merckens, C.; Klankenmayer, J.; Leitner, W.; *ChemCatChem* **2013**, 5, 439. g) Weickmann, D.; Plietker, B.; *ChemCatChem* **2013**, 5, 2170. h) Nagy, M.; David, K.; Britovsek, G. J. P.; Ragauskas, A. J.; *Holzforchung* **2009**, 63, 513. i) Kärkäs, M. D.; *ChemSusChem* **2017**, 10, 2111.

³ a) Son, S.; Toste, F. D. *Angew. Chem. Int. Ed.* **2010**, 49, 3791. b) Chan, J. M. W.; Bauer, S.; Sorek, H.; Sreekumar, S.; Wang, K.; Toste, F. D. *ACS Catal.* **2013**, 3, 1369.

⁴ a) Rahimi, A.; Azarpira, A.; Kim, H.; Ralph, J.; Stahl, S. S.; *J. Am. Chem. Soc.* **2013**, 135, 6415. b) Mitchell, L. J.; Moody, C. J.; *J. Org. Chem.* **2014**, 79, 11090. c) Hanson, S. K.; Baker, R. T.; *Acc. Chem. Res.* **2015**, 48, 2037.

⁵ a) Rahimi, A.; Ulbrich, A.; Coon, J. J.; Stahl, S. S.; *Nature* **2014**, 515, 249. b) Lancefield, C. S.; Ojo, O. S.; Tran, F.; Westwood, N. J. *Angew. Chem. Int. Ed.* **2015**, 54, 258. c) Lohr, T. L.; Li, Z.; Marks, T. J.; *ACS Catal.* **2015**, 5, 7004.

⁶ Wang, M.; Ma, J.; Liu, H.; Luo, N.; Zhao, Z.; Wang, F.; *ACS Catal.* **2018**, 8, 2129.

⁷ Crestini, C.; Crucianelli, M.; Orlandi, M.; Saladino, R.; *Catal. Today* **2010**, 156, 8.

yield of 11 %⁸. Another strategy based on the use of ionic liquids in order to improve lignin solubility has been reported by Wasserscheid. In presence of Mn(NO₃)₂, using [EMIM][CF₃SO₃] as solvent, at 100 °C, beech lignin was converted at 63 % after 24h. More interestingly, lowering the catalyst amount to 2% shifted the product selectivity from aromatic aldehydes to quinones⁹. On the other hand, photocatalytic approaches have been developed for lignin depolymerization, although most of them convert lignin directly into CO₂⁶. However, Li and co-workers studied the photocatalytic degradation of Kraft lignin with C₆₀-modified Bi₂TiO₄F₂ under visible light irradiation, affording a mixture of phenols, aldehydes and acids¹⁰. Besides the aforementioned complexes, other catalysts have shown an activity in lignin oxidative depolymerization to produce aromatic aldehydes, ketones and acids¹¹. For example, the catalytic activity of FeCl₃-derived complexes for oxidative lignin depolymerization in DMSO was confirmed, and it was discovered that the key reactive species facilitating the process are methyl radicals generated by H₂O₂ and DMSO¹². Finally, biomimetic catalysts such as metalloporphyrins can be used for lignin oxidative conversion, taking into account that naturally occurring enzymes such as lignin peroxidase and manganese dependent peroxidase are used by living organisms (*i.e.* fungi) in such reaction¹³. Commonly used metal porphyrins are based on Fe, Co, Mn and Ru. All these metals can form highly oxidized metal-oxo species, triggered by oxidants such as H₂O₂, ^tBuOOH, KHSO₅ and Magnesium monoperoxyphthalate^{13b,14}. This metal-oxo complex can subsequently oxidize the substrates through a mono electron-transfer process, abstracting the electron from either aryl positions or side-chain positions, leading to the formation of phenolic aldehydes, ketones and quinones¹⁵. Zheng and collaborators obtained the production of aromatic aldehydes from the heavy fraction of bio-oil (see *Chapter 1*), using a Cobalt porphyrin in presence of H₂O₂ as oxidant. Total yields (4.57 % w/w of vanillin and 1.58 % syringaldehyde) were low, but acceptable considering the very cheap starting material¹⁶. Furthermore, porphyrin systems can be immobilized on solid supports (SiO₂) in order to overcome the problems of homogeneous catalysts, such as the easy loss and the difficult recovery¹⁷.

In this field, also homogeneous Vanadium-based catalysts have been playing an important role. Toste et al. indeed studied complex **V9** in redox-neutral depolymerization of *Miscanthus giganteus*-

⁸ Partenheimer, W.; *Adv. Synth. Catal.* **2009**, 351, 456.

⁹ Stärk, K.; Taccardi, N.; Bösmann, A.; Wasserscheid, P.; *ChemSusChem* **2010**, 3, 719.

¹⁰ Du, Z. J.; Li, W. Z.; Xu, Z. P.; Wu, H.; Jameel, H.; Chang, H. M.; Ma, L. L.; *J. Wood. Chem. Technol.* **2016**, 36, 365.

¹¹ Liu, C.; Wu, S.; Zhang, H.; Xiao, R.; *Fuel Process. Technol.*, **2019**, 191, 181.

¹² Mottweiler, J.; Rinesch, T.; Besson, C.; Buendia, J.; Bolm, C.; *Green Chem.* **2015**, 17, 5001.

¹³ a) Li, C.; Zhao, X.; Wang, A.; Huber, G. W.; Zhang, T.; *Chem. Rev.* **2015**, 115, 11559. b) Vangeel, T.; Schutyser, W.; Renders, T.; Sels, B. F.; *Topics Curr. Chem.* **2018**, 376, 30. c) Zakeski, J.; Bruijninx, P. C.; Jongorius, A. L.; Weckhuysen, B. M.; *Chem. Rev.* **2010**, 110, 3552.

¹⁴ a) Zhu, C.; Ding, W.; Shen, T.; Tang, C.; Sun, C.; Xu, S.; Chen, Y.; Wu, J.; Ying, H.; *ChemSusChem* **2015**, 8, 1768. b) Crestini, C.; Saladino, R.; Tagliatesta, P.; Boschi, T.; *Bioorg. Med. Chem.* **1999**, 7, 1897.

¹⁵ Lange, H.; Decina, S.; Crestini, C.; *Eur. Polym. J.* **2013**, 49, 1151.

¹⁶ Li, Y.; Chang, J.; Ouyang, Y.; Zheng, X.; *B. Korean Chem. Soc.* **2014**, 35, 1654.

¹⁷ a) Ghiaci, M.; Molaie, F.; Sedaghat, M. E.; Dorostkar, N.; *Catal. Commun.* **2010**, 11, 694. b) Zucca, P.; Mocci, G.; Rescigno, A.; Sanjust, E.; *J. Mol. Catal. A-Chem.* **2007**, 278, 220. c) Crestini, C.; Pastorini, A.; Tagliatesta, P.; *J. Mol. Catal. A-Chem.* **2004**, 208, 195.

derived lignin^{3b}. Evidences of lignin oxidative degradation were provided by GPC and 2D-HSQC-NMR, since an extensive decrease in intensity of β -O-4 bond signals was detected, together with the increase in signals due to product deriving from redox neutral C-O cleavage¹⁸. More recently, Baker et al. reported other V(V) complexes (**V6**, **V15-16**) and a Cu-based system as effective catalysts in oxidative depolymerization of organosolv lignin¹⁹. In particular, by means of GPC and quantitative HSQC they verified a decrease in the molecular weight, a quantitative conversion of four kind of linkages and an increase in the oxidized syringyl and guaiacyl units. ³¹P NMR showed also a significant conversion of phenolic and aliphatic hydroxy-groups, as derived phosphite esters. However, in all these cases, the selectivity was directed either to C β -O cleavage or to C α -H cleavage, with no amount of aromatic aldehydes detected in the reaction mixtures. Parallel to this work, Wang and co-workers tested a system based on VOSO₄/TEMPO on organosolv Alcell lignin, obtaining 36 % oxidation of β -O-4 bonds after 24 h at 90 °C under O₂ (1 atm)²⁰. Bolm and co-workers prepared bimetallic Cu/V catalysts and homogeneous VO(acac)₂/Cu(NO₃)₂ catalytic system to be employed in lignin degradation²¹. Later, this system was also employed by the same research group to explore the selectivity of produced vanillin and vanillic acid, as well as their mutual transformation during the reaction²².

Currently, best of our knowledge, the state-of-art methods for obtaining aromatic aldehydes or acids from lignin are those published by Chornet et al.²³, Song et al.²⁴ and Stahl et al.^{4a}. The method developed by Chornet et al. employs Kraft lignin (see *Chapter 1*), treated with NaOH (135 % w/w), CuSO₄ (5 % w/w) and FeCl₃ (0.5 % w/w) under O₂ (14 atm) at 160 °C for 1 h, yielding 14 % of aldehydes²³. Song et al. employed commercially available organosolv lignin treated with CuSO₄ (5% w/w) supported on ionic liquids at 175 °C under O₂ (25 atm) and reported a 30 % yield in aromatic aldehydes²⁴. Finally, Stahl and collaborators developed a metal-free procedure for the oxidation of aspen lignin, using 4-AcNH-TEMPO in an acidic environment²⁵. Then, the oxidized lignin was subsequently cleaved using superstoichiometric amount of HCOONa/HCOOH, affording up to 50 % yield of syringyl- and guaiacyl- derived diketones through a non-oxidative C β -O bond cleavage (see also *Chapter 3*). However, all these methods suffer from the requirement of using high temperature and high pressures of pure oxygen, together with superstoichiometric amounts of strong acids/bases. Therefore, a pursuit of a milder depolymerization strategy which employs air or a lower oxygen pressure as terminal oxidant is needed.

¹⁸ Biannic, B.; Bozell, J. J. *Org. Lett.*; **2013**, 15, 2730.

¹⁹ Diaz-Urrutia, C.; Chen, W.; Crites, C. O.; Daccache, J.; Korobov, I.; Baker, T.; *RSC Adv.* **2015**, 5, 70502.

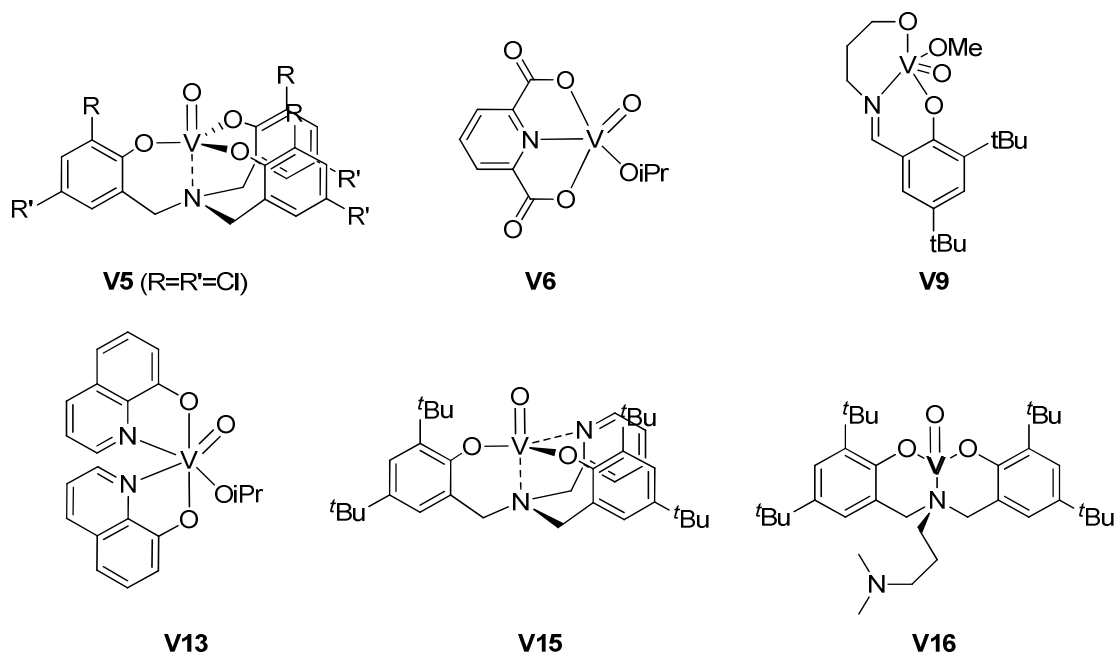
²⁰ Wang, M.; Lu, J.; Zhang, X.; Li, L.; Li, H.; Luo, N.; Wang, F.; *ACS Catal.* **2016**, 6, 6086.

²¹ Mottweiler, J.; Puche, M.; Rauber, C.; Schmidt, T.; Conception, P.; Corma, A.; Bolm, C.; *ChemSusChem* **2015**, 8, 2106.

²² Rinesch, T.; Mottweiler, J.; Puche, M.; Conception, P.; Corma, A.; Bolm, C.; *ACS Sust. Chem. Eng.* **2017**, 5, 9818.

²³ Wu, G.; Heitz, M.; Chornet, E.; *Ind. Eng. Chem. Res.* **1994**, 33, 718.

²⁴ Liu, S.; Shi, Z.; Li, L.; Yu, S.; Xie, C.; Song, Z.; *RSC Adv.* **2013**, 3, 5789.



After having obtained very promising results as regards aerobic oxidative cleavage of vicinal diols (*Chapter 2*) and oxidation of multimeric β -O-4 lignin models (*Chapter 3*) catalyzed by **VO-TPA(R,R')** complexes, we decided to start investigating the catalytic behavior of **V5** in depolymerization of lignin samples. To do this, I spent two weeks in prof. Kristin Bartik research group at ULB in Brussels, Belgium, in the framework of CARISMA COST Action FP1306 where we managed to find a suitable lignin source, that is as rich as possible in β -O-4 linkages. Lignin samples, prepared choosing wheat straw (WS)²⁵ and sugarcane bagasse (SCB)²⁶ as sources, were obtained in collaboration with prof. David Cannella at the ULB in Brussels, Belgium. WS raw lignin was hydrothermally pretreated using a Parr reactor, and then it was subjected to hydrolysis with excess of enzymes and to an organosolv treatment with aqueous ethanol, in order to obtain the final sample.

Sugarcane is the main feedstock for the production of sugar, accounting for nearly 67 % of the world production, and it is also the main raw material for the production of bio-ethanol²⁷. During the harvest of sugarcane, the stalks are transported to the mills where they are crushed in order to extract the juice which is used for the production of sugars and bio-ethanol. The fibrous matter that remains after juice extraction is called bagasse. Bagasse-derived lignin was isolated from lignocellulosic biomass using the previously discussed steam explosion method (*Chapter 1*) and a subsequent alkaline treatment with 1 % NaOH.

²⁵ Westereng, B.; Cannella, D.; Wittrup Agger, J.; Jorgensen, H.; Larsen Andersen, M.; Eijssink, V. G. H.; Felby, C.; *Sci. Rep.* **2015**, 5, 18561.

²⁶ Brenelli, L. B.; Mandelli, F.; Mercadante, A. Z.; De Moraes Rocha, G. J.; Rocco, S. A.; Craievich, A. F.; Squina, F. M.; *Industrial Crops and Products* **2016**, 83, 94.

²⁷ a) Santos, F.; Borém, A.; Caldas, C.; *Sugarcane: Bioenergy, Sugar and Ethanol – Technology and Prospects*, Universidad Federale de Vicosa, Vicosa, Brazil, **2012**. b) de Souza, A. P.; Grandis, A.; Leite, D. C. C.; Buckeridge, M. S.; *Bioenergy Res.* **2014**, 7, 24.

These treatments have been chosen since it is known that they provide the lowest degree of modification of lignin native structure²⁸, which is naturally rich in β -O-4 bonds, as previously stated. The aim of this chapter is to characterize these two lignin samples and to study their oxidation/depolymerization catalyzed by **V5** (10 % w/w), with a substrate concentration of 20 mg/mL, screening 1,4-dioxane and toluene as solvents, at 100 °C under an O₂ atmosphere. In particular, 2D HSQC NMR, ³¹P NMR (after derivatization), FT-IR, GPC and MALDI-TOF-MS are used as analytical techniques.

4.2 Lignin Samples Characterization

A first characterization of such samples was performed by 2D-HSQC-NMR, since all the main linkages present in lignin are characterized by a very specific value of $\delta(^1\text{H}-^{13}\text{C})$ ²⁹, as can be appreciated from Figure 4.1 and Table 4.1.

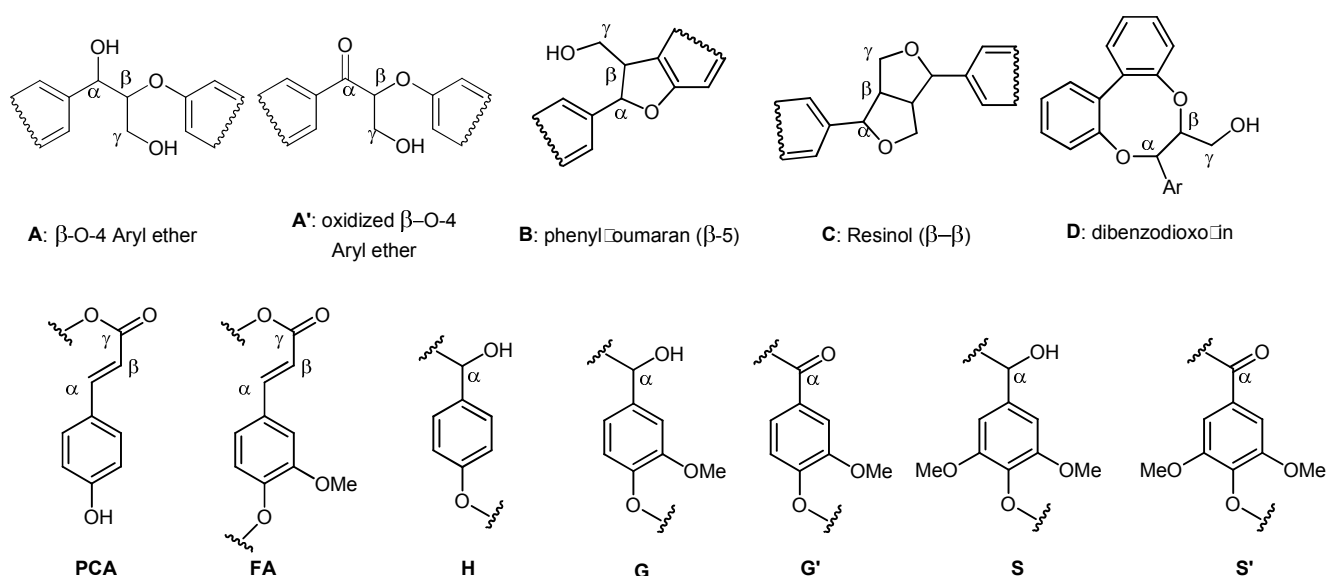


Figure 4.1: Most abundant linkages in lignin.

²⁸ Rocha, G. J. M.; Martín, C.; da Silva, V. F. N.; Gomez, E. O.; Gonçalves, A. R.; *Bioresource Technology* **2012**, 111, 447.

²⁹ a) del Río, J. C.; Lino, A. G.; Colodette, J. L.; Lima, C. F.; Gutierrez, A.; Martínez, A. T., Lu, F.; Ralph, J.; Rencoret, J.; *Biomass and Bioenergy* **2015**, 81, 322. b) Bauer, S.; Sorek, H.; Mitchell, V. D.; Ibanez, A. B.; Wemmer, D. E.; *J. Agric. Food Chem.* **2012**, 60, 8203. c) Ralph, S. A.; Ralph, J.; Landucci, L.; NMR Database of Lignin and Cell Wall Model Compounds, **2009**, www.glbrc.org/databases_and_software/nmrdatabase (September 2019). d) Yuan, T. Q.; Sun, S. N.; Xu, F.; Sun, R. C.; *J. Agric. Food Chem.* **2011**, 59, 6605.

Table 4.1: Chemical shifts of most abundant lignin linkages, recorded at 600 MHz in DMSO-d₆²⁹.

Entry	$\delta(\text{H}_\alpha/\text{C}_\alpha)$ (ppm)	$\delta(\text{H}_\beta/\text{C}_\beta)$ (ppm)	$\delta(\text{H}_{\gamma 1}/\text{C}_{\gamma 1})$ (ppm)	$\delta(\text{H}_{\gamma 2}/\text{C}_{\gamma 2})$ (ppm)
Phenylcoumaran (B)	5.46, 86.8	3.47, 52.8	3.65, 62.3	-
Resinol (C)	4.67, 84.8	3.07, 53.5	3.83, 70.9	4.20, 70.9
Dibenzodioxocin (D)	4.81, 83.3	4.09, 86.7	3.22, 60.66	3.86, 60.66
β -O-4 arylether (A)	4.87, 71.6	4.12, 85.9 ^a 4.29, 83.6 ^b	3.46, 59.3	3.70, 59.3
Oxidized β -O-4 arylether (A_{ox})	-	5.23, 82.8	-	-

^a $\delta(\text{H}_\beta/\text{C}_\beta)$ in β -O-4 substructures linked to a S unit ($\text{A}_{\beta(\text{S})}$). ^b $\delta(\text{H}_\beta/\text{C}_\beta)$ in β -O-4 substructures linked to a G unit ($\text{A}_{\beta(\text{G})}$).

Entry	$\delta(\text{H}_2/\text{C}_2)$ (ppm)	$\delta(\text{H}_3/\text{C}_3)$ (ppm)	$\delta(\text{H}_5/\text{C}_5)$ (ppm)	$\delta(\text{H}_6/\text{C}_6)$ (ppm)	$\delta(\text{H}_\alpha/\text{C}_\alpha)$ (ppm)	$\delta(\text{H}_\beta/\text{C}_\beta)$ (ppm)
<i>p</i> -hydroxyphenyl units (H)	7.23, 128.0	6.62, 114.5	6.62, 114.5	7.23, 128.0	-	-
Guaiacyl units (G)	7.00, 110.9	-	6.72, 114.9	6.77, 118.7 6.94, 118.7	-	-
Oxidized Guaiacyl units (G')	7.52, 111.5	-	-	-	-	-
Syringyl units (S)	6.69, 103.8	-	-	6.69, 103.8	-	-
Oxidized Syringyl units (S')	7.32, 106.1	-	-	7.32, 106.1	-	-
Ferulate moieties (FA)	7.32, 111.0	-	-	7.10, 123.3	7.41, 144.4	6.27, 113.5
<i>p</i> -coumarate moieties (PCA)	7.46, 130.0	6.77, 115.5	6.77, 115.5	7.46, 130.0	7.41, 144.4	6.27, 113.5

We therefore identified all the most common linkages present in our samples by comparison of $\delta(^1\text{H}-^{13}\text{C})$ with those reported in Table 4.1. Figure 4.2 reports the HSQC spectrum of WS organosolv lignin both in the aromatic (a) and aliphatic (b) regions.

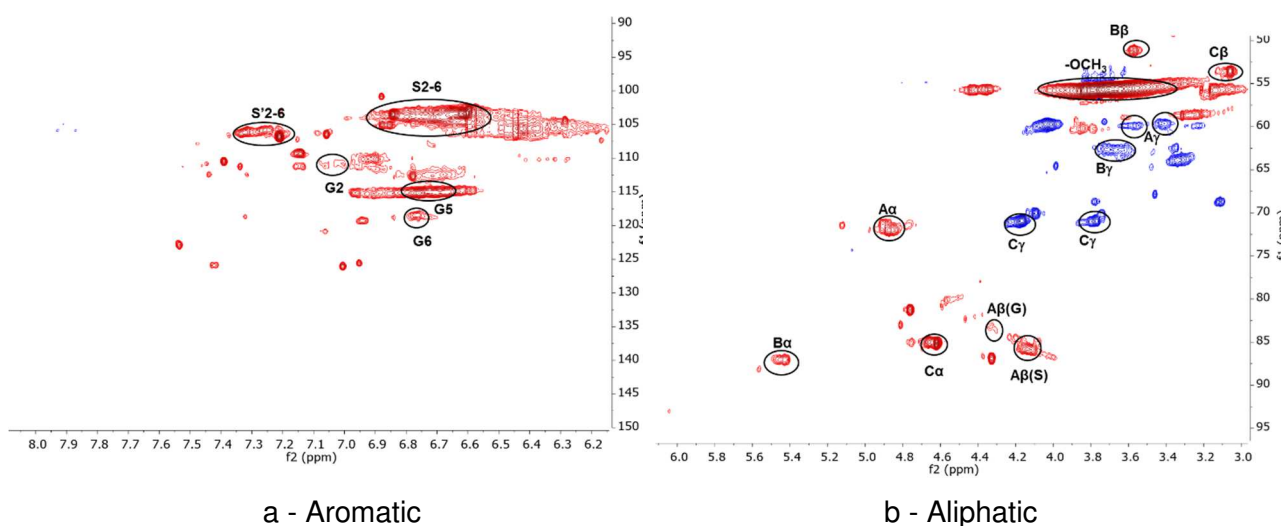


Figure 4.2: 2D-HSQC-NMR spectra (600 MHz, DMSO- d_6 , aliphatic ($\delta^1H/\delta^{13}C$ 3.0-6.0/50-95 ppm) and aromatic ($\delta^1H/\delta^{13}C$ 6.2-8.0/90-150 ppm) regions) of WS organosolv lignin. a: untreated lignin, aromatic region, b: untreated lignin, aliphatic region. See Table 4.1 for assignments and Figure 4.1 for the main lignin structures identified.

Looking into deep details to the aliphatic region (Figure 4.2a), it can be deduced that WS organosolv lignin structure is composed by the three most abundant linkages, namely β -O-4, resinol β - β and phenylcoumaran β -5, in a relative ratio of $A_\alpha:B_\alpha:C_\alpha = 1:0.42:1.39$. Moreover, from the aromatic region (Figure 4.2b) both syringyl and guaiacyl units were detected, in a relative ratio $S_{2-6}:G_2 = 8.4:1$. Interestingly, oxidized syringyl units were also present, in a ratio $S'_{2-6}:S_{2-6} = 0.14:1$.

As regards steam exploded SCB lignin (Figure 4.3), aliphatic region (a) clearly shows the presence of non-functionalized β -O-4 bonds, together with the almost total absence of other recurring linkages. Other signals in the spectrum are due to a hemicellulose residue, namely xylane, whose chemical shifts have been assigned according to literature^{29a} (Table 4.2). From volume integrations, it resulted that the ratio β -O-4 bonds (A_α):xylane (X_3) is 1:0.89. Looking into deeper details into the aromatic region, the most abundant aromatic units S, G and H were present in a relative ratio $S_{2-6}:G_2:H_{2-6} = 1.71:1:0.03$, whereas differently from WS lignin, *p*-coumarate (PCA) and ferulate (FA) units were detected, in a relative ratio $PCA_{2,6}:FA_2 = 0.99:1$.

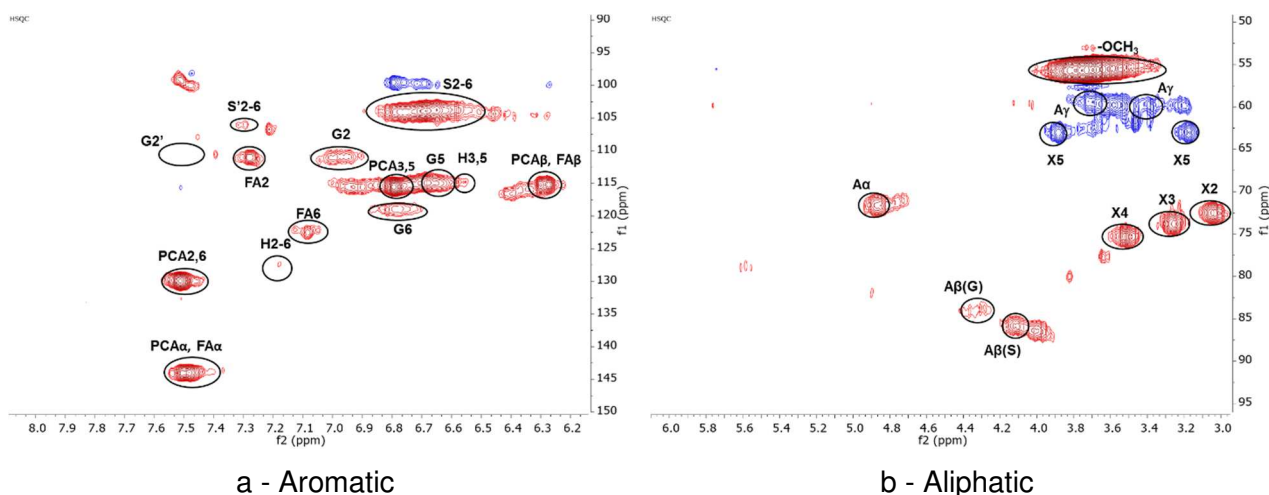


Figure 4.3: 2D-HSQC-NMR spectra (600 MHz, DMSO- d_6 , aliphatic ($\delta^1H/\delta^{13}C$ 3.0-6.0/50-95 ppm) and aromatic ($\delta^1H/\delta^{13}C$ 6.2-8.0/95-150 ppm) regions) of steam exploded SCB lignin. a: untreated lignin, aromatic region. b: untreated lignin, aliphatic region. See Table 4.1 for assignments and Figure 4.1 for the main lignin structures identified.

Due to the high amount of β -O-4 bonds, and the absence of other linkages which can complicate NMR interpretation, we started our investigation on the behavior of complex **V5** in the oxidative depolymerization of steam exploded SCB lignin sample.

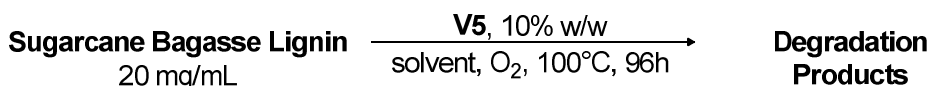
Table 4.2: Chemical shifts of xylane, recorded at 600 MHz in DMSO- d_6 ^{29a}.

Xylane	$\delta(H_2/C_2)$	$\delta(H_3/C_3)$	$\delta(H_4/C_4)$	$\delta(H_5/C_5)$
	(ppm)	(ppm)	(ppm)	(ppm)
Polysaccharide				
cross-peak signals	3.14, 72.9	3.32, 74.1	3.73, 75.6	3.26, 63.2 and 3.95, 63.2

4.3 Steam Exploded SCB and WS Organosolv Lignin Depolymerization

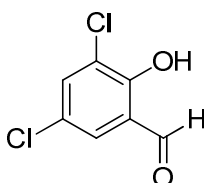
4.3.1 2D-HSQC NMR Spectroscopy

In *Chapter 3* we demonstrated that complex **V5** was still active in the oxidation of **LM4** and **LM5** using 1,4-dioxane as solvent. Considering the high solubility of SCB lignin (20 mg/mL) in such solvent, we decided to test the catalytic behavior of **V5** in 1,4-dioxane using reaction conditions already reported in the literature by Toste et al^{3b}, and monitoring the reaction by 2D-HSQC-NMR. (Eq. 4.1).



Eq. 4.1: Treatment of SCB lignin with **V5**.

After 96 h we performed the same 2D-HSQC NMR analysis (Figure 4.4a-b). A semiquantitative estimation of the amount of lignin subunits during the reaction is reported in Table 4.3. We chose a well-resolved signal (relative to FA₆ in ferulate moiety), which should remain unaffected by **V5**, as an internal standard, and therefore, all integrals have been normalized according to the intensity of this signal. We found the appearance of signals relative to the benzylic oxidation of β -O-4 system (5.21, 82.8 ppm, δ (H $_{\beta}$ /C $_{\beta}$) of oxidized β -O-4 bonds A_{ox}) in a ratio of 0.67:1 with respect to FA side chains, which corresponds to the oxidation of 15 % of β -O-4 bonds present in native lignin, a clear indication that our complex is active in the lignin oxidation. Non-oxidized β -O-4 linkages (A) decrease up to complete disappearance after 96 h of reaction. Furthermore, it can be noticed that xylane signals are maintained (only a 2 % decrease after 96 h), indicating that this compound remains almost unaffected from the action of **V5** during the reaction. As regards aromatic region, the presence of oxidized syringyl S' and guaiacyl G' moieties confirms that benzylic oxidation has occurred upon reaction with complex **V5**. After 96 h of reaction, the relative ratios S'₂₋₆:S₂₋₆ and G'₂:G₂ were respectively 0.93:1 and 3.02:1, whereas at the beginning the ratio S':S was 0.02:1 and no oxidized guaiacyl units G' were present at all. Other signals detected in this region were derived from catalyst degradation, which afford aldehyde **68**. The chemical shifts were assigned to this species (Figure 4.4 c) from comparison with those of the pure compound. Noticeably, control experiment (without catalyst) yielded no change in the composition of SCB lignin, indicating that **V5** is essential in order to have oxidation.



68

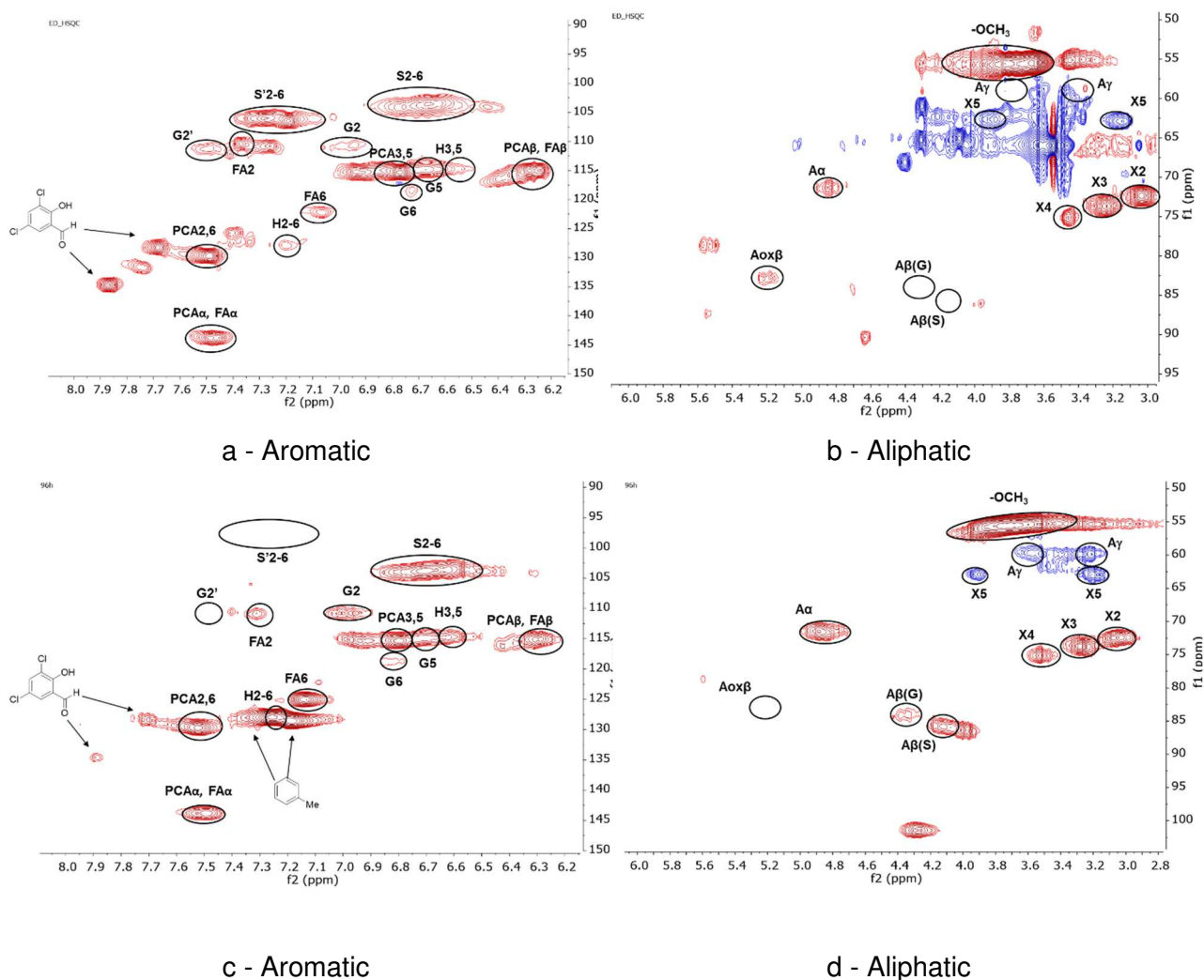


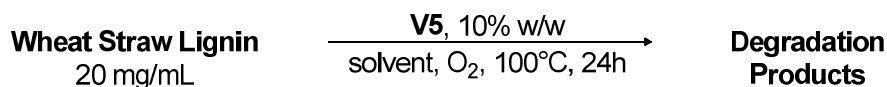
Figure 4.4: 2D-HSQC-NMR spectra (400 MHz, DMSO- d_6 , aliphatic ($\delta^1H/\delta^{13}C$ 3.0-6.0/50-95 ppm) and aromatic ($\delta^1H/\delta^{13}C$ 6.2-8.0/95-150 ppm) regions) of steam exploded SCB lignin a: lignin treated with **V5** (10 % w/w) after 96 h, dioxane, O₂, aromatic region, b: lignin treated with **V5** (10 % w/w) after 96 h, dioxane, O₂, aliphatic region. c: lignin treated with **V5** (10 % w/w) after 96 h, toluene, O₂, aromatic region, d: lignin treated with **V5** (10 % w/w) after 96 h, toluene, O₂, aliphatic region. See Table 4.1 for assignments and Figure 4.1 for the main lignin structures identified.

Since complex **V5** showed the best catalytic performances in aerobic oxidation of β -O-4 lignin models using toluene as solvent (*Chapter 3*), we run the reaction also in toluene, according to Eq. 4.1. However, the HSQC spectrum after 96 h of reaction was identical to that of native lignin (Figure 4.4c-d), indicating no β -O-4 bond oxidation occurring during the reaction. This can be attributed to the very low solubility of such sample in toluene.

Table 4.3: integrals of lignin subunits relative to $\delta(H_6/C_6)$ of ferulate moieties (FA) during the reaction of SCB lignin in 1,4-dioxane at 100 °C under O₂.

Unit	Integral vs FA ₆ at to	Integral vs FA ₆ at 24 h	Integral vs FA ₆ at 48 h	Integral vs FA ₆ at 96 h
A _α	4.54	2.43	1.21	1.01
A _{β(G)}	2.13	0.76	0.29	0
A _{β(S)}	2.55	0.79	0.54	0
A _{ox,β}	0	0.33	0.51	0.67
S ₂₋₆	14.06	11.32	9.96	8.97
S' ₂₋₆	0.33	7.06	8.85	8.39
G ₂	2.61	1.62	1.51	0.51
G' ₂	0	0.57	0.69	1.51
G ₆	2.62	1.61	1.50	0.50
H	2.03	1.25	0.87	0.72
X ₃	3.86	3.83	3.79	3.79

As regards WS organosolv lignin, the sample (20 mg/mL) was subjected to identical reaction conditions (**V5**, 10 % w/w, 1,4-dioxane or toluene, 100°C, O₂, 1 atm), according to Eq. 4.2 in order to verify the general applicability of catalyst **V5** to different kinds of lignin.



Eq. 4.2: Treatment of WS lignin with **V5**.

When running the reaction in 1,4-dioxane, remarkable changes in the HSQC spectrum were obtained already after 24 h of reaction as can be appreciated from Figure 4.5. In fact, looking first at the aromatic region (Figure 4.5a), a large amount of S units were converted to the corresponding oxidized moieties S', reaching a S'₂₋₆:S₂₋₆ ratio of 0.85:1 compared with 0.14:1 present in native lignin. Also G units were oxidized to G' (G'₂:G₂ ratio = 0.25:1 compared with no G' units in native lignin). Further confirmations of the occurred oxidative depolymerization are obtained also in the aliphatic region, resulting from the breakdown of all the main linkage motifs present in native lignin (β-O-4 (A), phenylcoumaran (B) and resinol (C), Figure 4.5b). A similar result was reported also by Baker et al. for catalysts **V15** and **V16** in the oxidative depolymerization of organosolv hardwood lignin¹⁹. Letting the reaction proceed for 96 h resulted in a further oxidation of S moieties (S'₂₋₆:S₂₋₆ ratio = 1.51:1) and a quantitative oxidation of G units, index of a great robustness of catalyst **V5** which after four days was still able to oxidize lignin.

Contrary to what found for SCB lignin, in the case of WS lignin catalyst **V5** was effective also in toluene, probably because of the enhanced solubility in organic solvents for organosolv lignin. The aromatic region of HSQC-NMR after 24 h of reaction (Figure 4.5c), showed an increase of S' and G' units as well (S'₂₋₆:S₂₋₆ ratio = 0.32:1 and G'₂:G₂ ratio = 0.55:1), indicating that complex **V5** is less

efficient in oxidizing S units in toluene with respect to 1,4-dioxane, but more efficient in the oxidation of G units. Looking into the aliphatic region (Figure 4.5d), once again A, B and C units disappeared although no signals of oxidized β -O-4 units ($A_{ox,\beta}$) appeared. Also in this case, after 96 h of reaction a quantitative formation of G' units was observed, whereas $S'_{2-6}:S_{2-6}$ ratio = 1:1.

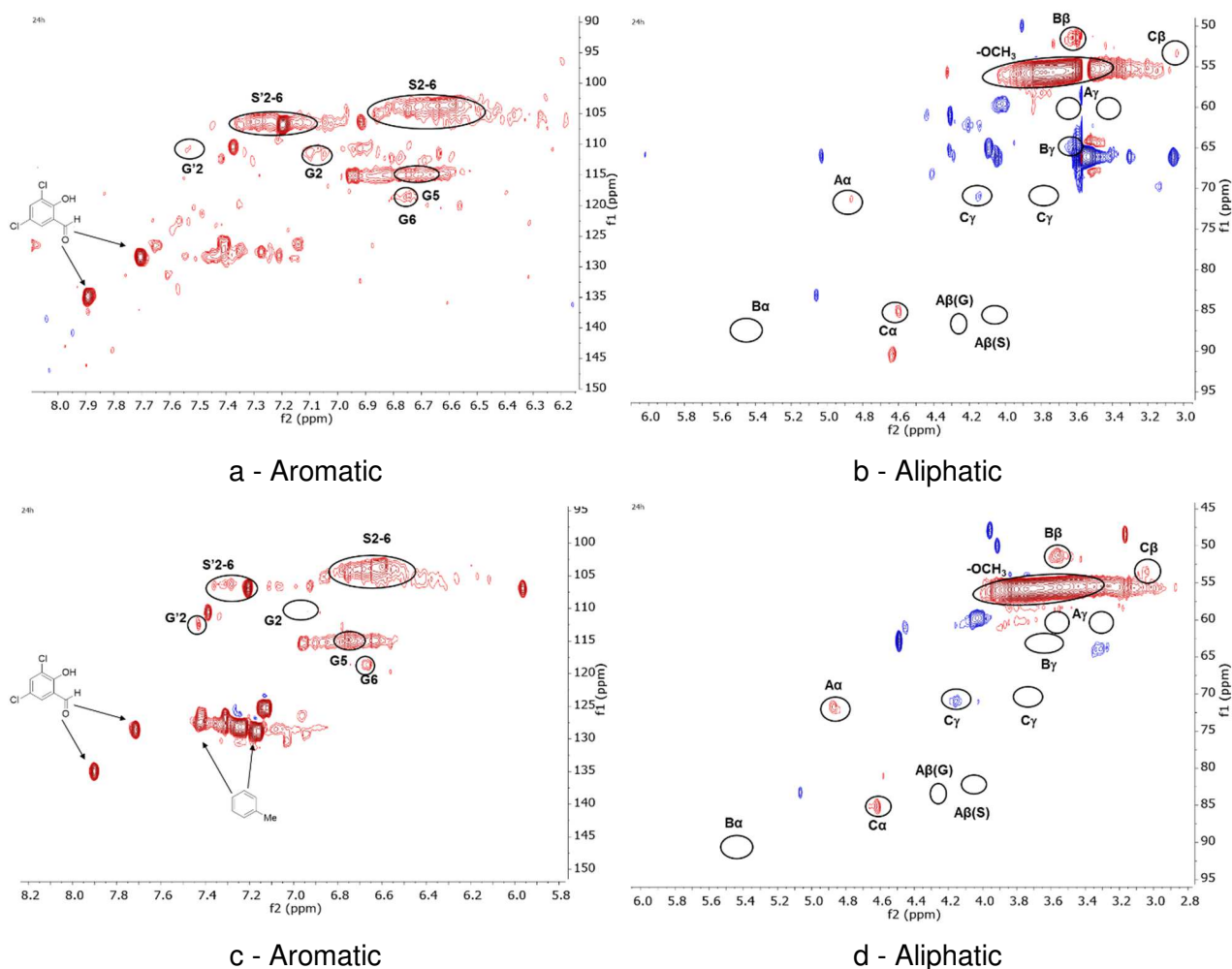
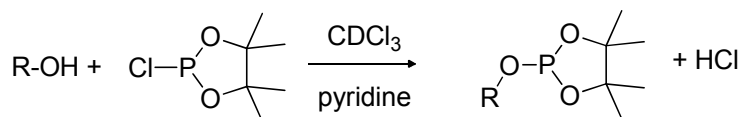


Figure 4.5: 2D-HSQC-NMR spectra (400 MHz, DMSO- d_6 , aliphatic ($\delta^1H/\delta^{13}C$ 3.0-6.0/50-95 ppm) and aromatic ($\delta^1H/\delta^{13}C$ 6.2-8.0/95-150 ppm) regions) of WS organosolv lignin a: lignin treated with **V5** (10 % w/w) after 24 h, dioxane, O_2 , aromatic region, b: lignin treated with **V5** (10 % w/w) after 24 h, dioxane, O_2 , aliphatic region. c: lignin treated with **V5** (10 % w/w) after 96 h, toluene, O_2 , aromatic region, d: lignin treated with **V5** (10 % w/w) after 96 h, toluene, O_2 , aliphatic region. See Table 4.1 for assignments and Figure 4.1 for the main lignin structures identified.

4.3.2 Quantitative ^{31}P NMR Spectroscopy

Derivatization by phosphitylation and subsequent NMR analysis is a very useful technique for the analysis of hydroxyl groups, especially in lignin, which is very rich in such functionalities. With an appropriate phosphorous reagent (TMDP), different -OH groups, including aliphatic, phenolic, and carboxylic, can be easily quantified (Eq. 4.3)



Eq. 4.3: Derivatization of hydroxyl groups with TMDP.

Table 4.4 reports the typical ^{31}P NMR chemical shift values for derivatized lignin subunits. Quantification was carried out via peak integration using NHND as internal standard.

Table 4.4: Typical integration regions for lignin in a ^{31}P -NMR spectrum³⁰.

Lignin Functional Group			Chemical Shift (ppm)
	5-5	Aliphatic OH	145.4 - 150.0
	4-O-5	Aliphatic OH	140.0 - 144.5
	S Syringyl	Aliphatic OH	141.2
	H p-hydroxyphenyl	Aliphatic OH	142.3
	G Guaiacyl	Aliphatic OH	142.7
	C5 substituted guaiacyl	Aliphatic OH	139.0 - 140.2
	Carboxylic acid OH	Carboxylic OH	137.8
			133.6-136.0

^{31}P -NMR spectra of native SCB lignin, control experiment (without **V5**) and oxidized lignin in 1,4-dioxane at 100 °C under O_2 for 96 h are reported in Figure 4.6, whereas integration values are reported in Table 4.5. As expected, the concentration of aliphatic hydroxyl groups after treatment of steam exploded SCB lignin with **V5** decreased substantially (86 %), indicating a further piece of evidence of β -O-4 bonds oxidation. Moreover, the amount of phenolic groups decreased during the reaction, especially G units to 0.21 mmol/g from 0.43 mmol/g present in native lignin, and S units to 0.06 mmol/g from 0.17 mmol/g. The amount of carboxylic OH groups is affected as well by our catalyst, since from the relative integrals a decrease of 32 % is detected.

³⁰ Pu, Y.; Cao, S.; Ragauskas, A. J.; *Energy Environ. Sci.* **2011**, 4, 3154.

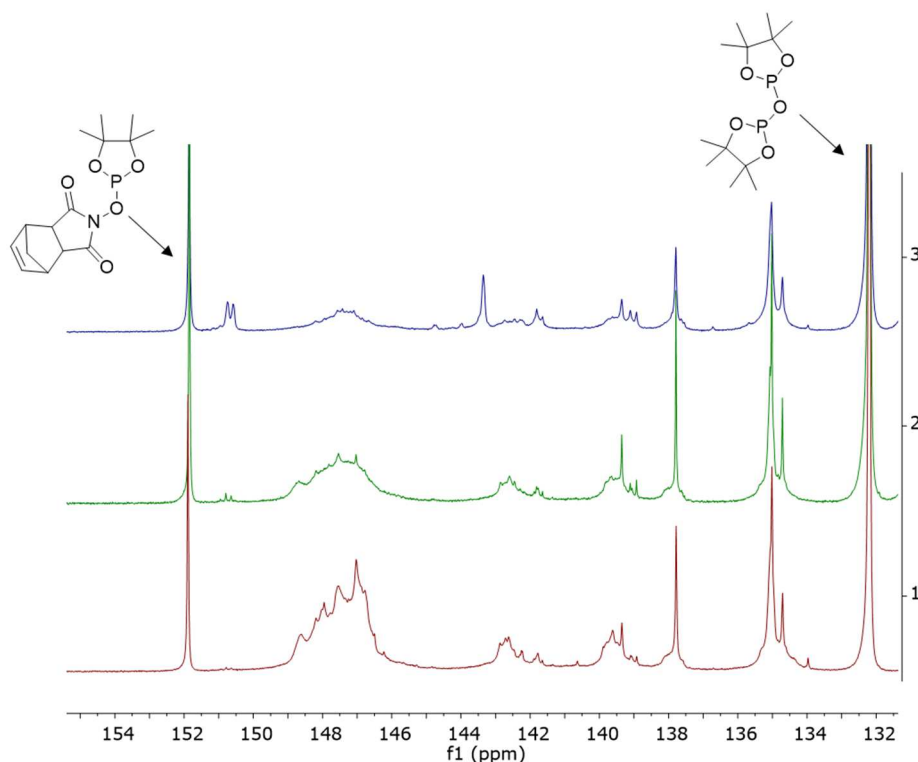


Figure 4.6: Quantitative $^{31}\text{P}\{^1\text{H}\}$ NMR spectra (161 MHz) of derived phosphite esters from: 1- steam-exploded SCB lignin, 2- control experiment (no catalyst), 3- residue after catalytic oxidation using **V5** (10 % w/w) in dioxane at 100 °C under O_2 after 96 h of reaction.

Table 4.5: Concentrations (mmol/g substrate) of SCB lignin derivatized phosphite esters determined by quantitative ^{31}P -NMR.

Lignin Subunit (mmol/g) δ (ppm)	Aliphatic OH 145.4-150.0	G 139.0-140.2	H 137.8	S 142.7	4-O-5 142.3	Carboxylic OH 133.6-136.0
Lignin	2.71	0.43	0.29	0.17	0.05	0.95
Control ^a	1.11	0.25	0.20	0.16	0.02	0.67
V5 -Dioxane-96h ^b	0.37	0.21	0.22	0.06	0.01	0.64

^a Control experiment run by heating lignin in dioxane at 100 °C under O_2 for 96 h. ^b Catalytic oxidation run using **V5** (10 % w/w) in dioxane at 100 °C under O_2 for 96 h.

As regards WS organosolv lignin, ^{31}P -NMR characterization is reported in Figure 4.7 and Table 4.6. Results indicate a remarkably different composition with respect to SCB lignin, especially as regards the amount of aliphatic OH (2.71 mmol/g for SCB lignin vs 1.25 mmol/g for WS lignin). The sample composition differs also from other organosolv WS lignin samples (extracted with dioxane) reported by Argyropoulos and Crestini³¹.

³¹ Argyropoulos, D. S.; Crestini, C.; *J. Agric. Food. Chem.* **1997**, 45, 1212.

This indicates that lignin composition is also strongly dependent upon the isolation treatment, and that also the same isolation treatment conducted in different solvent can afford different lignin compositions.

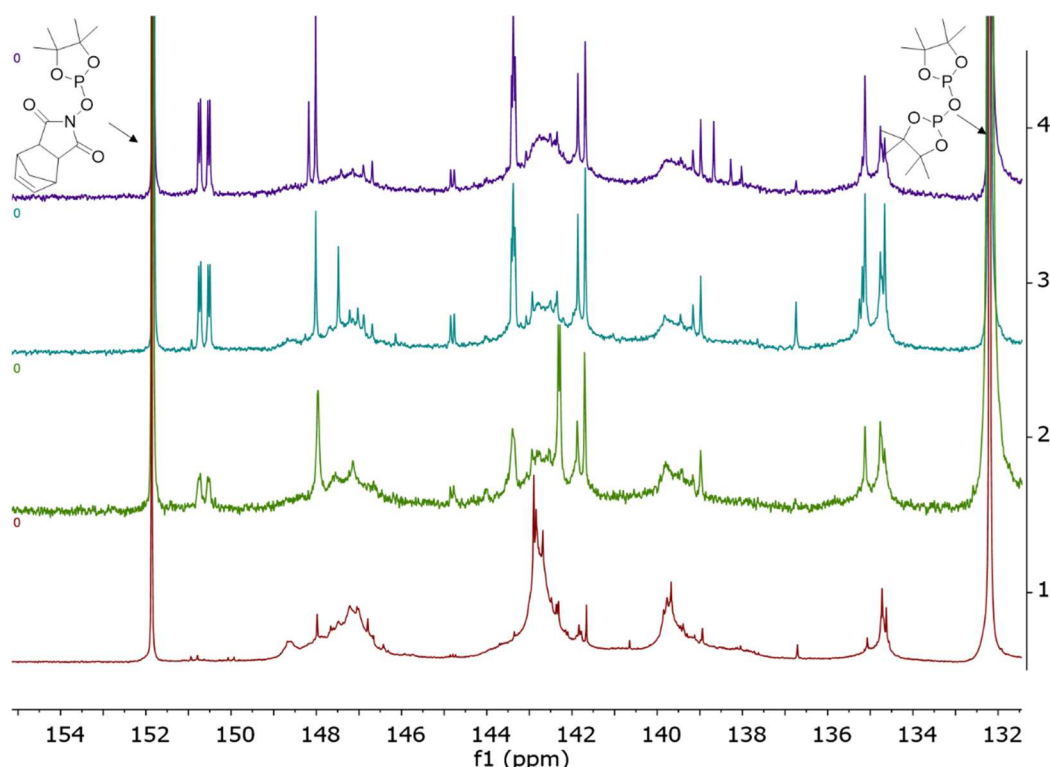


Figure 4.7: Quantitative $^{31}\text{P}\{^1\text{H}\}$ NMR spectra (161 MHz) of derived phosphite esters from: 1- organosolv WS lignin, 2- residue after catalytic oxidation using **V5** (10 % w/w) in dioxane at 100 °C under O_2 (1 atm) after 24 h of reaction, 3- residue after catalytic oxidation using **V5** (10 % w/w) in dioxane at 100 °C under O_2 (1 atm) after 96 h of reaction, 4- residue after catalytic oxidation using **V5** (10 % w/w) in toluene at 100 °C under O_2 (1 atm) after 96 h of reaction.

Table 4.6: Concentrations (mmol/g substrate) of WS lignin derivatized phosphite esters determined by quantitative ^{31}P -NMR.

Lignin Subunit (mmol/g) δ (ppm)	Aliphatic OH 145.4- 150.0	G 139.0-140.2	H 137.8	S (142.7) 4-O-5 (142.3) ^a	5-5 141.2	Carboxylic OH 133.6-136.0
Lignin	1.25	0.90	0	1.64	0	0.28
V5 -Dioxane-24h ^b	0.38	0.32	0	0.48	0	0.23
V5 -Dioxane-96h ^c	0.18	0.14	0	0.21	0	0.11
V5 -Toluene-96h ^d	0.22	0.07	0	0.13	0	0.12

^a Syringyl units 142.7 ppm overlap with 4-O-5 units at 142.3 ppm. ^b Catalytic oxidation run using **V5** (10 % w/w) in dioxane at 100 °C under O_2 for 24 h. ^c Catalytic oxidation run using **V5** (10 % w/w) in dioxane at 100 °C under O_2 for 96 h. ^d Catalytic oxidation run using **V5** (10 % w/w) in toluene at 100 °C under O_2 for 96 h.

Treatment of WS lignin with **V5** in dioxane at 100 °C under O₂ for 24 h (Figure 4.7) yielded a 70 % decrease in the concentration of aliphatic OH groups (Table 4.6), in line with the results obtained with SCB lignin (Table 4.5) and with HSQC-NMR (Figure 4.5a-b). As regards phenolic OH, both G and S units concentration decreased remarkably (64 % and 71 % respectively), whereas carboxylic acids were reduced only by 18 %. Increasing the reaction time to 96 h lead to a further depletion of all kinds of OH- groups (included carboxylic acids), confirming that oxidative depolymerization occurred in WS lignin (in analogy to what found also for SCB lignin, see Table 4.5). The reaction carried out in toluene after 96 h (Figure 4.7) showed a similar behavior, despite the amount of phenolic OH which was further depleted with respect to dioxane (more than 92 % concentration reduction for both G and S moieties).

4.3.3 FT-IR Analysis

Figure 4.8 shows FT-IR spectrum of steam exploded SCB lignin (solid blue line). The spectrum shows a wide absorption band at 3435 cm⁻¹, originated from O-H stretching vibrations in both phenolic and aliphatic groups, whereas the bands at 2918 cm⁻¹ and 2848 cm⁻¹ arise from C-H asymmetrical and symmetrical stretching in aliphatic -CH₂/-CH₃ and methoxy groups respectively³². Typical lignin bands at 1590 cm⁻¹, 1512 cm⁻¹ and 1422 cm⁻¹, derive from aromatic ring vibration, and a band at 1462 cm⁻¹ coming from C-H deformation vibrations in methoxy groups is also observed. Condensed S and G units give rise to a band at 1328 cm⁻¹, attributed to ring breathing, whereas that of G rings is found at 1263 cm⁻¹. In-plane bending of aromatic S units generates a band at 1123 cm⁻¹, that of G units is detected at 1036 cm⁻¹. Other significative bands can be attributed to C-C + C-O + C=O stretching (1222 cm⁻¹) and C-H out of plane deformation of S and G units (832 cm⁻¹). The band at 1691 cm⁻¹ can derive both from C=O stretching vibrations of conjugated ester groups or carboxylic acids (PCA and FA units)³³. It is worth mentioning that most lignin bands below 1430 cm⁻¹ are not derived from one single structural feature, but are complex bands resulting from various vibration modes. Finally, also residual xylane present in the sample generates a shoulder band at 1152 cm^{-1,34}.

If we compare the spectrum of the reaction outcome with **V5** (10 % w/w) in 1,4-dioxane at 100° C under O₂ (1 atm) (Figure 4.8, dashed red line) with the spectrum of native lignin, we can note a significant decrease in the intensity of the band at 1222 cm⁻¹, index of a significative β-O-4 bonds oxidation (benzylic C-OH stretching). This is confirmed also by the appearance of a shoulder band at 1716 cm⁻¹, which can indicate an increase in the presence of carbonyl compounds (oxidized β-O-4 bonds), in analogy with the results obtained for the same reaction from HSQC-NMR and ³¹P-NMR (Figures 4.4a-b and 4.6).

³² Li, J.; Zhang, J.; Zhang, S.; Go, Q.; Li, J.; Zhang, W.; *Ind. Crop. Prod.* **2018**, 120, 25.

³³ Faix, O.; Fourier Transform Infrared Spectroscopy. In *Methods in Lignin Chemistry*; Lin, S. Y.; Dence, C. W.; eds; Springer-Verlag: Berlin, **1992**.

³⁴ Kacurakova, M.; Capek, P.; Sasinkova, V.; Wellner, N.; Ebringerova, A.; *Carbohydr. Polym.* **2000**, 43, 195.

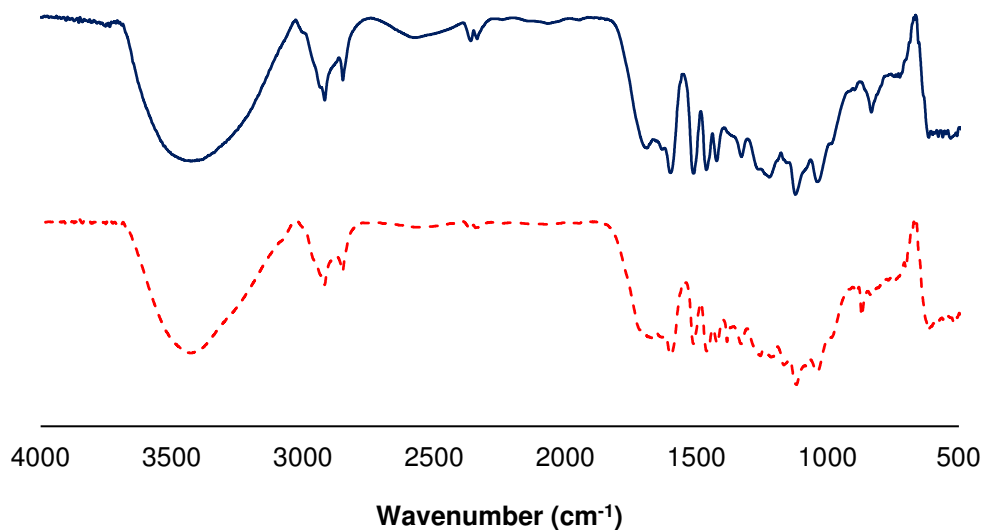
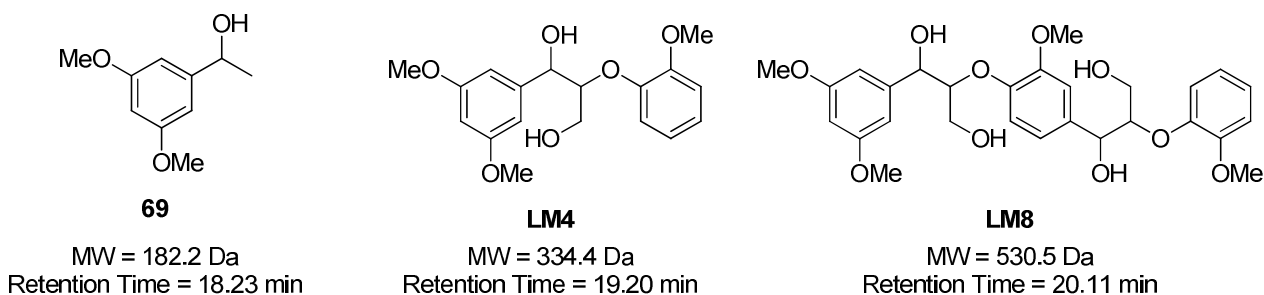


Figure 4.8: FT-IR spectra of steam exploded SCB lignin before (solid blue line) and after (dashed red line) reaction with **V5**.

4.3.4 GPC Analysis

The evaluation of the molecular weight of SCB and WS lignin before and after treatment with complex **V5** was performed by GPC, calibrating the instrument with polystyrene standards in the range of 850 Da - 10000 Da. However, due to the scarce affinity of PS structure to lignin structure³⁵, we added to the calibration curve more appropriate compounds, namely **69**, **LM4** and **LM8**, real representatives of β -O-4 bonds. Although more precise information on lignin MW is obtained with such technique, we can only accurately assign lignin MW distribution only for dimers and trimers, whereas for heavier oligomers (tetramers, pentamers, hexamers etc.) we can only have a rough estimation based on the correspondence with polystyrene MW. Taking these considerations into account we opted for a qualitative comparison of the chromatograms. We therefore characterized native SCB and WS lignin and their degradation products after reaction with complex **V5** (10 % w/w) using 1,4-dioxane and toluene as solvents, at 100 °C under O₂ (1 atm).

³⁵ a) Lange, H.; Rulli, F.; Crestini, C.; *ACS Sust. Chem. Eng.* **2016**, 4, 5167. b) Hortling, B.; Turunen, E.; Kokkonen, P.; *Handbook of Size Exclusion Chromatography and Related Techniques*; Dekker, M. Wayne, NJ., **1995**. c) Stewart, J. J.; Kadla, J. F.; Mansfield, S. D.; *Holzforchung* **2006**, 60, 111.



GPC analysis of native SCB lignin (Figure 4.9, solid line) yielded a broad signal with relative maxima corresponding to polystyrene MWs of *ca.* 921 Da and 711 Da, with other lower molecular weight compounds eluting at longer times (corresponding to MWs of *ca.* 464 Da and 198 Da). In particular, the most intense peak (464 Da) is consistent with a lignin composed mainly by trimers and dimers, in line with the results reported in literature for the same kind of lignin²⁶.

Control experiment performed in 1,4-dioxane at 100 °C under O₂ (1 atm) without catalyst (Figure 4.9, dashed line) did not produce any appreciable change in MW. The reaction with **V5** (Figure 4.9, dotted line) lead only to negligible differences in MW distribution as well. This lack in decrease of molecular weights prompted us to assume that the major reactivity of **V5** was benzylic oxidation of C_α in β-O-4 bonds, as indicated also by HSQC-NMR (Figure 4.4b) and ³¹P-NMR (Figure 4.5). This result can be better understood recalling that complex **V5** afforded mainly benzylic oxidation in dioxane for **LM4** (Table 3.4) and therefore, the same behavior has been found in SCB lignin.

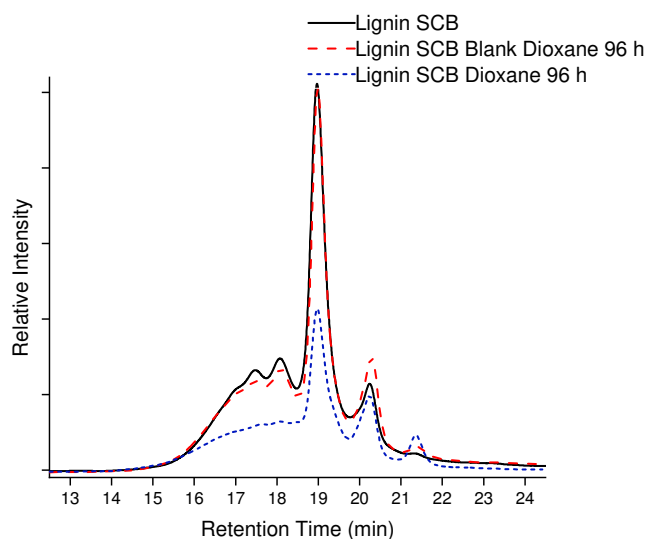


Figure 4.9: GPC data (solvent: THF, elution rate: 0.35 mL/min, 280 nm detection) for the catalytic oxidation of SCB lignin using **V5** (10 % w/w) in 1,4-dioxane at 100 °C for 96 h (dotted blue line) compared with the control experiment (same conditions with no catalyst, dashed red line) and untreated lignin (solid black line).

The reaction with complex **V5** in toluene at 100 °C under O₂ (1 atm) for 96 h (Figure 4.10, dashed line), shows a MW distribution profile almost identical to that of native lignin, even though we noticed a slight increase in the amount of lower MW components eluting at ca. 20.29 min (MW ~ 198 Da). This confirms the results obtained from HSQC-NMR (Figure 4.4c-d), that is an almost negligible reaction due to scarce lignin solubility of SCB lignin in toluene.

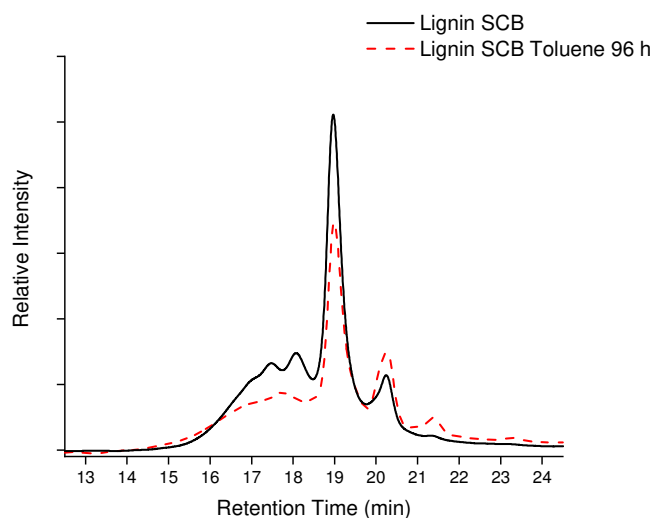


Figure 4.10: GPC data (solvent: THF, elution rate: 0.35 mL/min, 280 nm detection) for the catalytic oxidation of SCB lignin using **V5** (10 % w/w) in toluene at 100 °C for 96 h (dashed red line) compared with untreated lignin (solid black line).

GPC chromatogram of WS organosolv lignin (Figure 4.11, solid line) showed a broad peak centered at a polystyrene MW of 1138 Da, which can correspond to a mass range typical for pentamers and hexamers. This broad signal presents shoulders corresponding to a polystyrene MW of ca. 2930 Da (higher MW oligomers) and 669 Da (trimers and tetramers), while other signals can be attributed to species whose molecular weight corresponds to ca. 206 Da (for example MW of sinapyl alcohol = 210 Da). In this case MW distribution remarkably differs from that of SCB lignin, indicating that organosolv treatment affords a generally higher MW lignin with respect to steam explosion.

When WS lignin was subjected to the action of **V5** in 1,4-dioxane at 100 °C under O₂ (1 atm) for 24 h (Figure 4.11, dashed line), a remarkable change in the chromatogram was observed, although MW distribution remained almost the same. In particular, most intense peaks corresponding to a MW typical of tetramers, pentamers and hexamers were significantly reduced, whereas peaks corresponding to a MW of ca. 360 Da and 206 Da appeared, indicating an increase in the amount of dimers and monomers. At the moment, we are setting up suitable GC-MS and LC-MS methods in order to characterize such low molecular weight compounds, in order to have a more precise idea on their structure and composition. On the other hand, GPC analysis showed also a more defined peak at a polystyrene MW of ca. 3317 Da, indicating either that higher molecular weight oligomers

already present in native lignin are more recalcitrant towards depolymerization with **V5** or that some repolymerization of low MW compounds can occur in the reaction mixture. The reaction mixture composition after 96 h (Figure 4.11, dotted line) was similar to that after 24 h, confirming that in the case of WS lignin, the reaction was faster than SCB lignin, which took 96 h in order to reach completion, as reported in section 4.3.1 for HSQC-NMR.

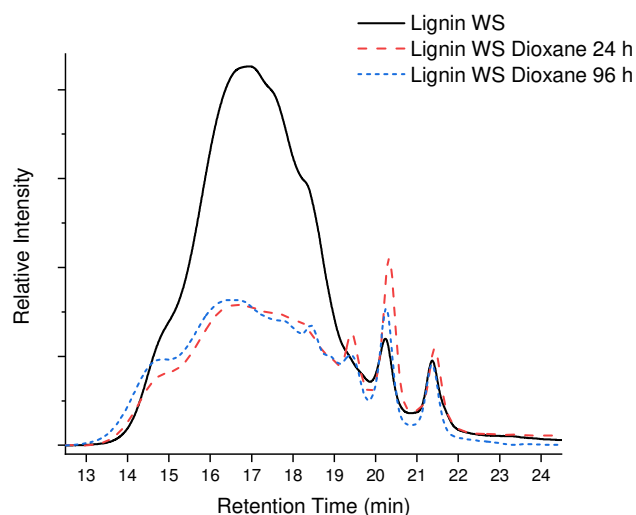


Figure 4.11: GPC data (solvent: THF, elution rate: 0.35 mL/min, 280 nm detection) for the catalytic oxidation of WS lignin using **V5** (10 % w/w) in 1,4-dioxane at 100 °C for 96 h (dotted blue line) compared with the catalytic oxidation of WS lignin using **V5** (10 % w/w) in 1,4-dioxane at 100 °C for 24 h (dashed red line) and untreated lignin (solid black line).

Differently from SCB lignin, which was scarcely soluble in toluene, organosolv WS lignin dissolved at a concentration of 20 mg/mL. Therefore, the effect of catalyst **V5** in aerobic oxidative depolymerization of WS lignin has been demonstrated also in toluene at 100 °C under O₂ (1 atm) (Figure 4.12).

In fact, already after 24 h of reaction (Figure 4.12, dashed line) the signal corresponding to a polystyrene MW of 1138 Da was significantly decreased, in favor of lower MW oligomers (see the increase of peaks corresponding to MW = 370 Da and 204 Da). After 96 h of reaction no appreciable changes were detected in MW distribution (figure 4.12 dotted line), as in the case of dioxane (Figure 4.11), meaning that 24 h are enough for reaction completion.

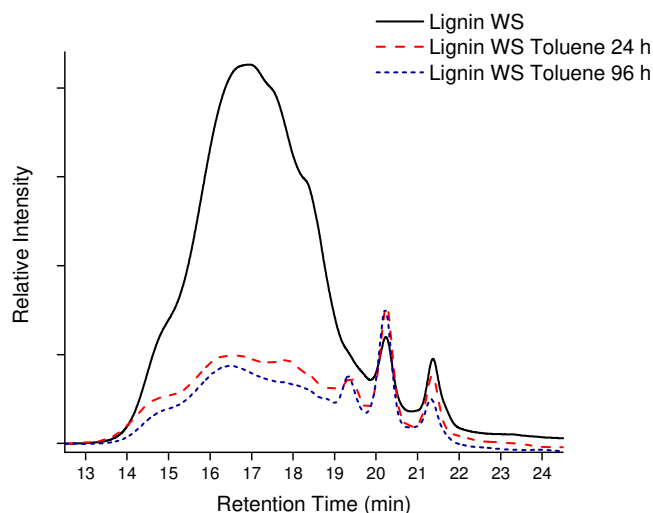


Figure 4.12: GPC data (solvent: THF, elution rate: 0.35 mL/min, 280 nm detection) for the catalytic oxidation of WS lignin using **V5** (10 % w/w) in toluene at 100 °C for 96 h (dotted blue line) compared with the catalytic oxidation of WS lignin using **V5** (10 % w/w) in toluene at 100 °C for 24 h (dashed red line) and untreated lignin (solid black line).

4.3.5 MALDI-TOF-MS Analysis

Although it is known that MALDI-TOF-MS application in lignin analysis is limited, due to its poor ionization efficiency³⁶, recently Lynn and co-workers reported an efficient method based on the use of DHAP as matrix and lithium cationization for lignin oligomers³⁷. The feasibility of this method was confirmed testing substrates **69**, **LM4** and **LM8**, respectively β -O-4 linkage monomer, dimer and trimer. In each case we observed lithium adducts at $m/z = 189$ [**69** + Li]⁺, 341 [**LM4** + Li]⁺ and 537 [**LM8** + Li]⁺, with minimal interference peaks due to the matrix: $m/z = 153$ [DHAP + H]⁺, 159 [DHAP + Li]⁺, 311 [2DHAP + Li]⁺.

We therefore used this procedure for characterizing SCB lignin and monitoring its oxidation with complex **V5**, for a comparison to what obtained by GPC. The MALDI-TOF-MS spectrum of SCB lignin in the scan range of $m/z = 130$ -1200 is reported in Figure 4.13. The most abundant ions over this mass range arise from dimeric phenylpropanes (one β -O-4 bond) ($m/z = 323$ -443, [M + Li]⁺), but we were able to identify also trimers ($m/z = 489$ -669, [M + Li]⁺), tetramers ($m/z = 655$ -895, [M + Li]⁺), pentamers ($m/z = 832$ -1121, [M + Li]⁺) and hexamers ($m/z = 987$ -1347, [M + Li]⁺).

³⁶ a) Richel, A.; Vanderghem, C.; Simon, M.; Wathelet, B.; Paquot, M.; *Anal. Chem. Insights* **2012**, 7, 79. b) Yoshioka, K.; Ando, D.; Watanabe, T.; *Phytochem Anal.* **2012**, 23, 248.

³⁷ Bowman, A. S.; Asare, S. O.; Lynn, B. C.; *Rapid Commun. Mass. Spectrom.* **2019**, 33, 811.

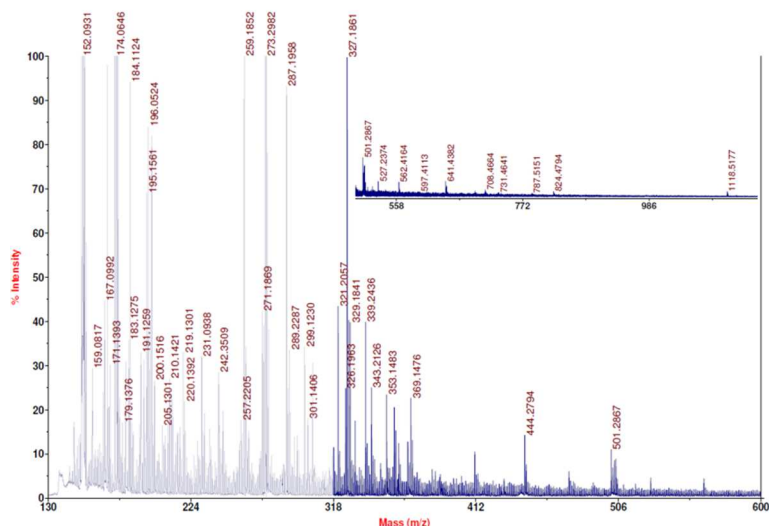


Figure 4.13: MALDI-TOF-MS spectrum of untreated SCB lignin, in the mass range of 130-600 Da with a zoom of the mass range of 500-1200 Da, at a sample concentration of 1 mg/mL obtained from DHAP containing 10 mM LiCl.

After treatment with complex **V5** (10 % w/w) in dioxane at 100 °C under O₂ (1 atm) for 96 h, tetramers and pentamers disappeared (Figure 4.14) and also signals in the trimeric region were significantly decreased. At lower MW we can observe that the signal at $m/z = 327$, which can for example be assigned to the β -O-4 dimer [**LM7** + Li]⁺, is significantly reduced. However, GC-MS of the reaction mixture showed only the presence of free *p*-coumaric acid, derived from PCA residues cleavage, with no detection of aromatic aldehydes (vanillin), in line to what reported in *Chapter 3* for **LM7** oxidation. This result is in line also with GPC analysis (Figure 4.9), which showed a slight decrease in the intensity of higher MW compounds.

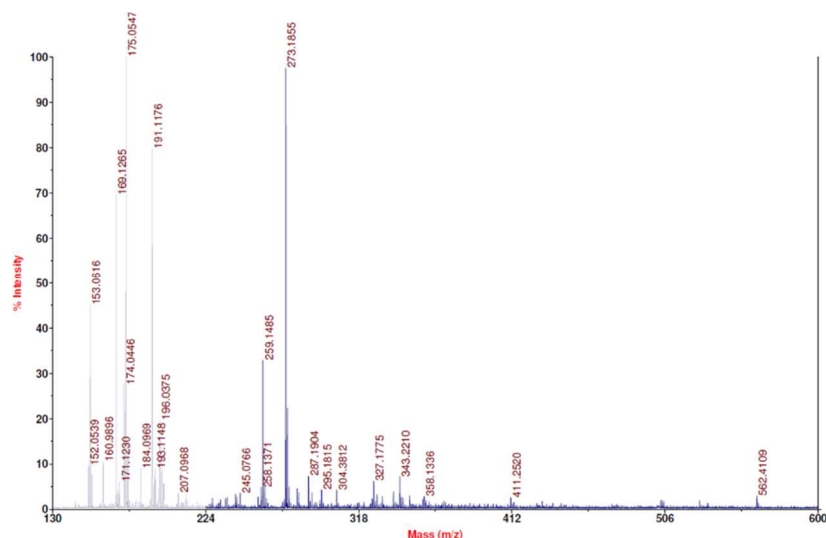


Figure 4.14: MALDI-TOF-MS spectrum of SCB lignin treated with 10 % w/w **V5** for 96 h in dioxane under O₂ atmosphere for 96 h, at a sample concentration of 1 mg/mL obtained from DHAP containing 10 mM LiCl.

Organosolv WS lignin MALDI-TOF-MS spectrum is reported in Figure 4.15. In this case, dimeric ($m/z = 323-443$, $[M + Li]^+$) and trimeric species ($m/z = 489-669$, $[M + Li]^+$) were well detected, as well as tetramers ($m/z = 655-895$, $[M + Li]^+$). However, pentamers and hexamers were not sufficiently ionized in order to be detected, demonstrating that MALDI-TOF-MS is not so reliable in determining actual MW distribution of WS lignin, since from GPC it emerged that this sample were mainly composed those species (Figure 4.11).

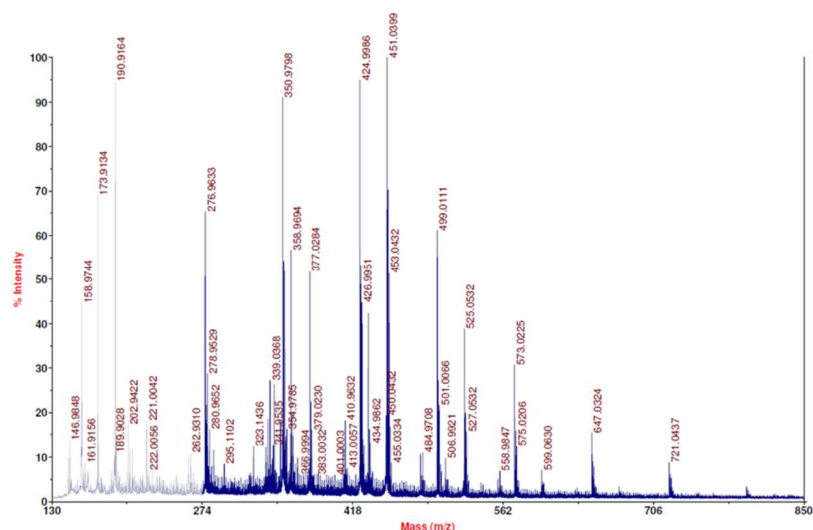


Figure 4.15: MALDI-TOF-MS spectrum of untreated WS lignin, in the mass range of 130-850 Da, at a sample concentration of 1 mg/mL obtained from DHAP containing 10 mM LiCl.

Reaction with complex **V5** (10 % w/w) in 1,4-dioxane under O_2 (1 atm) after 24 h yielded the disappearance of the higher MW signals ($m/z = 721$ and 647 , corresponding to tetramers and trimers), whereas signals relative to dimeric compounds were maintained ($m/z = 451$, 425 , 343) (Figure 4.16), in agreement with GPC results (Figure 4.11).

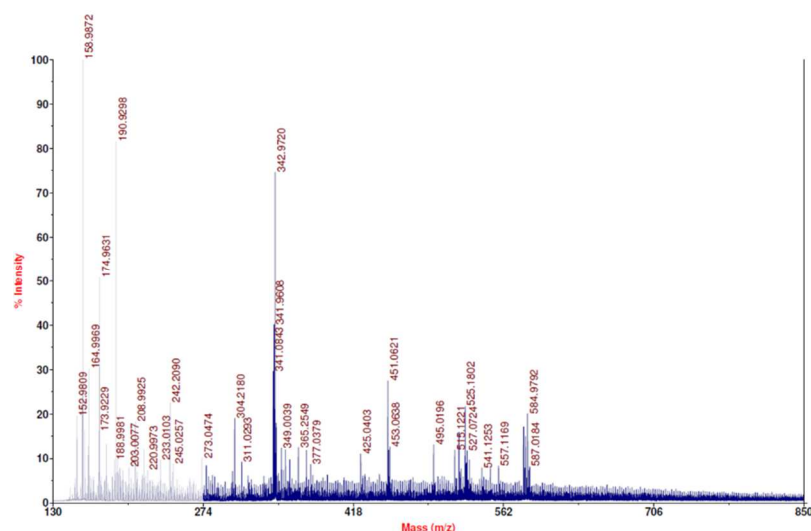


Figure 4.16: MALDI-TOF-MS spectrum of WS lignin treated with 10 % w/w **V5** for 96 h in dioxane under O₂ atmosphere, in the mass range of 130-850 Da, at a sample concentration of 1 mg/mL obtained from DHAP containing 10 mM LiCl.

To conclude this section, we were able to have a reliable estimation of the molecular weight distribution of organosolv WS and steam exploded SCB lignin samples by combining GPC and MALDI-TOF-MS techniques. In particular, results were more consistent for the latter sample, as it is composed mainly by trimers and dimers, which are sufficiently ionized in order to be detected by MALDI-TOF-MS. In the case of WS lignin, however, these two characterization techniques were not comparable, since MALDI-TOF-MS failed to detect pentamers and hexamers, which according to GPC were the major components of such sample. Nevertheless, it has been shown that MALDI can be effectively used in order to determine the exact structure of lower MW compounds coming from lignin depolymerization²⁵. Future work will be therefore based on the exact determination of such degradation products, in order to better understand the reaction outcome and to propose a more detailed mechanism.

4.4 Conclusions

In conclusion, lignin samples derived from wheat straw and sugarcane bagasse were fully characterized by means of 2D HSQC NMR, ^{31}P NMR, FT-IR, GPC and MALDI-TOF-MS. SCB lignin showed a very high amount of β -O-4 bonds present in dimeric and trimeric residues together with the depletion of other recurring linkages, making this sample an ideal candidate for studying its aerobic catalytic depolymerization. The sample was subjected to the action of complex **V5** in 1,4-dioxane, at 100 °C for 96h. After the reaction, HSQC spectra showed a complete conversion of β -O-4 bonds with the appearance of oxidized β -O-4 bonds (15 %), indicating the effectiveness of **V5** even in lignin oxidation. This was confirmed also from aromatic region, that displayed an increase in oxidized S and G units ($\text{S}'_{2-6}:\text{S}_{2-6}$ and $\text{G}'_2:\text{G}_2$ ratios respectively of 0.93:1 and 3.02:1). Moreover, residual hemicellulose xylane remained unaffected during the reaction. β -O-4 bonds oxidation was also confirmed by ^{31}P -NMR, from the decrease of the amount of aliphatic hydroxy groups (86 %) and FT-IR, from the decrease in intensity of the band relative to benzylic C-OH stretching. However, from GPC it emerged that average MW was only little affected by complex **V5**, indicating a poor extent of depolymerization, as β -O-4 bonds oxidation does not affect MW distribution that much. We have also to consider that native lignin is composed mainly by trimers and dimers, already of low MW, therefore depolymerization would afford only discrete modifications in MW distribution.

Organosolv WS lignin instead showed a significant depletion of β -O-4 bonds with respect to SCB lignin, in favor of other linkages (phenylcoumaran and resinol). However, oxidative depolymerization of this sample with **V5** (10 % w/w) was faster and effective also in toluene, where WS lignin is more soluble. Interestingly, HSQC-NMR and ^{31}P -NMR showed, besides the disappearance of β -O-4 bonds signals in aliphatic region, a depletion of also phenylcoumaran and resinol moieties, indicating that **V5** can be active even in the cleavage of other bonds present in lignin. Both S and G units were also oxidized respectively to S' and G' ($\text{S}'_{2-6}:\text{S}_{2-6}$ and $\text{G}'_2:\text{G}_2$ ratios respectively of 0.85:1 and 0.25:1) in 1,4-dioxane. In this case, GPC showed an extensive depolymerization of hexamers, pentamers and tetramers (WS lignin major components) to dimers, demonstrating a great potential of **V5** for lignocellulosic biomass valorization. Future work will be based on the investigation of **VO-TPA(R,R')** complexes in the oxidative cleavage of other lignin linkages, in order to build a robust depolymerization procedure generally effective with a wide array of lignin samples in terms of composition and molecular weight. Moreover, we are setting up suitable GC-MS and LC-MS methods for determination and quantification of volatile compounds, in order to verify the effectiveness of complex **V5** in yielding oxygenated aromatic compound from lignin degradation.

4.5 Experimental

General Remarks:

All chemicals and dry solvents were purchased from Sigma-Aldrich and used without further purification. Deuterated solvents (Sigma-Aldrich) were used without further purification. Other organic solvents, (Sigma-Aldrich) were used without further purification.

GC-MS spectra have been recorded with an Agilent 6850 Series GC System interfaced with an Agilent 5973 Network Mass Selective Detector. Carrier gas He, phase HP-5MS, column 30mt I.D. 0,25, film 0,25 μm , 5% diphenyl 95% dimethylsiloxane. Injector temperature has been set to 250 $^{\circ}\text{C}$, detector temperature has been set to 280 $^{\circ}\text{C}$ and the carrier gas is He (1 mL/min) with a HP-5MS column. ESI-MS spectra were recorded on an Agilent 1100 LC/MSD IonTrap spectrometer, in positive/negative modes, by direct flow injection using acetonitrile or methanol (both with 0.1 % v/v of HCOOH for analysis in positive mode) as mobile phase. FT-IR spectra has been recorded in the range (4000-600) cm^{-1} and resolution 4 cm^{-1} , on a Nicolet 5700 FT-IR instrument, using KBr pellets. HPLC analyses were performed on a Shimadzu HPLC equipped with a Knauer Eurospher II 100-5 C18 (5 μm of active phase, 250 x 4,6 mm column) operating at room temperature, eluent water /acetonitrile gradient, naphthalene/biphenyl as internal standard. The UV detector was set at $\lambda = 210$ nm. The concentration of both reagents and products was estimated from the calibration curves. GC-FID analyses were performed on a Shimadzu GC-2010, equipped with a Supelco column (phase: SPB^{T1}-1, length: 15 m, ID: 0.1 mm, 0.1 μm Film, 100% dimethylsiloxane). Carrier gas He (69 ml/min). Injector temperature has been set to 280 $^{\circ}\text{C}$, detector temperature has been set to 330 $^{\circ}\text{C}$. The concentration of both reagents and products was estimated from the calibration curves. GPC analyses were carried out in an Agilent Technologies 1260 Infinity HPLC/GPC system, equipped with an Agilent 1260 Infinity Variable Wavelength Detector (VWD) VL (280 nm target wavelength), the 1260 Infinity Refractive Index Detector (RID, 1260 Infinity Thermostated Column Compartment), using 0.35 mL/min THF at 40 $^{\circ}\text{C}$ with a guard column and two Phenomenex PhenogelTM 5 μm 50 \AA and 500 \AA columns connected in series. MALDI-TOF analyses were performed using a 4800 MALDI TOF-TOF Analyzer from Applied Biosystems.

NMR experiments

^1H , $^{13}\text{C}\{^1\text{H}\}$ NMR and 2D NMR spectra were obtained using a Bruker DMX 600 MHz equipped with a BBI *z-grad* probehead or a Bruker 400 MHz Avance III HD equipped with a BBI-*z grad* probehead. Chemical shifts (δ) have been reported in parts per million (ppm) relative to the residual undeuterated solvent as an internal reference (CDCl_3 : 7.26 ppm for ^1H -NMR and 77.0 ppm for ^{13}C NMR; $\text{DMSO-}d_6$: 2.50 ppm for ^1H -NMR and 39.52 ppm for ^{13}C NMR). For 2D-HSQC experiments, an aliquot of the reaction mixture was evaporated under reduced pressure and dissolved in $\text{DMSO-}d_6$. All the structural units of lignin samples were assigned by comparison from the lignin database reported in literature. The spectral width was set to 10 - 0 ppm in F2 dimension and 200 - 0 ppm in F1 dimension.

The recycle delay was set to 1.5 s. The number of collected points was 1024 for ^1H dimension. The number of scans was 128 with 256 increments. The Sine Square function was applied in both dimensions. All the structural units of the lignin substrates were assigned based on the lignin database and reported literature²⁹.

Quantitative ^{31}P -NMR was performed according to the following reported procedure³⁸: approximately 30 mg of native or oxidized lignin residue was dissolved in a mixture of pyridine/ CDCl_3 1.6/1 v/v (500 μL), then a solution of $\text{Cr}(\text{acac})_3$ (5 mg/mL) used as a relaxation agent and NHND (0.1 M) used as internal standard (100 μL) was added, and the mixture was stirred overnight until a homogeneous solution is formed. TMDP (100 μL) was subsequently added to the solution, which was stirred for 10 min at RT and transferred to an NMR tube. The spectrum was acquired using an inverse-gated decoupling pulse sequence with a 90° pulse angle, 10 s of interscan delay and 256 scans. All spectra were processed using MestReNova.

GPC Analysis

The GPC instrument was calibrated using polystyrene standards, although it has been demonstrated that such standards are of limited value for absolute determination of MW of branched macromolecules such as lignin. Therefore, we built a calibration curve including also lignin-related compounds **69**, **LM4** and **LM8** (according to ref 35a) and we opted for a qualitative comparison of the catalytic reactions with untreated lignin or control experiments in which lignin was subjected to identical conditions (solvent, temperature, etc.) in absence of **V5**. For GPC analysis an aliquot of the reaction mixture was evaporated and dissolved in THF (2.5 mg/mL).

MALDI-TOF-MS Analysis

The samples were prepared according to a procedure reported in literature, using DHAP as matrix and Lithium cationization³⁷. Lignin stock solutions were prepared in ACN at a concentration of 1 mg/mL. The DHAP matrix solution was prepared at 6.5 mg / mL in ACN. LiCl solution was prepared at a concentration of 10 mM in MeOH. The salt solution was spotted (1 μL) onto the stainless-steel plate and allowed to dry at RT under air. Next, lignin solutions (1 μL) were spotted above the salt spot and finally matrix solution (1 μL) was added and allowed to dry.

³⁸ Meng, X.; Crestini, C.; Ben, H.; Hao, N.; Pu, Y.; Ragauskas, A. J.; Argyropoulos, D. S.; *Nature Protocols* **2019**, 14, 2627.

Preparation of lignin samples

Wheat Straw organosolv lignin and steam exploded Sugarcane Bagasse lignin were provided by prof. D. Cannella at Université libre de Bruxelles, Brussels, Belgium. Before use, lignin samples were dried under vacuum to remove volatiles. The residues were then used without further purifications in all the experiments. The relative amounts of major structural units in the oxygenated aliphatic and aromatic regions were determined by 2D-HSQC-NMR, integrating the H_α/C_α correlations. For SCB lignin, the relative amount of the structural units was determined with respect to H₆ in ferulic acid residues, used as an internal standard.

Wheat Straw organosolv lignin²⁵

Wheat straw (*Triticum aestivum* L.) was pretreated in a 100 mL Parr reactor, at 194 °C with a residence time of 20 minutes, at 10% dry matter content in water. Solubilized sugars and degradation products were removed by a washing and pressing step after the pretreatment. The pretreated WS was dried and grinded in a coffee blender for 5 minutes prior to further use. The chemical composition of the solid fraction was determined using a modified version of the NREL method for lignocellulose biomasses³⁹, as glucans 53%, xylans 4%, lignin 34%, and ash 6%. Pretreated WS was then suspended in EtOH: H₂O = 1:1 solution at a 5:1 liquid to solid ratio and heated at 180 °C in a 1L Parr reactor for 80 minutes. After cooking, the residue was filtered at 75 °C. Solubilized lignin was precipitated by adding water at three times the original amount and recovered by filtration. The lignin enriched fraction was dried (40 °C) and grinded with a pestle and mortar.

Steam Explosion Treatment²⁶

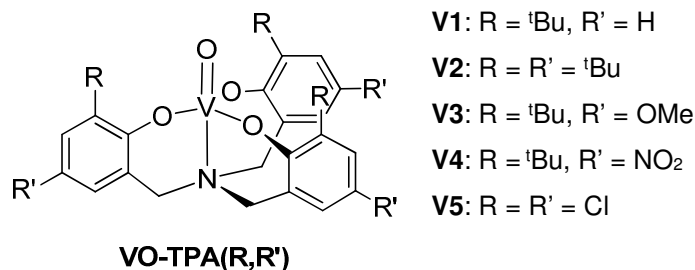
Dry bagasse was loaded into a stainless-steel reactor. The reactor was hermetically closed, and steam was injected until a pressure of approximately 1.3 MPa (equivalent to 190 °C) was achieved. After 15 min the reactor was suddenly depressurized, and the steam-exploded slurry was centrifuged for 10 min. The solid fraction (cellulignin), was separated, thoroughly washed with water and submitted to alkaline delignification in a stainless steel-coated cast iron reactor, equipped with a stirrer. A solution of NaOH 1% (w/v) was added, in a liquid-to-solid ratio of 20:1. The reaction mixture was heated at 100 °C and held under stirring (80 rpm) for 1 h. After that, raw cellulose was separated from the lignin-rich black liquor by centrifugation for 10 min. Lignin was isolated from the black liquors by precipitation after acidification with 98% H₂SO₄ until pH = 2.0 was reached. The precipitated lignin was separated by centrifugation (10 min) and washed with water until pH = 7.0 was reached. The washed lignin was finally dried at 70 °C.

³⁹ Cannella, D.; Hsieh, C. W.; Felby, C.; Jorgensen, H.; *Biotechnol. Biofuels* **2012**, 5, 26.

Procedure for the catalytic oxidation of organosolv WS steam exploded SCB lignin

In a 10 mL reactor, equipped with a stirring bar and a condenser under oxygen atmosphere (balloon), lignin (40 mg) was dissolved in the appropriate solvent (2 mL) and complex **V5** (4 mg, 10 % w/w) was added. The mixture was stirred (700 rpm) at 100 °C and the reaction was monitored by 2D-HSQC-NMR, taking aliquots corresponding to 10 mg of lignin at 24 h, 48 h and 96 h. After 96 h, the reaction was stopped, the solvent removed under vacuum and the mixture was analyzed by 2D-HSQC-NMR, ³¹P-NMR, FT-IR, GPC and MALDI-TOF-MS.

General Conclusions



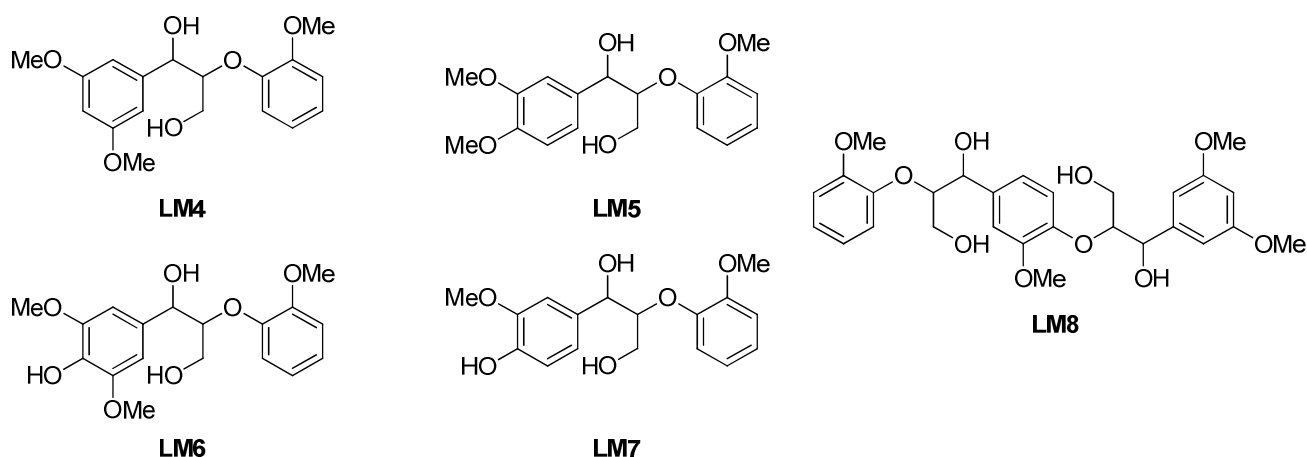
This thesis work describes the use of vanadium(V)-aminotriphenolate complexes **VO-TPA(R,R')** as catalysts for the efficient aerobic oxidative C-C cleavage of vicinal diols, β -O-4 lignin models and lignin itself. The facile manipulation of the phenolic framework of the aminotriphenolate structure provides a great opportunity for new ligands design: the introduction of a large variety of substituents allows to obtain a wide array of stereo-electronic properties to the complexes which effectively can be transferred to their behavior as catalysts. In fact, in the past decade such complexes have shown a very good activity in oxygen transfer reactions (sulfoxidations, haloperoxidations, amines oxidation), CO₂ activation for the synthesis of cyclic carbonate/polycarbonates, lactide living polymerization and as stereodynamic chiral probe. Among oxidation reactions, more recently the aerobic oxidative C-C bond cleavage catalyzed by **VO-TPA(R,R')** proved to be possible. The present work proves that these catalysts are effective not only with lignin models (1,2-diols and β -O-4 lignin models) but also lignin.

We developed an efficient and robust methodology for aerobic C-C cleavage of glycols catalyzed by **VO-TPA(R,R')**. The electron-poor hexachloro-substituted complex **V5** showed an impressive activity, yielding fast and complete substrate conversions towards the relative carbonyl compounds, reaching TONs up to 81,000 and TOFs up to 34,700 h⁻¹. A plethora of substrates were tested, demonstrating that our system is effective for tertiary, secondary and primary linear and cyclic glycols, bearing aliphatic and aromatic substituents and tolerant towards several functional groups. Based on some experimental evidence and DFT calculations a mechanism for the catalytic cycle was proposed. The catalytic cycle can be divided into three main steps: i. formation of a vanadium(V) non oxo-glycolate complex by reaction of **V5** with ethan-1,2-diol or pinacol with formal elimination of a water molecule, ii. C-C bond oxidative cleavage of the cyclic metal glycolate, yielding the carbonyl products by a two-fold electron transfer mechanism and generation of a V(III) complex intermediate. iii. re-oxidization to V(V) by O₂ addition, via formation of a V(V) peroxy and the a dinuclear V(IV)-peroxy-species and regeneration of catalyst **V5**.

The versatility of **VO-TPA(R,R')** complexes in oxidation reactions has been proven by their activity as catalysts for aldehyde oxidation to the corresponding carboxylic acids. Both aliphatic and aromatic

aldehydes were converted into the corresponding carboxylic acids in few hours, using O₂ as terminal oxidant in aromatic solvents at high temperatures (100-130°C). Preliminary tests are consistent with the occurrence of a radical processes (vanadium-mediated radical autooxidation). We are currently enlarging the substrate scope towards more appealing and useful compounds (HMF, citral, perillaldehyde) and verifying the chemoselectivity of the reaction in presence of other functional groups (-OH, alkenes, halogens, -CN, NO₂).

After having verified the ability of our **V5** based system in C-C cleavage of vicinal diols, we extended the substrate complexity to β-O-4 lignin linkage models **LM4-LM7**, including also a trimeric model bearing two consecutive β-O-4 bonds **LM8**.



A series of experiments could demonstrate that **V5** is capable of catalyzing the aerobic oxidation of these compounds down to catalyst loading of 1 mol %. With these substrates the chemoselectivity of the reaction is lower: we observed mainly benzylic oxidation (50-85 %), followed by C-C bond cleavage (13-32 %). C-O cleavage was also observed, even if in a minor extent (1-23%). In particular, further treatment of the oxidized reaction mixture of the trimeric model **LM8** (Baeyer-Villiger oxidation, H₂O₂/NaOH) yielded a quantitative C-C cleavage of the oxidized model **56a** with the reaction selectivity oriented towards the formation of carboxylic acids (70 % yield of 3,5-dimethoxybenzoic acid **19b** and 43 % yield of vanillic acid **39b**). This can represent an effective two-step lignin depolymerization strategy based on a first aerobic catalytic oxidation of α-OH groups yielding ketones and a subsequent cleavage process which employs mild oxidants and cheap reagents in order to afford benzoic acids. We also disentangled the effect of non-functionalized α-OH and γ-OH groups in β-O-4 models in benzylic oxidation, providing first insights in understanding such reaction.

Catalyst **V5** (10 % w/w) was also tested in the aerobic oxidation of lignin samples derived from wheat straw and sugarcane bagasse, particularly rich in β-O-4 linkages (at least 80 % of β-O-4 bonds). Reactions were run using a concentration of lignin of 20 mg/mL, at 100°C under O₂ (1 atm), screening 1,4-dioxane and toluene as solvents and monitored every 24 h up to 96 h when necessary. The lignin samples before and after the oxidative depolymerization were analyzed by HSQC-NMR, ³¹P-NMR (after derivatization to phosphite esters), FT-IR, GPC and MALDI-TOF-MS. A remarkable

activity was observed for SCB lignin with significant decrease or disappearance of β -O-4 linkages and formation of the corresponding ketones (15 % benzylic oxidation). The reaction with WS lignin yielded not only a quantitative conversion of β -O-4 bonds, but also phenylcoumaran and resinol linkages disappeared, with a concomitant depolymerization of lignin major components, namely hexamers and pentamers, indicating a great potential of this system for valorization of lignocellulosic biomass. We are currently setting up a suitable strategy for lignin degradation products determination, in order to identify and quantify the amount of low-molecular weight compounds produced from the reaction with **V5**.

Future work based on the results obtained in this PhD thesis will be mainly focused on clarifying the chemical processes previously reported. Despite the very good activity of complex **V5** in the aerobic oxidation of lignin models and lignin, the detailed reaction mechanism of the different oxidative pathways observed and the origin of the chemoselectivity have not been fully understood yet. We should concentrate on the clarification of all the parameters that control these reactions in order to design a more suitable and versatile catalyst. The versatility of TPAs scaffold together with the ease of its manipulation can be exploited also in order to build a more robust system, of crucial importance from an industrial point of view. For example, heterogenization of **VO-TPA(R,R')** complexes would provide several advantages, in terms of recyclability and easy separation from the reaction mixture. Moreover, novel approaches should be focused on tandem catalytic systems for oxidation/depolymerization, employing other transition metals (Cu(II)) or co-additives.

There is still a long way to go in order to find an effective method for lignocellulosic biomass valorization, despite the recent advances both in heterogeneous and homogeneous catalysis in this field. Although oxidation is not the only option for lignin valorization, this represents one of the greenest and most eco-friendly strategies that maintains the oxygen-based functionalization present in the starting material. The evolution to a carbon-neutral global economy, with the total depletion of fossil fuels is undoubtedly necessary but difficult in order to avoid catastrophic consequences of climate change. This thesis has contributed within the frame of developing a novel lignin oxidative depolymerization process based on the use of mild reaction conditions, homogeneous catalysis and O₂ as terminal oxidant.

List of Abbreviations

Ac	Acetyl
acac	Acetylacetonate
ACN	Acetonitrile
AcOEt	Ethyl Acetate
Ar	Aryl
atm	Atmosphere
Bn	Benzyl
bp	Boiling Point
BTX	Benzene, Toluene and Xylene
cat.	Catalyst
COD	1,5-Cyclooctadiene
conv.	Conversion
cy	Cyclohexyl
DAD	Diode Array Detector
DCE	1,2-dichloroethane
DCM	Dichloromethane
DFT	Density Functional Theory
DHAP	2',5'-dihydroxyacetophenone
DIPEA	Diisopropylethylamine
dipic	Dipicolinate
DMF	Dimethylformamide
DMSO	Dimethylsulfoxide
dtbbpy	4,4'-Di-tert-butyl-2,2'-dipyridyl
EMIM	Ethly-Methylimidazolium
ESI-MS	Electron Spray Ionization - Mass Spectrometry
ESI-TOF	Electron Spray Ionization Mass Spectrometry – Time of Flight
Et	Ethyl
Et₂O	Diethylether
EtOH	Ethanol
NEt₃	Triethylamine
FT	Fourier Transform
FT-IR	Fourier Transform - Infrared Spectroscopy
GC-FID	Gas Chromatography - Flame Ionization Detector
GC-MS	Gas Chromatography - Mass Spectrometry
GPC	Gel Permeation Chromatography

HMDSO	Hexamethyldisiloxane
HMF	Hydroxymethylfurfural
HMTA	Hexamethylenetetramine
HPLC	High Performance Liquid Chromatography
HQ	8-oxyquinolate
HRMS	High Resolution Mass Spectrometry
HSQC	Heteronuclear Spin Quantum Correlation
IL	Ionic Liquid
<i>i</i>Pr	Isopropyl
<i>i</i>PrO-	Isopropoxide
LC-MS	Liquid Chromatography - Mass Spectrometry
LDA	Lithium Diisopropylamide
MALDI-TOF-MS	Matrix Assisted Laser Desorption Ionization - Time of Flight - Mass Spectrometry
Me	Methyl
MeOH	Methanol
mim	3-Methylimidazole
MOM	Methoxymethyl
mp	Melting Point
MS	Molecular Sieves
MTO	Methyltrioxorhenium(VII)
MVL	Milled Wood Lignin
MW	Molecular Weight
NHND	N-hydroxy-5-norbornene-2,3-dicarboxylic acid imide
NHPI	N-Hydroxyphthalimide
NMR	Nuclear Magnetic Resonance
OCT	Octahedral Geometry
Ph	Phenyl
PINO	Phtalimide-N-Oxyl
PMA	Phosphomolybdic Acid
ppm	Part per Million
ppy	2-phenylpyridine
PS	Polystyrene
RT	Room Temperature
SCB	Sugarcane Bagasse
TBAB	Terabutylammonium Bromide
TBP	Trigonal Bipyramidal geometry

TBDMS	<i>tert</i> -butyldimethylsilyl
^tBu	<i>Tert</i> -butyl
TEMPO	2, 2, 6, 6-tetramethylpiperidine-N-oxyl
THF	Tetrahydrofuran
TLC	Thin Layer Chromatography
TMDP	2-Chloro-4,4,5,5-tetramethyl-1,3,2-dioxaphospholane
TMEDA	N,N,N',N'-tetramethylethylenediamine
TMS	Trimethylsilyl
TOF	Turn Over Frequency
TON	Turn Over Number
TPA	Triphenolamine
TfO	Trifluoromethanesulfonate
TsO	p-Toluenesulfonate
UFL	Upper Flammable Limit
UV-Vis	Ultraviolet - Visible
WS	Wheat Straw
% w/w	% weight/ weight
xantphos	4,5-Bis(diphenylphosphino)-9,9-dimethylxanthene